

**Chemical Modification of Proteins by Air Pollutants
and Metaproteomic Analysis of Atmospheric
Aerosol Samples by HPLC-MS Analyses**

Dissertation

zur Erlangung des Grades

‘Doktor rerum naturalium (Dr. rer. nat.)’

im Promotionsfach Chemie

am Fachbereich Chemie, Pharmazie und Geowissenschaften

der Johannes Gutenberg-Universität in Mainz

Fobang Liu

geb. am 20.07.1987

in Guangzhou (Guangdong), VR China

Mainz, 2017

I hereby declare that I wrote the dissertation submitted without any unauthorized external assistance and used only sources acknowledged in the work. All textual passages which are appropriated verbatim or paraphrased from published and unpublished texts as well as all information obtained from oral sources are duly indicated and listed in accordance with bibliographical rules. In carrying out this research, I complied with the rules of standard scientific practice as formulated in the statutes of Johannes Gutenberg University Mainz to insure standard scientific practice.

Abstract

Proteins are a major component of bioaerosols and can account for several percent of air particulate matter. They may influence the climate and public health depending on their properties, e.g., hygroscopicity, molecular composition and structure. The interaction with anthropogenic air pollutants can modify their physical, chemical and biological properties, thus altering their climate and health effects. In particular, chemical modifications of proteins (e.g., nitration and cross-linking) induced by air pollutants, have been linked to an enhanced potency of allergenic proteins. The mechanisms and kinetics of the underlying chemical processes, however, are not yet well understood.

In this thesis, the reaction products, kinetics and mechanisms of atmospheric protein chemistry were studied, and the proteome of atmospheric aerosol samples was characterized using high performance liquid chromatography coupled with diode array detection and fluorescence detection (HPLC-DAD and HPLC-DAD-FLD), and HPLC coupled to mass spectrometry (HPLC-MS/MS). The focus areas of this thesis can be summarized as follows:

1. Development of a method to characterize proteins from atmospheric aerosol samples using a mass spectrometry-based metaproteomic approach. Extraction solvents were optimized to overcome the interaction between proteins and glass fiber filters and achieve high protein recoveries. Size exclusion chromatography (SEC) was applied to remove matrix components. Sodium dodecyl sulfate polyacrylamide gel electrophoresis (SDS-PAGE) was applied for protein fractionation according to molecular size, followed by in-gel digestion. The digested peptides were analyzed using a hybrid Quadrupole-Orbitrap MS and database search functions. The developed method has been successfully applied for protein identification from filters samples collected in central Europe (Mainz, Germany). The presented method provides a tool for further studies of spatiotemporal variability of bioparticles and allergens in atmospheric aerosol samples.
2. Elucidation of the mechanisms and kinetics of protein nitration and oligomerization induced by ozone (O_3) and nitrogen dioxide (NO_2). Proteins were exposed to O_3 , and O_3/NO_2 mixtures in coated-wall flow-tube and bulk-solution experiments, using bovine serum albumin (BSA) as a model protein. An SEC-HPLC-DAD method was developed that enables the simultaneous detection of mono-, di-, tri-, and higher protein oligomers as well as their individual nitration degrees (NDs). In the reaction of BSA with O_3 , the formation of protein dimers, trimers and higher oligomers was observed. The SDS-PAGE

and fluorescence analysis results revealed that the protein cross-linking can be attributed to the formation of intermolecular dityrosine species. For the reactions of BSA with O₃ and NO₂, more tyrosine residues were found to react via the nitration pathways than via the oligomerization pathways. Depending on reaction conditions, oligomer mass fractions and NDs were in the range of 2.5-25% and 0.5-7%, respectively. The extent of protein nitration and oligomerization strongly depended on the phase state of proteins (i.e., amorphous solid, semi-solid, liquid) and hence the diffusivity of oxidants and protein molecules, which change with relative humidity. The experimental results can be explained and described by a kinetic multi-layer model of surface and bulk chemistry. The rates of both processes were sensitive to the increase of O₃ concentrations but rather insensitive to the change in ambient NO₂ concentrations.

3. Identification and quantification of free amino acids released upon oxidation of peptides and proteins by hydroxyl radicals. The oxidation products of proteins and peptides generated by hydroxyl radicals from Fenton reactions were analyzed using HPLC-MS/MS and HPLC-DAD-FLD. Free amino acids were identified as products by HPLC-MS/MS analysis. A site-selective formation of free amino acids was also observed, which may be due to a reaction pathway involving nitrogen-centered radicals. For protein oxidation reactions, the molar yields of glycine (Gly, ~32-55% for BSA, ~10-21% for ovalbumin (OVA)) were substantially higher than for the other identified amino acids (i.e., alanine, aspartic acid, and asparagine; ~5-12% for BSA, ~4-6% for OVA). Upon oxidation of tripeptides with Gly in C-terminal, mid-chain, or N-terminal positions, Gly was preferentially released when it was located at the C-terminal site.

The methods developed and reaction products, kinetics, and mechanisms studied in this thesis provide a basis for further investigations of atmospheric protein chemistry influenced by air pollutants. They shall help to understand the relations between air pollutant-modified aeroallergens and their enhanced allergenicity.

Zusammenfassung

Proteine sind eine Hauptkomponente biologischer Aerosolpartikeln können mehrere Prozent der gesamten Partikelmasse in der Luft ausmachen. Diese Proteine können abhängig von ihren Eigenschaften, wie Hygroskopizität, molekularer Zusammensetzung und Struktur, das Klima der Erde beeinflussen und sich auf die Gesundheit der Lebewesen auswirken. Durch die Wechselwirkungen mit anthropogenen Luftschadstoffen können die physikalischen, chemischen und biologischen Eigenschaften der Proteine modifiziert werden und demnach Auswirkungen auf das Klima und die Gesundheit haben. Insbesondere die von Luftschadstoffen hervorgerufene chemische Modifikationen von Proteinen (z.B. Nitrierung und Quervernetzung) konnten bereits mit einer verstärkten Allergenwirkung der entsprechenden Proteine in Zusammenhang gebracht werden. Allerdings sind weder die Mechanismen noch die Kinetik der zugrundeliegenden chemischen Prozesse ausreichend verstanden.

In der vorliegenden Doktorarbeit wurden basierend auf der Anwendung von Hochleistungsflüssigkeitschromatographie gekoppelt mit Diodenarray-Detektion und Fluoreszenzdetektion (HPLC-DAD und HPLC-FLD), sowie HPLC gekoppelt an Massenspektrometrie (HPLC-MS/MS) die Reaktionsprodukte, die Kinetik und die Mechanismen der Interaktion mit Luftschadstoffen untersucht und Proteine aus atmosphärischen Aerosolproben charakterisiert. Die Hauptpunkte dieser Arbeit können wie folgt zusammengefasst werden:

1. Entwicklung einer Methode zur Charakterisierung von Proteinen aus atmosphärischen Aerosolproben unter Anwendung eines metaproteomischen Ansatzes basierend auf Massenspektrometrie. Die Extraktionsmethode wurde optimiert, um die Interaktion zwischen Proteinen und Glasfaserfiltern zu überwinden und somit eine hohe Proteinrückgewinnung zu erreichen. Zur Entfernung von Matrixkomponenten wurde die Größenausschlusschromatographie (SEC) verwendet. Zur Auftrennung der Proteine anhand ihrer molekularen Größe, wurde Natriumdodecylsulfat-Polyacrylamidgellelektrophorese (SDS-PAGE) angewendet. Anschließend wurden die Proteine im Gel verdaut und die entstandenen Peptide mit Hilfe eines hybriden Quadrupol-Orbitrap-Massenspektrometers und Datenbanksuchfunktionen analysiert. Die entwickelte Methode konnte erfolgreich auf die Identifikation von Proteinen aus in Mitteleuropa (Mainz, Deutschland) gesammelten Filterproben angewendet werden. Zudem bietet sie ein

Werkzeug für weitere Studien über die räumliche und zeitliche Variabilität von Biopartikeln und Allergenen in atmosphärischen Aerosolproben.

2. Aufklärung des Mechanismus und der Kinetik der Nitrierung und Oligomerisierung von Tyrosinresten in Proteinen durch Ozon (O_3) und Stickstoffdioxid (NO_2). Hierfür wurden Proteine entweder auf die Wand eines Durchflussrohres aufgetragen oder in Lösung gebracht und O_3 oder einer Mischung aus O_3 und NO_2 ausgesetzt. Rinderserumalbumin (BSA) diente hierbei als Modellprotein. Des Weiteren wurde eine effiziente Methode mit SEC-HPLC-DAD entwickelt, welche die simultane Bestimmung von einfachen, zweifachen, dreifachen und höheren Proteinoligomeren sowie ihrer individuellen Nitrierungsgrade (NDs) ermöglicht. Für die Reaktion von BSA mit O_3 wurde die Bildung von Proteindimeren, -trimeren und höheren Oligomeren beobachtet. Die Ergebnisse von SDS-PAGE und Fluoreszenzanalyse zeigen, dass die Proteinquervernetzung auf die Bildung von intramolekularen Dityrosinen zurückzuführen ist. Für die Reaktion von BSA mit O_3 und NO_2 wurden mehr Tyrosinreste gefunden, die dem Nitrierungsweg folgen, als die den Weg der Oligomerisierung gehen. Abhängig von den Reaktionsbedingungen lag der Anteil an Oligomeren im Bereich von 2.5-25% und die NDs bei 0.5-7%. Das Ausmaß der Nitrierung und Oligomerisierung von Proteinen ist stark abhängig von ihrem Aggregatzustand (glasartig, halbfest, flüssig) und damit vom Diffusionsvermögen der Oxidationsmittel und Proteinmoleküle, das sich mit der relativen Luftfeuchtigkeit verändert. Die experimentellen Ergebnisse können unter Zuhilfenahme eines kinetischen Mehrschichtenmodells der Oberflächen- und Kernmaterialchemie beschrieben und erklärt werden. Die Reaktionsraten der beiden Prozesse reagierten feinfühlig auf einen Anstieg der O_3 -Konzentration, waren aber nahezu unempfindlich gegenüber Veränderungen in der umgebenden NO_2 -Konzentration.
3. Freisetzung von freien Aminosäuren als Folge der Oxidation von Peptiden und Proteinen durch Hydroxylradikale. Die Oxidationsprodukte von Proteinen und Peptiden, die durch Hydroxylradikale aus der Fenton-Reaktion entstanden sind, wurden mittels HPLC-MS/MS und HPLC-DAD-FLD analysiert. Freie Aminosäuren wurden durch HPLC-MS/MS-Analyse als Produkte identifiziert. Darüber hinaus wurde eine seitenselektive Bildung von freien Aminosäuren beobachtet, die durch einen Reaktionsweg erklärt werden könnte, der Stickstoff-zentrierte Radikale beinhaltet. Die molaren Ausbeuten für Oxidationsreaktionen waren wesentlich größer für Glycin (Gly, ~32-55 % für BSA, ~10-21 % für Ovalbumin (OVA)) als für andere identifizierte Aminosäuren (z.B. Alanin, Asparaginsäure, und

Asparagin; ~5-12 % für BSA, ~4-6 % für OVA). Bei der Oxidation von Tripeptiden mit Gly in C-terminaler, zentraler oder N-terminaler Position wurde Gly bevorzugt freigesetzt, wenn es sich zuvor am C-terminalen Ende befand.

Die in dieser Arbeit entwickelten Methoden, sowie die untersuchten Reaktionsprodukte, Mechanismen und Kinetik bieten eine Grundlage für weitere Untersuchungen der atmosphärischen Proteinchemie mit Luftschadstoffen. Sie sollen helfen, die Beziehungen zwischen durch Luftschadstoffe modifizierten Aeroallergenen und ihrer verstärkten Allergenität besser zu verstehen.

Contents

1. Introduction.....	1
1.1. Health and Climate Effects of Airborne Proteins	1
1.2. Atmospheric Chemistry of Proteins	2
1.2.1. Protein Nitration and Cross-Linking by Ozone and Nitrogen Dioxide	3
1.2.2. Protein Oxidation by Hydroxyl Radicals	5
1.3. Objectives	7
2. Results and Conclusions	8
2.1. Overview	8
2.2. Analytical Method Development	8
2.2.1. Metaproteomic Analysis of Atmospheric Aerosol Samples	8
2.2.2. Simultaneous Determination of Nitrated and Oligomerized Proteins.....	9
2.3. Protein Chemistry Induced by Reactive Oxygen Species.....	9
2.3.1. Protein Cross-Linking through Dityrosine Formation upon Exposure to Ozone .	9
2.3.2. Protein Nitration and Cross-Linking upon Exposure to Ozone and Nitrogen Dioxide	10
2.3.3. Release of Free Amino Acids upon Oxidation of Peptides and Proteins by Hydroxyl Radicals.....	10
2.4. Summary and Outlook	11
3. Bibliography	12
Appendix A. Personal List of Publications.....	17
Appendix B. Selected Publications.....	19
B.1. Liu et al., Anal. Bioanal. Chem., 2016	20
B.2. Liu et al., J. Chromatogr. A., 2017	46
B.3. Kampf et al., Environ. Sci. Technol., 2015	68
B.4. Liu et al., Farad. Discuss., 2017	82
B.5. Liu et al., Anal. Bioanal. Chem., 2017	97
Curriculum Vitae	xii

1. Introduction

1.1. Health and Climate Effects of Airborne Proteins

Primary biological aerosols, in short bioaerosols, play a vital role in the Earth system, climate and health (Després et al., 2012; Fröhlich-Nowoisky et al., 2016; Estillore et al., 2016; Pöschl and Shiraiwa, 2015). Primary biological aerosol particles (PBAPs) comprise bacteria, fungal spores, pollens, biogenic polymers, and others like plant or animal fragments. Proteins are a major component of PBAPs that can influence aerosol-cloud interactions and public health (Lang-Yona et al., 2016; D'amato et al., 2007; Pummer et al., 2015; Pöschl et al., 2010).

The adverse health effects caused by airborne proteins comprise allergies and associated respiratory diseases, which are mainly caused by allergenic proteins. Allergies pose an important concern for human health. The prevalence of allergic diseases has been increasing worldwide over the past few decades (Asher et al., 2006). A common type of allergy is mediated by the production of specific IgE antibodies against harmless proteins, the so called allergens. Important sources of aeroallergens are wind-dispersed pollen from trees, grasses, and weeds, fungal spores and hyphae, animal dander, and house-dust mite excretions (Buters et al., 2015; Twaroch et al., 2015; Fröhlich-Nowoisky et al., 2016).

The abundance and properties of aeroallergens can be influenced by air pollution and changes in climate (Reinmuth-Selzle et al., 2017). Increasing temperatures and higher carbon dioxide (CO₂) concentrations have been found to affect pollen production and the length of the pollination period, spore numbers, and allergen production of pollen and spores (Lang-Yona et al., 2013; Reid and Gamble, 2009; Reinmuth-Selzle et al., 2017). Air pollutants such as nitrogen oxides (NO, NO₂, etc.), sulfur dioxide (SO₂), and ozone (O₃) can also interact with pollen and fungal spores, damaging their envelopes and facilitating the release of allergens into polluted environments (Ouyang et al., 2016; Beck et al., 2013). On the other hand, exposure of aeroallergens to air pollutants may modify their allergenic potential, e.g., by changing their IgE binding capacity (Franze et al., 2005; Gruijthuijsen et al., 2006). Several studies have found an enhanced allergenicity of aeroallergens, such as birch pollen, ragweed pollen and *Aspergillus* spores, after their exposure to air pollutants (e.g., O₃ and NO₂) (Lang-Yona et al., 2016; Reinmuth-Selzle et al., 2014; Zhao et al., 2016). Such changes of allergenic properties may result from chemical modifications of allergens like nitration and cross-linking, induced by atmospheric oxidants. Gruijthuijsen et al. (2006) showed that the nitrated major birch pollen allergen Bet v 1a resulted in enhanced levels of specific IgE in murine models, possibly due to the formation of neoepitopes. Nitration of Bet v 1a also resulted in enhanced presentation of

allergen-derived peptides by antigen presenting cells (APC) (Karle et al., 2012). Moreover, oligomers and aggregates of certain allergenic proteins were found to enhance immune responses compared to the monomeric form (Vrtala et al., 2011; Rouvinen et al., 2010).

Proteinaceous matter in aerosol particles (e.g., proteins, protein fragments, free amino acids) also play an important role in cloud formation and precipitation. Steiner et al. (2015) found that the submicron pollen particles (SPP) released from pollen grains under humid conditions can act as cloud condensation nuclei (CCN). The composition analysis indicated that SPP mainly contains carbohydrates and proteins. Mikhailov et al. (2004) showed that in aerosol particles composed of proteins and salts, proteins were enriched at the surface and formed an envelope. This envelope inhibits the ability of water vapor to reach the particle core and leads to kinetic limitations of hygroscopic growth, phase transitions, and microstructural rearrangement processes. Other proteinaceous matter, like amino acids and other amine compounds, have been suggested to affect the atmospheric water cycle and the atmospheric radiation balance (Zhang and Anastasio, 2003; Qiu and Zhang, 2013).

The role of proteins in the ability of PBAPs to serve as ice nuclei (IN) is a topic of increasing interest (Hill et al., 2014; O'Sullivan et al., 2016). It has been shown that many bacteria are IN-active because they possess an IN-active protein in the outer cell wall, which has structural similarities to the crystal lattice of ice (Hoose and Möhler, 2012). In general, only certain sections on the surface of an IN particle participates in ice nucleation--so called active sites. Biological macromolecules can become INs by themselves (Pummer et al., 2015). Proteins, saccharides, and lipids may play a role as ice nucleating macromolecules (INMs), depending on their properties such as size, composition and heat tolerance (Hoose and Möhler, 2012; Pummer et al., 2015). It has been shown that the INMs of certain bacterial and fungal species are proteins, while polysaccharides are suggested to be the INMs of birch pollen (Hill et al., 2014; Pummer et al., 2015; Murray et al., 2015). However, the characteristic structures of INMs, which are responsible for the IN activity, are subject of ongoing scientific research and discussions.

1.2. Atmospheric Chemistry of Proteins

Fig.1 schematically summarizes the chemical reactions of proteins with atmospheric oxidants. Atmospheric protein chemistry induced by ambient reactive oxygen species (ROS) and reactive nitrogen species (RNS) mainly includes oxidation, nitration, cross-linking, and degradation of proteins. These modifications can lead to changes in the structure of protein

macromolecules, and affect protein stability and other properties such as hydrophobicity and acidity of binding sites (Reinmuth-Selzle et al., 2017). Such transformations may affect the allergenic potential of aeroallergens, the role of proteins (or proteinaceous matter) involved in the CCN activity of atmospheric particles, and the ability of proteins to act as IN. Thus, it is important to elucidate the mechanisms and kinetics of protein chemistry induced by atmospheric ROS/RNS.

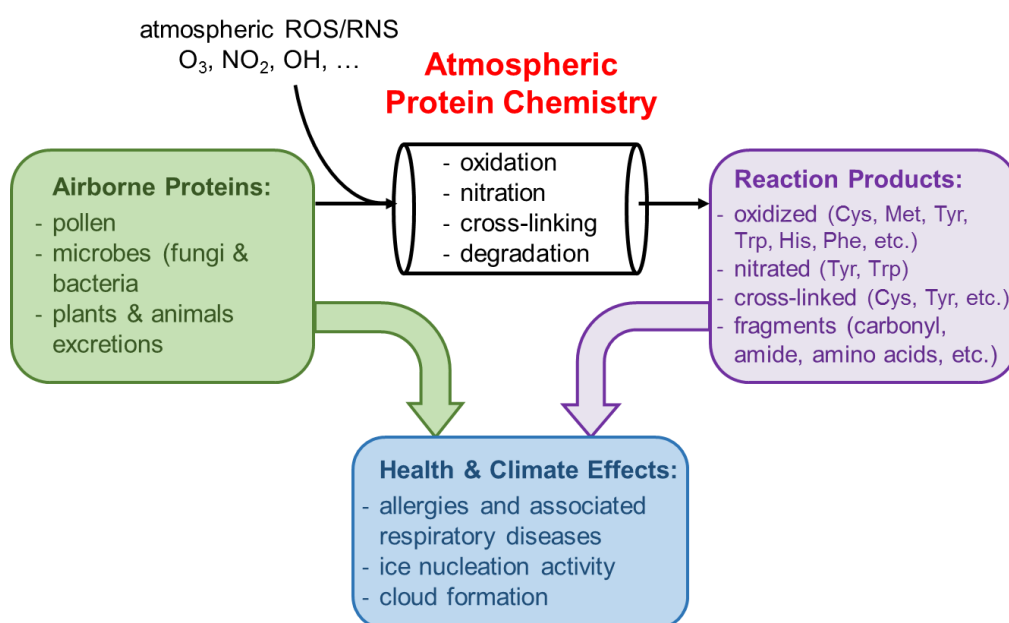


Fig.1 Proteins in the atmosphere: airborne proteins transported in the atmosphere by aerosols of biological origin may affect public health and climate; they may also undergo heterogeneous reactions with atmospheric ROS/RNS leading to complex products and altering their health and climate effects.

1.2.1. Protein Nitration and Cross-Linking by Ozone and Nitrogen Dioxide

Previous studies have investigated the general mechanisms and kinetics of protein nitration upon exposure to O₃ and NO₂ (Shiraiwa et al., 2012; Reinmuth-Selzle et al., 2014; Sandhiya et al., 2014). Reactions of proteins with O₃ and NO₂ mainly lead to the nitration of the aromatic amino acid tyrosine (Tyr) forming 3-nitrotyrosine (NTyr). Shiraiwa et al. (2012) proposed that the reactions follow a two-step mechanism involving the formation of long-lived reactive oxygen intermediates (ROIs) by the reaction of O₃ with protein Tyr residues, likely tyrosyl radicals, and followed by the nitration via exposure to NO₂. Kinetic experiments and modeling showed that the reaction rates are limited by the phase state of proteins and the diffusivity of

oxidants and proteins, which change with relative humidity (RH) and temperature (T) (Reinmuth-Selzle et al., 2014; Sandhiya et al., 2014).

Product analysis by mass spectrometry found that the nitration is site selective, depending on the nitrating agents, reaction conditions, and molecular structures of proteins (primary, secondary and tertiary structures) (Abello et al., 2009; Zhang et al., 2011; Reinmuth-Selzle et al., 2014). Those Tyr residues found to be efficiently nitrated usually have a high solvent accessibility, are located in loop or α -helix secondary structures, and/or within a hydrophobic environment. Upon exposure of Bet v 1a to O₃/NO₂, NTyr residues were mainly identified in the C-terminal helix and in the hydrophobic cavity, which are both key positions for the binding of specific IgE as well as ligands like fatty acids, cytokines, and flavonoids (Reinmuth-Selzle et al., 2017).

In addition to nitration, tyrosyl radicals can also undergo cross-linking to form dityrosine (DTyr) derivatives. It has been demonstrated that O₃ can induce protein cross-linking in solution via the formation of DTyr species (Verweij et al., 1982). Shiraiwa et al. (2012) showed mass spectra of dimeric protein species after the exposure of aerosolized proteins to O₃, and suggested that the ROIs reacted with each other to form protein dimers. However, investigations of the kinetics and chemical mechanisms of protein oligomerization processes at atmospherically relevant concentrations of O₃ are limited.

Under physiological conditions, Pfeiffer et al. (2000) found that DTyr was a major product of Tyr modification caused by low steady-state concentrations of peroxyxynitrite, while high fluxes ($> 2 \mu\text{M s}^{-1}$) of nitrogen oxide/superoxide anion (NO/O₂⁻) are required to render peroxyxynitrite an efficient trigger of Tyr nitration. The mechanism for peroxyxynitrite-mediated Tyr modification also involves the generation of tyrosyl radicals. Thus, a kinetic competition between Tyr nitration and dimerization (or oligomerization) upon protein exposure to O₃ and NO₂ can be expected, which needs to be explored in detail to assess relevant atmospheric conditions favoring the one or the other protein modification.

The levels of DTyr in proteins have been quantified in numerous studies based on the intrinsic fluorescence properties of DTyr (DiMarco and Giulivi, 2007; Malencik et al., 1996). However, the sites for Tyr cross-linking might differ from the sites for Tyr nitration, as the nitration involves one more site-selective reaction step than the pure ozonolysis. Also, the effect of steric hindrance for Tyr cross-linking is likely more important than for Tyr nitration (Heijnis et al., 2010).

Thus, to explicitly explore the kinetics and competition between Tyr nitration and cross-linking, together with the quantification of oligomeric species, studies should consider the mass spectrometric identification of DTyr as well as NTyr modification sites in proteins. However, the identification of DTyr cross-linked peptides is challenging because of their complex fragmentation patterns and a lack of bioinformatics tools for the localization of cross-linked residues. In a recent study, the fragmentation characteristics of known DTyr-linked peptides were studied, which enabled identification of the cross-linked positions and provided generic rules to identify these oxidative modifications in the oxidized human serum albumin (Annibal et al., 2016). This strategy may also be applied to other proteins for identifying DTyr cross-linked sites.

Apart from Tyr, O₃ can also react with other amino acids, i.e., cysteine (Cys), tryptophan (Trp), methionine (Met), phenylalanine (Phe) and histidine (His). The oxidation of Cys induced by O₃ could also form protein oligomers via intermolecular disulfide cross-linking, while the ozonolysis of Trp, Met, Phe and His doesn't contribute to the formation of oligomer species (Sharma and Graham, 2010). The reactivity order for the O₃-mediated oxidation of amino acids at neutral pH is: Cys > Trp > Met > Tyr > Phe ≈ His (Sharma and Graham, 2010; Pryor and Uppu, 1993). But a pH dependency for the reactivity is also observed; at pH < 4: Trp > Met > Cys > Tyr > all others (including Phe and His) (Pryor and Uppu, 1993). It should be noted that the reactivity order of amino acids in peptides and/or proteins might differ from that of free amino acids, probably owing to micro-structural and steric effects (Kotiaho et al., 2000). These findings indicate that the reaction system between proteins and O₃/NO₂ is complex with multiple reaction pathways and products. Thus, robust and state-of-the-art analytical techniques are needed for the quantification of reaction products and identification of the site-selectivity of protein modifications by O₃/NO₂. For kinetic studies and modelling, a holistic and flexible chemical mechanism may improve its applicability towards the complex reaction system.

1.2.2. Protein Oxidation by Hydroxyl Radicals

The hydroxyl radical, OH, plays a key role in the atmosphere as well as in biological systems because of its very high reactivity (Pöschl and Shiraiwa, 2015). It exhibits a very short lifetime (less than one second) and low mixing ratio (sub-ppt, i.e., < pmol mol⁻¹) in the lower troposphere. The major sources of OH in the lower troposphere include the photolysis of O₃, NO₂, nitric acids (HONO), etc. (Gligorovski et al., 2015). In biological systems, OH can be

generated endogenously and exogenously, and the sources include a variety of different processes such as cellular metabolic processes, radiolysis, photolysis, and Fenton chemistry (Watson et al., 2009; Apel and Hirt, 2004; Doan et al., 2010; Xu and Chance, 2007).

The mechanism and kinetics of the OH-mediated oxidation of amino acids, peptides, and proteins in aqueous solutions or under physiologically relevant conditions have been extensively studied over the past few decades (Xu and Chance, 2007; Davies, 2005). The oxidation products (i.e., carbonylated products) are commonly used as markers of protein damage (Davies, 2016). The OH radicals have a high reactivity with all amino acid residues, with rate constants $> 10^{-14} \text{ cm}^3 \text{ s}^{-1}$ (Sharma and Rokita, 2012). With respect to the peptide backbone cleavage induced by OH, the main reaction pathway is initiated by an H-abstraction at the α -carbon positions of the protein backbone. This is followed by a reaction with O_2 to produce a peroxy radical, which ultimately results in fragmentation and cleavage of the backbone of the protein, thereby mainly forming amide and carbonyl fragments (Xu and Chance, 2007). The high reactivity of proteins with OH radicals, however, may result in various products due to different reaction pathways. Further studies quantifying specific (and/or various) oxidation products are required to fully elucidate the mechanisms and kinetics of OH-mediated protein oxidation (Morgan et al., 2012).

The oxidation of airborne proteins induced by OH under atmospherically relevant conditions (e.g., heterogeneous reactions at different relative humidities), to the author's knowledge, have not yet been well investigated. The reaction mechanisms of airborne proteins with OH are expected to be similar to that in aqueous media or under physiological conditions. The degradation products might play an important role in the abundance of atmospheric amine, amide and carbonyl compounds (Qiu and Zhang, 2013). These compounds, (e.g. amines) are involved in the nucleation and growth of nanoparticles, which contribute to climate change (Ge et al., 2011; Qiu and Zhang, 2013). So far, the contribution of protein oxidation/degradation on the abundance of atmospheric amines and amino compounds is still largely unknown. This timely topic is highly interesting and should be investigated in future studies.

1.3. Objectives

Airborne proteins, originating from various biological species with different properties, may undergo physical and chemical transformation processes upon interaction with air pollutants, and thus affect the climate system and human health. The aims of this PhD work were to develop methods for the characterization of aerosol proteins, and to elucidate the reaction products, mechanisms and kinetics of proteins reacting with air pollutants, in order to provide insights into the impact of airborne proteins on climate and human health. The specific objectives of the PhD work can be summarized as follows:

1. Develop a method to characterize proteins from atmospheric aerosol samples using a mass spectrometry-based metaproteomics approach, providing information about the taxonomic composition of bioaerosols.
2. Develop a method to enable a simultaneous detection of mono-, di-, tri-, and higher protein oligomers, as well as their individual nitration degrees.
3. Investigate the formation of oligomers of proteins upon their exposure to atmospherically relevant concentrations of O₃, and study the mechanisms and kinetics of protein oligomerization under varying environmental conditions.
4. Elucidate the oxidation, nitration and oligomerization reactions of proteins induced by O₃ and NO₂, and their predominance under different atmospherically-relevant conditions.
5. Identify and quantify amino acids as oxidation products of proteins and peptides generated by hydroxyl radicals from the Fenton reaction.

2. Results and Conclusions

2.1. Overview

The results of this PhD research are described in five manuscripts for publication in peer-reviewed scientific journals (four first-author and one co-first-author papers). The manuscripts are attached in Appendix B. All of them have been accepted for publication. The PhD research focused on the development of analytical methods and their application in the identification of proteins in atmospheric aerosol samples, as well as products and mechanisms studies of protein modification induced by air pollutants or ROS. An overview of the studies is shown in Fig.2, and summaries of the individual studies are included below.

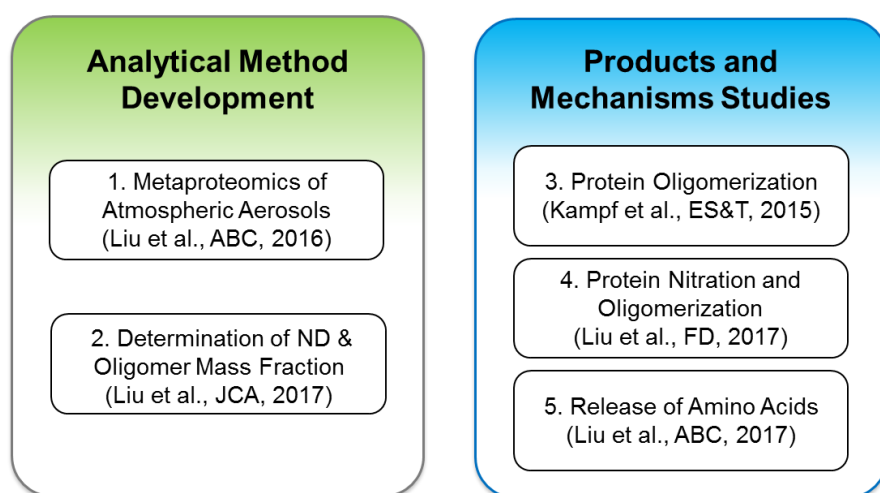


Fig.2 Individual studies of the PhD research in two core areas: 1) analytical method development, and 2) products and mechanisms studies. The analytical techniques applied for method development and products analysis mainly include: mass spectrometry (quadrupole time-of-flight, orbitrap), high performance liquid chromatography (size exclusion and reversed phase chromatography), spectrophotometry (UV-Vis, fluorescence), gel electrophoresis (SDS-PAGE) and protein quantification assay (bicinchoninic acid assay). For kinetic and mechanistic studies (sub-projects 3 and 4), two kinetic models, i.e., a box model for homogeneous reactions and kinetic multilayer model for aerosol surface and bulk chemistry (KM-SUB) (Shiraiwa et al., 2010) are also introduced for data interpretation in cooperation with modeling partners.

2.2. Analytical Method Development

2.2.1. Metaproteomic Analysis of Atmospheric Aerosol Samples

This study presents an efficient method for the extraction and analysis of proteins from glass fiber filter samples of airborne particulate matter. Extraction solvents were optimized to

overcome the interaction between proteins and filter material and achieve high protein recoveries. The metaproteomic analysis allows a profiling of proteins in atmospheric aerosols. Proteins in airborne particulate matter were found to mainly originate from plants, microorganisms, and animals, which is in line with the major categories of PBAPs. Allergenic pollen proteins, e.g., from perennial ryegrass, were found in fine particles, which can penetrate deep into the lower part of the respiratory tract. In addition, the molecular size dependent analysis of proteins extracted from the aerosol samples revealed the presence of fragmented proteins in atmospheric aerosol sample extracts.

For details see Appendix B.1, Liu et al., *Anal. Bioanal. Chem.*, 2016.

2.2.2. Simultaneous Determination of Nitrated and Oligomerized Proteins

A size exclusion high performance liquid chromatography coupled to photodiode array detection (SEC-HPLC-DAD) method was developed that enables a simultaneous detection of mono-, di-, tri-, and higher protein oligomers, as well as their individual nitration degrees (NDs). The validation of the results showed a good agreement between this new method and a well-established method. Importantly, the NDs for individual oligomer fractions can be obtained from the new method. Overall, the new method provides a single run analysis for the determination of NDs and oligomer mass fractions, reducing analysis time and sample consumption. The new method has been successfully applied in Liu et al., *Farad. Discuss.*, 2017 for the investigation of reaction kinetics and mechanisms of protein tyrosine nitration and cross-linking by O₃/NO₂.

For details see Appendix B.2, Liu et al., *J. Chromatogr. A.*, accepted.

2.3. Protein Chemistry Induced by Reactive Oxygen Species

2.3.1. Protein Cross-Linking through Dityrosine Formation upon Exposure to Ozone

The chemical mechanism and kinetics of protein oligomerization upon exposure to atmospherically relevant concentrations of O₃ was studied in coated-wall flow-tube and bulk-solution experiments, using bovine serum albumin as a model protein. The formation of protein dimers, trimers, and higher oligomers was observed. The cross-linking was attributed to the formation of intermolecular DTyr cross-links, which was demonstrated by SDS-PAGE and fluorescence analysis. The oligomerization proceeds fast on the surface of protein films, while the bulk oligomerization, characterized by limited diffusion of O₃ and protein molecules, occurred at much slower rates. From the experimental data, a chemical mechanism and rate

equations were derived for a kinetic multi-layer model of surface and bulk reaction, thus enabling a prediction of oligomer formation under atmospherically relevant conditions.

For details see Appendix B.3, Kampf et al., *Environ. Sci. Technol.*, 2015.

2.3.2. Protein Nitration and Cross-Linking upon Exposure to Ozone and Nitrogen Dioxide

The chemical kinetics and mechanisms of protein tyrosine nitration and oligomerization upon simultaneous exposure of O₃ and NO₂ were investigated in coated-wall flow-tube and bulk-solution experiments under atmospherically relevant conditions, using bovine serum albumin as a model protein. Tyrosine residues were more prone to react via nitration pathways than via oligomerization pathways. The extent of nitration and oligomerization strongly depended on the phase state of proteins (i.e., amorphous solid, semi-solid, liquid), which changes with relative humidity. Dimeric and nitrated species were the major products in the liquid phase, while protein oligomers became the dominant oligomerization products at solid and semi-solid protein states. From the experimental and kinetic modelling results, the rates of both processes were found to be sensitive to ambient O₃ concentrations, but rather insensitive to different NO₂ levels.

For details see Appendix B.4, Liu et al., *Farad. Discuss.*, accepted.

2.3.3. Release of Free Amino Acids upon Oxidation of Peptides and Proteins by Hydroxyl Radicals

The oxidation products of proteins and peptides generated by OH from Fenton reactions were analyzed by HPLC tandem mass spectrometry (HPLC-MS/MS) and by HPLC with diode array detection and fluorescence detection (HPLC-DAD-FLD). Free amino acids were identified as products in the OH-induced oxidation of proteins and peptides by HPLC-MS/MS analysis. For protein oxidation reactions, the molar yields of glycine were substantially higher than for the other identified amino acids (i.e., alanine, aspartic acid, and asparagine). Upon oxidation of tripeptides with known amino acid compositions, the molar yields of individual amino acids strongly depended on the sequence of amino acids, as well as the reactivity of amino acid residues with OH.

For details see Appendix B.5, Liu et al., *Anal. Bioanal. Chem.*, 2017.

2.4. Summary and Outlook

Understanding the role of airborne proteins in human health and climate requires the characterization of proteins from atmospheric aerosols and the elucidation of the reaction mechanisms and kinetics of atmospheric protein chemistry. This PhD research established a mass spectrometric approach for the identification of proteins in atmospheric aerosol samples, and also elucidated the reaction products, mechanisms, and kinetics of protein modification induced by atmospheric ROS.

The metaproteomic analysis presented in this PhD research provides a tool for further studies of spatiotemporal variability of bioparticles and allergens in airborne particulate matter. The development of an efficient method for the simultaneous determination of protein nitration degrees and oligomer mass fractions will facilitate further kinetic and mechanistic studies of protein nitration and cross-linking, particularly for allergenic proteins, which are generally expensive and available only in small quantities.

The kinetic and mechanistic insights of atmospheric protein chemistry with air pollutants show that the reactions are highly complex and yield a variety of products including nitrated, oxidized, oligomerized, and degraded proteins. Hence, further investigations are recommended on the allergenic and immunogenic effects induced by chemically-modified aeroallergens. Of particular interest are nitrated and oligomerized proteins, which are believed to have enhanced allergenicity. In terms of the climate effects caused by airborne proteins, future challenges include the investigations of the ice nucleation activity and the hygroscopicity (etc.) of air pollutant-modified (aged) proteins.

3. Bibliography

- Abello, N., Kerstjens, H. A., Postma, D. S., and Bischoff, R.: Protein tyrosine nitration: selectivity, physicochemical and biological consequences, denitration, and proteomics methods for the identification of tyrosine-nitrated proteins, *Journal of proteome research*, 8, 3222-3238, 2009.
- Annibal, A., Colombo, G., Milzani, A., Dalle-Donne, I., Fedorova, M., and Hoffmann, R.: Identification of dityrosine cross-linked sites in oxidized human serum albumin, *Journal of Chromatography B*, 1019, 147-155, 2016.
- Apel, K., and Hirt, H.: Reactive oxygen species: metabolism, oxidative stress, and signal transduction, *Annual Review of Plant Biology*, 55, 373-399, 2004.
- Asher, M. I., Montefort, S., Björkstén, B., Lai, C. K., Strachan, D. P., Weiland, S. K., Williams, H., and Group, I. P. T. S.: Worldwide time trends in the prevalence of symptoms of asthma, allergic rhinoconjunctivitis, and eczema in childhood: ISAAC Phases One and Three repeat multicountry cross-sectional surveys, *The Lancet*, 368, 733-743, 2006.
- Beck, I., Jochner, S., Gilles, S., McIntyre, M., Buters, J. T., Schmidt-Weber, C., Behrendt, H., Ring, J., Menzel, A., and Traidl-Hoffmann, C.: High environmental ozone levels lead to enhanced allergenicity of birch pollen, *PLoS One*, 8, e80147, 2013.
- Buters, J., Prank, M., Sofiev, M., Pusch, G., Albertini, R., Annesi-Maesano, I., Antunes, C., Behrendt, H., Berger, U., and Brandao, R.: Variation of the group 5 grass pollen allergen content of airborne pollen in relation to geographic location and time in season, *Journal of Allergy and Clinical Immunology*, 136, 87-95. e86, 2015.
- D'amato, G., Cecchi, L., Bonini, S., Nunes, C., Annesi-Maesano, I., Behrendt, H., Liccardi, G., Popov, T., and Van Cauwenberge, P.: Allergenic pollen and pollen allergy in Europe, *Allergy*, 62, 976-990, 2007.
- Davies, M. J.: The oxidative environment and protein damage, *Biochimica et Biophysica Acta (BBA)-Proteins and Proteomics*, 1703, 93-109, 2005.
- Davies, M. J.: Protein oxidation and peroxidation, *Biochemical Journal*, 473, 805-825, 2016.
- Després, V. R., Huffman, J. A., Burrows, S. M., Hoose, C., Safatov, A. S., Buryak, G., Fröhlich-Nowoisky, J., Elbert, W., Andreae, M. O., and Pöschl, U.: Primary biological aerosol particles in the atmosphere: a review, *Tellus B*, 64, 2012.
- DiMarco, T., and Giulivi, C.: Current analytical methods for the detection of dityrosine, a biomarker of oxidative stress, in biological samples, *Mass spectrometry reviews*, 26, 108-120, 2007.
- Doan, H. Q., Davis, A. C., and Francisco, J. S.: Primary Steps in the Reaction of OH Radicals with Peptide Systems: Perspective from a Study of Model Amides, *The Journal of Physical Chemistry A*, 114, 5342-5357, 2010.

- Estillore, A. D., Trueblood, J. V., and Grassian, V. H.: Atmospheric chemistry of bioaerosols: heterogeneous and multiphase reactions with atmospheric oxidants and other trace gases, *Chemical Science*, 7, 6604-6616, 2016.
- Franze, T., Weller, M. G., Niessner, R., and Pöschl, U.: Protein nitration by polluted air, *Environmental science & technology*, 39, 1673-1678, 2005.
- Fröhlich-Nowoisky, J., Kampf, C. J., Weber, B., Huffman, J. A., Pöhlker, C., Andreae, M. O., Lang-Yona, N., Burrows, S. M., Gunthe, S. S., and Elbert, W.: Bioaerosols in the Earth system: Climate, health, and ecosystem interactions, *Atmospheric Research*, 182, 346-376, 2016.
- Ge, X., Wexler, A. S., and Clegg, S. L.: Atmospheric amines—Part I. A review, *Atmospheric Environment*, 45, 524-546, 2011.
- Gligorovski, S., Streckowski, R., Barbati, S., and Vione, D.: Environmental implications of hydroxyl radicals ($\cdot\text{OH}$), *Chemical reviews*, 115, 13051-13092, 2015.
- Grujthuisen, Y., Grieshuber, I., Stöcklinger, A., Tischler, U., Fehrenbach, T., Weller, M., Vogel, L., Vieths, S., Pöschl, U., and Duschl, A.: Nitration enhances the allergenic potential of proteins, *International archives of allergy and immunology*, 141, 265-275, 2006.
- Heijnis, W. H., Dekker, H. L., de Koning, L. J., Wierenga, P. A., Westphal, A. H., de Koster, C. G., Gruppen, H., and van Berkel, W. J.: Identification of the peroxidase-generated intermolecular dityrosine cross-link in bovine α -lactalbumin, *Journal of agricultural and food chemistry*, 59, 444-449, 2010.
- Hill, T. C., Moffett, B. F., DeMott, P. J., Georgakopoulos, D. G., Stump, W. L., and Franc, G. D.: Measurement of ice nucleation-active bacteria on plants and in precipitation by quantitative PCR, *Applied and environmental microbiology*, 80, 1256-1267, 2014.
- Hoose, C., and Möhler, O.: Heterogeneous ice nucleation on atmospheric aerosols: a review of results from laboratory experiments, *Atmos. Chem. Phys.*, 12, 9817-9854, 2012.
- Karle, A. C., Oostingh, G. J., Mutschlechner, S., Ferreira, F., Lackner, P., Bohle, B., Fischer, G. F., Vogt, A. B., and Duschl, A.: Nitration of the pollen allergen bet v 1.0101 enhances the presentation of bet v 1-derived peptides by HLA-DR on human dendritic cells, *PLoS One*, 7, e31483, 2012.
- Kotiaho, T., Eberlin, M. N., Vainiotalo, P., and Kostianen, R.: Electrospray mass and tandem mass spectrometry identification of ozone oxidation products of amino acids and small peptides, *Journal of the American Society for Mass Spectrometry*, 11, 526-535, 2000.
- Lang-Yona, N., Levin, Y., Dannemiller, K. C., Yarden, O., Peccia, J., and Rudich, Y.: Changes in atmospheric CO_2 influence the allergenicity of *Aspergillus fumigatus*, *Global change biology*, 19, 2381-2388, 2013.
- Lang-Yona, N., Shuster-Meiseles, T., Mazar, Y., Yarden, O., and Rudich, Y.: Impact of urban air pollution on the allergenicity of *Aspergillus fumigatus* conidia: Outdoor exposure study supported by laboratory experiments, *Science of the Total Environment*, 541, 365-371, 2016.

- Malencik, D. A., Sprouse, J. F., Swanson, C. A., and Anderson, S. R.: Dityrosine: preparation, isolation, and analysis, *Analytical biochemistry*, 242, 202-213, 1996.
- Mikhailov, E., Vlasenko, S., Niessner, R., and Pöschl, U.: Interaction of aerosol particles composed of protein and salt with water vapor: hygroscopic growth and microstructural rearrangement, *Atmospheric Chemistry and Physics*, 4, 323-350, 2004.
- Morgan, P. E., Pattison, D. I., and Davies, M. J.: Quantification of hydroxyl radical-derived oxidation products in peptides containing glycine, alanine, valine, and proline, *Free Radical Biology and Medicine*, 52, 328-339, 2012.
- Murray, B., Ross, J., Whale, T., Price, H., Atkinson, J., Umo, N., and Webb, M.: The relevance of nanoscale biological fragments for ice nucleation in clouds, *Scientific reports*, 5, 8082, 2015.
- O'Sullivan, D., Murray, B. J., Ross, J. F., and Webb, M. E.: The adsorption of fungal ice-nucleating proteins on mineral dusts: a terrestrial reservoir of atmospheric ice-nucleating particles, *Atmospheric Chemistry and Physics*, 16, 7879-7887, 2016.
- Ouyang, Y., Xu, Z., Fan, E., Li, Y., and Zhang, L.: Effect of nitrogen dioxide and sulfur dioxide on viability and morphology of oak pollen, *International forum of allergy & rhinology*, 2016, 95-100.
- Pfeiffer, S., Schmidt, K., and Mayer, B.: Dityrosine Formation Outcompetes Tyrosine Nitration at Low Steady-state Concentrations of Peroxynitrite IMPLICATIONS FOR TYROSINE MODIFICATION BY NITRIC OXIDE/SUPEROXIDE IN VIVO, *Journal of Biological Chemistry*, 275, 6346-6352, 2000.
- Pöschl, U., Martin, S., Sinha, B., Chen, Q., Gunthe, S., Huffman, J., Borrmann, S., Farmer, D., Garland, R., Helas, G., Jimenez, J., King, S., Manzi, A., Mikhailov, E., Pauliquevis, T., Petters, M., Prenni, A., Roldin, P., Rose, D., Schneider, J., Su, H., Zorn, S., Artaxo, P., and Andreae, M. O.: Rainforest aerosols as biogenic nuclei of clouds and precipitation in the Amazon, *Science*, 329, 1513-1516, 2010.
- Pöschl, U., and Shiraiwa, M.: Multiphase chemistry at the atmosphere–biosphere interface influencing climate and public health in the Anthropocene, *Chemical reviews*, 115, 4440-4475, 2015.
- Pryor, W., and Uppu, R.: A kinetic model for the competitive reactions of ozone with amino acid residues in proteins in reverse micelles, *Journal of Biological Chemistry*, 268, 3120-3126, 1993.
- Pummer, B., Budke, C., Augustin-Bauditz, S., Niedermeier, D., Felgitsch, L., Kampf, C., Huber, R., Liedl, K., Loerting, T., and Moschen, T.: Ice nucleation by water-soluble macromolecules, *Atmospheric Chemistry and Physics*, 15, 4077-4091, 2015.
- Qiu, C., and Zhang, R.: Multiphase chemistry of atmospheric amines, *Physical Chemistry Chemical Physics*, 15, 5738-5752, 2013.
- Reid, C. E., and Gamble, J. L.: Aeroallergens, allergic disease, and climate change: impacts and adaptation, *Ecohealth*, 6, 458-470, 2009.

- Reinmuth-Selzle, K., Ackaert, C., Kampf, C. J., Samonig, M., Shiraiwa, M., Kofler, S., Yang, H., Gadermaier, G., Brandstetter, H., and Huber, C. G., Duschl, A., Oostingh, G.J., Pöschl U.: Nitration of the birch pollen allergen Bet v 1.0101: efficiency and site-selectivity of liquid and gaseous nitrating agents, *Journal of proteome research*, 13, 1570-1577, 2014.
- Reinmuth-Selzle, K., Kampf, C. J., Lucas, K., Lang-Yona, N., Fröhlich-Nowoisky, J., Shiraiwa, M., Lakey, P. S. J., Lai, S., Liu, F., Kunert, A. T., Ziegler, K., Shen, F., Sgarbanti, R., Weber, B., Weller, M. G., Bellinghausen, I., Saloga, J., Duschl, A., Delfef, S., and Pöschl, U.: Air pollution and climate change effects on allergies in the Anthropocene, *submitted to Environmental science & technology*, 2017.
- Rouvinen, J., Jänis, J., Laukkanen, M.-L., Jylhä, S., Niemi, M., Päivinen, T., Mäkinen-Kiljunen, S., Haahtela, T., Söderlund, H., and Takkinen, K.: Transient dimers of allergens, *PLoS One*, 5, e9037, 2010.
- Sandhiya, L., Kolandaivel, P., and Senthilkumar, K.: Oxidation and Nitration of Tyrosine by Ozone and Nitrogen Dioxide: Reaction Mechanisms and Biological and Atmospheric Implications, *The Journal of Physical Chemistry B*, 118, 3479-3490, 2014.
- Sharma, V. K., and Graham, N. J.: Oxidation of amino acids, peptides and proteins by ozone: a review, *Ozone: Science & Engineering*, 32, 81-90, 2010.
- Sharma, V. K., and Rokita, S. E.: Oxidation of Amino Acids, Peptides, and Proteins: Kinetics and Mechanism, John Wiley & Sons, 2012.
- Shiraiwa, M., Pfrang, C., and Pöschl, U.: Kinetic multi-layer model of aerosol surface and bulk chemistry (KM-SUB): the influence of interfacial transport and bulk diffusion on the oxidation of oleic acid by ozone, *Atmospheric Chemistry and Physics*, 10, 3673-3691, 2010.
- Shiraiwa, M., Selzle, K., Yang, H., Sosedova, Y., Ammann, M., and Pöschl, U.: Multiphase chemical kinetics of the nitration of aerosolized protein by ozone and nitrogen dioxide, *Environmental science & technology*, 46, 6672-6680, 2012.
- Steiner, A. L., Brooks, S. D., Deng, C., Thornton, D. C., Pendleton, M. W., and Bryant, V.: Pollen as atmospheric cloud condensation nuclei, *Geophysical Research Letters*, 42, 3596-3602, 2015.
- Twaroch, T. E., Curin, M., Valenta, R., and Swoboda, I.: Mold allergens in respiratory allergy: from structure to therapy, *Allergy, asthma & immunology research*, 7, 205-220, 2015.
- Verweij, H., Christianse, K., and Van Steveninck, J.: Ozone-induced formation of O, O'-dityrosine cross-links in proteins, *Biochimica et Biophysica Acta (BBA)-Protein Structure and Molecular Enzymology*, 701, 180-184, 1982.
- Vrtala, S., Fohr, M., Campana, R., Baumgartner, C., Valent, P., and Valenta, R.: Genetic engineering of trimers of hypoallergenic fragments of the major birch pollen allergen, Bet v 1, for allergy vaccination, *Vaccine*, 29, 2140-2148, 2011.
- Watson, C., Janik, I., Zhuang, T., Charvátová, O., Woods, R. J., and Sharp, J. S.: Pulsed electron beam water radiolysis for submicrosecond hydroxyl radical protein footprinting, *Analytical chemistry*, 81, 2496-2505, 2009.

- Xu, G., and Chance, M. R.: Hydroxyl radical-mediated modification of proteins as probes for structural proteomics, *Chemical reviews*, 107, 3514-3543, 2007.
- Zhang, Q., and Anastasio, C.: Free and combined amino compounds in atmospheric fine particles (PM_{2.5}) and fog waters from Northern California, *Atmospheric Environment*, 37, 2247-2258, 2003.
- Zhang, Y., Yang, H., and Pöschl, U.: Analysis of nitrated proteins and tryptic peptides by HPLC-chip-MS/MS: site-specific quantification, nitration degree, and reactivity of tyrosine residues, *Analytical and bioanalytical chemistry*, 399, 459-471, 2011.
- Zhao, F., Elkelish, A., Durner, J., Lindermayr, C., Winkler, J. B., Ruëff, F., Behrendt, H., Traidl-Hoffmann, C., Holzinger, A., and Kofler, W.: Common ragweed (*Ambrosia artemisiifolia* L.): allergenicity and molecular characterization of pollen after plant exposure to elevated NO₂, *Plant, cell & environment*, 39, 147-164, 2016.

Appendix A. Personal List of Publications

Journal Articles

1. Liu, F., Lakey, P. S. J., Berkemeier, T., Tong, H., Kunert, A.T., Meusel, H., Cheng, Y., Su, H., Fröhlich-Nowoisky, J., Shiraiwa, M., Lai, S., Weller, M. G., Pöschl, U., Kampf, C. J. “Atmospheric protein chemistry influenced by anthropogenic air pollutants: protein nitration and oligomerization upon exposure to ozone and nitrogen dioxide”, *Faraday Discussions*, *accepted*.
2. Liu, F., Reinmuth-Selzle, K., Lai, S., Weller, M. G., Pöschl, U., Kampf, C. J. “Simultaneous determination of nitrated and oligomerized proteins by size exclusion high performance liquid chromatography coupled to photodiode array detection”, *Journal of Chromatography A*, *accepted*.
3. Liu, F., Lai, S., Tong, H., Lakey, P. S. J., Shiraiwa, M., Weller, M. G., Pöschl, U., Kampf, C. J. “Release of free amino acids upon oxidation of peptides and proteins by hydroxyl radicals”, *Analytical and Bioanalytical Chemistry*. 2017; 1-10.
4. Reinmuth-Selzle, K., Kampf, C. J., Lucas, K., Lang-Yona, N., Fröhlich-Nowoisky, J., Shiraiwa, M., Lakey, P. S. J., Lai, S., Liu, F., Kunert, A.T., Ziegler, K., Shen, F., Sgarbanti, R., Weber, B., Weller, M. G., Bellinghausen, I., Saloga, J., Duschl, A., Schuppan, D., Pöschl, U. “Air pollution and climate change effects on allergies in the Anthropocene”, submitted to *Environmental science & technology*.
5. Liu, F., Lai, S., Reinmuth-Selzle, K., Scheel, J. F., Fröhlich-Nowoisky, J., Després, V. R., Hoffmann, T., Pöschl, U., Kampf, C. J. “Metaproteomic analysis of atmospheric aerosol samples” *Analytical and Bioanalytical Chemistry*. 2016; 408(23): 6337-48.
6. Zhao, Y., Zhang, Y., Fu, P., Ho, S. S., Ho, K. F., Liu, F., Zou, S., Wang, S., Lai, S. “Non-polar organic compounds in marine aerosols over the northern South China Sea: Influence of continental outflow” *Chemosphere*. 2016; 153: 332-9.
7. Tong, H., Arangio, A. M., Lakey, P. S. J., Berkemeier, T., Liu, F., Kampf, C. J., Brune, W. H., Pöschl, U., Shiraiwa, M. “Hydroxyl radicals from secondary organic aerosol decomposition in water” *Atmospheric Chemistry and Physics*. 2016; 16(3): 1761-71.
8. Kampf, C. J., Liu, F., Reinmuth-Selzle, K., Berkemeier, T., Meusel, H., Shiraiwa, M., Pöschl, U. “Protein cross-linking and oligomerization through dityrosine formation upon exposure to ozone” *Environmental science & technology*. 2015; 49(18): 10859-66.
9. Zhang, Y., Lai, S., Zhao, Z., Liu, F., Chen, H., Zou, S., Xie, Z., Ebinghaus, R. “Spatial distribution of perfluoroalkyl acids in the Pearl River of Southern China” *Chemosphere*. 2013; 93(8): 1519-25.
10. Liu, J., Li, J., Lin, T., Liu, D., Xu, Y., Chaemfa, C., Qi, S., Liu, F., Zhang, G. “Diurnal and nocturnal variations of PAHs in the Lhasa atmosphere, Tibetan Plateau: implication for

local sources and the impact of atmospheric degradation processing” *Atmospheric Research*. 2013; 93(8): 1519-25.

11. Liu, F., Xu, Y., Liu, J., Liu, D., Li, J., Zhang, G., Li, X., Zou, S., Lai, S. “Atmospheric deposition of polycyclic aromatic hydrocarbons (PAHs) to a coastal site of Hong Kong, South China” *Atmospheric Environment*. 2013; 69: 265-72.

Oral Presentations

1. Liu, F., Lai, S., Reinmuth-Selzle, K., Scheel, J. F., Fröhlich-Nowoisky, J., Després, V. R., Hoffmann, T., Pöschl, U., Kampf, C.J. Metaproteomic analysis of atmospheric aerosol samples, European Aerosol Conference, Tours, France, 4th - 9th Sep, 2016.
2. Liu, F., Mass spectrometry based metaproteomics of atmospheric aerosol samples, MPGS PhD Symposium, Mainz, Germany, 17th - 18th Mar, 2016.
3. Liu, F., Protein oligomerization upon exposure to ozone, Doktorandenseminar (DoSe), Mainz, Germany, 20th Oct, 2015.
4. Liu, F., Kampf, C. J., Reinmuth-Selzle, K., Berkemeier, T., Shiraiwa, M., Pöschl, U. Protein cross-linking and oligomerization through dityrosine formation upon exposure to ozone, European Geophysical Union General Assembly, Vienna, Austria, 12th -17th Apr, 2015.
5. Liu, F., Protein cross-linking and oligomerization through dityrosine formation upon exposure to ozone, IMPRS PhD Symposium, Mainz, Germany, 8th -10th Dec, 2014.

Poster Presentations

1. Liu, F., Reinmuth-Selzle, K., Després, V. R., Pöschl, U., Kampf, C. J.. Proteome analysis in ambient fine and coarse particles, European Aerosol Conference, Milano, Italy, 6th - 11th Sep, 2015.

Appendix B. Selected Publications

1. Liu, F., Lai, S., Reinmuth-Selzle, K., Scheel, J. F., Fröhlich-Nowoisky, J., Després, V. R., Hoffmann, T., Pöschl, U., Kampf, C. J. “Metaproteomic analysis of atmospheric aerosol samples” *Analytical and Bioanalytical Chemistry*. 2016; 408 (23): 6337-48.
2. Liu, F., Reinmuth-Selzle, K., Lai, S., Weller, M. G., Pöschl, U., Kampf, C. J. “Simultaneous determination of nitrated and oligomerized proteins by size exclusion high performance liquid chromatography coupled to photodiode array detection”, *Journal of Chromatography A*, *accepted*.
3. Kampf, C. J., Liu, F., Reinmuth-Selzle, K., Berkemeier, T., Meusel, H., Shiraiwa, M., Pöschl, U. “Protein cross-linking and oligomerization through dityrosine formation upon exposure to ozone” *Environmental science & technology*. 2015; 49 (18): 10859-66.
4. Liu, F., Lakey, P. S. J., Berkemeier, T., Tong, H., Kunert, A.T., Meusel, H., Cheng, Y., Su, H., Fröhlich-Nowoisky, J., Shiraiwa, M., Lai, S., Weller, M. G., Pöschl, U., Kampf, C. J. “Atmospheric protein chemistry influenced by anthropogenic air pollutants: protein nitration and oligomerization upon exposure to ozone and nitrogen dioxide”, *Faraday Discussions*, *accepted*.
5. Liu, F., Lai, S., Tong, H., Lakey, P. S. J., Shiraiwa, M., Weller, M. G., Pöschl, U., Kampf, C. J. “Release of free amino acids upon oxidation of peptides and proteins by hydroxyl radicals”, *Analytical and Bioanalytical Chemistry*. 2017; 1-10.

B.1. Liu et al., Anal. Bioanal. Chem., 2016

Metaproteomic analysis of atmospheric aerosol samples

Fobang Liu¹, Senchao Lai^{1,2}, Kathrin Reinmuth-Selzle¹, Jan Frederik Scheel¹, Janine Fröhlich-Nowoisky¹, Viviane R. Després³, Thorsten Hoffmann⁴, Ulrich Pöschl¹, and Christopher J. Kampf^{4, 1,*}

¹Department of Multiphase Chemistry, Max Planck Institute for Chemistry, Hahn-Meitner-Weg 1, 55128 Mainz, Germany

²School of Environment and Energy, South China University of Technology, Higher Education Mega Center, Guangzhou 510006, P.R. China

³Institute of General Botany, Johannes Gutenberg University Mainz, Johannes-von-Müller-Weg 6, 55128 Mainz, Germany

⁴Institute for Inorganic and Analytical Chemistry, Johannes Gutenberg University Mainz, Duesbergweg 10-14, 55128 Mainz, Germany

*Correspondence to Christopher J. Kampf, email: c.kampf@mpic.de

Analytical and Bioanalytical Chemistry, 2016, 408 (23): 6337-48.

Metaproteomic analysis of atmospheric aerosol samples

Fobang Liu¹ · Senchao Lai^{1,2} · Kathrin Reinmuth-Selzle¹ · Jan Frederik Scheel¹ ·
Janine Fröhlich-Nowoisky¹ · Viviane R. Després³ · Thorsten Hoffmann⁴ ·
Ulrich Pöschl¹ · Christopher J. Kampf^{1,4}

Received: 1 March 2016 / Revised: 19 April 2016 / Accepted: 27 June 2016 / Published online: 13 July 2016
© The Author(s) 2016. This article is published with open access at Springerlink.com

Abstract Metaproteomic analysis of air particulate matter provides information about the abundance and properties of bioaerosols in the atmosphere and their influence on climate and public health. We developed and applied efficient methods for the extraction and analysis of proteins from glass fiber filter samples of total, coarse, and fine particulate matter. Size exclusion chromatography was applied to remove matrix components, and sodium dodecyl sulfate polyacrylamide gel electrophoresis (SDS-PAGE) was applied for protein fractionation according to molecular size, followed by in-gel digestion and LC-MS/MS analysis of peptides using a hybrid Quadrupole-Orbitrap MS. Maxquant software and the Swiss-Prot database were used for protein identification. In samples collected at a suburban location in central Europe, we found proteins that originated mainly from plants, fungi, and bacteria, which constitute a major fraction of primary biological aerosol particles (PBAP) in the atmosphere. Allergenic proteins were found in coarse and fine particle

samples, and indications for atmospheric degradation of proteins were observed.

Keywords Metaproteomics · Atmospheric aerosols · Bioanalytical methods · HPLC · Mass spectrometry

Introduction

Primary biological aerosol particles (PBAP) including bacteria, fungal spores, pollen, biogenic polymers, and others like plant or animal fragments, are ubiquitous components of the atmospheric aerosol [1–3]. They likely have an influence on clouds and precipitation [4, 5] and have been linked to many adverse health effects such as infectious, respiratory, and allergic diseases [6–8]. Proteins, contained in PBAP from different sources and with distinct properties, are also known to influence atmospheric microphysics and public health [9–11].

Proteins can be found in coarse mode particles (>2.5 μm aerodynamic diameter) as well as in fine mode particles (<2.5 μm) [12]. It has been shown that bacteria are most frequently observed in ~2–4 μm particles [13, 14], fungal spores in the range of 2–10 μm [15, 16], pollen grains between 10 and 100 μm [1], and smaller pollen compartments, such as pollen cytoplasmic granules (PCGs; subcellular compartments) released from the rupture of pollen grains due to high humidity and moisture, are in the range of 30 nm to 4 μm [17, 18]. Proteinaceous material in different size modes of atmospheric aerosols have different penetration depths into the human respiratory tract, i.e., fine mode particles are able to pass through the upper respiratory tract and deposit in the small airway and alveoli [19], thus affecting potential health impacts.

Proteins in aerosol particles have been suggested to be good tracers for PBAP in the atmosphere [20]. Many

Electronic supplementary material The online version of this article (doi:10.1007/s00216-016-9747-x) contains supplementary material, which is available to authorized users.

✉ Christopher J. Kampf
c.kampf@mpic.de

- ¹ Department of Multiphase Chemistry, Max Planck Institute for Chemistry, Hahn-Meitner-Weg 1, 55128 Mainz, Germany
- ² School of Environment and Energy, South China University of Technology, Higher Education Mega Center, Guangzhou 510006, People's Republic of China
- ³ Institute of General Botany, Johannes Gutenberg University Mainz, Johannes-von-Müller-Weg 6, 55128 Mainz, Germany
- ⁴ Institute for Inorganic and Analytical Chemistry, Johannes Gutenberg University Mainz, Duesbergweg 10-14, 55128 Mainz, Germany

studies have focused on the measurement of total protein content in airborne particles using biological assays, e.g., bicinchoninic acid (BCA) assay, nano-orange, and Bradford assay and found proteins to account for up to 5 % of particles in mass concentration [21–23]. Some specific proteins, mostly allergens, have been investigated using immunoassays, such as enzyme-linked immunosorbent assay (ELISA) or Western blot, etc. For example, Buters et al. [24] determined the major birch pollen allergen Bet v 1 in ambient aerosols of different size fractions with an allergen-specific ELISA. Miyajima et al. [25] developed a fiber-optic chemifluorescence immunoassay for the detection of the airborne major dust mite allergen Der f 1. Although these immunoassays have the advantage of low detection limits and can quantify the targeted proteins, the antigen specificity of these assays limits their use in metaproteomic analysis of ambient aerosol particles. The term metaproteomics has been proposed for the characterization of the entire protein complement of environmental samples at a given point in time [26, 27]. Mass spectrometry-based metaproteomics has been successfully applied in studies of soils, lake sediments, and marine environments [28–31]. With regard to atmospheric aerosols, bioaerosol mass spectrometry has been used for the rapid identification of individual aerosolized microbial particles [32, 33]. Moreover, metaproteomic analysis has recently been applied to soils in Asian desert dust storm deposition regions [34, 35].

In this study, we develop a method to characterize proteins from atmospheric aerosol samples using a mass spectrometry-based metaproteomics approach, providing information about the taxonomic composition of bioaerosols. To our knowledge, this approach has previously not been established and applied for atmospheric aerosol samples. The critical step for protein identification is to efficiently extract proteins from the air filter samples. Besides considering the differences in protein properties such as solubility, also interactions between proteins, particles, and filter material need to be overcome by the extraction method. We evaluated the effects of soot particles and ammonium sulfate on protein recovery during filter extraction using BCA assays and sodium dodecyl sulfate polyacrylamide gel electrophoresis (SDS-PAGE). Furthermore, aerosol samples of different particle size fractions (total suspended, fine, and coarse particles) were analyzed using nano-HPLC coupled with a Hybrid Quadrupole-Orbitrap mass spectrometer after in-gel digestion. The method developed in this study allows for the characterization of aerosol proteins, simultaneously yielding insights into atmospheric protein transformation processes. A schematic overview of the analytical procedure for protein identification in ambient aerosol samples is shown in Fig. 1.

Materials and methods

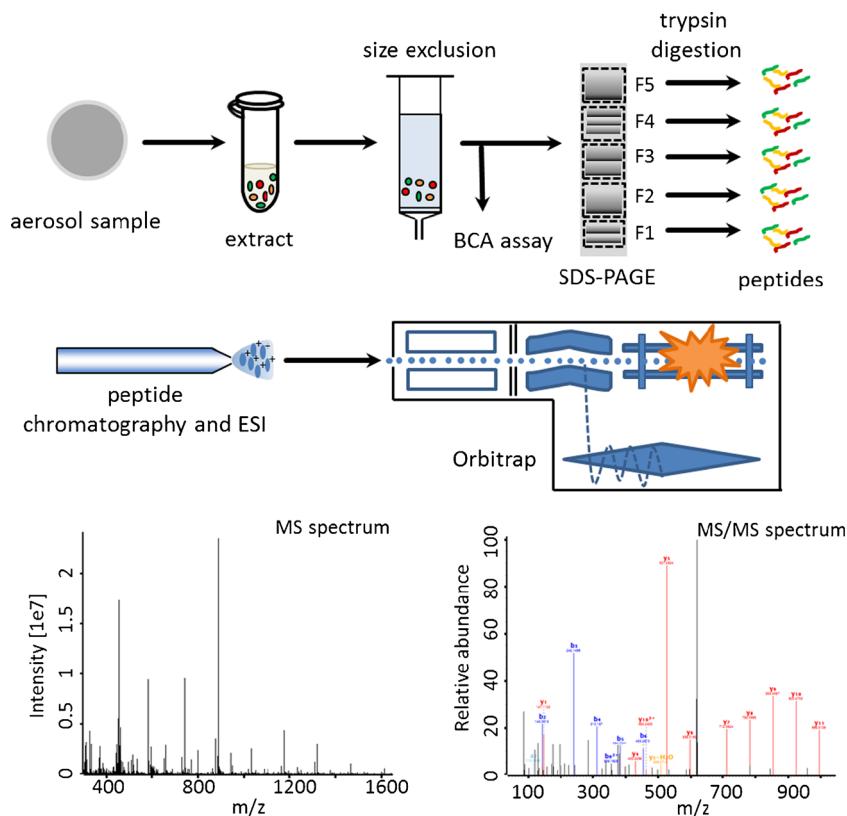
Reagents

Bovine serum albumin (BSA; A5611), phosphate-buffered saline tablet (PBS; P4417), glycine (G7126), β -mercaptoethanol (M-6250), dithiothreitol (DTT; D5545), iodoacetamide (IAM; I6125), acetonitrile (ACN; 34967), ammonium bicarbonate (A6141), and trypsin from porcine pancreas (T6567) were supplied by Sigma-Aldrich (Germany). Ten times Tris/glycine/SDS (161-0732) and two times Lamli sample buffer (161-0737) were from Bio-Rad Laboratories (USA). Trifluoroacetic acid (TFA; 400028) was from Applied Biosystem (UK). Formic acid (28905) and C18 spin tubes (89870) for desalting were obtained from ThermoFisher Scientific (Germany). Diesel particulate matter (SRM 2975) was purchased from the National Institute for Standards and Technology (NIST; USA). Ammonium sulfate (>99 %) was obtained from Acros Organics. Sodium dodecyl sulfate (H5113) was from Promega (USA). Glass fiber filters (type MN 85/90, 406015, Duren, Germany) for sampling of total suspended particles (TSP) and protein recovery tests during the development of the extraction method were purchased from Macherey-Nagel (Germany). A second set of glass fiber filters (type A/A, 102-mm diameter) for sampling coarse and fine particles was obtained from Pall Corporation (UK). High-purity water (18.2 M Ω m) was taken from an ELGA LabWater system (PURELAB Ultra, ELGA LabWater Global Operations, UK) and autoclaved before use if not specified otherwise.

Aerosol sampling

Aerosol samples were collected at the roof of the Max Planck Institute for Chemistry (MPIC; Mainz, Germany) in 2010 and 2015; the sampling period was generally 7 days. Sampling details are provided in Fröhlich-Nowoisky et al. [15]. Briefly, coarse and fine aerosol particles were collected onto a pair of glass fiber filters (prebaked at 500 °C overnight) by a self-built high-volume dichotomous sampler [36] operated at 300 L/min. Coarse particles with aerodynamic diameters larger than the cutoff diameter ($\approx 3 \mu\text{m}$) were collected through a virtual impactor operated in line with the inlet ($\approx 30 \text{ L/min}$), and fine particles with aerodynamic diameters smaller than the cutoff were collected from the main gas flow perpendicular to the inlet ($\approx 270 \text{ L/min}$). As a result of the air flow design of the virtual impactor, 10 % of the fine particles are collected on the coarse particle fraction. Furthermore, TSP samples were collected on 150 mm glass fiber filters (baked overnight at 290 °C) using a self-standing high-volume sampler (Digital DHA-80) operated at 100 L/min. A list of all investigated air filter samples is given in Electronic supplementary material (ESM) 1 Table S1. The loaded samples were stored in

Fig. 1 Schematic overview of the developed method for the metaproteomic analysis of atmospheric aerosol samples. Aerosol filter samples were extracted and subjected to size exclusion chromatography to remove sample matrix before BCA assay and SDS-PAGE analysis. Five molecular size fractions were excised from SDS-PAGE gels and in-gel digested before nano-LC-MS/MS with a Hybrid Quadrupole-Orbitrap mass spectrometer. Proteins were identified using the MaxQuant software for database searches against the Swiss-Prot database



decontaminated aluminum foil bags at $-80\text{ }^{\circ}\text{C}$. To detect possible contaminations from the samplers and sample handling, blank samples were taken as well. Blank sample filters were mounted in the sampler like for regular sampling, but the pump was turned on only for up to 30 s.

Protein extraction

Figure S1 in ESM 1 illustrates the extraction method development. The effects of the vial material, the extraction solvent and technique, as well as the enrichment method on protein recovery were investigated. In these experiments, 200 μg of BSA dissolved in 100 μL H_2O were spiked on prebaked filters. The parameters of interest were varied individually, while keeping the remaining parameters constant (see ESM 1 for details). The corresponding effects were evaluated by BSA recovery obtained by BCA assay, which has been widely applied for the measurement of total protein concentration in ambient aerosol samples [22, 37], as outlined in “[Bicinchoninic acid assay](#)”. All spiking experiments were performed in triplicate.

The optimized extraction method (discussed in “[Development of extraction method](#)”) was applied to aerosol filter samples. Briefly, filter aliquots ($\sim 40\text{ cm}^2$) were cut out from the whole filter and extracted twice with 2.0 mL $1\times$ Tris/Gly/SDS buffer in a 15-mL polypropylene (PP) vial by sonication (frequency, 35 kHz; Bandelin, Sonorex Super 10P,

Germany) for 1 h. It should be noted that low protein binding microcentrifuge tubes (525-0134, VWR International, Germany) were used in following steps in order to minimize protein loss. After the first extraction, the extract was centrifuged (15,000 rpm, 15 min) and the supernatant was collected before extracting the filter material the second time. Subsequently, the supernatants were lyophilized separately (Christ Alpha 2-4 LD, Germany). The dried residues were resuspended in 500 μL H_2O and subjected to size exclusion chromatography (28-9180-08, PD MinitrapTM G-25, exclusion limit 5 kDa, GE Healthcare, Germany) according to the supplier’s instruction, before BCA assay and SDS-PAGE analysis. Also, blank filter samples (see “[Aerosol sampling](#)”) were treated in the same way.

Assessment of matrix interferences on BCA assay and SDS-PAGE silver staining

The effects of ammonium sulfate and soot particles interfering with protein concentration determination by BCA assay were investigated. Experiments were conducted in triplicate using aliquots of 26 mg ammonium sulfate, 0.4 mg soot with or without spiking BSA solution (final concentration 250 mg/L) in 500 μL Tris/Gly/SDS buffer, representing the estimated mass of ammonium sulfate and soot collected on the ambient filter samples based on a study by Poulain et al. [38], and the average protein concentration on our filter samples as

determined by BCA assay. The mixture was sonicated for 1 h and afterwards centrifuged (15,000 rpm) for 15 min. The supernatant (450 μ L) was pipetted into a size exclusion column (PD MinitrapTM G-25) while a 50- μ L aliquot was kept as the sample before size exclusion treatment. Both samples, before and after size exclusion treatment, were analyzed by BCA assay.

In addition, 0.4 mg soot samples with or without spiking BSA (200 ng) in 500 μ L Tris/Gly/SDS buffer were used to investigate the effect of soot on SDS-PAGE silver staining. The same procedures of sonication and size exclusion treatment were performed as described above. Afterwards, the eluate was lyophilized and resuspended in 40 μ L 1 \times Lamlli sample buffer for SDS-PAGE and silver staining, as detailed in “[SDS-PAGE and in-gel digestion](#)”.

Bicinchoninic acid assay

The protein concentrations of spiked BSA and ambient aerosol filter sample extracts were determined with the BCA assay (BCA1-1 KT, Sigma-Aldrich). In brief, the assay was performed in 96-well microplates and calibrated with solutions of BSA dissolved in the corresponding extractants. Volumes of 10 μ L of standard and sample solutions, respectively, were pipetted into the microwells (three wells per sample solution), and 200 μ L freshly prepared working reagent was added. The microplate was incubated at 60 $^{\circ}$ C for 15 min, and then cooled to room temperature (\sim 22 $^{\circ}$ C). The absorbance was measured on a microplate photometer (Thermo Scientific Multiskan EX) at 560 nm. Prebaked blank filters and sample handling blanks were assayed according to the same procedure, and results were used to correct laboratory and ambient filter results for blank values.

SDS-PAGE and in-gel digestion

SDS-PAGE was performed using a 4 to 20 % gradient Mini-PROTEAN[®] TGXTM Gel (456-1093, Bio-Rad, USA). Briefly, after lyophilization, the ambient filter sample extracts were resuspended in 40 μ L 1 \times Lamlli sample buffer containing 2.5 % β -mercaptoethanol, then incubated at 95 $^{\circ}$ C in a thermomixer (Thermomixer Comfort, Eppendorf, Germany) for 5 min prior to SDS-PAGE separation. A molecular weight marker (Precision Plus Protein Unstained Standards, 161-0363, Bio-Rad, USA) was used for molecular weight scale calibration. Gels were run at a constant voltage of 110 V and silver-stained with a Pierce Silver Stain for Mass Spectrometry kit (24600, ThermoFisher Scientific, USA) according to the supplier's instruction. Subsequently, the gels were scanned on a ChemiDoc MP Imaging system using the Image Lab software (version 4.1, Bio-Rad).

The gels were cut into five fractions (F1-F5) as illustrated in Fig. 3, corresponding to molecular weights of \sim 10–15 kDa

(F1), \sim 15–25 kDa (F2), \sim 25–50 kDa (F3), \sim 50–100 kDa (F4), and \sim 100–250 kDa (F5) for in-gel digestion. The excised pieces were destained using the reagents and procedure provided in the Pierce Silver Stain for Mass Spectrometry kit. The following in-gel digestion was conducted according to the protocol of Shevchenko et al. [39]. Briefly, 10 mM DTT was applied at 56 $^{\circ}$ C for reduction of disulfide bonds and 55 mM IAM at room temperature in the dark for alkylation of cysteine residues. Trypsin digestion was performed at 37 $^{\circ}$ C overnight. Typically, 200 μ L or more DTT, IAM, and trypsin solution were added to completely cover the gel pieces in the corresponding step, depending on the volume of gel matrix. After digestion, peptides were extracted from the gel pieces by adding 400 μ L 5 % formic acid/ACN (*v/v*) and incubating for 15 min at 37 $^{\circ}$ C. Subsequently, the supernatants were collected and dried down by a SpeedVac concentrator (Christ RVC 2-25, Germany). The dried extracts were dissolved in 100 μ L 5 % ACN in H₂O with 0.5 % TFA and desalted with conditioned C18 spin tubes according to the manufacturer's instructions. Finally, the tryptic peptides were eluted using 20 μ L 50 % ACN in H₂O with 0.1 % formic acid for MS analysis.

Nano-LC-MS/MS analysis

Peptide mixtures were analyzed with a Thermo Q Exactive Plus Hybrid Quadrupole-Orbitrap mass spectrometer coupled to an EASY nLC 1000 uHPLC system. Self-packed NewObjective silica tip columns (25 cm length, 75 μ m inner diameter) packed with C18 stationary phase material (ReproSil-Pur 120 C18-AQ 1.9, 120 Å pore size, 1.9 μ m particle size, Dr. Maisch) were used for peptide separation. The column was operated in a column oven at 35 $^{\circ}$ C to reduce back pressure and coupled to a nano-electrospray ion source [40]. Eluents were H₂O with 0.1 % formic acid (buffer A) and 80 % ACN in H₂O with 0.1 % formic acid (buffer B). Peptides were eluted with a linear gradient from 2 to 5 % buffer B for 2 min, 5 to 40 % B for 19 min, 40 to 95 % B for 4 min, and 95 % B for 5 min at a flow rate of 225 nL/min. Then the mobile phase was reset to initial condition within 4 min and equilibrated for 4 min before the next run. The sample injection volume was 9 μ L. The Q Exactive Plus Orbitrap was operated in a HCD Top 10 mode with dynamic selection of the ten most intense peaks from each survey scan (*m/z* 300–1650) with collision energy of 25 eV for fragmentation. The resolution for full scan (*m/z* 300–1650) was 70,000 and 17,500 for MS/MS scan. Dynamic exclusion time was 20 s.

Database searches were performed with Maxquant (version 1.4.1.2, <http://www.maxquant.org/>) against the database Swiss-Prot (release 2013_08, www.uniprot.org). Trypsin/P was specified as a cleavage enzyme. Carbamidomethyl (C) was set as a fixed modification. Variable modifications were

acetyl (protein N-term) and oxidation (methionine (M)). Initial peptide mass tolerance was set to 20 ppm, and fragment mass tolerance was set to 4.5 ppm. Two missed cleavages were allowed, and the minimum peptide length was seven amino acids. The maximum false-discovery rate (FDR) was set to 0.01 for both the peptides and proteins. The maximal posterior error probability (PEP), which is the individual probability of each peptide to be a false hit considering identification score and peptide length, was set to 0.1. Only proteins with a minimum of two identified peptides, one of which needs to be unique, and without simultaneous detection in blank and wash samples were regarded as positively identified.

Results and discussion

Development of extraction method

The effects of vial materials, extraction solvents and techniques, as well as enrichment methods on protein recovery from spiked filter samples were investigated (for details, see “Protein extraction”; Fig. S1 in ESM 1). The presented extraction method is primarily aimed at proteins that are already released or easily extractable from pollen, fungal spores, bacteria, and other cells and cellular fragments in the primary biological fraction of air particulate matter.

We first compared the influence of vial materials used for extraction, i.e., PP and glass, on BSA recovery from glass fiber filters. No significant difference in BSA recovery was observed ($\Delta_{\text{recovery}} \sim 1\%$). Polypropylene vials were selected for further method development steps. Physical extraction methods tested were sonication and stirring. Sonication and stirring were both carried out for 1 h at room temperature. Protein recoveries of sonicated samples were 13 % higher than of stirred samples. Sample enrichment methods tested were freeze drying and protein precipitation using trichloroacetic acid (TCA). Protein recovery of freeze drying was 22 % higher compared with TCA precipitation. Trichloroacetic acid precipitation is efficient for protein separation from sample matrix but lower protein recoveries were obtained. Thus, for maximum protein recovery, freeze drying was used for protein enrichment. It should be noted that a commercial kit for protein extraction from soils (NoviPure[®] Soil Protein Extraction Kit, Mo-Bio) was also tested but showed a comparatively low recovery ($8.5 \pm 3.6\%$, data not shown) for BSA spiked on test filters. Further tests and procedure optimizations for extraction methods aiming to extract proteins also from intact cells collected on air filter samples, including lysis methods, are required and shall be pursued in follow-up studies.

The comparison of extraction solvents was performed among H₂O (as reference), 50 % ACN in H₂O (common extraction solvent for organic aerosol constituents), and aqueous buffer solutions commonly used in aerosol protein

extraction (PBS) and biological research (PBS and Tris/Gly/SDS). The highest protein recovery ($88 \pm 6\%$) was observed for Tris/Gly/SDS buffer (25 mM Tris, 192 mM glycine, 0.1 % SDS in aqueous solution), followed by Gly/SDS (192 mM glycine and 0.1 % SDS in aqueous solution), 0.1 % (w/v) SDS in H₂O, H₂O, 10 % PBS in H₂O, and 50 % ACN in H₂O, respectively, as shown in Fig. 2. Sodium dodecyl sulfate (SDS), as an anionic detergent, can denature secondary and non-disulfide-linked tertiary structures of proteins and therefore facilitates the solubilization of otherwise water-insoluble proteins as well as water-soluble proteins. Watanabe et al. [41] reported that the amount of protein extracted from food increased 10- to 100-fold when the extraction solvent contained SDS and β -ME and assumed that SDS helps solubilize proteins by disrupting most of their non-covalent bonds. Indeed, all extraction solvents containing SDS resulted in a high protein recovery. Therefore, Tris/Gly/SDS buffer was selected to enable extraction of water-soluble and water-insoluble proteins and to minimize other potential non-covalent interactions between proteins and components (e.g., soot, dust) of ambient aerosol samples and the filter material.

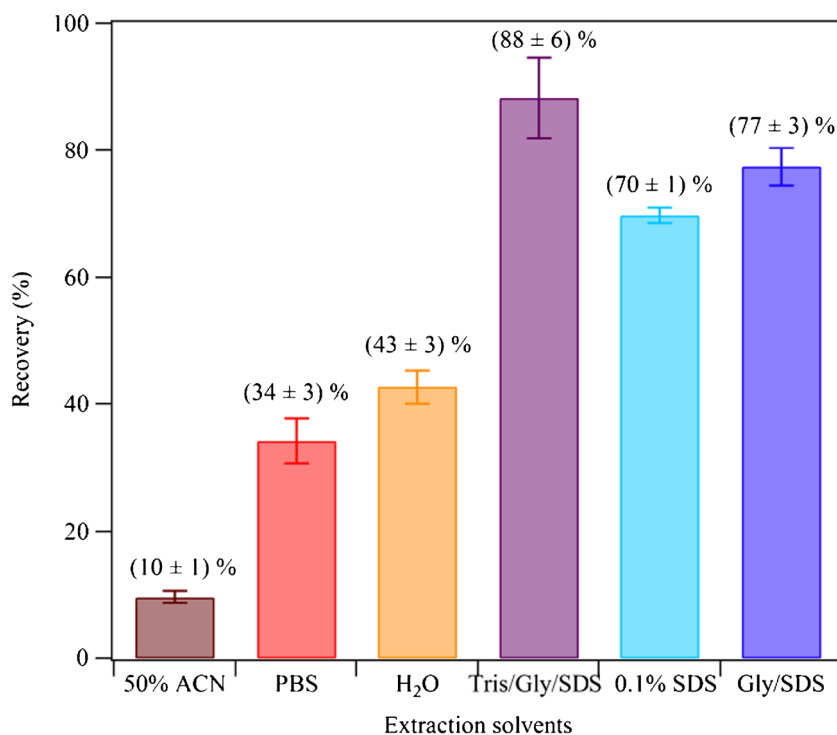
In summary, in the optimized method, samples were sonicated using Tris/Gly/SDS buffer as the extraction solvent, followed by freeze drying of the obtained extracts for sample enrichment.

BCA assay and SDS-PAGE silver staining analysis of aerosol samples—interferences caused by ammonium sulfate and soot particles

Previous studies have shown that aerosol components such as ammonium sulfate and humic-like substances (HULIS) may hamper protein determination by protein quantitation kits [42]. They found that protein concentrations measured by the protein quantitation kit (nano-orange assay) were six times higher than the concentrations determined by hydrolysis of proteinaceous material and concluded that the discrepancy could be caused by matrix interferences. In addition, also soot particles, which are mostly present in the fine fraction of atmospheric aerosols, may cause interferences in protein concentration determination by protein quantitation kits. Here, we estimate the effects of ammonium sulfate and soot on protein concentration determination by BCA assay (details in “Assessment of matrix interferences on BCA assay and SDS-PAGE silver staining”). Figure 3a illustrates that ammonium sulfate and soot are causing signals in the BCA assay (signals were converted into equivalent BSA concentrations) and thus the calculated recovery of BSA was $>100\%$ in Fig. 3b, when ammonium sulfate or soot were present in the protein solution.

Low molecular weight interfering substances, i.e., ammonium sulfate, can be efficiently removed by size exclusion

Fig. 2 Protein recoveries obtained for different extraction solvents used for the extraction of test filters spiked with 200 μg BSA. The filter extraction procedure and solvents are detailed in “Protein extraction”



chromatography (SEC), as suggested by Franze et al. [22] and illustrated in Fig. 3. The BCA assay signal caused by ammonium sulfate is reduced by around one order of magnitude after SEC, bringing the observed recovery of the BSA/ammonium sulfate mixture close to 100 %. Also for soot particles, a threefold reduction in the BSA equivalent concentration was observed after SEC and >65 % of the interference in the mixed BSA/soot sample could be removed. BCA assay analysis of ambient aerosol samples also show a reduction of BSA equivalent protein concentration of ~60–90 % after SEC

(see Fig. S2 in ESM 1). This reduction in the observed signal may either be caused by an over determination of the protein content in the presence of the aforementioned interferences or by the removal of proteins attached to soot particles. A combination with other protein purification techniques, e.g., dialysis or affinity chromatography, may further improve protein concentration determination of aerosol samples by BCA assay.

For SDS-PAGE analysis, no influence of ammonium sulfate was observed, but soot particles were found to affect the

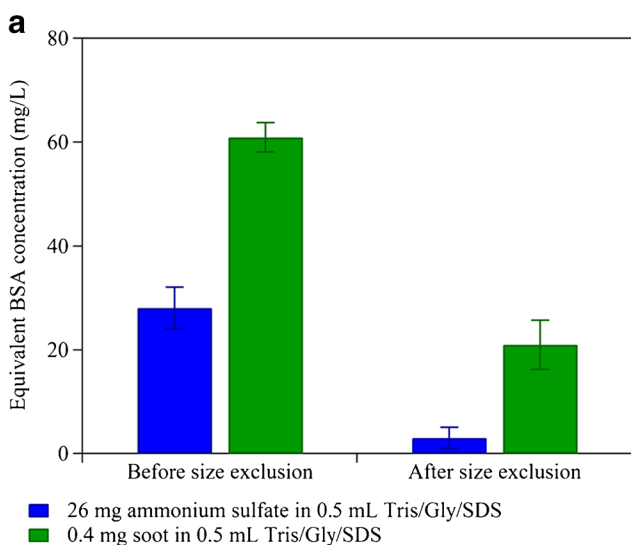
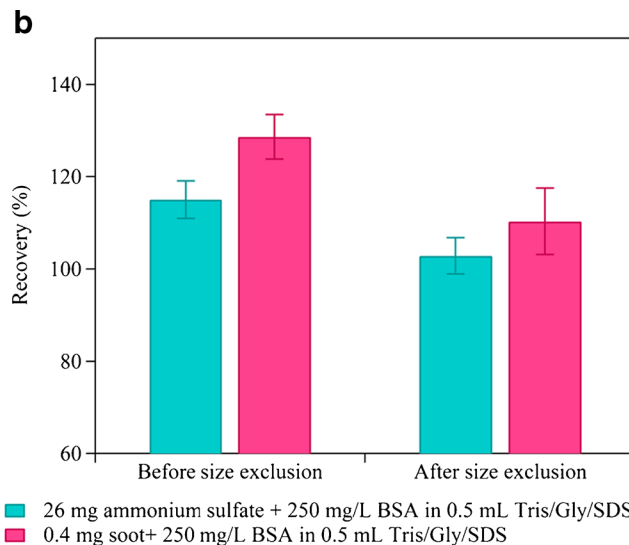


Fig. 3 Influence of soot particles and ammonium sulfate on total protein content analysis by BCA assay: **a** equivalent BSA concentration of soot particle and ammonium sulfate standards in Tris/Gly/SDS buffer before



and after size exclusion; **b** observed BSA recovery for soot + BSA and ammonium sulfate + BSA mixtures before and after size exclusion

appearance of the gel after silver staining. Figure 4 lane A shows the separation of an ambient aerosol (TSP) sample extract after silver staining, whereby no clear bands could be resolved over the strong background. Coomassie-stained SDS-PAGE gels of filter extracts did not show any visible bands (data not shown; EZBlue, G1041, Sigma-Aldrich, Germany, detection sensitivity 5 ng), indicating that overloading of gels is no major issue and silver staining was selected because of its higher sensitivity (<1 ng protein) [43]. Additional experiments were performed to investigate the influence of soot particles on the lane background after silver staining (see Fig. 4; Fig. S3 in ESM 1). The background of lanes showing separations of samples with soot standard (lane B and D in Fig. 4; lane B in Fig. S3 in ESM 1) appears in a darker color after silver staining compared with the background of lanes without the addition of soot (lane C Fig. 4; Fig. S3 in ESM 1). Furthermore, the intensities of the protein bands were weaker in the presence of soot particles (lane D in Fig. 4; lane B in Fig. S3 in ESM 1). However, the location of the BSA monomer band remained unaffected by the soot particles (lanes C and D in Fig. 4). It should be noted that the soot standard used here might have different properties than aged soot in the atmosphere, as soot morphology changes and coatings by organic substances have been observed for atmospherically aged soot particles [44]. Alternative or optimized staining methods shall be investigated in follow-up studies to minimize the effect of soot particles in the staining step.

Soot particles were found to affect both BCA assay and SDS-PAGE analysis of atmospheric aerosol samples and

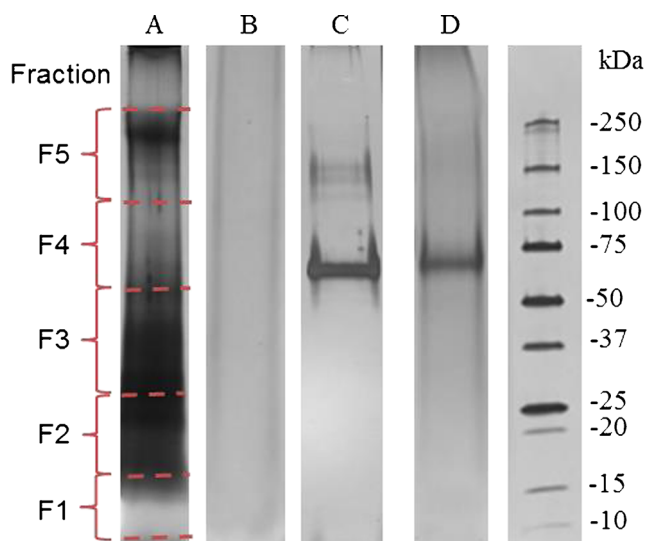


Fig. 4 SDS-PAGE of filter extracts after silver staining, BSA and/or soot in Tris/Gly/SDS buffer: *Lane A*, filter sample (Mz02c, TSP); *lane B*, 0.4 mg soot in 500 µL Tris/Gly/SDS buffer; *lane C*, 200 ng BSA in 500 µL Tris/Gly/SDS buffer; *lane D*, 200 ng BSA mixed with 0.4 mg soot in 500 µL Tris/Gly/SDS buffer. *Right lane*, protein molecular weight marker

should be considered when reporting the corresponding protein concentrations. Nevertheless, the soot particles did not affect SDS-PAGE protein separation itself, thus in-gel digestion of aerosol sample extracts and subsequent peptide LC-MS/MS have been performed and will be discussed in the next section.

Protein identification in ambient aerosol samples

Ambient aerosol samples collected in Mainz, Germany, a sampling site in central Europe influenced by urban and rural boundary layer air masses, have been analyzed. A list of the identified proteins and their taxonomic classification is given in ESM 2. The Maxquant output file for the observed peptides of the identified proteins and protein groups, respectively, is provided in ESM 3.

Five, twenty-one, and thirty-three proteins were successfully identified in the coarse, fine, and TSP aerosol sample, respectively. There seems to be a gap in the number of identified proteins from the investigated aerosol samples compared with the metaproteomic analysis of other environmental samples, e.g., soils or sediments [28–31]. The low number of proteins identified in this work might be related to the applied extraction method, for which the aims were outlined above. Also, larger sample sizes (whole filters, longer sampling times) might be used to increase the number of identified proteins, considering the potentially low amounts of individual proteins contributing to the total protein mass analyzed per filter aliquot (~250 µg) due to the diversity of protein sources including various plants, fungi, and bacteria. Furthermore, as will be discussed below, we observed the presence of partly degraded proteins in the aerosol filter sample extracts, which may further hamper protein identification. Note that the higher number of identified proteins in the fine fraction aerosol sample compared with the coarse fraction aerosol sample is likely due to the higher sampling flow rate of the fine fraction aerosol sample. Protein databases (e.g., Swiss-Prot) only provide sequence information for a subset of known proteins [45]. Therefore, only those proteins listed in the databases can be identified, which is particularly important for the identification of fungal and bacterial proteins.

Many database-listed proteins of bacteria and fungi are inferred from homology, i.e., indicating that the existence of a protein is probable because clear orthologs exist in closely related species, while no direct experimental evidence for the existence of these proteins exists on a transcript or protein level. For example, the genome of *Neurospora crassa* (a fungi from the class of Sordariomycetes in the phylum of Ascomycota) has been sequenced due to its use as a model organism in biology [46], providing information about predicted protein-coding sequences. Still, proteins identified to originate from *N. crassa*, which was also found in air filter samples collected in Mainz in March 2006 using DNA

analysis [15], are partly inferred from homology (entries 18, 19, 47, and 48 in ESM 2). For other identified proteins, experimental evidence is available at the transcript level (entries 2 and 20 in ESM 2), while experimental evidence at the protein level is only available for one of them (entry 49 in ESM 2).

Some of the identified proteins are expressed by a variety of organisms with only minor changes in the primary protein

structure (i.e., the amino acid sequence of the protein). Thus, the taxonomic level to which identified proteins can be assigned varies depending on the uniqueness of the measured peptides among the database-listed proteins. In most cases kingdom (83 %) and phylum (80 %) level assignments are reasonable. The identified proteins mainly originated from plants (68 % in TSP, 31 % in fine particles), microorganisms

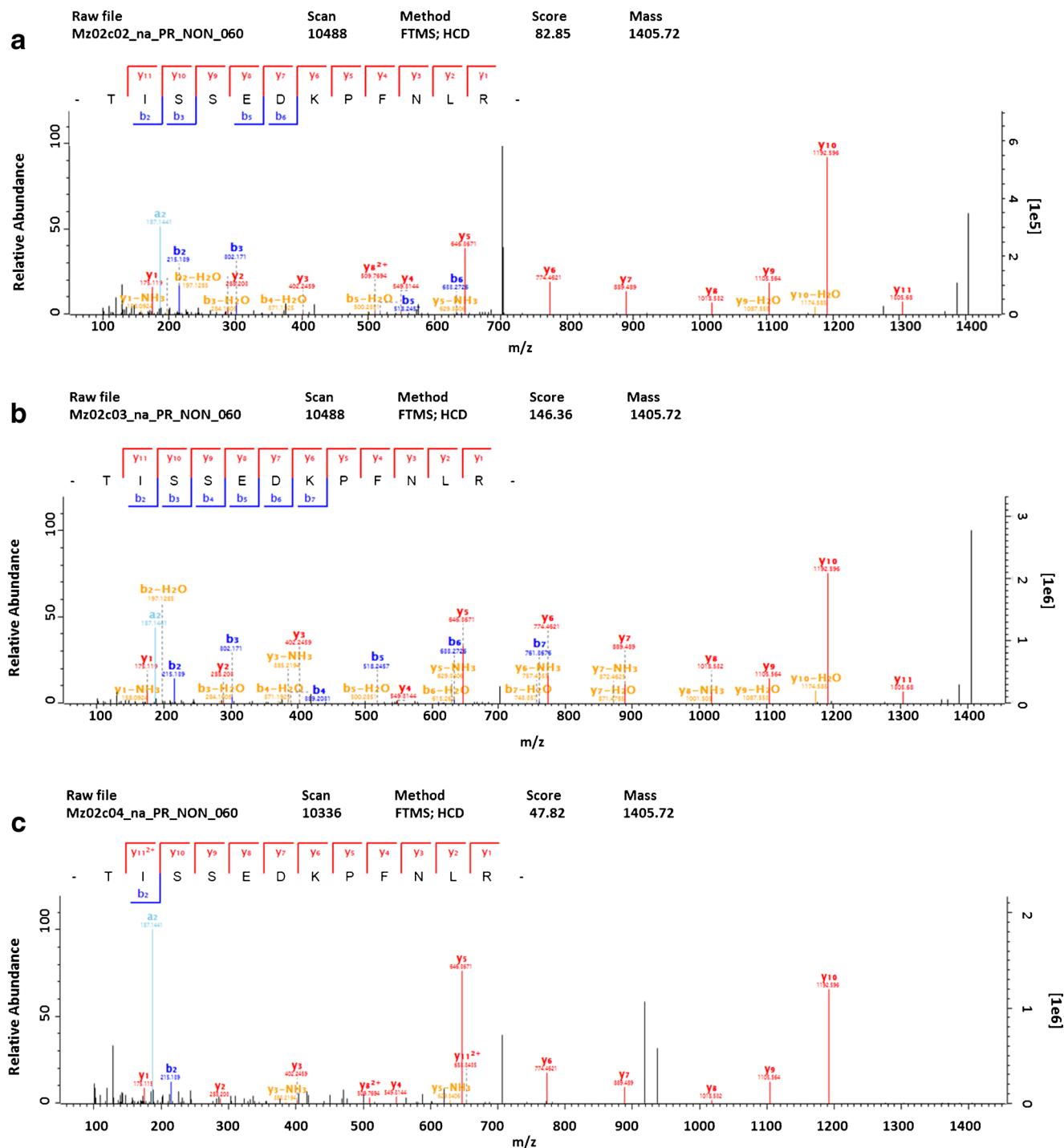


Fig. 5 Exemplary MS/MS spectra of the tryptic peptide TISSEDKPFNLR (a unique peptide of Beta-conglycinin, alpha chain from soybean) identified in fraction F2 (a), F3 (b), and F4 (c) of the TSP sample (Mz02c)

(fungi, bacteria, Amoebozoa, etc., 25 % in TSP, 50 % in fine particles) and animals (7 % in TSP, 19 % in fine particles), which is in line with the major categories of PBAP [1]. Notably, in the coarse particle sample one protein has been assigned to a bacterium (*Rhodococcus rhodochrous*) [47], which is used as a soil inoculant in agriculture, while potential assignments of proteins identified in the fine particle and TSP sample to the kingdom of bacteria were not unambiguous on the kingdom level.

Also lower taxonomic ranks down to family and genus level may be assigned, e.g., in the case of the well-studied plant pollen proteins. Here, also seasonal influences are reflected in the identified proteins. Particularly for the TSP sample collected beginning of July 2015, several proteins from different grass (Poaceae) genera were identified, which is in accordance with the main grass flowering period from May to July in central Europe [10]. Grass pollen proteins identified were all allergens from the genera *Lolium*, *Dactylis*, and *Phleum*. Notably, also nine proteins originating from *Glycine max* (soybean), eight having a molecular weight >20 kDa, were identified in the TSP sample. Potentially, the occurrence of these proteins can be attributed to soy unloading and industrial processing by a local manufacturing site producing among others soy oil and soy flour. Soy flour dust is known to contain high levels of proteins with MW >20 kDa [48].

Allergenic proteins were found in TSP, coarse, and fine particle samples. Polcalcin Phl p 7 from common timothy (*Phleum pratense*), which is one of the most abundant sources of airborne grass pollen [10], was identified in the TSP and coarse particle sample, while for example, the major perennial ryegrass (*Lolium perenne*) pollen protein Lol p 5a and the hydrophobic seed protein (Gly m 1), an allergen from soybean (*G. max*), were identified in the TSP and fine particle sample. Allergens associated with different aerosol size fractions can

be inhaled and transported to different regions of the respiratory tract depending on their size (i.e., smaller particles can enter deeper into the respiratory tract), and thus have distinct health implications such as allergic asthma [49, 50].

The molecular weight-dependent proteomic analysis of aerosol samples showed the presence of protein fragments in the atmospheric aerosol sample extracts. SDS-PAGE gels were divided into five molecular weight fractions (F1-F5, see “Assessment of matrix interferences on BCA assay and SDS-PAGE silver staining”) and some of the identified proteins could be detected in multiple gel fractions (Table 1), i.e., also in fractions corresponding to lower MW than that of the intact protein. For example, beta-conglycinin, alpha chain from soybean (*G. max*), MW 70.3 kDa, was simultaneously identified in fractions F2, F3, and F4 in the TSP sample. Corresponding to its MW, the protein should only be detected in fraction F4. Figure 5 shows exemplary MS/MS spectra of TISSEDKPFNLR, a representative unique peptide of beta-conglycinin, alpha chain, identified in the different MW fractions, respectively. Tandem mass spectra (MS/MS) of other (razor and unique) peptides of beta-conglycinin, alpha chain are shown in Fig. S3 (ESM 1). In general, several processes may lead to the observed protein degradation, including proteolytic degradation during sample preparation and in the environment, as well as degradation by reactive oxygen species (e.g., OH, HO₂) [51] and acid-catalyzed hydrolysis [52] in the environment. To differentiate between environmental protein degradation and degradation during sample preparation, it is planned to conduct experiments with and without the addition of protease inhibitors [53]. Nevertheless, these first results could motivate studies concerning the fate of proteins in the atmosphere, especially under the rising air pollutant concentrations encountered in the Anthropocene, the present era of steeply increasing human influence on planet Earth [54, 55]. Environmental protein degradation might be a source of

Table 1 Exemplary results of protein identification in SDS-PAGE molecular size fractions for the TSP and fine particle sample extracts

Sample ID (size range)	Protein name	Family/species	Sum of peptides	Unique peptides	MW (kDa)	(Unique) Peptide counts				
						F1	F2	F3	F4	F5
Mz02c (TSP)	Glycinin G4	Fabaceae/ <i>Glycine max</i> (soybean)	2	1	63.6	1 (0)	2 (1)	1 (0)	1 (0)	
	Glycinin G1	Fabaceae/ <i>G. max</i> (soybean)	7	4	55.7	4 (3)	5 (3)	3 (1)	1 (1)	
	Glycinin G2	Fabaceae/ <i>G. max</i> (soybean)	8	4	54.4	1 (0)	5 (3)	4 (2)		
	Beta-conglycinin, alpha chain	Fabaceae/ <i>G. max</i> (soybean)	9	6	70.3		2 (2)	9 (5)	4 (4)	
	Beta-conglycinin, alpha' chain	Fabaceae/ <i>G. max</i> (soybean)	4	2	74.3			4 (2)		
	Major pollen allergen Lol p 5a	Poaceae/ <i>Lolium perenne</i> (perennial ryegrass)	6	6	30.9		6 (2)	2 (2)		
344b (<3 μm)	ATP synthase subunit beta	Saccharomycetaceae (yeasts)/–	7	1	54.8	5 (1)	3 (1)	6 (1)	3 (0)	1 (0)
	Elongation factor 2	Saccharomycetaceae (yeasts)/–	3	1	93.2	3 (1)	1 (1)			

Molecular size fractions: F1 (~10–15 kDa), F2 (~15–25 kDa), F3 (~25–50 kDa), F4 (~50–100 kDa), F5 (~100–250 kDa)

peptides, amino acids, amino, and carbonyl compounds in the atmosphere and thus contribute to various atmospheric processes and ecosystem interactions of atmospheric aerosols [56, 57].

Conclusions

Mass spectrometric identification of proteins in atmospheric aerosol samples was carried out after development of a method optimized to extract proteins from air filter samples. Soot particles contained in the aerosol samples were found to interfere with BCA assay analysis, a common technique to measure total protein contents, as well as staining methods, i.e., silver staining, used to visualize SDS-PAGE results. The interference of the soot particles could be minimized by performing size exclusion chromatography of air filter sample extracts.

The metaproteomic analysis presented here allows a first profiling of proteins in atmospheric aerosols. More in-depth analysis of specific post-translational modifications (PTM) of health-relevant proteins (aeroallergens) in the atmosphere (e.g., protein nitration) [58–61], requires specific and efficient enrichment and purification methods, e.g., antibody-based affinity enrichment, which will be addressed in follow-up studies. Furthermore, improvements of protein databases, e.g., by providing proteome information for a larger number of species including fungi and bacteria present in the atmosphere are needed to provide more complete information about the abundance and proportions of different biological kingdoms present in the aerosol metaproteome.

The molecular size-dependent analysis of proteins extracted from the aerosol samples revealed the presence of fragmented proteins in the sample extracts. Such fragments may arise partly from proteolytic degradation during sample preparation and degradation of proteins in the environment, which will be examined in follow-up studies. Environmental protein degradation processes might be of relevance for ecosystem interactions, e.g., nutrient cycling, as well as health implications of protein-containing aerosols due to a potential loss of protein activity upon degradation.

The presented profiles of extractable proteins in atmospheric aerosol particles show that proteins encountered in ambient air particulate matter mainly originate from plants, fungi, and bacteria, which is in line with the major categories of PBAP. Allergenic pollen proteins, e.g., from perennial ryegrass, were found in coarse and fine particles, which can penetrate deep into the lower part of the respiratory tract.

Complementary to antibody or DNA-based methods, the metaproteomic analysis of atmospheric aerosol samples provides a tool to study bioparticles and allergens in air particulate matter. Potential applications include investigations of the

spatiotemporal variability of bioaerosol composition and corresponding implications for human health.

Acknowledgments Open access funding provided by Max Planck Society. F.L. and S.L. acknowledge financial support from China Scholarship Council (CSC), C.J.K. acknowledges financial support by the German Research Foundation (DFG; grant no. KA4008/1-1). Support in nano-LC-MS/MS analysis by the Institute of Molecular Biology (IMB; Mainz) Proteomic Core Facility is gratefully acknowledged. The authors thank Jörn Wehking and Daniel Pickersgill for technical support.

Compliance with ethical standards

Conflict of interest The authors declare that they have no competing interests.

Ethical approval This article does not contain any research with human participants or animals. All authors of this manuscript were informed and agreed for submission.

Open Access This article is distributed under the terms of the Creative Commons Attribution 4.0 International License (<http://creativecommons.org/licenses/by/4.0/>), which permits unrestricted use, distribution, and reproduction in any medium, provided you give appropriate credit to the original author(s) and the source, provide a link to the Creative Commons license, and indicate if changes were made.

References

- Després VR, Huffman JA, Burrows SM, Hoose C, Safatov AS, Buryak G et al. Primary biological aerosol particles in the atmosphere: a review. *Tellus B*. 2012; 64.
- Matthias-Maser S, Jaenicke R. The size distribution of primary biological aerosol particles with radii $>0.2 \mu\text{m}$ in an urban/rural influenced region. *Atmos Res*. 1995;39:279–86.
- Carslaw K, Boucher O, Spracklen D, Mann G, Rae J, Woodward S, et al. A review of natural aerosol interactions and feedbacks within the Earth system. *Atmos Chem Phys*. 2010;10:1701–37.
- Pöschl U, Martin S, Sinha B, Chen Q, Gunthe S, Huffman J, et al. Rainforest aerosols as biogenic nuclei of clouds and precipitation in the Amazon. *Science*. 2010;329:1513–6.
- Huffman JA, Prenni A, DeMott P, Pöhlker C, Mason R, Robinson N, et al. High concentrations of biological aerosol particles and ice nuclei during and after rain. *Atmos Chem Phys*. 2013;13:6151–64.
- Żukiewicz-Sobczak W. The role of fungi in allergic diseases. *Postep Derm Alergol*. 2013;30:42–5.
- Douwes J, Thorne P, Pearce N, Heederik D. Bioaerosol health effects and exposure assessment: progress and prospects. *Ann Occup Hyg*. 2003;47:187–200.
- Singh A. Pollen and fungal aeroallergens associated with allergy and asthma in India. *Glob J Immunol Allerg Dis*. 2014;2:19–28.
- Lang-Yona N, Shuster-Meiseles T, Mazar Y, Yarden O, Rudich Y. Impact of urban air pollution on the allergenicity of *Aspergillus fumigatus* conidia: outdoor exposure study supported by laboratory experiments. *Sci Total Environ*. 2016;541:365–71.
- D'Amato G, Cecchi L, Bonini S, Nunes C, Annesi-Maesano I, Behrendt H, et al. Allergenic pollen and pollen allergy in Europe. *Allergy*. 2007;62:976–90.
- Pummer B, Budke C, Augustin-Bauditz S, Niedermeier D, Felgitsch L, Kampf C, et al. Ice nucleation by water-soluble macromolecules. *Atmos Chem Phys*. 2015;15:4077–91.

12. Riediker M, Koller T, Monn C. Differences in size selective aerosol sampling for pollen allergen detection using high-volume cascade impactors. *Clin Exp Allergy*. 2000;30:867–73.
13. Tong Y, Lighthart B. The annual bacterial particle concentration and size distribution in the ambient atmosphere in a rural area of the Willamette Valley. *Oregon Aerosol Sci Technol*. 2000;32:393–403.
14. Wang CC, Fang GC, Lee L. Bioaerosols study in central Taiwan during summer season. *Toxicol Ind Health*. 2007;23:133–9.
15. Fröhlich-Nowoisky J, Pickersgill DA, Després VR, Pöschl U. High diversity of fungi in air particulate matter. *Proc Natl Acad Sci U S A*. 2009;106:12814–9.
16. Elbert W, Taylor P, Andreae M, Pöschl U. Contribution of fungi to primary biogenic aerosols in the atmosphere: wet and dry discharged spores, carbohydrates, and inorganic ions. *Atmos Chem Phys*. 2007;7:4569–88.
17. Taylor P, Flagan R, Miguel A, Valenta R, Glovsky M. Birch pollen rupture and the release of aerosols of respirable allergens. *Clin Exp Allergy*. 2004;34:1591–6.
18. Visez N, Chassard G, Azarkan N, Naas O, Sénéchal H, Sutra J-P, et al. Wind-induced mechanical rupture of birch pollen: potential implications for allergen dispersal. *J Aerosol Sci*. 2015;89:77–84.
19. Guarnieri M, Balmes JR. Outdoor air pollution and asthma. *Lancet*. 2014;383:1581–92.
20. Staton SJ, Woodward A, Castillo JA, Swing K, Hayes MA. Ground level environmental protein concentrations in various Ecuadorian environments: potential uses of aerosolized protein for ecological research. *Ecol Indic*. 2015;48:389–95.
21. Miguel AG, Cass GR, Glovsky MM, Weiss J. Allergens in paved road dust and airborne particles. *Environ Sci Technol*. 1999;33:4159–68.
22. Franze T, Weller MG, Niessner R, Pöschl U. Protein nitration by polluted air. *Environ Sci Technol*. 2005;39:1673–8.
23. Menetrez M, Foarde K, Dean T, Betancourt D, Moore S. An evaluation of the protein mass of particulate matter. *Atmos Environ*. 2007;41:8264–74.
24. Buters J, Thibaudon M, Smith M, Kennedy R, Rantio-Lehtimäki A, Albertini R, et al. Release of Bet v 1 from birch pollen from 5 European countries. Results from the HIALINE study. *Atmos Environ*. 2012;55:496–505.
25. Miyajima K, Suzuki Y, Miki D, Arai M, Arakawa T, Shimomura H, et al. Direct analysis of airborne mite allergen (Der f 1) in the residential atmosphere by chemifluorescent immunoassay using bioaerosol sampler. *Talanta*. 2014;123:241–6.
26. Rodriguez-Valera F. Environmental genomics, the big picture? *FEMS Microbiol Lett*. 2004;231:153–8.
27. Wilmes P, Bond PL. The application of two-dimensional polyacrylamide gel electrophoresis and downstream analyses to a mixed community of prokaryotic microorganisms. *Environ Microbiol*. 2004;6:911–20.
28. Williams MA, Taylor EB, Mula HP. Metaproteomic characterization of a soil microbial community following carbon amendment. *Soil Biol Biochem*. 2010;42:1148–56.
29. Wang DZ, Xie ZX, Zhang SF. Marine metaproteomics: current status and future directions. *J Proteomics*. 2014;97:27–35.
30. Barnett JP, Scanlan DJ, Blindauer CA. Protein fractionation and detection for metalloproteomics: challenges and approaches. *Anal Bioanal Chem*. 2012;402:3311–22.
31. Thompson EL, Taylor DA, Nair SV, Birch G, Hose GC, Raftos DA. Proteomic analysis of Sydney Rock oysters (*Saccostrea glomerata*) exposed to metal contamination in the field. *Environ Pollut*. 2012;170:102–12.
32. Shah HN, Gharbia S, editors. *Mass spectrometry for microbial proteomics*. Chichester: Wiley; 2010.
33. Tobias HJ, Schafer MP, Pitesky M, Ferguson DP, Horn J, Frank M, et al. Bioaerosol mass spectrometry for rapid detection of individual airborne *Mycobacterium tuberculosis* H37Ra particles. *Appl Environ Microbiol*. 2005;71:6086–95.
34. Sekhon SS, Ahn JY, Min J, Kim YH. Toxicoproteomic approaches for analysis of microbial community inhabiting Asian dust particles. *Mol Cell Toxicol*. 2015;11:287–94.
35. Sekhon SS, Kim M, Um HJ, Kobayashi F, Iwasaka Y, Shi G, et al. Proteomic analysis of microbial community inhabiting Asian dust source region. *Clean-Soil Air Water*. 2016;44:25–8.
36. Solomon PA, Moyers JL, Fletcher RA. High-volume dichotomous virtual impactor for the fractionation and collection of particles according to aerodynamic size. *Aerosol Sci Technol*. 1983;2:455–64.
37. Kang H, Xie Z, Hu Q. Ambient protein concentration in PM₁₀ in Hefei, central China. *Atmos Environ*. 2012;54:73–9.
38. Poulain L, Spindler G, Birmili W, Plass-Dülmer C, Wiedensohler A, Herrmann H. Seasonal and diurnal variations of particulate nitrate and organic matter at the IfT research station Melpitz. *Atmos Chem Phys*. 2011;11:12579–99.
39. Shevchenko A, Henrik Tomas JH, Olsen JV, Mann M. In-gel digestion for mass spectrometric characterization of proteins and proteomes. *Nat Protoc*. 2007;1:2856–60.
40. Wilm M, Mann M. Analytical properties of the nanoelectrospray ion source. *Anal Chem*. 1996;68:1–8.
41. Watanabe Y, Aburatani K, Mizumura T, Sakai M, Muraoka S, Mamegosi S, et al. Novel ELISA for the detection of raw and processed egg using extraction buffer containing a surfactant and a reducing agent. *J Immunol Methods*. 2005;300:115–23.
42. Mandalakis M, Apostolaki M, Tziaras T, Polymenakou P, Stephanou EG. Free and combined amino acids in marine background atmospheric aerosols over the Eastern Mediterranean. *Atmos Environ*. 2011;45:1003–9.
43. Weiss W, Weiland F, Görg A. Protein detection and quantitation technologies for gel-based proteome analysis. *Proteomics*. 2009;564:59–82.
44. Qiu C, Khalizov AF, Zhang R. Soot aging from OH-initiated oxidation of toluene. *Environ Sci Technol*. 2012;46:9464–72.
45. Gattiker A, Michoud K, Rivoire C, Auchincloss AH, Coudert E, Lima T, et al. Automated annotation of microbial proteomes in SWISS-PROT. *Comput Biol Chem*. 2003;27:49–58.
46. Galagan JE, Calvo SE, Borkovich KA, Selker EU, Read ND, Jaffe D, et al. The genome sequence of the filamentous fungus *Neurospora crassa*. *Nature*. 2003;422:859–68.
47. Dinamarca MA, Orellana L, Aguirre J, Baeza P, Espinoza G, Canales C, et al. Biotransformation of dibenzothiophene and gas oil using a bioreactor containing a catalytic bed with *Rhodococcus rhodochrous* immobilized on silica. *Biotechnol Lett*. 2014;36:1649–52.
48. Gómez-Ollés S, Cruz M, Bogdanovic J, Wouters I, Doekes G, Sander I, et al. Assessment of soy aeroallergen levels in different work environments. *Clin Exp Allergy*. 2007;37:1863–72.
49. Riediker M, Koller T, Monn C. Determination of birch pollen allergens in different aerosol sizes. *Aerobiologia*. 2000;16:251–4.
50. Taylor PE, Flagan RC, Valenta R, Glovsky MM. Release of allergens as respirable aerosols: a link between grass pollen and asthma. *J Allergy Clin Immunol*. 2002;109:51–6.
51. Stadtman ER. Protein oxidation and aging. *Free Rad Res*. 2006;40:1250–8.
52. Oliyai C, Borchardt RT. Chemical pathways of peptide degradation. IV. Pathways, kinetics, and mechanism of degradation of an aspartyl residue in a model hexapeptide. *Pharm Res*. 1993;10:95–102.
53. Zhang N, Chen R, Young N, Wishart D, Winter P, Weiner JH, et al. Comparison of SDS- and methanol-assisted protein solubilization and digestion methods for *Escherichia coli* membrane proteome analysis by 2-D LC-MS/MS. *Proteomics*. 2007;7:484–93.
54. Crutzen PJ. Geology of mankind. *Nature*. 2002;415:23.

55. Pöschl U, Shiraiwa M. Multiphase chemistry at the atmosphere–biosphere interface influencing climate and public health in the anthropocene. *Chem Rev.* 2015;115:4440–75.
56. Zhang Q, Anastasio C. Free and combined amino compounds in atmospheric fine particles (PM_{2.5}) and fog waters from Northern California. *Atmos Environ.* 2003;37:2247–58.
57. Nguyen TB, Crounse JD, Teng AP, Clair JMS, Paulot F, Wolfe GM, et al. Rapid deposition of oxidized biogenic compounds to a temperate forest. *Proc Natl Acad Sci U S A.* 2015;112:E392–401.
58. Gruijthuijsen Y, Grieshuber I, Stöcklinger A, Tischler U, Fehrenbach T, Weller M, et al. Nitration enhances the allergenic potential of proteins. *Int Arch Allergy Immunol.* 2006;141:265–75.
59. Karle AC, Oostingh GJ, Mutschlechner S, Ferreira F, Lackner P, Bohle B, et al. Nitration of the pollen allergen bet v 1.0101 enhances the presentation of bet v 1-derived peptides by HLA-DR on human dendritic cells. *PLoS One.* 2012;7:e31483.
60. Ackaert C, Kofler S, Horejs-Hoeck J, Zulehner N, Asam C, von Grafenstein S, et al. The impact of nitration on the structure and immunogenicity of the major birch pollen allergen Bet v 1.0101. *PloS one.* 2014;9:e104520.
61. Reinmuth-Selzle K, Ackaert C, Kampf CJ, Samonig M, Shiraiwa M, Kofler S, et al. Nitration of the birch pollen allergen Bet v 1.0101: efficiency and site-selectivity of liquid and gaseous nitrating agents. *J Proteome Res.* 2014;13:1570–7.

Electronic Supplementary Material 1

Metaproteomic analysis of atmospheric aerosol samples

Analytical and Bioanalytical Chemistry

Fobang Liu¹, Senchao Lai^{1,2}, Kathrin Reinmuth-Selzle¹, Jan Frederik Scheel¹, Janine Fröhlich-Nowoisky¹, Viviane R. Després³, Thorsten Hoffmann⁴, Ulrich Pöschl¹, and Christopher J. Kampf^{4,1,*}

¹Department of Multiphase Chemistry, Max Planck Institute for Chemistry, Hahn-Meitner-Weg 1, 55128 Mainz, Germany

²School of Environment and Energy, South China University of Technology, Higher Education Mega Center, Guangzhou 510006, P.R. China

³Institute of General Botany, Johannes Gutenberg University Mainz, Johannes-von-Müller-Weg 6, 55128 Mainz, Germany

⁴Institute for Inorganic and Analytical Chemistry, Johannes Gutenberg University Mainz, Duesbergweg 10-14, 55128 Mainz, Germany

*Correspondence to Christopher J. Kampf, email: c.kampf@mpic.de, phone: +49 6131 305 6206

Electronic Supplementary 2 - 216_2016_9747_MOESM2_ESM.pdf

Electronic Supplementary 3 - 216_2016_9747_MOESM3_ESM.pdf

Table S1. Overview of all investigated air filter samples in this study.

Sample ID	Size range	Sampling period	Sampled air volume (m ³)	Protein concentration (µg/m ³)
344a	> 3 µm (coarse)	22/06/2010-29/06/2010	302	0.27 ± 0.01
344b	< 3 µm (fine)	22/06/2010-29/06/2010	2722	0.13 ± 0.01
Mz01a	> 3 µm (coarse)	02/06/2015-09/06/2015	301	0.32 ± 0.02
Mz01b	< 3 µm (fine)	02/06/2015-09/06/2015	2705	0.11 ± 0.01
Mz01c	TSP	02/06/2015-09/06/2015	1002	1.14 ± 0.11
Mz02c	TSP	01/07/2015-07/07/2015	975	1.27 ± 0.03

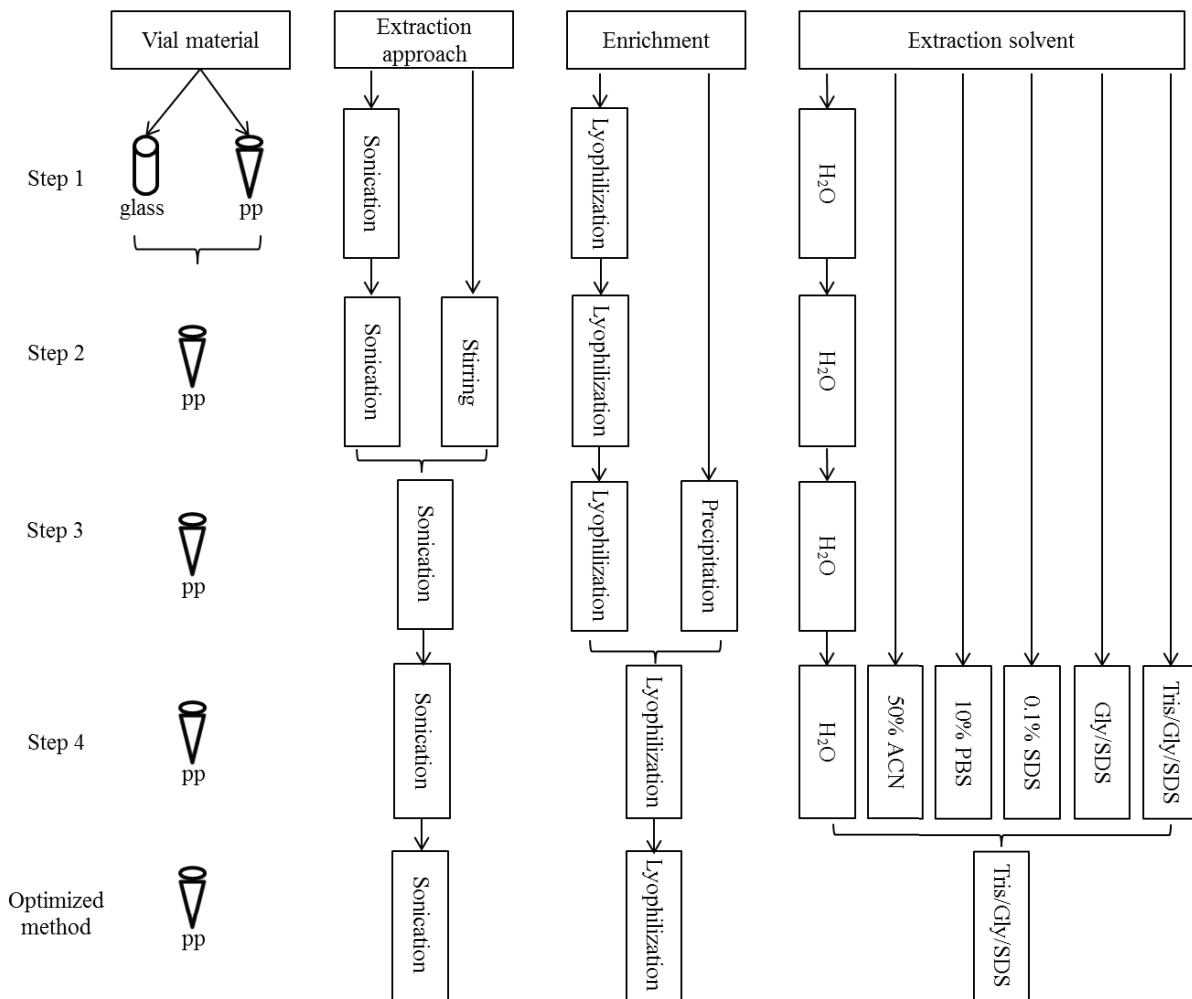


Fig. S1 Scheme of the development of extraction method. Sonication and stirring (step 2) were both conducted twice with 2 mL corresponding solvent for 1h. Precipitation (step 3) was performed with 100% trichloroacetic acid (TCA). Briefly, 0.37 mL 100% TCA was added to each c.a. 1.5 mL extract and incubated at -20°C for 1 h. Then the extract was centrifuged (15,000 rpm, 5 min) and the liquid was removed as much as possible. Subsequently 0.5 mL ice cold acetone was added to wash protein pellets for three times and afterwards the pellets were dried in a hood.

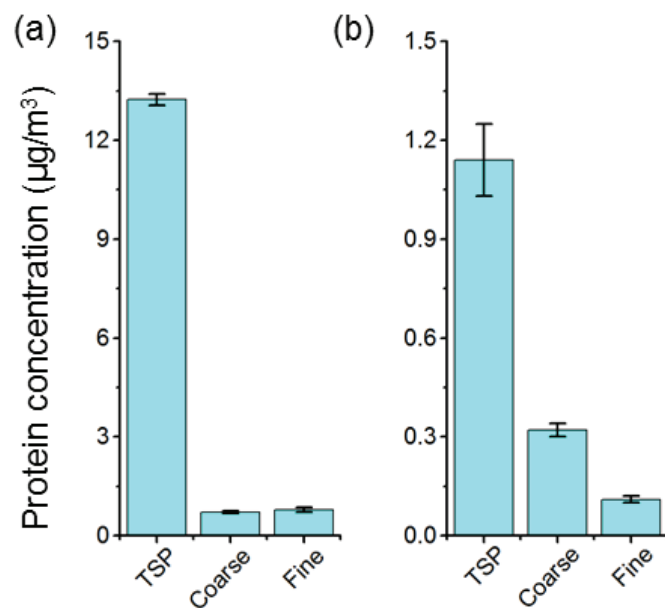
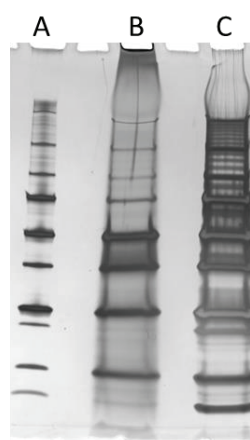


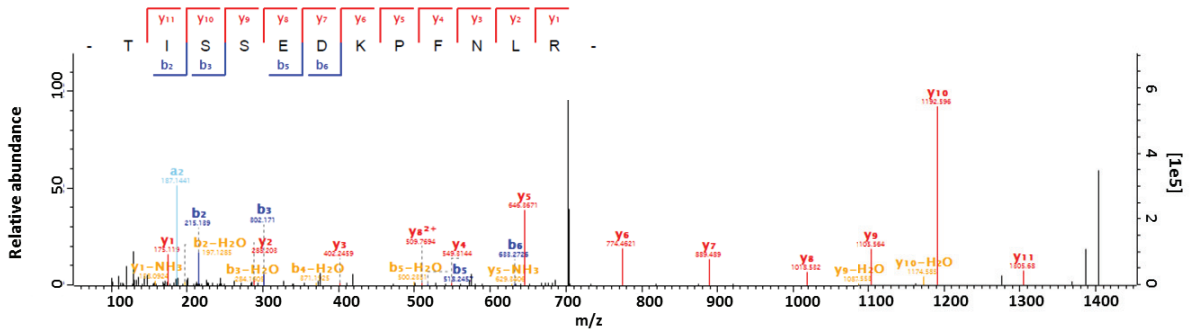
Fig. S2 Protein concentrations before (a) and after (b) size exclusion in ambient TSP (Mz01c), coarse (Mz01a) and fine (Mz01b) fraction particles, sampling in 02/06/2015-09/06/2015.



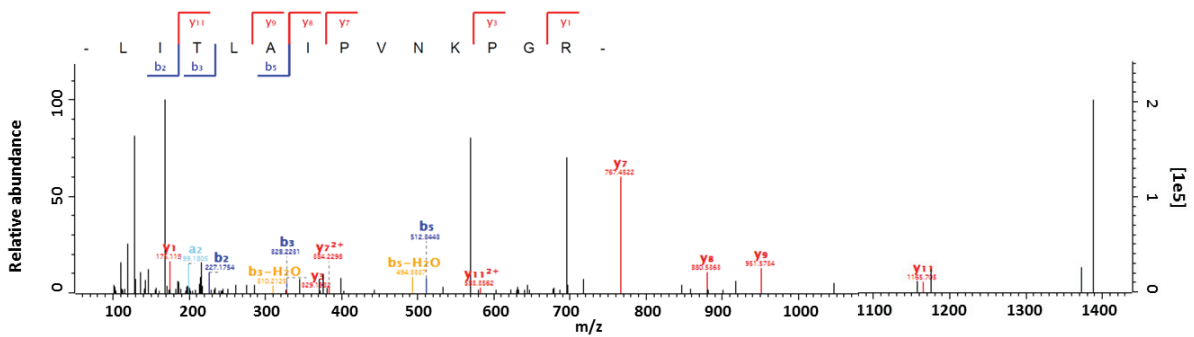
A: 0.5µL MW marker
 B: 0.4 mg soot + 2.5 µL MW marker
 C: 2.5 µL MW marker

Fig. S3 SDS-PAGE of protein molecular weight (MW) marker after silver staining.

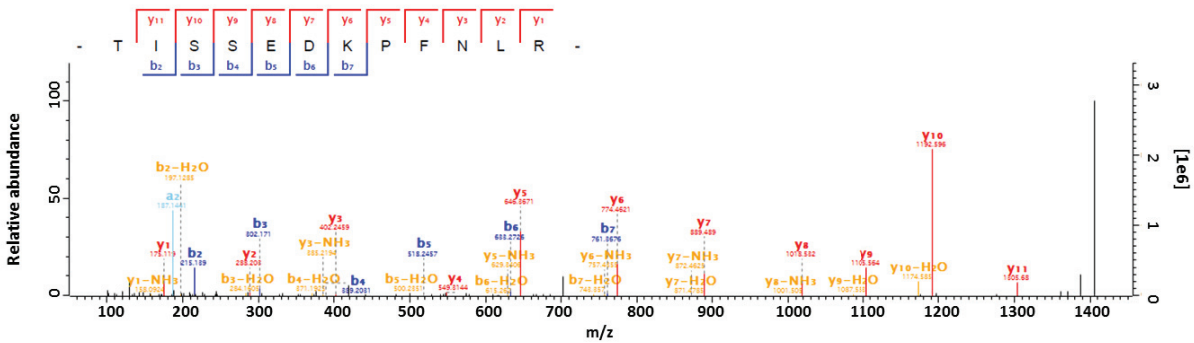
(a) Raw file: Mz02c02_na_PR_NON_060 Scan: 10488 Method: FTMS; HCD Score: 82.85 Mass: 1405.72



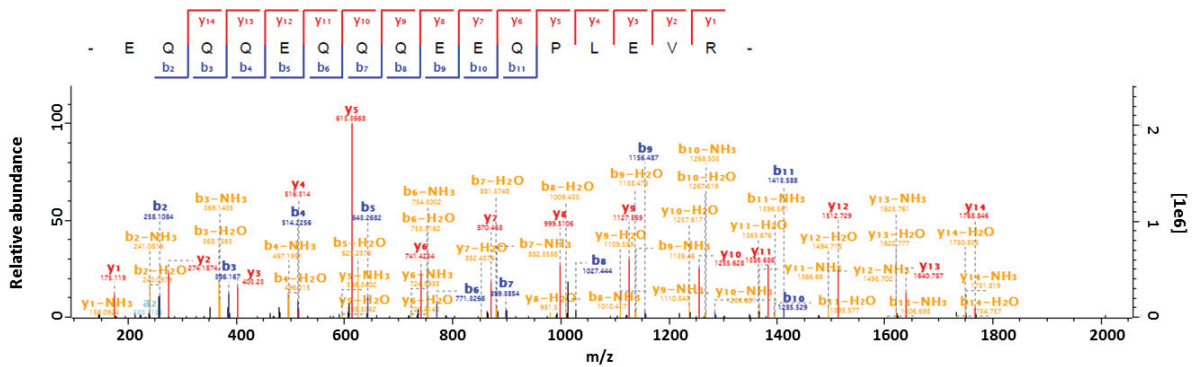
Raw file: Mz02c02_na_PR_NON_060 Scan: 10593 Method: FTMS; HCD Score: 48.04 Mass: 1390.866

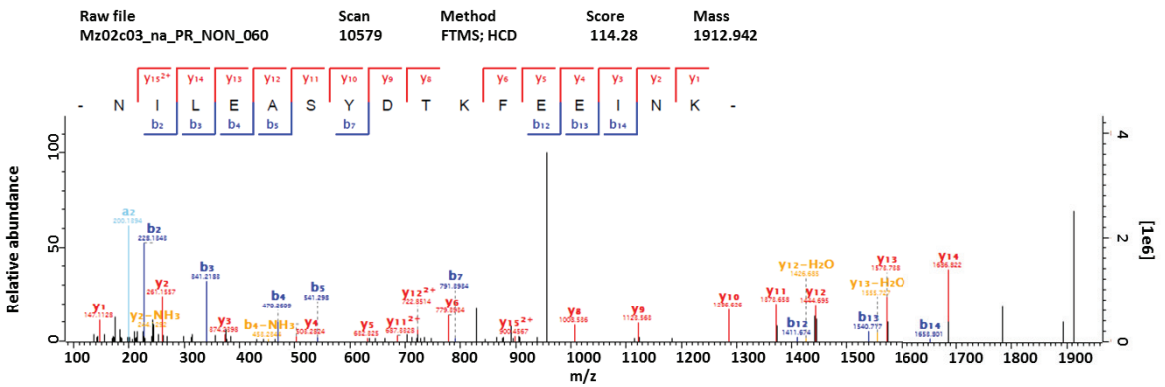
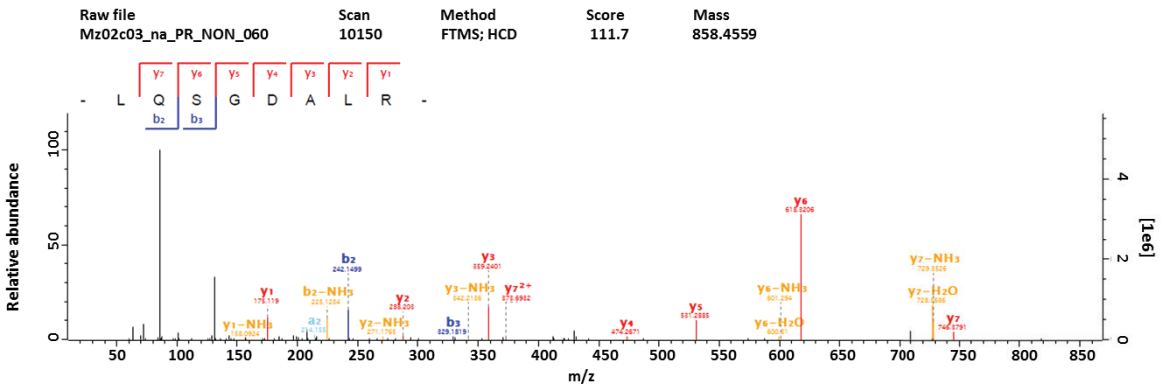
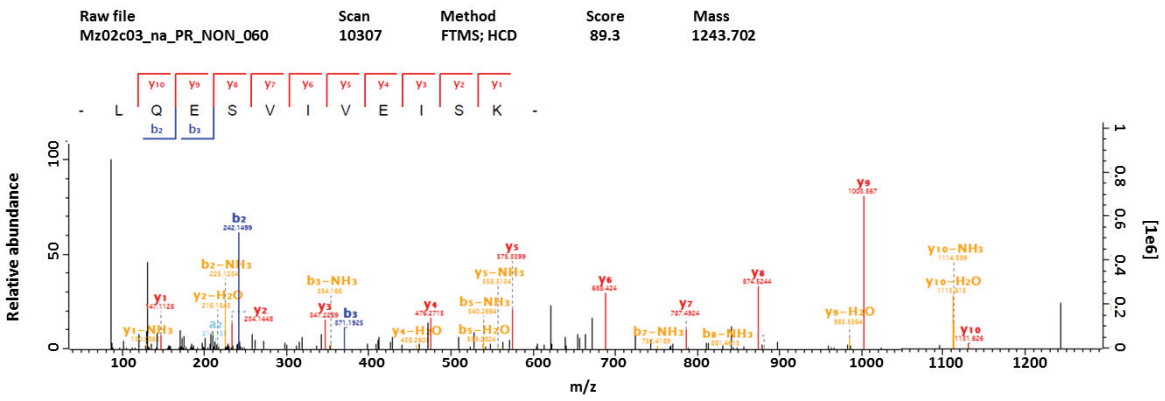
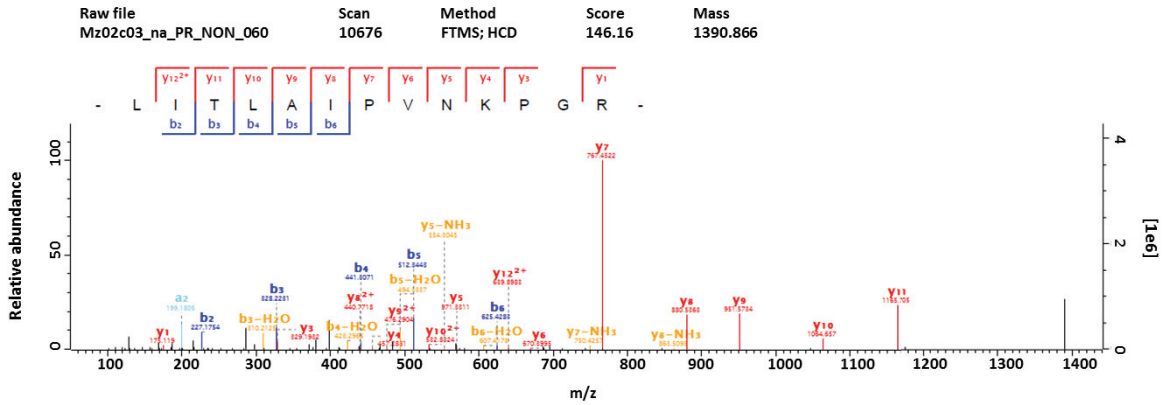


(b) Raw file: Mz02c03_na_PR_NON_060 Scan: 10488 Method: FTMS; HCD Score: 146.36 Mass: 1405.72

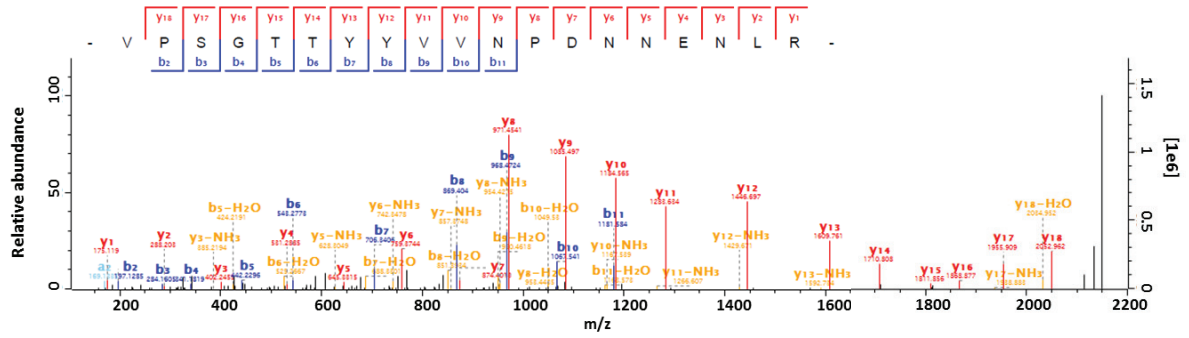


Raw file: Mz02c03_na_PR_NON_060 Scan: 9895 Method: FTMS; HCD Score: 428.85 Mass: 2024.94

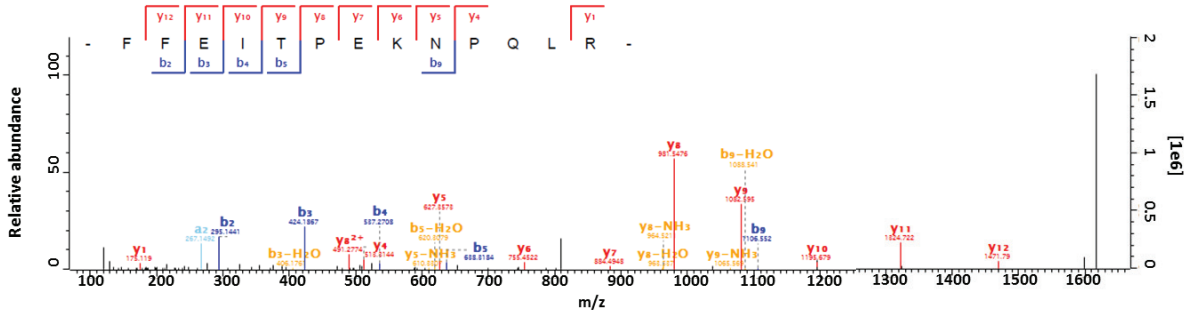




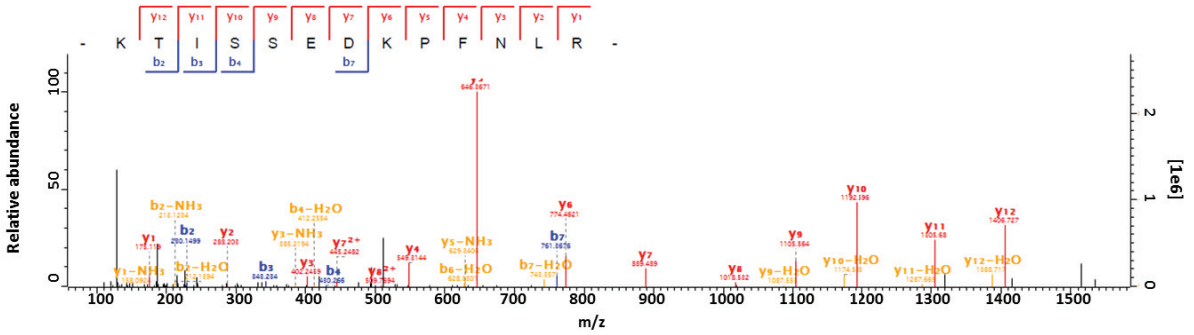
Raw file: Mz02c03_na_PR_NON_060 Scan: 10004 Method: FTMS;HCD Score: 275.37 Mass: 2151.023



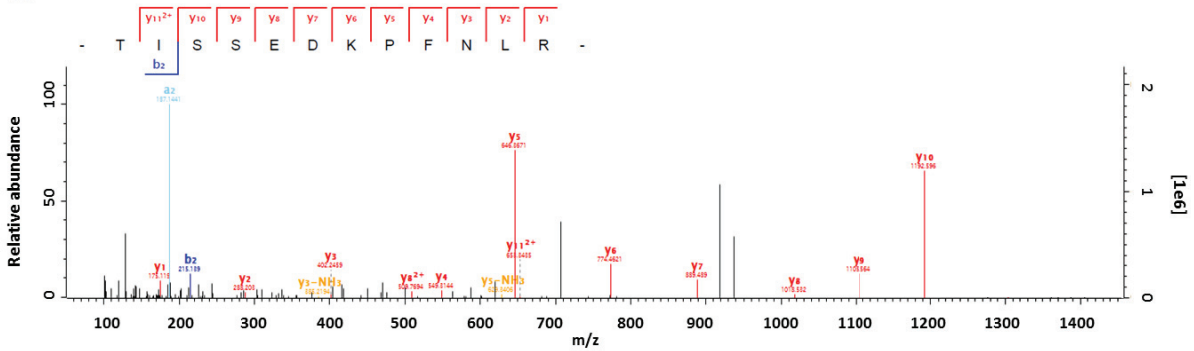
Raw file: Mz02c03_na_PR_NON_060 Scan: 10645 Method: FTMS;HCD Score: 134.56 Mass: 1617.852



Raw file: Mz02c03_na_PR_NON_060 Scan: 10722 Method: FTMS;HCD Score: 124.07 Mass: 1533.815



(c) Raw file: Mz02c04_na_PR_NON_060 Scan: 10336 Method: FTMS;HCD Score: 47.82 Mass: 1405.72



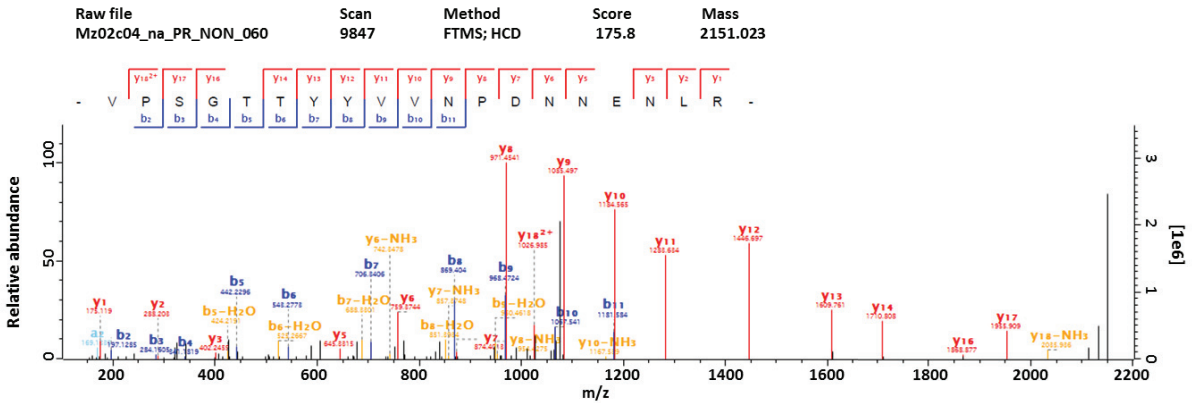
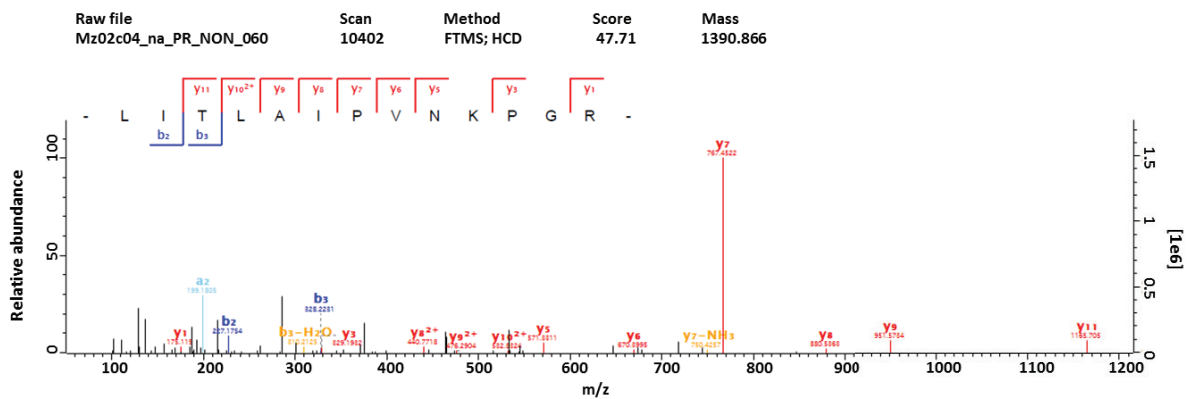
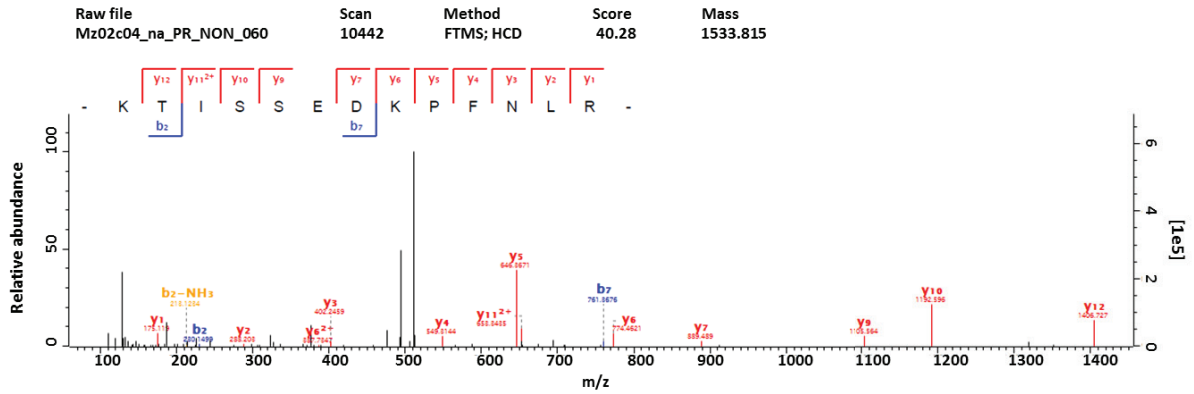


Fig. S4 MS/MS spectra of tryptic peptides of Beta-conglycinin, alpha chain in fraction F2 ((a), two unique peptides), F3 ((b), five unique peptides and four razor peptides) and F4 ((c), four unique peptides) in the TSP (Mz02c) sample.

31	Cubulin	Q9UNW5 P01861 P01860 P01859 P02026; protein inferred from homology P02026 P02024 P01861	protein inferred from homology	Fungi	Ascomycota	Ascomycota/ Clasophora	Sordariomycetes/ Eurotiomycetes/ Oligosporales	Magnaporales/ Glomeriales/ Sordariales/ Ospendales	Glomeriales/ Sordariales/ Heterotheliales	Magnaporales/ Glomeriales/ Sordariales/ Heterotheliales/ Aspergillales/ Eurotiomycetes	Magnaporales/ Glomeriales/ Sordariales/ Heterotheliales/ Aspergillales/ Eurotiomycetes	8	Magnaporales	2	2	2	2	1	17.0	16.1	6.29E-32	9.14E-07	
32	ADP-ATP carrier protein	Q90148	experimental evidence at transcript level	Fungi	Ascomycota	Schizosaccharomycetes	Schizosaccharomycetes	Schizosaccharomycetes	Schizosaccharomycetes	Schizosaccharomycetes	Schizosaccharomycetes	1	Schizosaccharomycetes	3	3	1	2	1	1	35.0	9	2.04E-09	3.71E-07
33	Histone H4	P09122 Q9NR03 Q9H113 Q75AX1 Q75TK Q9P169 P09101 Q9T784 Q9ZXX3 P09123 9	experimental evidence at protein level	Fungi	Animal	Ascomycota/ Basidiomycota/ Ascomycota/ Clasophora/ Ascomycota	Schizosaccharomycetes/ Saccharomycetes/ Eurotiomycetes/ Eurotiomycetes/ Eurotiomycetes/ Eurotiomycetes	Schizosaccharomycetes/ Saccharomycetes/ Eurotiomycetes/ Eurotiomycetes/ Eurotiomycetes/ Eurotiomycetes	Schizosaccharomycetes/ Saccharomycetes/ Eurotiomycetes/ Eurotiomycetes/ Eurotiomycetes/ Eurotiomycetes	Schizosaccharomycetes/ Saccharomycetes/ Eurotiomycetes/ Eurotiomycetes/ Eurotiomycetes/ Eurotiomycetes	Schizosaccharomycetes/ Saccharomycetes/ Eurotiomycetes/ Eurotiomycetes/ Eurotiomycetes/ Eurotiomycetes	Schizosaccharomycetes/ Saccharomycetes/ Eurotiomycetes/ Eurotiomycetes/ Eurotiomycetes/ Eurotiomycetes	10	Schizosaccharomycetes	2	2	1	2	1	11.4	29.1	9.38E-08	3.12E-08
34	Eradase	P12040	experimental evidence at protein level	Fungi	Ascomycota	Dothidiomycetes	Capnodiales	Cladospirales	Cladospirales	Cladospirales	Cladospirales	1	Dendrofulva	2	2	2	1	2	47.5	6.8	3.16E-129	1.41E-08	
35	Tetrahymenaphthalase reductase	P87025	protein inferred from homology	Fungi	Ascomycota	Sordariomycetes	Glomeriales	Glomeriales	Glomeriales	Glomeriales	Glomeriales	1	Glomeriales	2	2	2	1	2	29.8	7.8	9.45E-08	8.65E-07	
36	ATP-dependent RNA helicase dBFA	Q6U336 A0QVY2 Q7RV88 A6R181 Q2H E7A332 L2AR61 A1CT51 P19161 Q6 CDV4 P10041 A0ZQ11 Q6FQ06 A7TK55; A16B91 Q6_A0Z Q6B181 P1706 A1D VMI A15G78 Q5B181 Q11426 A2Q5N1; Q11P13	protein inferred from homology	Fungi	Ascomycota	Dothidiomycetes/ Sordariomycetes/ Eurotiomycetes/ Eurotiomycetes/ Eurotiomycetes/ Eurotiomycetes	Phycomycetes/ Eurotiomycetes/ Eurotiomycetes/ Eurotiomycetes/ Eurotiomycetes/ Eurotiomycetes	Phycomycetes/ Eurotiomycetes/ Eurotiomycetes/ Eurotiomycetes/ Eurotiomycetes/ Eurotiomycetes	Phycomycetes/ Eurotiomycetes/ Eurotiomycetes/ Eurotiomycetes/ Eurotiomycetes/ Eurotiomycetes	Phycomycetes/ Eurotiomycetes/ Eurotiomycetes/ Eurotiomycetes/ Eurotiomycetes/ Eurotiomycetes	Phycomycetes/ Eurotiomycetes/ Eurotiomycetes/ Eurotiomycetes/ Eurotiomycetes/ Eurotiomycetes	Phycomycetes/ Eurotiomycetes/ Eurotiomycetes/ Eurotiomycetes/ Eurotiomycetes/ Eurotiomycetes	24	Phycomycetes	3	3	2	1	2	44.5	8.8	5.66E-07	1.45E-08
37	Mitral dehydrogenase 1	E18266 B0BQ9N N1U6 P81373 Q9ZP 06 Q9ER A1Q4744 P17783 Q9N86 P95 02 P06074 Q7V84	protein inferred from homology for bacteria experimental evidence at protein/transcript level for plant protein	Bacteria/ Plant	Proteobacteria/ Streptophyta	Gamma-proteobacteria/ Magnetotactales	Proteobacteria/ Rosales/ Rhodiales/ Circulinales/ Sphaerales	Proteobacteria/ Rosales/ Rhodiales/ Circulinales/ Sphaerales	Proteobacteria/ Rosales/ Rhodiales/ Circulinales/ Sphaerales	Proteobacteria/ Rosales/ Rhodiales/ Circulinales/ Sphaerales	Proteobacteria/ Rosales/ Rhodiales/ Circulinales/ Sphaerales	12	Actinobacteria/ Heterotheliales/ Eurotiomycetes/ Eurotiomycetes/ Eurotiomycetes/ Eurotiomycetes	2	2	2	1	1	2	33.4	3.8	8.79E-403	9.27E-07
38	Ovalbumin	P01012	experimental evidence at protein level	Animal	Chordata	Aves	Galliformes	Phasianales	Phasianales	Gallus	Gallus	1	Gallus gallus	2	2	1	1	1	42.9	8.5	1.09E-05	4.27E-07	
39	Lactin	P82615	experimental evidence at protein level	Animal	Chordata	Mammalia	Perissodactyla	Equidae	Equidae	Equus	Equus	1	Equus caballus	3	3	1	3	2	24.7	15.8	2.10E-27	1.36E-08	

assignment of taxonomic rank antigens at higher rank
assignment of taxonomic rank antigens at phylum level

Information available on this website is provided for informational purposes only. It is not intended to be used for any purpose other than that for which it was intended. The information is provided "as is" without any warranty, express or implied, and without any liability for damages, including consequential, special, or punitive damages. The information is provided on an "as is" basis and is subject to change without notice. The information is provided on an "as is" basis and is subject to change without notice. The information is provided on an "as is" basis and is subject to change without notice.

Account Name	Account Type	Account Number	Account Balance	Account Status	Account Description	Account Location	Account Manager	Account Contact	Account Email	Account Phone	Account Fax	Account Website	Account Address	Account City	Account State	Account Zip	Account Country	Account Currency	Account Language	Account Timezone	Account Date	Account Time	Account User	Account Role	Account Permissions	Account Groups	Account Roles	Account Profiles	Account Settings	Account Preferences	Account Security	Account Audit	Account Logs	Account Reports	Account Analytics	Account Metrics	Account KPIs	Account Dashboards	Account Widgets	Account Tools	Account Integrations	Account Extensions	Account Add-ons	Account Plugins	Account Themes	Account Templates	Account Widgets	Account Tools	Account Integrations	Account Extensions	Account Add-ons	Account Plugins	Account Themes	Account Templates
Account 1	Account Type 1	Account Number 1	Account Balance 1	Account Status 1	Account Description 1	Account Location 1	Account Manager 1	Account Contact 1	Account Email 1	Account Phone 1	Account Fax 1	Account Website 1	Account Address 1	Account City 1	Account State 1	Account Zip 1	Account Country 1	Account Currency 1	Account Language 1	Account Timezone 1	Account Date 1	Account Time 1	Account User 1	Account Role 1	Account Permissions 1	Account Groups 1	Account Roles 1	Account Profiles 1	Account Settings 1	Account Preferences 1	Account Security 1	Account Audit 1	Account Logs 1	Account Reports 1	Account Analytics 1	Account Metrics 1	Account KPIs 1	Account Dashboards 1	Account Widgets 1	Account Tools 1	Account Integrations 1	Account Extensions 1	Account Add-ons 1	Account Plugins 1	Account Themes 1	Account Templates 1								

B.2. Liu et al., J. Chromatogr. A., 2017

Simultaneous determination of nitrated and oligomerized proteins by size exclusion high performance liquid chromatography coupled to photodiode array detection

Fobang Liu^a, Kathrin Reinmuth-Selzle^a, Senchao Lai^{b,a}, Michael G. Weller^c, Ulrich Pöschl^a,
and Christopher J. Kampf^{cd,e,a,*}

^a Multiphase Chemistry Department, Max Planck Institute for Chemistry, Hahn-Meitner-Weg
1, 55128 Mainz, Germany

^b School of Environment and Energy, South China University of Technology, Higher
Education Mega Center, Guangzhou 510006, P.R. China

^c Division 1.5 Protein Analysis, Federal Institute for Materials Research and Testing (BAM),
Richard-Willstätter-Str. 11, 12489 Berlin, Germany

^d Institute for Organic Chemistry, Johannes Gutenberg University, Duesbergweg 10-14,
55128 Mainz, Germany

^e Institute for Inorganic and Analytical Chemistry, Johannes Gutenberg University,
Duesbergweg 10-14, 55128 Mainz, Germany

*Correspondence to Christopher J. Kampf, email: c.kampf@mpic.de

Journal of Chromatography A, 2017, accepted

Simultaneous determination of nitrated and oligomerized proteins by size exclusion high-performance liquid chromatography coupled to photodiode array detection

Fobang Liu^a, Kathrin Reinmuth-Selzle^a, Senchao Lai^{b,a}, Michael G. Weller^c, Ulrich Pöschl^a, and Christopher J. Kampf^{d,e,a,*}

^a *Multiphase Chemistry Department, Max Planck Institute for Chemistry, Hahn-Meitner-Weg 1, 55128 Mainz, Germany*

^b *School of Environment and Energy, South China University of Technology, Higher Education Mega Center, Guangzhou 510006, P.R. China*

^c *Division 1.5 Protein Analysis, Federal Institute for Materials Research and Testing (BAM), Richard-Willstätter-Str. 11, 12489 Berlin, Germany*

^d *Institute for Organic Chemistry, Johannes Gutenberg University, Duesbergweg 10-14, 55128 Mainz, Germany*

^e *Institute for Inorganic and Analytical Chemistry, Johannes Gutenberg University, Duesbergweg 10-14, 55128 Mainz, Germany*

*Correspondence to Christopher J. Kampf, email: kampfch@uni-mainz.de, phone: +49 6131 39 22417

Highlights

- simultaneous detection of protein oligomers and their individual nitration degrees (ND)
- calculation of individual protein oligomer concentrations from their measured ND
- method validation against a well-established method for the determination of the ND of proteins
- suitable for the investigation of kinetics and mechanisms of protein tyrosine nitration and cross-linking

Abstract

Chemical modifications such as nitration and cross-linking may enhance the allergenic potential of proteins. The kinetics and mechanisms of the underlying chemical processes, however, are not yet well understood. Here, we present a size-exclusion chromatography/spectrophotometry method (SEC-HPLC-DAD) that allows a simultaneous detection of mono-, di-, tri-, and higher protein oligomers, as well as their individual nitration degrees (NDs). The ND results of proteins from this new method agree well with the results from an alternative well-established method, for the analysis of tetranitromethane (TNM)- and nitrogen dioxide and ozone (NO₂/O₃)-nitrated protein samples. Importantly, the NDs for individual oligomer fractions can be obtained from the new method, and also, we provide a proof of principle for the calculation of the concentrations for individual protein oligomer fractions by their determined NDs, which will facilitate the investigation of the kinetics and mechanism for protein tyrosine nitration and cross-linking.

Keywords: size exclusion chromatography; HPLC-DAD; protein nitration degree; protein oligomer analysis, nitrotyrosine.

1. Introduction

The determination of 3-nitrotyrosine (NTyr) in proteins is of central importance, as it can serve as a biomarker for inflammation, asthma and a wide range of diseases [1, 2]. Protein nitration leading to the formation of 3-nitrotyrosine, may occur endogenously and/or exogenously with different nitrating agents [3]. For example, protein tyrosine (Tyr) residues can be nitrated by peroxynitrite (ONOO^-) under physiological conditions [4]. In addition, the nitration of proteins was also observed upon their exposure to nitrogen dioxide (NO_2) and ozone (O_3) in synthetic gas mixtures and polluted urban air [3, 5]. This post-translational modification (PTM) of proteins has been associated with the enhancement of allergic diseases by air pollution [6].

Several analytical techniques have been developed to determine the extent of Tyr nitration in proteins/peptides, such as immunochemical and chromatographic methods. A summary of analytical methods for the NTyr detection and quantification can be found in a recent review [7]. Most of the current approaches enable and focus on the detection of nitrotyrosine as a free amino acid, or in digested peptides as well as in “whole” proteins [8-11]. However, the modifications induced by endogenous and exogenous reactive oxygen species (ROS) may also result in aggregation or fragmentation of proteins, modifying the allergenic potential of the proteins [12, 13]. Indeed, it has been shown that protein dimers and higher oligomers were formed through dityrosine formation upon exposure to atmospherically relevant concentrations of O_3 [14]. Therefore, in order to investigate the kinetics and mechanism for protein tyrosine nitration and dimerization (or oligomerization) by ROS (e.g., ONOO^- or NO_2/O_3) [14, 15] and thus to better evaluate the immunological effects induced by each detected molecular weight (MW) fraction,

an efficient method for the detection of nitration degrees (NDs) in individual oligomer fractions of proteins is required.

Here, we developed a size-exclusion chromatography/spectrophotometry method to enable the simultaneous detection of mono-, di-, tri-, and higher protein oligomers as well as their individual NDs, on the basis of a simple and efficient method recently established for determination of NDs for the birch pollen allergen Bet v 1 [16]. The applicability of the new method is validated by a comparison with the well-established method [16]. Also, we provide a proof of principle for the calculation of the concentrations for monomer, dimer and trimer by their determined NDs.

2. Materials and methods

2.1 Chemicals

Bovine serum albumin (BSA, A5611), tetranitromethane (TNM, T25003), L-3-nitrotyrosine (NTyr, ALX-106-020-G001), L-tyrosine (Tyr, 93829), sodium phosphate monobasic monohydrate ($\text{NaH}_2\text{PO}_4 \cdot \text{H}_2\text{O}$, 71504), methanol (MeOH, 494291) and acetonitrile (ACN, 34967) were purchased from Sigma-Aldrich (Germany). Water with 0.1 % (v/v) trifluoroacetic acid (TFA, LiChrosolv, 480112) was obtained from Merck KGaA (Germany). Sodium hydroxide (NaOH, 0583) was from VWR (Germany). PD-10 desalting columns were obtained from GE Healthcare (Germany). High purity water (18.2 M Ω cm) for Chromatography and UV spectrophotometry was taken from a Milli-Q Integral 3 water purification system (Merck Millipore, USA). For other purposes, high purity water (18.2 M Ω cm) was autoclaved before used if not specified otherwise.

2.2 Preparation of TNM-nitrated proteins

Protein nitration by TNM was carried out as described in Yang et al. [10]. Briefly, aliquots of aqueous protein solutions (20 mg mL⁻¹, 2.5 mL) were mixed with different amounts of TNM/MeOH (4%, v/v), yielding TNM/Tyr molar ratios of 1/3, 2/3, 1/1 and 2/1. Reaction mixtures were stirred for 3h at room temperature. Each reaction mixture was then eluted with ultrapure water on a PD-10 size exclusion chromatography column, according to the manufacturer's instructions, to remove excess TNM. The PD-10 columns separate compounds according to their molecular weight with a cutoff value of about 5 kDa. Each column was pre-equilibrated with 30 mL ultrapure water before use. After elution, eluates were diluted ten times and analyzed according to the reference method by Selzle et al. [16] and the newly developed SEC-HPLC-DAD method.

2.3 Nitration of proteins by NO₂/O₃ exposure

Aliquots of aqueous BSA solutions (0.13 mg mL⁻¹, 1.5 mL) were exposed to NO₂/O₃ mixtures. Briefly, O₃ was produced from synthetic air passed through a UV lamp (L.O.T.-Oriol GmbH & Co.KG, Germany) at ~1.98 L min⁻¹. The air flow was then mixed with another flow (20 mL min⁻¹) containing ~5 ppmV NO₂ in N₂ (Air Liquide, Germany). The resulting air gas mixtures were bubbled directly through the aqueous BSA solutions with a Teflon tube (ID: 1.59 mm) at a flow rate of 60 mL min⁻¹. The concentrations of O₃ and NO₂ were monitored by commercial monitoring instruments (Ozone analyzer, 49i, Thermo Scientific, Germany; NO_x analyzer, 42i-TL, Thermo Scientific, Germany), respectively. After exposure, the proteins were lyophilized and resuspended in 150 µL H₂O to concentrate the sample for further analysis.

2.4 Determination of scaling factors f and k by UV/Vis spectrophotometry

Selzle et al. [16] have introduced the scaling factors f and k (Eqs. 1 and 2) to calculate protein NDs (Eq. 3) according to Eq. 4 based on the Beer-Lambert Law using Reversed Phase (RP)-HPLC-DAD. In Eqs 1-4, $\varepsilon_{Tyr, 280}$, $\varepsilon_{NTyr, 280}$, and $\varepsilon_{NTyr, 357}$ are the molar extinction coefficients of Tyr at the wavelength of 280 nm, and of NTyr at wavelengths of 280 and 357 nm, respectively. The ND is defined as the concentration of NTyr (c_{NTyr} , in moles per liter) divided by the sum of the concentrations of NTyr and Tyr ($c_{NTyr} + c_{Tyr}$) [16]. $A_{all,280}$ and $A_{NTyr,280}$ are the absorbance signals of the intact proteins at wavelengths of 280 and 357 nm. The scaling factors were determined by analyzing the UV/Vis absorbance of three different concentrations of the free amino acids Tyr and NTyr, thereby eliminating the need of nitrated protein standards for calibration.

$$f = \frac{\varepsilon_{NTyr,280}}{\varepsilon_{Tyr,280}} \quad (1)$$

$$k = \frac{\varepsilon_{NTyr,280}}{\varepsilon_{NTyr,357}} \quad (2)$$

$$ND = \frac{c_{NTyr}}{c_{NTyr} + c_{Tyr}} \quad (3)$$

$$ND = \frac{A_{NTyr,357}}{A_{NTyr,357} + \frac{f}{k}(A_{all,280} - kA_{NTyr,357})} \quad (4)$$

Here, aiming to measure the individual ND of protein monomers and oligomers by SEC-HPLC-DAD analysis (details in “SEC-HPLC-DAD analysis”), we determined the scaling factor of f and k in the running buffer used for the analysis at pH 7. The scaling factors f and k were determined by measuring the absorbance of three different concentrations (0.05, 0.10, and 0.20 mM) of Tyr and NTyr (10 replicates each) in 150 mM NaH₂PO₄ buffer (pH 7) at wavelengths of 280 nm and 357 nm on a Lambda 25 UV/Vis spectrophotometer (Perkin Elmer, USA),

respectively. Scaling factors $k=2.50 \pm 0.04$ (linear regression, $n=3$) and $f=3.50 \pm 0.04$ (linear regression, $n=3$) at pH 7 were determined as shown in Fig. 1.

2.5 SEC-HPLC-DAD analysis

All samples were analyzed using high-performance liquid chromatography coupled to diode array detection (HPLC-DAD, Agilent Technologies 1200 series). The HPLC system consisted of a binary pump (G1379B), an autosampler with thermostat (G1330B), a column thermostat (G1316B), and a photodiode array detector (DAD, G1315C). ChemStation software (Rev. B.03.01, Agilent) was used for system control and data analysis. Molecular weight separation by size exclusion chromatography (SEC) was carried out using an AdvanceBio SEC column (Agilent, 300 Å, 300 × 4.6 mm, 2.7 μm). The mobile phase for isocratic separation was 150 mM NaH₂PO₄ buffer (pH 7, adjusted by adding 10 N NaOH). The flow rate was 0.35 mL min⁻¹ and the sample injection volume was 40 μL. The settings of DAD were as follows: full spectra were recorded at wavelengths of 200-800 nm every 2 s with a slit width of 4 nm and in steps of 2 nm. Chromatograms at wavelengths of 220, 280 and 357 nm were used for analysis. Each chromatographic run was performed in duplicate.

The determination of protein oligomer fractions was carried out as described in Kampf et al. [14]. Briefly, a protein standard mix 15-600 kDa (69385, Sigma-Aldrich, Germany) was used for the molecular weight (MW) calibration (elution time vs log MW; calibration curve provided in Fig. 2). The BSA oligomer fractions are reported as the ratios of the respective oligomer fractions (monomer, dimer, trimer, and higher oligomers with $n \geq 4$) to the sum of monomer and all oligomer peak areas at 220 nm [14]. Assuming that the molar extinction coefficients of the individual protein oligomer fractions are multiples of the monomer extinction coefficient, the

calculated oligomer ratios correspond to the oligomer mass fractions (ω , percentage by mass of the individual oligomers to the mass of the total protein). Exemplary chromatograms at 280 nm for a native BSA sample, TNM-nitrated BSA and NO₂/O₃-nitrated BSA are provided in Fig. 3. The commercially available native BSA contains monomer, dimer and trimer variants of the protein according to the molecular weights calculated by the calibration curve for the chromatographic signals in Fig. 3a. The oligomer mass fractions ω reported in Fig. 5 were corrected for this background.

The ND of individual oligomers was calculated according to Eq. 4 introduced by Selzle et al. [16], using the peak areas of respective oligomer signals monitored at wavelengths of 280 nm and 357 nm. The total protein ND was calculated using the sum of the peak areas of all MW fractions at wavelengths of 280 nm and 357 nm, respectively.

In addition to the calculation of the respective oligomer fractions outlined above, we provide a proof of principle for the calculation of the concentrations of monomer, dimer and trimer in the protein solution as follows:

$$C_P = C_M + 2C_D + 3C_T \quad (5)$$

where C_P , C_M , C_D and C_T are the concentrations of the total protein, monomer, dimer and trimer in solution.

The combined ND of the monomer plus dimer fraction ($ND_{(M+D)}$), and of the monomer plus trimer fraction ($ND_{(M+T)}$) can be formulated as Eq.6 and Eq.7, respectively, according to the definition of ND (Eq.3; [16]) and assuming the extinction coefficients of the individual protein oligomer fractions are multiples of the monomer extinction coefficients for the specific wavelengths:

$$ND_{(M+D)} = \frac{n_{Tyr}C_M ND_M + 2n_{Tyr}C_D ND_D}{n_{Tyr}C_M + 2n_{Tyr}C_D} \quad (6)$$

$$ND_{(M+T)} = \frac{n_{Tyr}C_M ND_M + 3n_{Tyr}C_T ND_T}{n_{Tyr}C_M + 3n_{Tyr}C_T} \quad (7)$$

where n_{Tyr} is the number of Tyr residues in the investigated protein, i.e., 20 for BSA [17], and ND_M , ND_D and ND_T are the individual ND of the protein monomer, dimer and trimer, respectively. Thus, the C_D and C_T can be generalized using the following expressions:

$$C_D = \frac{C_M(ND_M - ND_{(M+D)})}{2(ND_{(M+D)} - ND_D)} \quad (8)$$

$$C_T = \frac{C_M(ND_M - ND_{(M+T)})}{3(ND_{(M+T)} - ND_T)} \quad (9)$$

Therefore, Eq.5 can be re-formulated as:

$$C_P = C_M + \frac{C_M(ND_M - ND_{(M+D)})}{(ND_{(M+D)} - ND_D)} + \frac{C_M(ND_M - ND_{(M+T)})}{(ND_{(M+T)} - ND_T)} \quad (10)$$

Note that the $ND_{(M+D)}$ and $ND_{(M+T)}$ can be calculated from Eq.4. Thus, we can derive C_M , C_D and C_T from Eqs.8-10, assuming the concentration of the investigated protein is known or has been determined.

2.6 HPLC-DAD analysis

For comparison with an established method, total protein NDs were determined according to Selzle et al. [16], using the same HPLC-DAD system as described above, equipped with a monofunctionally bound C_{18} column (Vydac 238TP, 250 mm×2.1 mm inner diameter, 5 μ m particle size; Grace Vydac, Alltech) for chromatographic separation. Briefly, samples were separated using the following gradient of 0.1% (v/v) trifluoroacetic acid in water (eluent A) and ACN (eluent B): the solvent gradient started at 3 % B followed by a linear gradient to 90 % B within 15 min, flushing back to 3% B within 0.2 min, and maintaining 3 % B for additional 2.8 min. Column re-equilibration time was 5 min before the next run. Note that the elution method has been applied for the determination of protein NDs in laboratory studies on the nitration of

individual proteins by different nitrating agents, i.e., the nitration of the major birch pollen allergen Bet v 1 by TNM, peroxyxynitrite, as well as O₃/NO₂ [3]. However, for the analysis of protein mixtures, different elution methods should be considered. Settings of the DAD were as follows: full spectra were recorded at wavelengths of 200–600 nm every 2 s with a slit width of 4 nm and in steps of 2 nm. The peak areas of the protein signal at wavelengths of 280 and 357 nm were used for the determination of NDs according to Eq. 4.

3. Results and discussion

For validation, the total protein NDs obtained for TNM-nitrated and NO₂/O₃-nitrated BSA samples using the newly developed SEC-HPLC-DAD method were compared with the results obtained by the established HPLC-DAD method, as shown in Fig. 4.

Both methods agree very well for the two ranges of total protein NDs resulting from the two different nitration setups. The TNM-nitrated protein samples show a high ND, ranging from 0.1 to 0.3, while the NDs of NO₂/O₃-nitrated protein samples were about one magnitude lower (0.03~0.06). In both correlation plots the slopes are close to 1 and show high correlation coefficients (>0.997 for TNM-nitrated BSA, Fig. 4a; >0.988 for NO₂/O₃-nitrated BSA, Fig. 4b), which confirms the applicability of the SEC-HPLC-DAD method for the ND determination of protein samples. With regard to the ND, the detection limit of our method was found to be 0.012, determined by nine consecutive measurements of unmodified BSA samples (1.33 mg L⁻¹). It should be noted, that Tyr and NTyr extinction coefficients at 280 and 357 nm are higher in acidic solutions (~pH 3) than in neutral solutions (pH 7), respectively [18]. Therefore, the SEC-HPLC-DAD limit of detection for ND determination of BSA is higher than that previously reported [10, 16]. Indeed, we found that in neutral solutions the extinction coefficient of BSA is about 0.6

times that in acidic solution for the wavelength of 280 nm and ~ 0.5 for 357 nm by a division of the corresponding integrated peak areas. Additionally, the absorption of tryptophan (Trp) at 280 nm should be taken into account as a potential interference for this method. However, our results showed that this interference has little influence on BSA samples, which may be explained by a much higher number of tyrosines than tryptophans in BSA (20 Tyr, 2 Trp). Also, no interference was found for ovalbumin (OVA, 10 Tyr, 3 Trp), as demonstrated in our previous study [16].

In addition to the determination of the total protein ND, SEC-HPLC-DAD analysis yields NDs of the individual oligomer fractions in nitrated protein samples as shown in Fig. 5a and b. Fig. 5a shows a positive relationship between NDs for monomeric, dimeric and trimeric BSA and molar ratios of TNM/Tyr residues in the protein. Fig. 5b shows the temporal evolution of BSA monomer and dimer NDs for different exposure times to a NO_2/O_3 mixture. In both cases the ND decreases as the oligomerization state of the protein increases. Note that corresponding to the definition of the ND (Eq. 3), the same number of NTyr residues in a BSA monomer and dimer (or trimer), will yield a factor of 2 (or 3) difference in the individual NDs, because a BSA dimer (or trimer) contains twice (or triple) the number of Tyr residues compared to the monomer.

Table 1 shows concentrations of monomeric, dimeric, and trimeric BSA species (C_M , C_D and C_T) calculated from the NDs of the individual oligomer fractions obtained for TNM-nitrated BSA samples as outlined in the section "SEC-HPLC-DAD analysis". The C_M , C_D and C_T in the four samples were very similar, with an average of 16.61 ± 0.33 , 1.72 ± 0.04 and 0.48 ± 0.04 mM, respectively. The C_O values were not calculated, because the corresponding chromatographic peaks could not be well separated. For example, Fig. 3c shows higher concentrations of oligomers formed in the NO_2/O_3 -nitrated BSA samples in the dashed box labeled "O", which illustrates the difficulty in estimating their molecular weight due to the non-

optimal peak shape, resulting from low concentrations of higher oligomers and chromatographic resolution limitations of the applied SEC. Nevertheless, the results indicate that oligomerization is a minor pathway compared to nitration in the TNM/BSA reaction system.

4. Conclusions

In this study, we developed a SEC-HPLC-DAD method for the simultaneous detection of mono-, di-, tri- and higher protein oligomers as well as their individual ND. The ND determination of the new method has been validated using a series of nitrated BSA samples against the original method [16]. The results of the validation show a very good agreement between both methods with correlation plot slopes of ~ 1 and correlation coefficients >0.988 . Further, we introduce a formalism to calculate concentrations of monomeric, dimeric and trimeric protein species in single protein solutions through the determined NDs. The new method combines and improves methods by Selzle et al. [16] and Kampf et al. [14] to reduce analysis time and sample consumption. Overall, the new method provides a single run analysis for the simultaneous investigation of reaction kinetics and mechanisms of protein tyrosine nitration and cross-linking by ROS (e.g., NO_2/O_3 , ONOO^-). Furthermore, additional information about the NDs of individual oligomer fractions can be obtained, which will be useful in follow-up studies on the immunogenicity of nitrated/non-nitrated variants of individual protein oligomer fractions.

Acknowledgment

F.L. and S.L. acknowledge the financial support from China Scholarship Council (CSC). C.J.K. acknowledges support by the Max Planck Graduate Center with the Johannes Gutenberg University Mainz (MPGC) and financial support by the German Research Foundation (DFG,

grant no. KA4008/1-2). K. R-S. acknowledges financial support by Max Planck Graduate Center with the Johannes Gutenberg University Mainz (MPGC). We thank Dr. Pascale S. J. Lakey (Max Planck Institute for Chemistry) for helpful discussions during the revision of the manuscript.

References

- [1] S. Ghosh, A.J. Janocha, M.A. Aronica, S. Swaidani, S.A. Comhair, W. Xu, L. Zheng, S. Kaveti, M. Kinter, S.L. Hazen, Nitrotyrosine proteome survey in asthma identifies oxidative mechanism of catalase inactivation, *J. Immunol.* 176 (2006) 5587-5597.
- [2] G. Saravanabhavan, E. Blais, R. Vincent, P. Kumarathasan, A high performance liquid chromatography-electrochemical array method for the measurement of oxidative/nitrative changes in human urine, *J. Chromatogr. A* 1217 (2010) 3269-3274.
- [3] K. Reinmuth-Selzle, C. Ackaert, C.J. Kampf, M. Samonig, M. Shiraiwa, S. Kofler, H. Yang, G. Gadermaier, H. Brandstetter, C.G. Huber, A. Duschl, G.J. Oostingh, U. Pöschl, Nitration of the birch pollen allergen Bet v 1.0101: efficiency and site-selectivity of liquid and gaseous nitrating agents, *J. Proteome. Res.* 13 (2014) 1570-1577.
- [4] R. Radi, Protein tyrosine nitration: biochemical mechanisms and structural basis of functional effects, *Accounts. Chem. Res.* 46 (2012) 550-559.
- [5] N. Lang-Yona, T. Shuster-Meiseles, Y. Mazar, O. Yarden, Y. Rudich, Impact of urban air pollution on the allergenicity of *Aspergillus fumigatus* conidia: Outdoor exposure study supported by laboratory experiments, *Sci. Total. Environ.* 541 (2016) 365-371.
- [6] U. Pöschl, M. Shiraiwa, Multiphase chemistry at the atmosphere–biosphere interface influencing climate and public health in the Anthropocene, *Chem. Rev.* 115 (2015) 4440-4475.
- [7] D. Teixeira, R. Fernandes, C. Prudêncio, M. Vieira, 3-Nitrotyrosine quantification methods: Current concepts and future challenges, *Biochimie.* 125 (2016) 1-11.

- [8] J. Guo, K. Prokai-Tatrai, L. Prokai, Relative quantitation of protein nitration by liquid chromatography–mass spectrometry using isotope-coded dimethyl labeling and chemoprecipitation, *J. Chromatogr. A* 1232 (2012) 266-275.
- [9] C. Massip, P. Riollot, E. Quemener, C. Bayle, R. Salvayre, F. Couderc, E. Causse, Choice of different dyes to label tyrosine and nitrotyrosine, *J. Chromatogr. A* 979 (2002) 209-215.
- [10] H. Yang, Y. Zhang, U. Pöschl, Quantification of nitrotyrosine in nitrated proteins, *Anal. Bioanal. Chem.* 397 (2010) 879-886.
- [11] Y. Zhang, H. Yang, U. Pöschl, Analysis of nitrated proteins and tryptic peptides by HPLC-chip-MS/MS: site-specific quantification, nitration degree, and reactivity of tyrosine residues, *Anal. Bioanal. Chem.* 399 (2011) 459-471.
- [12] S. Kofler, C. Ackaert, M. Samonig, C. Asam, P. Briza, J. Horejs-Hoeck, C. Cabrele, F. Ferreira, A. Duschl, C. Huber, Stabilization of the dimeric birch pollen allergen Bet v 1 impacts its immunological properties, *J. Biol. Chem.* 289 (2014) 540-551.
- [13] E.R. Stadtman, Protein oxidation and aging, *Free. Radical. Res.* 40 (2006) 1250-1258.
- [14] C.J. Kampf, F. Liu, K. Reinmuth-Selzle, T. Berkemeier, H. Meusel, M. Shiraiwa, U. Pöschl, Protein cross-linking and oligomerization through dityrosine formation upon exposure to ozone, *Environ. Sci Technol.* 49 (2015) 10859-10866.
- [15] P. Ahmad, A. Ali, Peroxynitrite induced structural changes result in the generation of neo-epitopes on human serum albumin, *Int. J. Biol. Macromol.* 59 (2013) 349-356.
- [16] K. Selzle, C. Ackaert, C.J. Kampf, A.T. Kunert, A. Duschl, G.J. Oostingh, U. Pöschl, Determination of nitration degrees for the birch pollen allergen Bet v 1, *Anal. Bioanal. Chem.* 405 (2013) 8945-8949.
- [17] A. Hesse, M.G. Weller, Protein quantification by derivatization-free high-performance liquid chromatography of aromatic amino acids, *J. Amino. Acids.* 2016 (2016) 1-8.
- [18] V. De Filippis, R. Frasson, A. Fontana, 3–Nitrotyrosine as a spectroscopic probe for investigating protein–protein interactions, *Protein Sci.* 15 (2006) 976-986.

Figure captions

Fig. 1. Determination of scaling factors k and f by UV photometry of tyrosine (Tyr) and nitrotyrosine (NTyr) in 150 mM NaH_2PO_4 (aq, adjusted to pH 7 by 10 N NaOH): (a) Scaling factor $k = 2.50 \pm 0.04$ ($R^2 = 0.99$, $n=3$) was determined as the slope of a linear least squares fit by plotting the absorbance signal of NTyr at 280 nm ($A_{\text{NTyr}, 280 \text{ nm}}$) against the absorbance signal of NTyr at 357 nm ($A_{\text{NTyr}, 357 \text{ nm}}$); (b) Scaling factor $f = 3.50 \pm 0.04$ ($R^2 = 0.99$, $n=3$) was determined as the slope of a linear least squares fit by plotting the absorbance signal of NTyr at 280 nm ($A_{\text{NTyr}, 280 \text{ nm}}$) against the absorbance signal of Tyr at 280 nm ($A_{\text{Tyr}, 280 \text{ nm}}$). Three different concentrations (0.05, 0.10, and 0.20 mM) were measured and the error bars represent the standard deviation of 10 experimental replicates for each concentration.

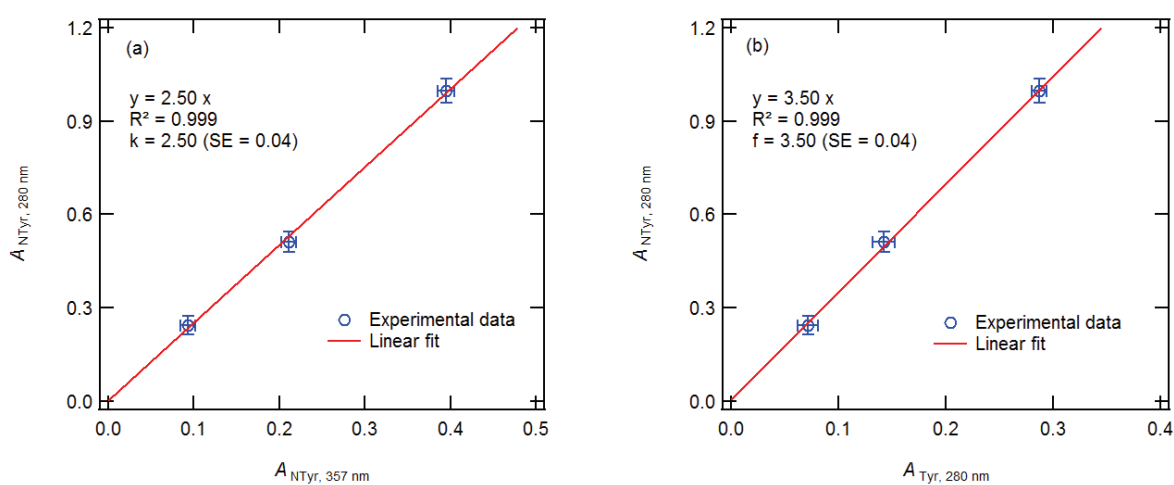


Fig. 2. Calibration curve plotting the logarithm of molecular weight ($\log(\text{MW})$) against retention time (RT) of the protein standard mix. The fitting equation was $y = -0.42x + 5.21$, $R^2 = 0.99$. The protein standard mix 15–600 kDa (69385, Sigma-Aldrich, Steinheim, Germany) contains bovine thyroglobulin (MW = 670 kDa), γ -globulins from bovine blood (MW = 150 kDa), albumin chicken egg grade VI (MW = 44.3 kDa), and ribonuclease A (MW = 13.7 kDa).

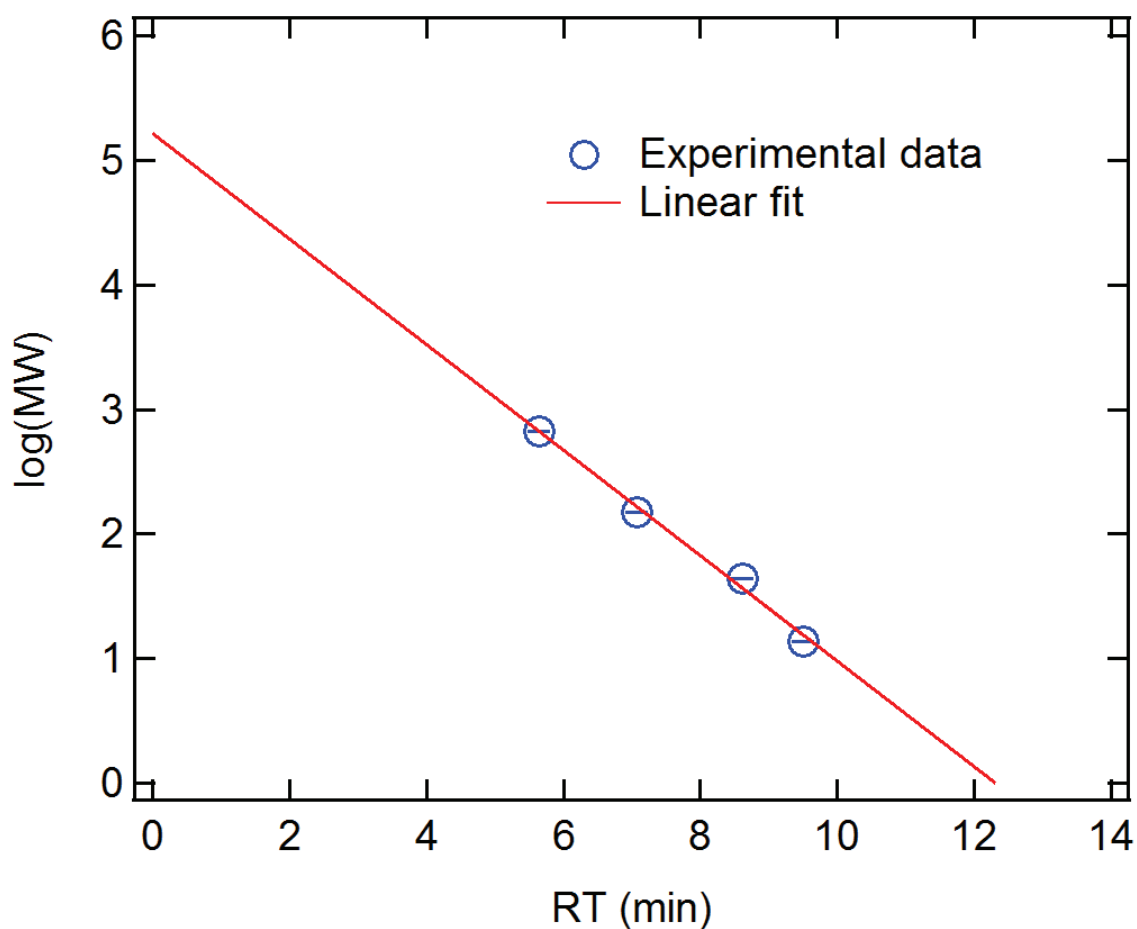


Fig. 3. SEC-HPLC-DAD chromatograms at 280 nm for native BSA and nitrated BSA in aqueous solutions. (a) 1.3 mg mL⁻¹ BSA, (b) 1.1 mg mL⁻¹ TNM-nitrated BSA (TNM/Tyr = 1/3, mol/mol), 3 h reaction, (c) 1.3 mg mL⁻¹ NO₂/O₃-nitrated BSA, 200 ppb O₃/50ppb NO₂, 1 h reaction.

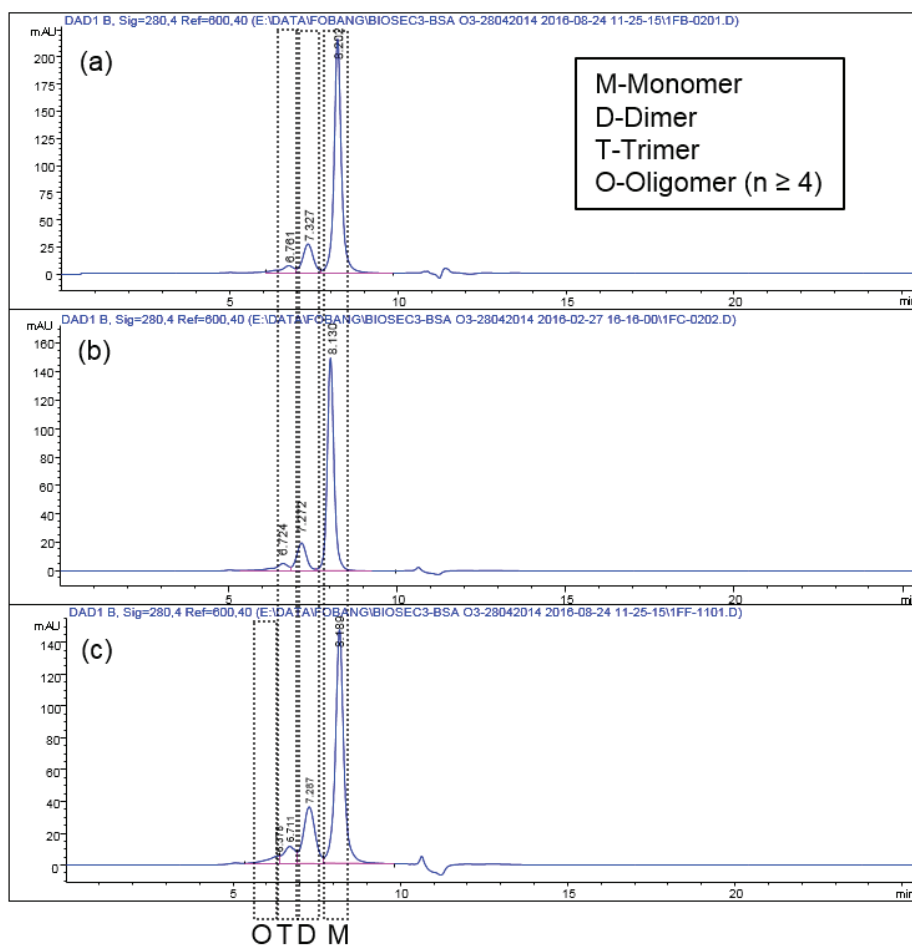


Fig. 4. Method comparison for: (a) TNM-nitrated BSA samples and (b) NO₂/O₃-nitrated BSA samples. NDs from HPLC-DAD calibrated with the amino acids Tyr and NTyr at pH 3 are plotted against NDs from SEC-HPLC-DAD calibrated with the amino acids Tyr and NTyr at pH 7.

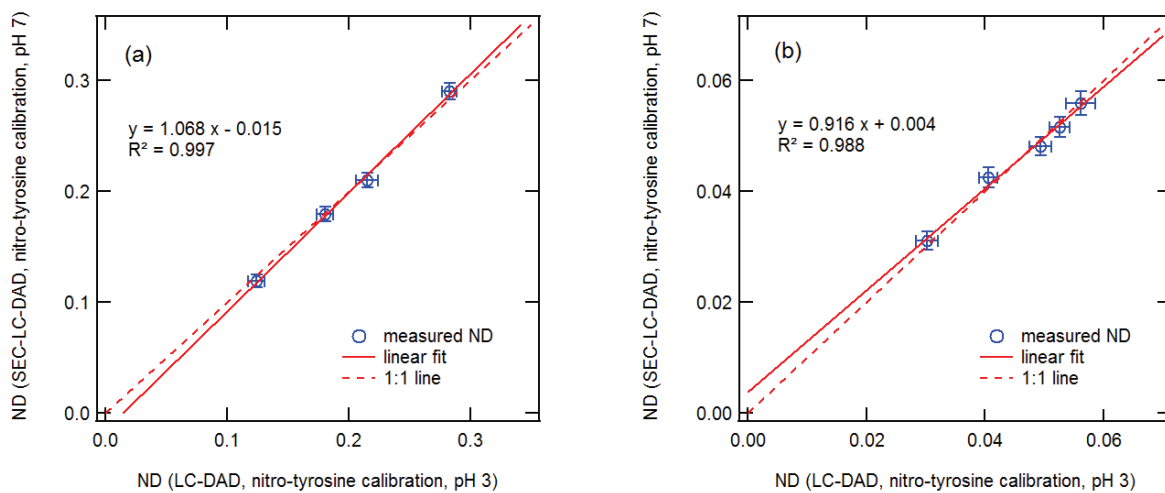


Fig. 5. (a) NDs of monomer, dimer and trimer vs. molar ratio of TNM to tyrosine residues in nitrated BSA samples. (b) Temporal evolution of NDs for monomer, dimer in the aqueous phase reaction of BSA with 200 ppb O₃ and 50 ppb NO₂. (c) The variation of dimer and trimer mass fractions in TNM-nitrated BSA samples. (d) Temporal evolution of protein dimer, trimer and oligomer mass fractions in the aqueous phase reaction of BSA with 200 ppb O₃ and 50 ppb NO₂.

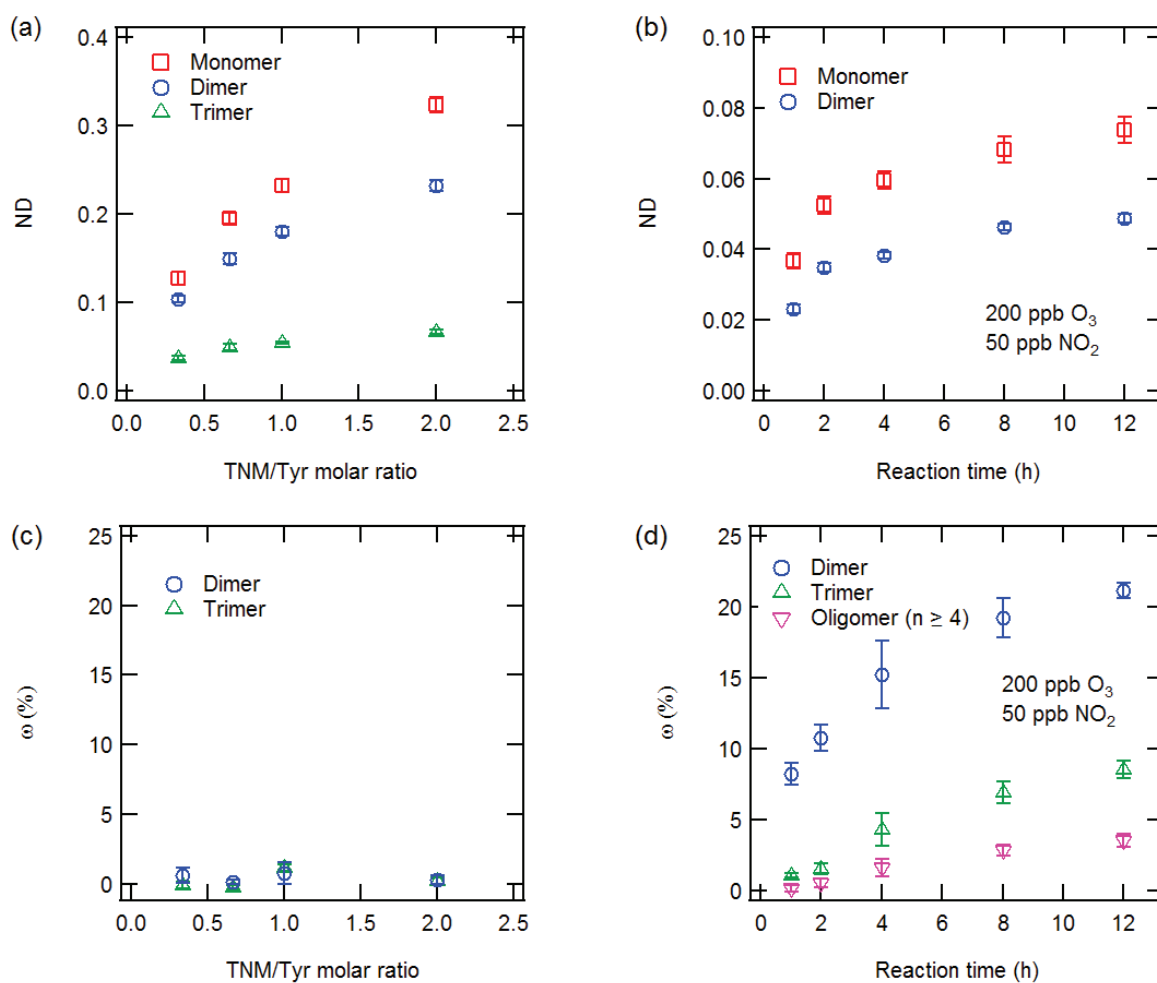


Table 1 The concentrations of monomer, dimer and trimer in the TNM nitrated-BSA samples, calculated from their determined NDs. The calculation method is outlined in the section “SEC-HPLC-DAD analysis”.

Sample	TNM/Tyr (mol/mol)	C_M (μM)	C_D (μM)	C_T (μM)
TNM-nitro-BSA-1	1/3	16.94 ± 0.02	1.68 ± 0.02	0.40 ± 0.02
TNM-nitro-BSA-2	2/3	16.84 ± 0.02	1.69 ± 0.03	0.43 ± 0.02
TNM-nitro-BSA-3	1/1	16.29 ± 0.03	1.75 ± 0.03	0.57 ± 0.03
TNM-nitro-BSA-4	2/1	16.38 ± 0.03	1.76 ± 0.03	0.53 ± 0.03
Mean \pm S.D.:		16.61 ± 0.33	1.72 ± 0.04	0.48 ± 0.04

B.3. Kampf et al., Environ. Sci. Technol., 2015

**Protein cross-linking and oligomerization through dityrosine formation
upon exposure to ozone**

Christopher J. Kampf^{1,2,#,*}, Fobang Liu^{2,#}, Kathrin Reinmuth-Selzle², Thomas Berkemeier²,
Hannah Meusel², Manabu Shiraiwa², Ulrich Pöschl²

¹Institute of Inorganic and Analytical Chemistry, Johannes Gutenberg University, Mainz,
Germany

²Multiphase Chemistry Department, Max Planck Institute for Chemistry, Mainz, Germany

#these authors contributed equally

*Correspondence to Christopher J. Kampf, email: kampf@uni-mainz.de

Environmental science & technology, 2015, 49(18):10859-66.

Protein Cross-Linking and Oligomerization through Dityrosine Formation upon Exposure to Ozone

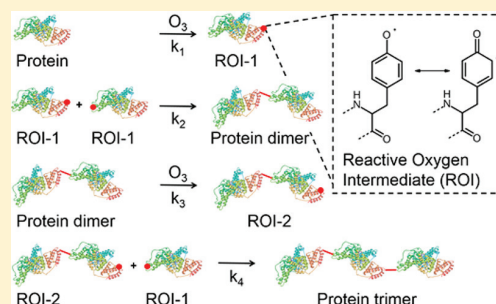
Christopher J. Kampf,^{*,†,‡,§} Fobang Liu,^{‡,§} Kathrin Reinmuth-Selzle,[‡] Thomas Berkemeier,[‡] Hannah Meusel,[‡] Manabu Shiraiwa,[‡] and Ulrich Pöschl[‡]

[†]Institute of Inorganic and Analytical Chemistry, Johannes Gutenberg University Mainz, 55128 Mainz, Germany

[‡]Multiphase Chemistry Department, Max Planck Institute for Chemistry, 55128 Mainz, Germany

S Supporting Information

ABSTRACT: Air pollution is a potential driver for the increasing prevalence of allergic disease, and post-translational modification by air pollutants can enhance the allergenic potential of proteins. Here, the kinetics and mechanism of protein oligomerization upon ozone (O_3) exposure were studied in coated-wall flow tube experiments at environmentally relevant O_3 concentrations, relative humidities and protein phase states (amorphous solid, semisolid, and liquid). We observed the formation of protein dimers, trimers, and higher oligomers, and attribute the cross-linking to the formation of covalent intermolecular dityrosine species. The oligomerization proceeds fast on the surface of protein films. In the bulk material, reaction rates are limited by diffusion depending on phase state and humidity. From the experimental data, we derive a chemical mechanism and rate equations for a kinetic multilayer model of surface and bulk reaction enabling the prediction of oligomer formation. Increasing levels of tropospheric O_3 in the Anthropocene may promote the formation of protein oligomers with enhanced allergenicity and may thus contribute to the increasing prevalence of allergies.



1. INTRODUCTION

The prevalence of allergies is increasing worldwide,^{1,2} and air pollution has been identified as one of the factors potentially responsible for this trend,³ but the underlying chemical mechanisms remain unclear.³ Air pollutants can directly affect the immune system, e.g., by inducing inflammation or oxidative stress,^{4–7} and reactive trace gases like ozone (O_3) and nitrogen dioxide (NO_2) can induce post-translational modifications altering the immunogenicity of proteins.^{8–12}

Atmospheric aerosols carry a variety of allergenic proteins in plant pollen, fungal spores, animal secretions and excrements. Besides these mostly larger particles (coarse mode particles, $>1–2 \mu\text{m}$ diameter), several processes might also lead to the occurrence of allergenic proteins in fine mode particles ($<1 \mu\text{m}$), which may enter deeper into the respiratory tract. Such processes include the release of cytoplasmic granules from pollen (PCGs),¹³ fragmentation of airborne cellular material,¹⁴ and transfer of allergenic proteins onto fine mode particles (e.g., refs 14 and 15). Therefore, airborne allergenic proteins can be directly exposed to air pollution, such as O_3 and NO_2 , promoting post-translational modifications like tyrosine (Tyr, Y) nitration.¹⁶ Although a number of studies already investigated general mechanisms and kinetics of protein O_3 uptake and nitration,^{17–19} analysis of site selectivity of protein nitration by O_3 and NO_2 ,²⁰ or specifically studied specific relevant aeroallergens, e.g., the major birch pollen allergen Bet v 1,^{8,21,22} much less is known about oligomerization processes for proteins at atmospherically relevant concentrations of O_3 .

The (transient) formation of homodimers or oligomers has been reported for a number of allergenic proteins.^{23–29} Such dimers, typically formed by colocalization at high protein concentrations encountered in living cells, were observed in 80% of 55 allergen crystal structures and should show an enhanced allergenicity due to facilitated cross-linking of IgE antibodies at FcεRI receptors on effector cells.³⁰ For Bet v 1.0101, it has recently been shown that the wild-type allergen partly contains a YSC mutation and that a disulfide-bridge mediated stabilization of a dimeric form, which preferentially induced a T_H2 immune response.²⁸

In this study, we investigate the formation of oligomers of proteins upon their exposure to atmospherically relevant concentrations of O_3 . Bovine serum albumin (BSA) was used as a model protein, because O_3 uptake kinetics and rate constants are available in the literature.¹⁷ Coated-wall flow tube and liquid phase experiments were performed to study the mechanism and kinetics of protein oligomerization under varying environmental conditions using size exclusion chromatography, fluorescence spectroscopy, gel electrophoresis, and a kinetic modeling approach.

Received: February 11, 2015

Revised: August 18, 2015

Accepted: August 19, 2015

Published: August 19, 2015

2. EXPERIMENTAL SECTION

2.1. Materials. Bovine serum albumin (BSA, A5611-1G), ammonium acetate (>98%, 32301-500G), trifluoroethanol (TFE, T63002), ammonium bicarbonate (A6141-25G), dithiothreitol (DTT, D5545-5G), and iodoacetamide (IAM, I6125-5G) were purchased from Sigma-Aldrich (Germany). 10× Tris/glycine/SDS (161-0732), 2× Lamml sample buffer (161-0737) were from Bio-Rad Laboratories (USA). PD-10 desalting columns were obtained from GE Healthcare (Germany). Sodium hydroxide (NaOH) was purchased from Merck (Germany). High purity water (18.2 MΩ m) for chromatography was taken from an ELGA LabWater system (PURELAB Ultra, ELGA LabWater Global Operations, UK). For other purposes, high purity water (18.2 MΩ m) was autoclaved before used if not specified otherwise.

2.2. Protein O₃ Exposure Setup. BSA solutions (0.6 mL; 3.33, 0.33, 0.07, and 0.03 mg mL⁻¹ concentrations were used to achieve 2, 0.2, 0.04, and 0.02 mg of BSA coating for experiments discussed in section 3.2; for all other reactions, 0.33 mg mL⁻¹ BSA solutions were used) were loaded into the glass tube and dried by passing a N₂ (99.999%) flow of ~2.3 L min⁻¹ through the rotated tube before the exposure experiment. The BSA-coated glass tube was then connected to the experimental setup. Figure S1 of the Supporting Information shows a schematic of the experimental setup. Ozone was produced from synthetic air passed through a mercury vapor lamp (Jelight Company, Inc., Irvine, USA) at 1.9 L min⁻¹. The O₃ concentration was controlled by varying the intensity of UV irradiation with an adjustable cover on the mercury vapor lamp. To control the relative humidity (RH), the gas flow was split; one flow was passed through a Nafion gas humidifier (MH-110-12F-4, PermaPure, Toms River, NJ, USA) operated with autoclaved high purity water, while the other flow remained dry. RH could be varied in a wide range by adjusting the ratio between the dry and humidified air flow. During the experiments, the standard deviation from the set RH values was <2% RH. The resulting air flow was then passed through the BSA-coated glass tube. O₃ concentration and RH were measured by commercial monitoring instruments (Ozone analyzer, 49i, Thermo Scientific, Germany; RH sensor FHA 646-E1C with an ALMEMO 2590-3 instrument, Ahlborn, Mess- und Regelungstechnik GmbH, Holzkirchen). After the respective exposure, the proteins were extracted from the glass tube with 1.5 mL of 1× Tris/glycine/SDS buffer to avoid precipitation of protein oligomers in the extract solution.

Additionally, to investigate further the role of protein phase state for the oligomerization process, the homogeneous reaction of dissolved protein and reactants were studied using a setup described in our previous study.²² Briefly, O₃/synthetic air gas mixtures were bubbled directly through 1.5 mL 0.15 mg mL⁻¹ BSA aqueous solutions (pH 7.1 ± 0.1; pH meter model WTW multi 350i; WTW, Weilheim, Germany) at a flow rate of 60 mL min⁻¹.

2.3. SEC-HPLC-DAD Analysis. Product analysis was performed using high-performance liquid chromatography coupled to diode array detection (HPLC-DAD, Agilent Technologies 1200 series). The HPLC-DAD system consisted of a binary pump (G1379B), an autosampler with thermostat (G1330B), a column thermostat (G1316B), and a photodiode array detector (DAD, G1315C). ChemStation software (Rev. B.03.01, Agilent) was used for system control and data analysis. Molecular weight (MW) separation by size exclusion

chromatography (SEC) was carried out using a Bio SEC-3 HPLC column (Agilent, 300 Å, 150 × 4.6 mm, 3 μm) at a temperature of 30 °C. The mobile phase was 50 mM ammonium acetate (pH 6.8). The flow rate was 0.35 mL min⁻¹ and the sample injection volume was 40 μL. The absorbance was monitored with the DAD at wavelengths of 220 and 280 nm.

A protein standard mix 15–600 kDa (69385, Sigma-Aldrich, Steinheim, Germany) containing thyroglobulin bovine (MW = 670 kDa), γ-globulins from bovine blood (MW = 150 kDa), albumin chicken egg grade VI (MW = 44.3 kDa), and Ribonuclease A (MW = 13.7 kDa) was used for the SEC column calibration (elution time vs log MW). For details, see the Supporting Information. It should be noted that SEC separates molecules according to their hydrodynamic sizes, thus only approximate molecular masses can be obtained by this calibration method. We report the formation of BSA oligomers as the temporal evolution in the ratios of the respective oligomers (dimer, trimer, and higher oligomers with $n \geq 4$) to the sum of monomer and all oligomer peak areas. The commercially available BSA contained also dimer and trimer variants of the protein. Therefore, the reported values were corrected for this background.

2.4. SDS-PAGE Analysis. Sodium dodecyl sulfate polyacrylamide gel electrophoresis (SDS-PAGE) was performed using Mini-PROTEAN TGX Any kD Stain-Free precast gels (Bio-Rad) according to the manufacturer's instructions. Briefly, samples were mixed with Lamml sample buffer and heated at 95 °C for 5 min prior to SDS-PAGE separation. A molecular weight marker (Precision Plus Protein Unstained Standards, 161-0363, Bio-Rad) was used for the calibration of the molecular weight scale. After the SDS-PAGE run, the gels were visualized on a ChemiDoc MP Imaging system with Image Lab software (Version 5.1, Bio-Rad). Molecular weights were determined using the MW Analysis Tool of the Image Lab software.

2.5. Fluorescence Spectroscopy. Fluorescence spectra were recorded on a LS 45 luminescence spectrometer (PerkinElmer, Inc., Waltham, MA, USA). A detailed instrument description is given in Pöhlker et al.³¹ Samples were analyzed in a 10 × 10 × 40 mm UV quartz cuvette (Hellma Analytics, Müllheim, Germany). The photomultiplier tube detector voltage was 600 V. Excitation wavelengths were 240–400 nm (10 nm increments), whereas emission was recorded from 280 to 560 nm (0.5 nm increments). Excitation and emission slit widths were both set to 10 nm and a scan speed of 1500 nm min⁻¹ was used.

3. RESULTS AND DISCUSSION

3.1. Protein Ozone Exposure Results in the Formation of Dityrosine Cross-Links. In a previous study, it has been demonstrated that O₃ can induce protein cross-linking in solution via the formation of dityrosine species. In this study, we explore this process and its kinetics for the heterogeneous and homogeneous reactions of proteins with O₃ at atmospherically relevant conditions.

For one set of homogeneous bulk solution experiments, the BSA samples were pretreated with DTT and IAM, according to the method described in Zhang, Yang, and Poschl²⁰ to exclude oligomer formation due to disulfide bridging. The alkylated BSA samples were then desalted with PD-10 columns according to the manufacturer's instructions and the eluates were used for the exposure experiments. Exemplary results are

illustrated in Figure 1. The BSA dimer (MW 141.9 kDa) and trimer (MW 195.8 kDa) bands clearly increased in intensity,

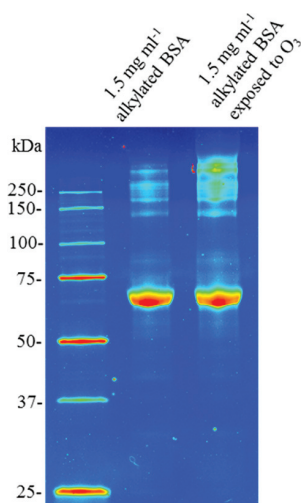


Figure 1. SDS-PAGE analysis of the homogeneous oligomerization of alkylated BSA exposed to 200 ppb O_3 for 2 h (false color illustration).

whereas the intensity of the monomer band (MW 65.1 kDa) is reduced. Interestingly, further bands at MWs higher than 250 kDa were found as well, indicating further oligomerization or agglomeration of BSA. Clearly, an O_3 induced formation of oligomers occurred and, more importantly, the cross-linking could not be attributed to the formation of intermolecular

disulfide bonds because the thiol groups of the protein had been protected by alkylation before the exposure experiment. Additionally, the formation of dityrosine species in the reacted samples was confirmed by fluorescence spectrometry. Excitation and emission wavelengths of dityrosine in alkaline solution were taken from the literature (320 and 400 nm, respectively).³² Accordingly, the pH of our samples was adjusted to 9.7 with 0.1 M NaOH before measurement. Figure 2a–c shows the excitation/emission matrices (EEM) of nonexposed and exposed BSA samples for increasing reaction times, whereas Figure 2d) shows the fluorescence spectra of native BSA and BSA exposed to O_3 in the liquid phase at $\lambda_{ex} = 320$ nm. Clearly, the fluorescence intensity at 400–430 nm increased in the reacted compared to the unreacted BSA samples, which we attribute to the formation of dityrosine species. From the combined SDS-PAGE and fluorescence analysis results, we can infer that ozone induced protein oligomerization occurs via the formation of covalent intermolecular dityrosine cross-links, which is consistent with a previous study.³³

In another set of homogeneous bulk solution experiments, we investigated the reaction kinetics of the formation of BSA dimers and trimers at O_3 concentrations of 50 and 200 ppb. A series of exposure experiments were conducted for both O_3 concentrations with reaction times between 3 (200 ppb O_3) and 6 (50 ppb O_3) minutes and 2 h. The samples were analyzed by SEC-HPLC-DAD as described above (for exemplary chromatograms, see Supporting Information Figure S3) and the results are shown in Figure 3. Signals corresponding to the molecular weight of BSA dimers, trimers, and even higher oligomers have been observed in the exposed samples. For the

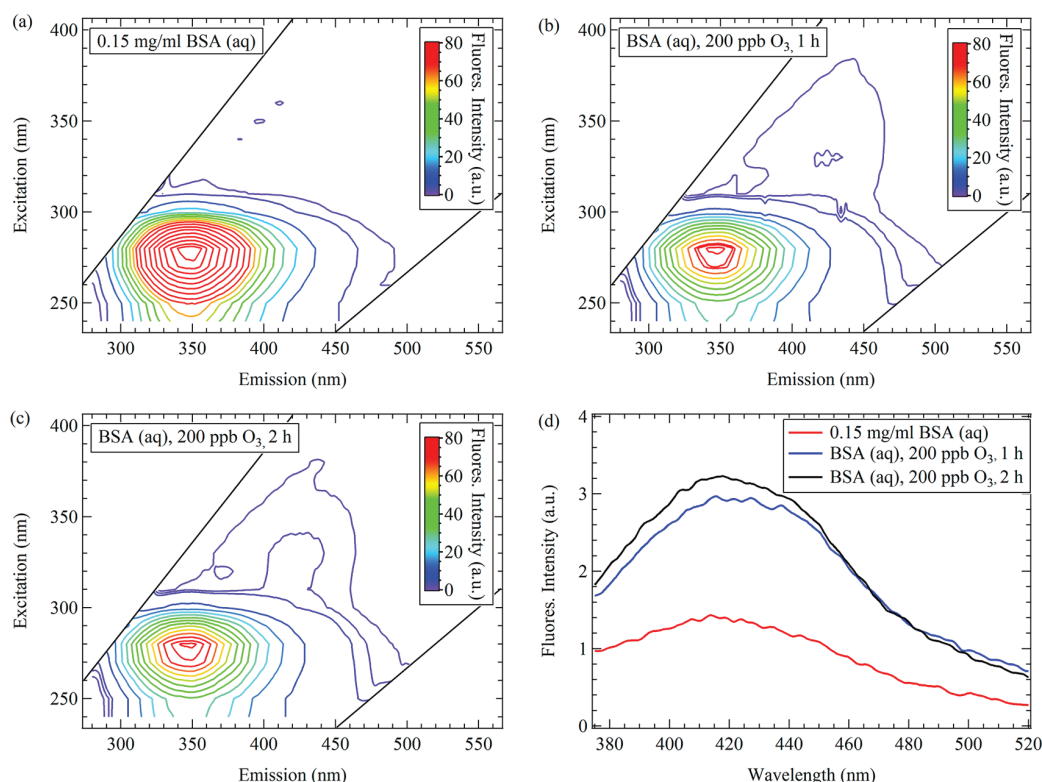


Figure 2. Fluorescence excitation–emission matrices (EEMs) of native BSA (a), and BSA after 1 h (b) and 2 h (c) exposure of 200 ppb O_3 in the liquid phase; (d) fluorescence emission spectra at $\lambda_{ex} = 320$ nm (dityrosine signal).

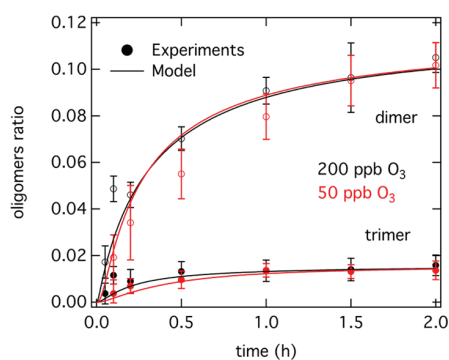


Figure 3. Temporal evolution of protein oligomer content in the aqueous phase reaction of BSA (initial pH 7.1 ± 0.1) with ozone at gas phase concentrations of 50 and 200 ppb O_3 . BSA oligomer formation is reported as the temporal evolution of the ratio of the UV signal area (220 nm) of the respective oligomer (dimer, trimer) to the total signal area (sum of monomer and all oligomer signal areas), see section 2.3. The reported values were corrected for the background of dimers and trimers observed in the commercial BSA. The solid lines are results of the kinetic model.

higher oligomers ($MW > MW_{\text{trimer}}$), peak shape and retention time varied among different samples. However, according to their retention times, they span a range from tetramers up to decamers.

It should be noted that the ozonolysis of amino acid residues, e.g., Tyr, histidine (His), methionine (Met), and tryptophan (Trp) also results in the formation of oxidized products incorporating O atoms,^{34,35} e.g., Tyr + O_3 yields an *o*-quinone derivate.³⁶ However, in a recent study on the oxidation and nitration of Tyr by O_3 and NO_2 , ab initio calculations showed that O_3 can induce H abstraction from the hydroxyl group of

the Tyr phenol ring, resulting in the formation of a tyrosyl radical.³⁷ This reaction was found to have a similar energy barrier as the attack of ozone at the phenol ring in ortho position to the hydroxyl group (3.9 vs 3.6 kcal/mol in aqueous medium).

Oxidative protein cross-links can form upon (a) tyrosyl radical coupling to form dityrosine, (b) Schiff-base cross-linking by reaction of an oxidation-derived protein carbonyl with the ϵ -amino group of lysine and (c) intra- or intermolecular disulfide cross-linking, in part after reductive separation of pre-existing disulfide bridges.³⁸ Because we can exclude the formation of intermolecular disulfide bonds as outlined above, the combined SDS-PAGE and fluorescence analysis results, strongly indicate that the observed O_3 induced protein oligomerization can be attributed to the formation of covalent intermolecular dityrosine cross-links.

The formation of tyrosyl radicals during the ozonolysis of BSA may also lead to the formation of O_3^- , which can be rapidly converted into OH radicals. Further, during ozonolysis reactions, 1O_2 (singlet oxygen) and H_2O_2 (hydrogen peroxide) are known to occur.³⁹ These reactive oxygen species (ROS) likely induce secondary reactions, such as oxidation, ring opening of aromatic amino acid side chains, and protein backbone cleavage.^{40–42} However, the role of this secondary chemistry in atmospheric protein modification and degradation needs to be investigated in follow-up studies.

The focus of this study was to investigate the chemical process and the kinetics of protein oligomerization under environmentally relevant O_3 and RH conditions. However, the reaction of O_3 with the Tyr residues in BSA likely is site selective. Likely Tyr candidates for this reaction could be inferred from previous work on Tyr nitration in BSA.²⁰ Protein Tyr nitration by O_3 and NO_2 is a two-step mechanism

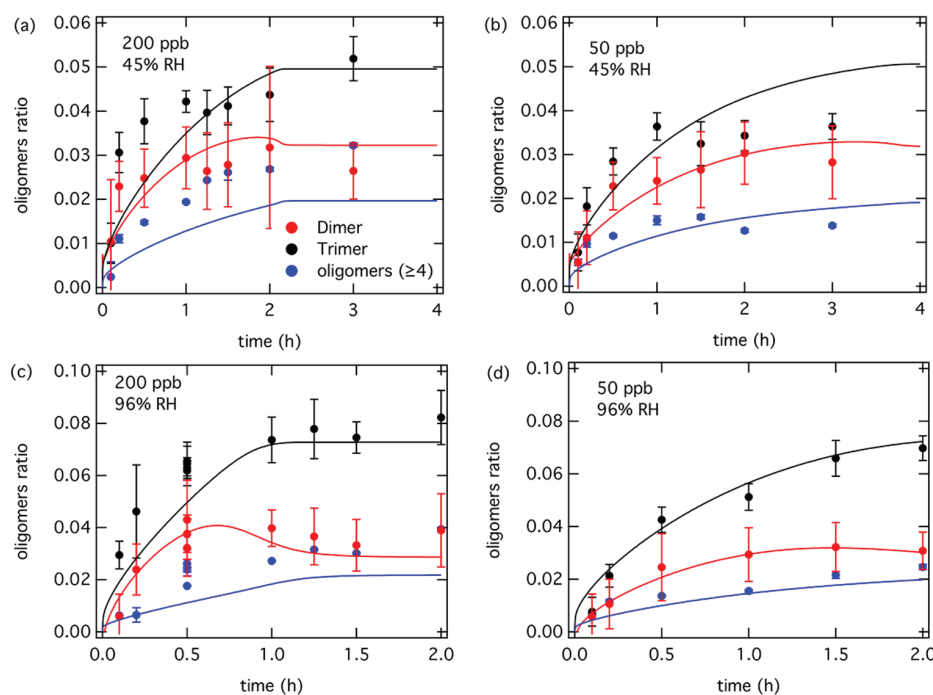


Figure 4. Temporal evolution of protein oligomer content (dimer, red; trimer, black; higher oligomers, blue) upon ozone exposure of BSA films (thickness 34 nm; calculated according to ref 34): (a) 45% RH, 200 ppb O_3 ; (b) 45% RH, 50 ppb O_3 ; (c) 96% RH, 200 ppb O_3 ; (d) 96% RH, 50 ppb O_3 . Details on experimental conditions and analysis are provided in section 2.3. The solid lines are the results of the kinetic model.

involving the attack of O_3 as the first step, which is followed by the addition of NO_2 to form 3-nitrotyrosine.¹⁸ Three nitrated Tyr residues (Y161, Y364, and Y520) were found, Y161 was fully nitrated ($ND_{Y161} = 1$), whereas the others exhibited only low nitration degrees ($ND_{Y364} = 0.003$, $ND_{Y520} = 0.006$).²⁰ However, also other Tyr residues in BSA might be reactive toward O_3 , as the nitration involves one more site-selective reaction step than the pure ozonolysis. It should be noted, that for potential dimerization sites, the effect of steric hindrance likely is more important than for the nitration reaction. Further, in a recent study, peroxidase-generated intermolecular dityrosine cross-links in bovine α -lactalbumin were found to be site selective and occurred at sterically favored sites.⁴³ Tryptophan residues in cytochrome C were observed to be resistant to O_3 , whereas Trp in BSA and human serum albumin (HSA) were found to be susceptible to O_3 .⁴⁴ Such potentially protein structure related resistance may also apply to Tyr in some proteins.

3.2. Kinetics of the Oligomerization Process. Figures 3 and 4 show experimental data and kinetic modeling results to explore and characterize the reaction kinetics of protein oligomerization by ozone. We performed experiments for the reaction of thin protein films (i.e., five layers of protein as detailed below) at 45% RH and 96% RH and proteins in aqueous solution with O_3 gas phase concentrations of 200 and 50 ppb. Oligomer signals were found to increase with exposure time.

Figure 5 illustrates the influence of protein film thickness on the observed increase of oligomer signals after an exposure of

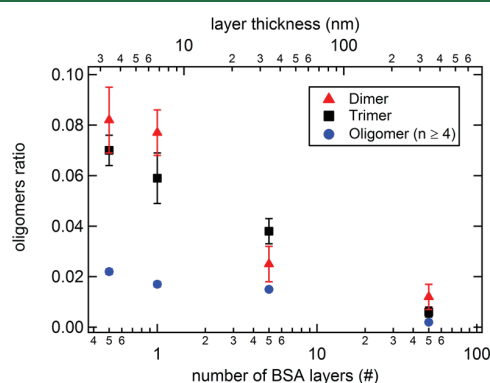
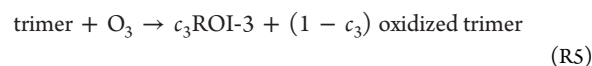
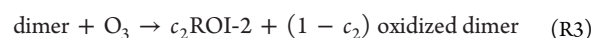
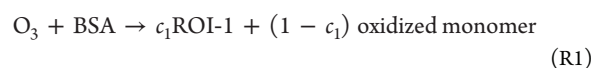


Figure 5. Influence of protein coating thickness on oligomer formation observed after 30 min of ozone exposure (200 ppb O_3 , 45% RH).

200 ppb of O_3 for 30 min at 45% RH. For spherical molecules, the number of layers (n) coating the inner surface of the reaction tube can be estimated from their molecular radius (r_m) and the inner diameter (d) and length (l) of the tube: $n = m_{BSA} r_m^2 N_A / (M_{BSA} d l)$, where N_A is the Avogadro constant, $6.022 \times 10^{23} \text{ mol}^{-1}$, $r_m = 3.4 \text{ nm}$,⁴⁵ $M_{BSA} = 66430 \text{ Da}$. In principle, 2 mg of BSA can form 50 layers on the tube's inner surface. By coating 0.2, 0.04, and 0.02 mg of BSA, five layers, a monolayer, and half of a monolayer can be formed, respectively, assuming an ideal distribution of BSA molecules on the tube's surface. Therefore, when the tube is coated with 0.02 or 0.04 mg of BSA, the reaction with O_3 could be dominated by surface reactions, whereas for 0.2 mg and 2 mg BSA bulk diffusion and reactions plays an increasing role. We found oligomers ratio to be reduced for both the dimer and the trimer with increasing initial BSA mass. Consequently, proteins located on the film

surface were oligomerized efficiently, whereas the bulk oligomerization occurred at much slower rates when reactive sites on the surface were consumed, confirming the bulk diffusion limitation result of the kinetic modeling as detailed below.

The observations support that the dimerization of proteins by O_3 proceeds through a chemical mechanism involving two steps, as suggested in previous studies.^{18,46} The first step is the reaction of a Tyr residue with O_3 forming phenoxy radical derivatives (tyrosyl radicals) as long-lived reactive oxygen intermediates (ROI-1).¹⁹ It should be noted that O_3 can also oxidize other amino acid residues in proteins such as Trp.³⁶ However, from other amino acid residues with a high reactivity toward O_3 , i.e., cysteine (Cys), Trp, Met, and His,⁴⁷ only Cys is able to cross-link proteins directly upon O_3 exposure.^{36,48} Cross-linking by O_3 induced intermolecular disulfide bridge formation could be excluded in our experiments (see section 3.1). In the second step of the process, the ROI-1 react with each other to form dimers. A dimer itself can react further with O_3 forming tyrosyl radicals, forming a second type of reactive oxygen intermediate (ROI-2), which may react with ROI-1 to form a trimer. Oxidation of trimer and formation of tetramer is also considered. Further oligomerization was not considered as such products were not detected in significant amount in experimental studies. These reactions can be summarized as follows



where c_1 , c_2 , and c_3 are stoichiometric coefficients for R1, R3, and R5, respectively. The above chemical mechanism was applied in the kinetic model to fit the experimental data. The kinetic parameters were varied using a global optimization method that utilizes a uniformly sampled Monte Carlo search to seed a genetic algorithm (MCGA method^{49,50}). The genetic algorithm was terminated when the correlation between experimental data and model output converged into an optimum. Since the optimization of the kinetic parameters to the experimental data was not unique in all kinetic parameters, repeated execution of the MCGA method yields a range of kinetic parameters, which can be used to describe the experimental data (Figure S4). The time and O_3 concentration dependence of dimer and trimer formation in the aqueous phase was reproduced very well, as shown with the solid lines in Figure 3. Concentration of O_3 in the aqueous phase was estimated using a Henry's law constant of 0.011 M atm^{-1} .⁵¹ The second-order rate coefficients for R1 and R3 were found to be fast at $(0.1-5) \times 10^{-14} \text{ cm}^3 \text{ s}^{-1}$, which is consistent with previous studies;³⁶ the oligomerization rates R2, R4, R6, and R7 were consistently several orders of magnitude lower (see Figure S4). The stoichiometric coefficients c_1 and c_2 were found to be ~ 0.2 , and c_3 was found to be ~ 0.1 .

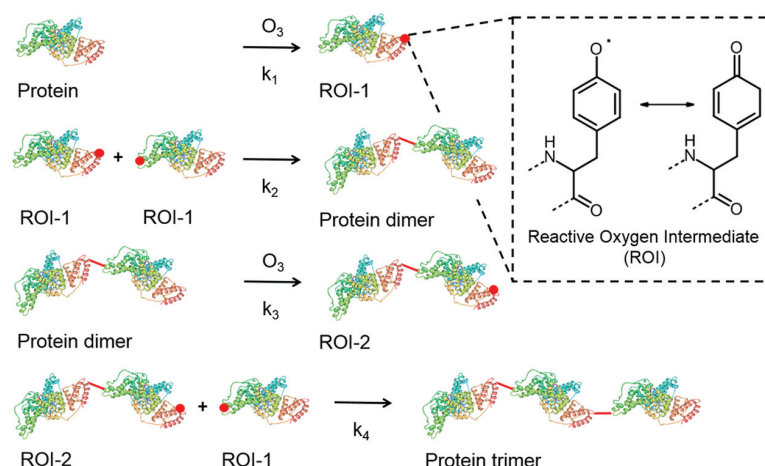


Figure 6. Schematic overview of the most relevant reactions and intermediates for protein oligomerization observed in flowtube experiments upon exposure to environmentally relevant O_3 concentrations. The molecular structure of the protein (bovine serum albumin, BSA; PDB accession number 3V03) was created using the RCSB PDB protein workshop (4.2.0) software.

The reactivity of a Tyr residue is strongly influenced by hydration-level and acidity (pH) of the environment. For instance, phenolate ions are much more reactive toward O_3 than phenols, i.e., by a factor of $\sim 10^6$.³⁹ However, it is difficult to determine the amounts of conjugated ions of Tyr in our flowtube experiments. Local pH and exact pK_a (of the phenolic hydrogen) values for the individual Tyr residues are hard to determine under these experimental conditions. For aqueous phase experiments, one could calculate the amounts of conjugated Tyr ions according to the Henderson–Hasselbalch equation using the pK_a of the phenolic hydrogen of free Tyr (10.07). According to this equation, $\sim 10^{-5}$ to $\sim 10^{-3}$ dissociated ions per residue should be present at pH 5–7, respectively. By a simple division of the rate constant of Tyr + O_3 calculated by the model in this study ($\sim 6 \times 10^5$ – 3×10^7 $M^{-1} s^{-1}$) with the rate constant of phenolate + O_3 reported by Mvula and von Sonntag (1.4×10^9 $M^{-1} s^{-1}$),³⁹ we may estimate that $\sim 4 \times 10^{-4}$ to $\sim 2 \times 10^{-2}$ of the reactive Tyr residues in BSA were present in the form of dissociated ions under the experimental conditions applied in this study, indicating neutral to slightly acidic pH in the flow tube experiments. Further, rate constants of Tyr + O_3 reported in the literature (0.7 – 2.8×10^6 $M^{-1} s^{-1}$ in neutral pH,⁵² and 7.2×10^7 $M^{-1} s^{-1}$ in aqueous medium at 298 K calculated using variational transition state theory³⁷) are in fairly good agreement with our model results.

Figure 4 shows the temporal evolution of the oligomers ratio (for more details see section 3.1; dimer (red), trimer (black) and oligomers with $n \geq 4$ monomer units (blue)) for O_3 exposure to protein films with gas phase O_3 concentrations of 200 and 50 ppb at 45% and 96% RH. Here, we model the formation of oligomers using the kinetic multilayer model for aerosol surface and bulk chemistry (KM-SUB).⁵³ KM-SUB explicitly resolves surface-bulk exchange, bulk diffusion and chemical reactions from the gas-particle interface to the particle core, resolving concentration gradients and diffusion throughout the particle bulk. The model fitting to the experimental data for different RH and in aqueous solution was performed using the MCGA method. Optimized parameters include the second-order reaction rate coefficients (see Figure S4), the bulk diffusion coefficients of O_3 in BSA, and the self-diffusion coefficient of the protein.

The solid lines in Figure 4 show the results of model simulations, reproducing the observed evolution of dimer, trimer, and oligomer ($n \geq 4$) concentrations well. The reactive turnover is higher at 96% RH compared to 45% RH, which can be explained by a moisture-induced phase transition of the protein matrix: the phase state of BSA is amorphous solid with high viscosity at 45% RH, whereas it is semisolid or liquid-like with low viscosity at 96% RH.¹⁷ On the basis of the model fitting, the bulk diffusion coefficients of O_3 were estimated to be 10^{-9} – 10^{-8} $cm^2 s^{-1}$ at 45% RH and $\sim 10^{-7}$ $cm^2 s^{-1}$ at 96% RH; self-diffusion coefficients of protein were estimated to be $\sim 10^{-17}$ $cm^2 s^{-1}$ at 45% RH and $\sim 10^{-15}$ $cm^2 s^{-1}$ at 96% RH. Protein oxidation followed by oligomerization can be kinetically limited by bulk diffusion particularly at lower RH. In summary, our flow tube experiments show that thin protein films, e.g., on the surface of bioaerosol particles, can be efficiently oligomerized by atmospheric O_3 . The most relevant reactions for this process are illustrated in Figure 6.

Temperature also affects the reaction rate of tyrosyl radical formation by ozonolysis. In a recent publication by Sandhiya et al. (2014),³⁷ the effect of temperature on rate constants of the Tyr + O_3 reactions was studied using ab initio calculations. The rate constant for the formation of tyrosyl radicals in aqueous medium ranged from 3.6×10^6 to 2.7×10^8 $M^{-1} s^{-1}$ over the temperature range of 278–308 K.

Numerous studies indicate that anthropogenic air pollution has led to a massive increase of aerosol and oxidant concentrations in the lower atmosphere. For example, the average mixing ratios of O_3 in continental background air have increased by factors of 2–4 from around 10–20 ppb from the beginning of the 19th century to 30–40 ppb in the 21st century.^{54–61} This increase of O_3 concentration in the Anthropocene likely resulted in an increased occurrence of oligomeric proteins in the atmosphere, which in turn may be related to the increase in the prevalence of allergies that has been observed around the globe. The allergenicity of birch pollen has recently been shown to be enhanced at high O_3 concentrations,⁶² and the dimeric proteins were found to have higher allergenicity than the monomeric species.²⁸ On the basis of our observation of higher oligomers formed upon O_3 exposure, we suggest further investigation of the allergenicity of protein oligomers beyond the dimer level.

In the atmosphere, also, photooxidation of proteins may lead to oligomer formation.⁶³ Photoinduced radicals can trigger secondary reactions, which have been shown to result in protein cross-linking in the absence of UV radiation.⁶⁴ Thus, the reaction mechanism and kinetics presented in this study can be regarded as a lower limit of protein oligomer formation in the atmospheric environment.

■ ASSOCIATED CONTENT

📄 Supporting Information

The Supporting Information is available free of charge on the ACS Publications website at DOI: 10.1021/acs.est.5b02902.

Protein O₃ exposure setup (Figure S1), molecular weight calibration of the size exclusion chromatography (Figure S2), exemplary chromatograms from the SEC-DAD analysis of exposed protein samples (Figure S3) and the second-order reaction rate coefficients determined by applying KM-SUB to experimental data (Figure S4) (PDF).

■ AUTHOR INFORMATION

Corresponding Author

*C. J. Kampf. Phone: +49 (0)6131 39 25877. Fax: +49 (0)6131 39 25336. E-mail: kampf@c.uni-mainz.de.

Author Contributions

§These authors contributed equally.

Notes

The authors declare no competing financial interest.

■ ACKNOWLEDGMENTS

F.L. acknowledges financial support from the China Scholarship Council (CSC). T.B. was supported by the Max Planck Graduate Center with the Johannes Gutenberg-Universität Mainz (MPGC), and C.K. acknowledges financial support from the German Research Foundation (DFG Project KA 4008/1-1).

■ REFERENCES

- Holgate, S. T. The epidemic of allergy and asthma. *Nature* **1999**, *402* (6760), B2–B4.
- Holgate, S. T. The epidemic of asthma and allergy. *J. R. Soc. Med.* **2004**, *97* (3), 103–110.
- D'Amato, G.; Baena-Cagnani, C. E.; Cecchi, L.; Annesi-Maesano, I.; Nunes, C.; Ansotegui, I.; D'Amato, M.; Liccardi, G.; Sofia, M.; Canonica, W. G. Climate change, air pollution and extreme events leading to increasing prevalence of allergic respiratory diseases. *Multidiscip. Respir. Med.* **2013**, *8*, 12.
- Bernstein, J. A.; Alexis, N.; Barnes, C.; Bernstein, I. L.; Nel, A.; Peden, D.; Diaz-Sanchez, D.; Tarlo, S. M.; Williams, P. B.; Bernstein, J. A. Health effects of air pollution. *J. Allergy Clin. Immunol.* **2004**, *114* (5), 1116–1123.
- Kampa, M.; Castanas, E. Human health effects of air pollution. *Environ. Pollut.* **2008**, *151* (2), 362–367.
- Yang, W.; Omaye, S. T. Air pollutants, oxidative stress and human health. *Mutat. Res., Genet. Toxicol. Environ. Mutagen.* **2009**, *674* (1–2), 45–54.
- Connor, A. J.; Laskin, J. D.; Laskin, D. L. Ozone-induced lung injury and sterile inflammation. Role of toll-like receptor 4. *Exp. Mol. Pathol.* **2012**, *92* (2), 229–235.
- Ackaert, C.; Kofler, S.; Horejs-Hoecel, J.; Zulehner, N.; Asam, C.; von Grafenstein, S.; Fuchs, J. E.; Briza, P.; Liedl, K. R.; Bohle, B.; Ferreira, F.; Brandstetter, H.; Oostingh, G. J.; Duschl, A. The Impact of Nitration on the Structure and Immunogenicity of the Major Birch Pollen Allergen Bet v 1.0101. *PLoS One* **2014**, *9* (8), e104520.
- Grujthuisen, Y. K.; Grieshuber, I.; Stocklinger, A.; Tischler, U.; Fehrenbach, T.; Weller, M. G.; Vogel, L.; Vieths, S.; Poschl, U.; Duschl, A. Nitration enhances the allergenic potential of proteins. *Int. Arch. Allergy Immunol.* **2006**, *141* (3), 265–275.
- Cuñica, L. G.; Abreu, I.; Esteves da Silva, J. Effect of air pollutant NO₂ on *Betula pendula*, *Ostrya carpinifolia* and *Carpinus betulus* pollen fertility and human allergenicity. *Environ. Pollut.* **2014**, *186* (0), 50–55.
- Karle, A. C.; Oostingh, G. J.; Mutschlechner, S.; Ferreira, F.; Lackner, P.; Bohle, B.; Fischer, G. F.; Vogt, A. B.; Duschl, A. Nitration of the Pollen Allergen Bet v 1.0101 Enhances the Presentation of Bet v 1-Derived Peptides by HLA-DR on Human Dendritic Cells. *PLoS One* **2012**, *7* (2), e31483.
- Hochscheid, R.; Schreiber, N.; Kotte, E.; Weber, P.; Cassel, W.; Yang, H.; Zhang, Y.; Poschl, U.; Müller, B. Nitration of protein without allergenic potential triggers modulation of antioxidant response in Type II pneumocytes. *J. Toxicol. Environ. Health, Part A* **2014**, *77* (12), 679–695.
- Motta, A. C.; Marliere, M.; Peltre, G.; Sterenberg, P. A.; Lacroix, G. Traffic-related air pollutants induce the release of allergen-containing cytoplasmic granules from grass pollen. *Int. Arch. Allergy Immunol.* **2006**, *139* (4), 294–298.
- Taylor, P. E.; Flagan, R. C.; Miguel, A. G.; Valenta, R.; Glovsky, M. M. Birch pollen rupture and the release of aerosols of respirable allergens. *Clin. Exp. Allergy* **2004**, *34* (10), 1591–1596.
- Schappi, G. F.; Taylor, P. E.; Staff, I. A.; Suphioglu, C.; Knox, R. B. Source of Bet v 1 loaded inhalable particles from birch revealed. *Sex. Plant Reprod.* **1997**, *10* (6), 315–323.
- Franze, T.; Weller, M. G.; Niessner, R.; Poschl, U. Protein nitration by polluted air. *Environ. Sci. Technol.* **2005**, *39* (6), 1673–1678.
- Shiraiwa, M.; Ammann, M.; Koop, T.; Pöschl, U. Gas uptake and chemical aging of semisolid organic aerosol particles. *Proc. Natl. Acad. Sci. U. S. A.* **2011**, *108* (27), 11003–11008.
- Shiraiwa, M.; Selzle, K.; Yang, H.; Sosedova, Y.; Ammann, M.; Poschl, U. Multiphase Chemical Kinetics of the Nitration of Aerosolized Protein by Ozone and Nitrogen Dioxide. *Environ. Sci. Technol.* **2012**, *46* (12), 6672–6680.
- Shiraiwa, M.; Sosedova, Y.; Rouviere, A.; Yang, H.; Zhang, Y. Y.; Abbatt, J. P. D.; Ammann, M.; Poschl, U. The role of long-lived reactive oxygen intermediates in the reaction of ozone with aerosol particles. *Nat. Chem.* **2011**, *3* (4), 291–295.
- Zhang, Y. Y.; Yang, H.; Poschl, U. Analysis of nitrated proteins and tryptic peptides by HPLC-chip-MS/MS: site-specific quantification, nitration degree, and reactivity of tyrosine residues. *Anal. Bioanal. Chem.* **2011**, *399* (1), 459–471.
- Selzle, K.; Ackaert, C.; Kampf, C. J.; Kunert, A. T.; Duschl, A.; Oostingh, G. J.; Poschl, U. Determination of nitration degrees for the birch pollen allergen Bet v 1. *Anal. Bioanal. Chem.* **2013**, *405* (27), 8945–8949.
- Reinmuth-Selzle, K.; Ackaert, C.; Kampf, C. J.; Samonig, M.; Shiraiwa, M.; Kofler, S.; Yang, H.; Gadermaier, G.; Brandstetter, H.; Huber, C. G.; Duschl, A.; Oostingh, G. J.; Poschl, U. Nitration of the Birch Pollen Allergen Bet v 1.0101: Efficiency and Site-Selectivity of Liquid and Gaseous Nitrating Agents. *J. Proteome Res.* **2014**, *13* (3), 1570–1577.
- Verdino, P.; Westritschnig, K.; Valenta, R.; Keller, W. The cross-reactive calcium-binding pollen allergen, Phl p 7, reveals a novel dimer assembly. *EMBO J.* **2002**, *21* (19), S007–S016.
- Lascombe, M. B.; Gregoire, C.; Poncet, P.; Tavares, G. A.; Rosinski-Chupin, I.; Rabillon, J.; Goubran-Botros, H.; Mazie, J. C.; David, B.; Alzari, P. M. Crystal structure of the allergen Equ c 1 - A dimeric lipocalin with restricted IgE-reactive epitopes. *J. Biol. Chem.* **2000**, *275* (28), 21572–21577.
- Maleki, S. J.; Kopper, R. A.; Shin, D. S.; Park, C. W.; Compadre, C. M.; Sampson, H.; Burks, A. W.; Bannon, G. A. Structure of the major peanut allergen Ara h 1 may protect IgE-binding epitopes from degradation. *J. Immunol.* **2000**, *164* (11), S844–S849.

- (26) Niemi, M.; Jylha, S.; Laukkanen, M.-L.; Soderlund, H.; Makinen-Kiljunen, S.; Kallio, J. M.; Hakulinen, N.; Haahtela, T.; Takkinen, K.; Rouvinen, J. Molecular interactions between a recombinant IgE antibody and the beta-lactoglobulin allergen. *Structure* **2007**, *15* (11), 1413–1421.
- (27) Niemi, M. H.; Rytönen-Nissinen, M.; Janis, J.; Virtanen, T.; Rouvinen, J. Structural aspects of dog allergies: The crystal structure of a dog dander allergen Can f 4. *Mol. Immunol.* **2014**, *61* (1), 7–15.
- (28) Kofler, S.; Ackaert, C.; Samonig, M.; Asam, C.; Briza, P.; Horejs-Hoek, J.; Cabrele, C.; Ferreira, F.; Duschl, A.; Huber, C.; Brandstetter, H. Stabilization of the Dimeric Birch Pollen Allergen Bet v 1 Impacts Its Immunological Properties. *J. Biol. Chem.* **2014**, *289* (1), 540–551.
- (29) Magler, I.; Nuss, D.; Hauser, M.; Ferreira, F.; Brandstetter, H. Molecular metamorphosis in polcalcin allergens by EF-hand rearrangements and domain swapping. *FEBS J.* **2010**, *277* (12), 2598–2610.
- (30) Rouvinen, J.; Janis, J.; Laukkanen, M.-L.; Jylha, S.; Niemi, M.; Paivinen, T.; Makinen-Kiljunen, S.; Haahtela, T.; Soderlund, H.; Takkinen, K. Transient Dimers of Allergens. *PLoS One* **2010**, *5* (2), e9037.
- (31) Pöhlker, C.; Huffman, J. A.; Poschl, U. Autofluorescence of atmospheric bioaerosols - fluorescent biomolecules and potential interferences. *Atmos. Meas. Tech.* **2012**, *5* (1), 37–71.
- (32) Malencik, D. A.; Sprouse, J. F.; Swanson, C. A.; Anderson, S. R. Dityrosine: Preparation, isolation, and analysis. *Anal. Biochem.* **1996**, *242* (2), 202–213.
- (33) Verweij, H.; Christianse, K.; Vansteveninck, J. Ozone-induced formation of O,O'-dityrosine cross-links in proteins. *Biochim. Biophys. Acta, Protein Struct. Mol. Enzymol.* **1982**, *701* (2), 180–184.
- (34) Lloyd, J.; Spraggins, J.; Johnston, M.; Laskin, J. Peptide ozonolysis: Product structures and relative reactivities for oxidation of tyrosine and histidine residues. *J. Am. Soc. Mass Spectrom.* **2006**, *17* (9), 1289–1298.
- (35) Kotiaho, T.; Eberlin, M. N.; Vainiotalo, P.; Kostianen, R. Electrospray mass and tandem mass spectrometry identification of ozone oxidation products of amino acids and small peptides. *J. Am. Soc. Mass Spectrom.* **2000**, *11* (6), 526–535.
- (36) Sharma, V. K.; Graham, N. J. D. Oxidation of Amino Acids, Peptides and Proteins by Ozone: A Review. *Ozone: Sci. Eng.* **2010**, *32* (2), 81–90.
- (37) Sandhiya, L.; Kolandaivel, P.; Senthilkumar, K. Oxidation and Nitration of Tyrosine by Ozone and Nitrogen Dioxide: Reaction Mechanisms and Biological and Atmospheric Implications. *J. Phys. Chem. B* **2014**, *118* (13), 3479–3490.
- (38) Stadtman, E. R. Protein oxidation and aging. *Free Radical Res.* **2006**, *40* (12), 1250–1258.
- (39) Mvula, E.; von Sonntag, C. Ozonolysis of phenols in aqueous solution. *Org. Biomol. Chem.* **2003**, *1* (10), 1749–1756.
- (40) Xu, G.; Chance, M. R. Hydroxyl Radical-Mediated Modification of Proteins as Probes for Structural Proteomics. *Chem. Rev.* **2007**, *107* (8), 3514–3543.
- (41) Davies, M. J. Reactive species formed on proteins exposed to singlet oxygen. *Photochem. Photobiol. Sci.* **2004**, *3* (1), 17–25.
- (42) Winterbourn, C. C.; Metodieva, D. Reactivity of biologically important thiol compounds with superoxide and hydrogen peroxide. *Free Radical Biol. Med.* **1999**, *27* (3–4), 322–328.
- (43) Heijnis, W. H.; Dekker, H. L.; de Koning, L. J.; Wierenga, P. A.; Westphal, A. H.; de Koster, C. G.; Gruppen, H.; van Berkel, W. J. Identification of the peroxidase-generated intermolecular dityrosine cross-link in bovine α -lactalbumin. *J. Agric. Food Chem.* **2011**, *59* (1), 444–449.
- (44) Mudd, J. B.; Dawson, P. J.; Tseng, S.; Liu, F.-P. Reaction of Ozone with Protein Tryptophans: Band III, Serum Albumin, and Cytochrome C. *Arch. Biochem. Biophys.* **1997**, *338* (2), 143–149.
- (45) González Flecha, F. L.; Levi, V. Determination of the molecular size of BSA by fluorescence anisotropy. *Biochem. Mol. Biol. Educ.* **2003**, *31* (5), 319–322.
- (46) Shiraiwa, M.; Selzle, K.; Poschl, U. Hazardous components and health effects of atmospheric aerosol particles: reactive oxygen species, soot, polycyclic aromatic compounds and allergenic proteins. *Free Radical Res.* **2012**, *46* (8), 927–939.
- (47) Pryor, W. A.; Uppu, R. M. A kinetic model for the competitive reactions of ozone with amino acid residues in proteins in reverse micelles. *J. Biol. Chem.* **1993**, *268* (5), 3120–3126.
- (48) Cataldo, F. On the action of ozone on proteins. *Polym. Degrad. Stab.* **2003**, *82* (1), 105–114.
- (49) Berkemeier, T.; Huisman, A. J.; Ammann, M.; Shiraiwa, M.; Koop, T.; Pöschl, U. Kinetic regimes and limiting cases of gas uptake and heterogeneous reactions in atmospheric aerosols and clouds: a general classification scheme. *Atmos. Chem. Phys.* **2013**, *13* (14), 6663–6686.
- (50) Arangio, A. M.; Slade, J. H.; Berkemeier, T.; Pöschl, U.; Knopf, D. A.; Shiraiwa, M. Multiphase Chemical Kinetics of OH Radical Uptake by Molecular Organic Markers of Biomass Burning Aerosols: Humidity and Temperature Dependence, Surface Reaction, and Bulk Diffusion. *J. Phys. Chem. A* **2015**, *119* (19), 4533–4544.
- (51) Sander, R. Compilation of Henry's law constants (version 4.0) for water as solvent. *Atmos. Chem. Phys.* **2015**, *15* (8), 4399–4981.
- (52) Pryor, W. A.; Giamalva, D. H.; Church, D. F. Kinetics of ozonation. 2. Amino acids and model compounds in water and comparisons to rates in nonpolar solvents. *J. Am. Chem. Soc.* **1984**, *106* (23), 7094–7100.
- (53) Shiraiwa, M.; Pfrang, C.; Poschl, U. Kinetic multi-layer model of aerosol surface and bulk chemistry (KM-SUB): the influence of interfacial transport and bulk diffusion on the oxidation of oleic acid by ozone. *Atmos. Chem. Phys.* **2010**, *10* (8), 3673–3691.
- (54) Akimoto, H. Global air quality and pollution. *Science* **2003**, *302* (5651), 1716–1719.
- (55) Lelieveld, J.; van Aardenne, J.; Fischer, H.; de Reus, M.; Williams, J.; Winkler, P. Increasing ozone over the Atlantic Ocean. *Science* **2004**, *304* (5676), 1483–1487.
- (56) Vingarzan, R. A review of surface ozone background levels and trends. *Atmos. Environ.* **2004**, *38* (21), 3431–3442.
- (57) Parrish, D. D.; Millet, D. B.; Goldstein, A. H. Increasing ozone in marine boundary layer inflow at the west coasts of North America and Europe. *Atmos. Chem. Phys.* **2009**, *9* (4), 1303–1323.
- (58) Tanimoto, H.; Ohara, T.; Uno, I. Asian anthropogenic emissions and decadal trends in springtime tropospheric ozone over Japan: 1998–2007. *Geophys. Res. Lett.* **2009**, *36*, L23802.
- (59) Cooper, O. R.; Parrish, D. D.; Stohl, A.; Trainer, M.; Nédélec, P.; Thouret, V.; Cammas, J. P.; Oltmans, S. J.; Johnson, B. J.; Tarasick, D. Increasing springtime ozone mixing ratios in the free troposphere over western North America. *Nature* **2010**, *463* (7279), 344–348.
- (60) Fishman, J.; Creilson, J. K.; Parker, P. A.; Ainsworth, E. A.; Vining, G. G.; Szarka, J.; Booker, F. L.; Xu, X. An investigation of widespread ozone damage to the soybean crop in the upper Midwest determined from ground-based and satellite measurements. *Atmos. Environ.* **2010**, *44* (18), 2248–2256.
- (61) Pöschl, U.; Shiraiwa, M. Multiphase Chemistry at the Atmosphere–Biosphere Interface Influencing Climate and Public Health in the Anthropocene. *Chem. Rev.* **2015**, *115* (10), 4440–4475.
- (62) Beck, I.; Jochner, S.; Gilles, S.; McIntyre, M.; Buters, J. T. M.; Schmidt-Weber, C.; Behrendt, H.; Ring, J.; Menzel, A.; Traidl-Hoffmann, C. High Environmental Ozone Levels Lead to Enhanced Allergenicity of Birch Pollen. *PLoS One* **2013**, *8* (11), e80147.
- (63) Pattison, D. I.; Rahmanto, A. S.; Davies, M. J. Photo-oxidation of proteins. *Photochem. Photobiol. Sci.* **2012**, *11* (1), 38–53.
- (64) Dubbelman, T. M. A. R.; Haasnoot, C.; van Steveninck, J. Temperature dependence of photodynamic red cell membrane damage. *Biochim. Biophys. Acta, Biomembr.* **1980**, *601* (0), 220–227.

SUPPORTING INFORMATION

Protein Cross-Linking and Oligomerization through Dityrosine Formation upon Exposure to Ozone

**Christopher J. Kampf^{1,2,#}, Fobang Liu^{2,#}, Kathrin Reinmuth-Selzle², Thomas Berkemeier², Hannah Meusel², Manabu Shiraiwa², Ulrich Pöschl²*

¹Institute for Inorganic and Analytical Chemistry, Johannes Gutenberg University Mainz, Mainz, Germany

²Multiphase Chemistry Department, Max Planck Institute for Chemistry, Mainz, Germany

*Corresponding author: Christopher J. Kampf, Johannes Gutenberg University Mainz, Duesbergweg 10-14, 55128 Mainz, Germany, phone: +49 6131 39 25877, fax: +49 6131 39 25336, Email: kampfch@uni-mainz.de

[#]These authors contributed equally

Summary

Figure S1	Page S2
Figure S2	Page S2
Figure S3	Page S3
Figure S4	Page S4

Protein ozone exposure setup

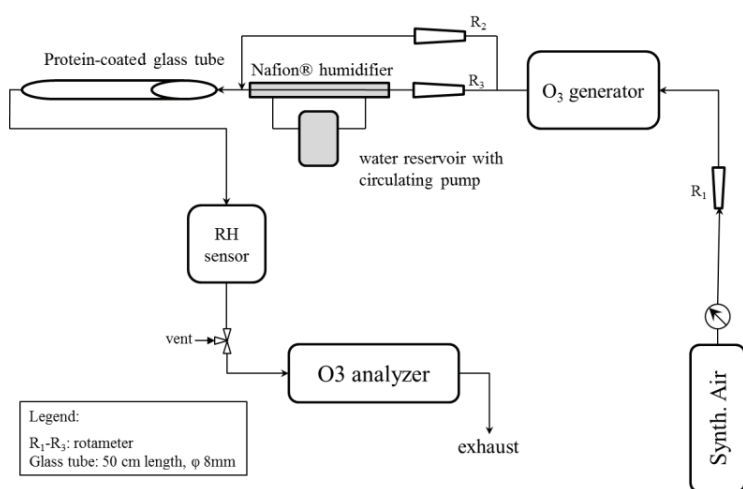


Figure S1. Experimental setup for protein ozone exposure.

Molecular weight calibration of size exclusion chromatography (SEC)

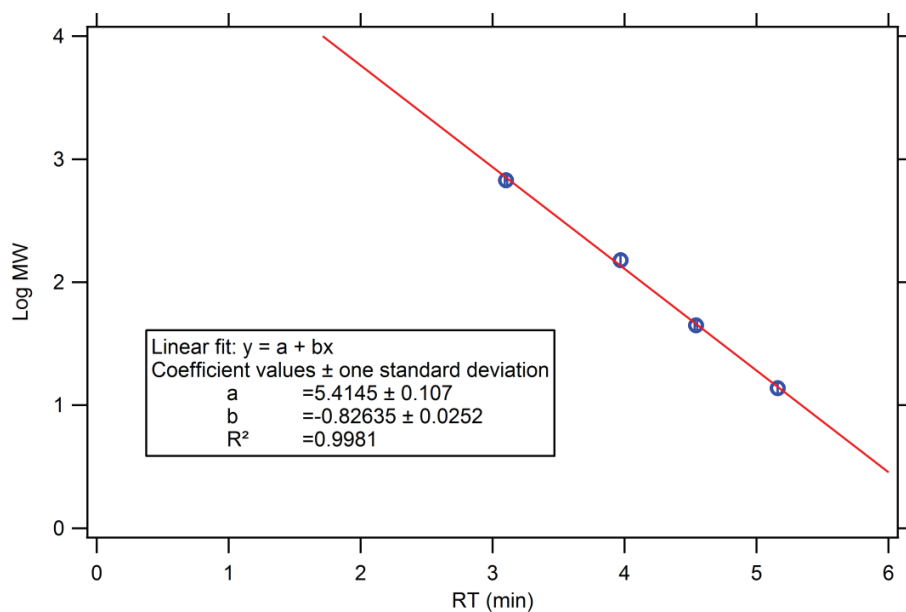


Figure S2. Calibration curve plotting the logarithm of molecular weight (Log MW) against retention time (RT) of the protein standard mix. The fitting equation was $y = -0.83x + 5.41$, $R^2 = 0.998$.

DAD analysis of exposed protein samples

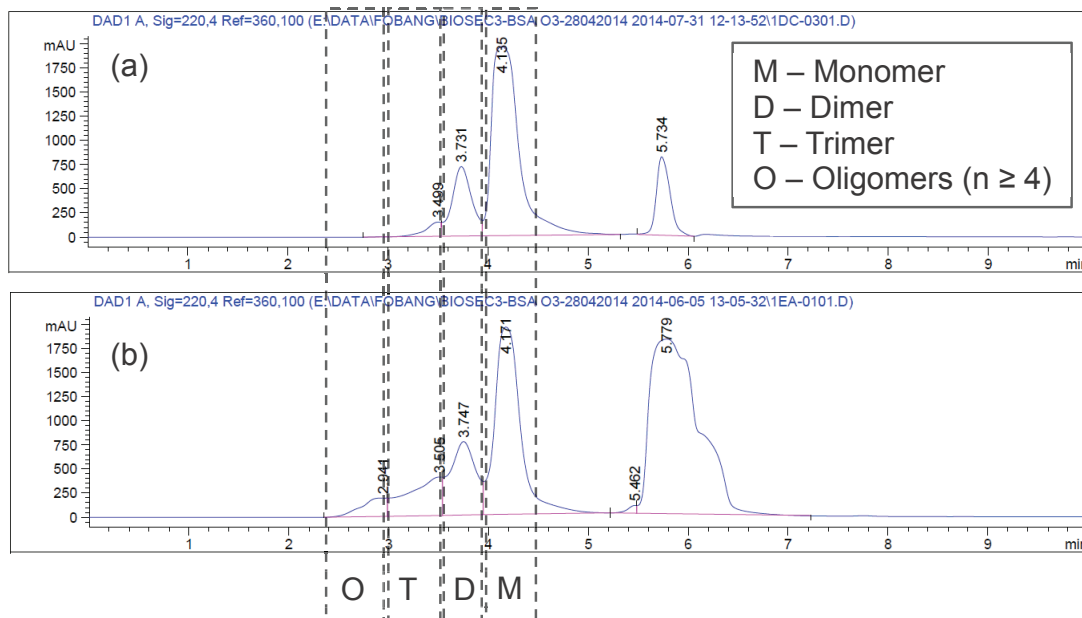


Figure S3. Exemplary chromatograms of native BSA and exposed BSA samples. (a) 1.3 mg/mL BSA in 1×Tris/Glycine/SDS buffer, (b) BSA, 200 ppb O₃, 96% RH, 30 min exposure.

The signal at 5.6 – 6.4 min retention time in Figure S3 a) and b) is caused by the SDS buffer used to elute the protein from the reaction tube after the experiment; SDS buffer concentration in b) is ten times higher than in a).

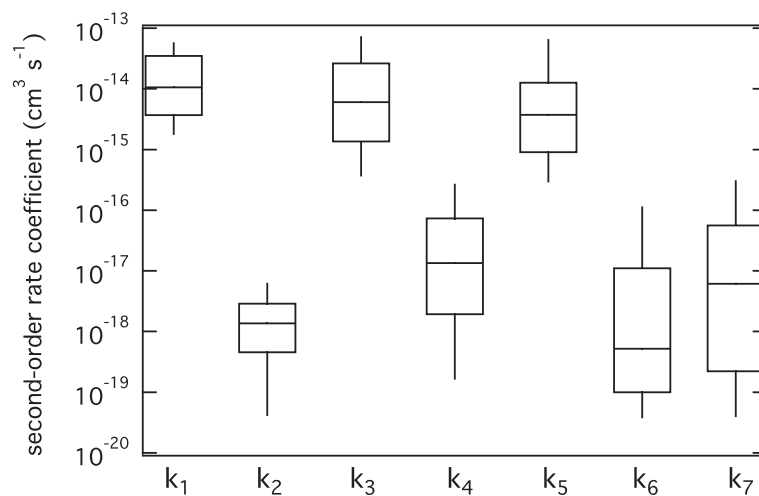


Figure S4. The second-order reaction rate coefficients (k) for (R1)-(R7) determined by optimizing KM-SUB model results to experimental data. The model fitting was performed in a least-squares fashion using a genetic algorithm (Matlab software) preceded by a uniformly-sampled Monte-Carlo search as global optimization routine. Multiple optimizations yielded 20 sets of possible parameter combinations that describe the experimental data equally well. The ranges parameters k_1 - k_7 spanned is depicted as a box-whisker plot (the percentiles of 10, 25, 50, 75, and 90 % are shown).

B.4. Liu et al., Farad. Discuss., 2017

Atmospheric protein chemistry influenced by anthropogenic air pollutants: nitration and oligomerization upon exposure to ozone and nitrogen dioxide

Fobang Liu¹, Pascale S. J. Lakey¹, Thomas Berkemeier^{1,2}, Haijie Tong¹, Anna Theresa Kunert¹, Hannah Meusel¹, Yafang Cheng¹, Hang Su¹, Janine Fröhlich-Nowoisky¹, Senchao Lai³, Michael G. Weller⁴, Manabu Shiraiwa⁵, Ulrich Pöschl¹, Christopher J. Kampf^{6,1*}

¹Multiphase Chemistry Department, Max Planck Institute for Chemistry, Hahn-Meitner-Weg 1, 55128 Mainz, Germany

²School of Chemical & Biomolecular Engineering, Georgia Tech, Atlanta, GA, USA

³School of Environment and Energy, South China University of Technology, Higher Education Mega Center, Guangzhou 510006, P.R. China

⁴Division 1.5 Protein Analysis, Federal Institute for Materials Research and Testing (BAM), Richard-Willstätter-Str. 11, 12489 Berlin, Germany

⁵Department of Chemistry, University of California, Irvine, CA, USA

⁶Institute for Organic Chemistry, Johannes Gutenberg University Mainz, Duesbergweg 10-14, 55128 Mainz, Germany

*Correspondence to Christopher J. Kampf, email: kampf@uni-mainz.de

Faraday Discussions, 2017, accepted.



View Article Online
DOI: 10.1039/C7FD00005G

Faraday Discussions

ARTICLE

Atmospheric protein chemistry influenced by anthropogenic air pollutants: nitration and oligomerization upon exposure to ozone and nitrogen dioxide

Received 4th January 2017,
Accepted 00th January 20xx

DOI: 10.1039/x0xx00000x

www.rsc.org/

Fobang Liu,^a Pascale S. J. Lakey,^a Thomas Berkemeier,^{a,b} Haijie Tong,^a Anna Theresa Kunert,^a Hannah Meusel,^a Yafang Cheng,^a Hang Su,^a Janine Fröhlich-Nowoisky,^a Senchao Lai,^c Michael G. Weller,^d Manabu Shiraiwa,^e Ulrich Pöschl^a and Christopher J. Kampf^{f*,f,a}

The allergenic potential of airborne proteins may be enhanced *via* posttranslational modification induced by air pollutants like ozone (O₃) and nitrogen dioxide (NO₂). The molecular mechanisms and kinetics of the chemical modifications enhancing the allergenicity of proteins, however, are still not fully understood. Here, protein tyrosine nitration and oligomerization upon simultaneous exposure of O₃ and NO₂ were studied in coated-wall flow-tube and bulk-solution experiments under varying atmospherically-relevant conditions (5–200 ppb O₃, 5–200 ppb NO₂, 45–96% RH), using bovine serum albumin as a model protein. Generally, more tyrosine residues were found to react *via* the nitration pathway than *via* the oligomerization pathway. Depending on reaction conditions, oligomer mass fractions and nitration degrees were in the range of 2.5–25% and 0.5–7%, respectively. The experimental results were well-reproduced by the kinetic multi-layer model of aerosol surface and bulk chemistry (KM-SUB). The extent of nitration and oligomerization strongly depended on relative humidity (RH) due to moisture-induced phase transition of proteins, highlighting the importance of cloud processing conditions for accelerated protein chemistry. Dimeric and nitrated species were major products in the liquid phase, while protein oligomerization was observed to greater extent at solid and semi-solid phase states of proteins. Our results showed that the rate of both processes was sensitive towards ambient ozone concentration, but rather insensitive towards different NO₂ levels. An increase of tropospheric ozone concentrations in the Anthropocene may thus promote pro-allergic protein modifications and contribute to the observed increase of allergies over the past decades.

1. Introduction

Allergies represent an important issue for human health and the prevalence of allergic diseases has been increasing worldwide over the past decades.^{1,2} Among other explanations, air pollution has been proposed as a potential driver for this increase.^{3–6} It is well established that air pollutants, especially diesel exhaust particles (DEPs), can act as adjuvants and facilitate on the allergic sensitization in the human body.^{7,8} Air pollutants like nitrogen dioxide (NO₂), sulfur dioxide (SO₂), and ozone (O₃), have been shown to interact with and modify allergen carriers like pollen grains and fungal spores, increasing

the release of allergenic proteins.^{8,9} Moreover, post-translational modifications (PTM) of allergenic proteins can be induced by reactive trace gases such as O₃ and NO₂ and modify their structure and activity, thus altering the immunogenicity of the proteins.^{10–13}

Airborne allergenic proteins (aeroallergens) are contained not only in coarse biological particles such as pollen grains¹⁴, but also in the fine fraction of air particulate matter (aerodynamic diameter < 2.5 μm).^{15–17} The occurrence of allergenic proteins in fine particles can be explained by several processes, including the release of pollen cytoplasmic granules (PCGs) from the rupture of pollen grains,⁹ fragmentation of airborne cellular material,¹⁸ and contact transfer of allergenic proteins onto fine particles.^{18,19} Therefore, aeroallergens can be directly exposed to ambient O₃ and NO₂, promoting chemical modifications like tyrosine (Tyr) nitration and oligomerization.

Laboratory and field investigations have shown that proteins can be oxidized, nitrated and/or oligomerized upon exposure to NO₂ and O₃ in synthetic gas mixtures or polluted urban air.^{11, 12, 15, 20} The mechanisms of protein nitration by O₃ and NO₂, and protein cross-linking (oligomerization) by O₃, both involve the formation of long-lived reactive oxygen intermediates (ROIs), which are most likely tyrosyl radicals, as proposed earlier.^{12, 20–24} The ROIs can subsequently react with each other forming dityrosine (DTyr) crosslinks, with NO₂ to form nitrotyrosine (NTyr) residues, or undergo further oxidation reactions. Using quantum chemical methods, Sandhiya *et al.*²² showed that six different intermediates

^a Multiphase Chemistry Department, Max Planck Institute for Chemistry, Hahn-Meitner-Weg 1, 55128 Mainz, Germany.

^b School of Chemical & Biomolecular Engineering, Georgia Tech, Atlanta, GA, USA.

^c School of Environment and Energy, South China University of Technology, Higher Education Mega Center, Guangzhou 510006, P.R. China.

^d Division 1.5 Protein Analysis, Federal Institute for Materials Research and Testing (BAM), Richard-Willstätter-Str. 11, 12489 Berlin, Germany.

^e Department of Chemistry, University of California, Irvine, CA, USA.

^f Institute for Organic Chemistry, Johannes Gutenberg University Mainz, Duesbergweg 10-14, 55128 Mainz, Germany. Email: kampfc@uni-mainz.de

Electronic Supplementary Information (ESI) available: Chemical mechanism and corresponding parameters used in kinetic modelling (Table S1), schematic experimental setup (Fig. S1), and SEC calibration curve (Fig. S2). See DOI: 10.1039/x0xx00000x

can be formed through the initial oxidation of Tyr residues by O₃, out of which the tyrosyl radical is favorable due to a small energy barrier, particularly in the aqueous phase. In the absence of NO₂, tyrosyl radicals can undergo self-reaction to stabilize in the form of dimers. Under physiological conditions, Pfeiffer *et al.*²⁵ found that DTyr was a major product of Tyr modification caused by low steady-state concentrations of peroxyxynitrite, while high fluxes (> 2 μM s⁻¹) of nitrogen oxide/superoxide anion (NO/O₂⁻) are required to render peroxyxynitrite an efficient trigger of Tyr nitration. Thus, a kinetic competition between Tyr nitration and dimerization (or oligomerization) upon protein exposure to O₃ and NO₂ can be expected, which needs to be explored in detail to assess relevant atmospheric conditions favoring potentially health relevant protein modifications.

In this study, we explored the oxidation, nitration, and oligomerization reactions of proteins induced by O₃ and NO₂, and their kinetics under different atmospherically relevant conditions using bovine serum albumin (BSA) as a model protein. Coated-wall flow-tube and bulk solution experiments were performed to study the kinetics of protein nitration and oligomerization at O₃ and NO₂ concentrations of 5-200 ppb, and relative humidity (RH) of 45 and 96%, utilizing a size exclusion chromatography/spectrophotometry method. Additionally, we used the kinetic multi-layer model of aerosol surface and bulk chemistry (KM-SUB)²⁶ to investigate which chemical reactions and transport processes control the concentration and time dependence of protein oligomerization and nitration.

2. Experimental

2.1. Materials

Bovine serum albumin (BSA, A5611) and sodium phosphate monobasic monohydrate (NaH₂PO₄·H₂O, 71504), were purchased from Sigma-Aldrich (Germany). Sodium hydroxide (NaOH, 0583) was from VWR (Germany). 10×Tris/Glycine/SDS (161-0732) was from Bio-Rad Laboratories (USA). High purity water (18.2 MΩ cm) for chromatography was taken from a Milli-Q Integral 3 water purification system (Merck Millipore, USA). The high purity water (18.2 MΩ·cm) was autoclaved before use if not specified otherwise.

2.2. Protein O₃/NO₂ exposure setup

Reactions of BSA with O₃/NO₂ mixtures were performed both homogeneously in aqueous solutions and heterogeneously *via* the exposure of BSA-coated glass tubes to gaseous O₃/NO₂ at different levels of relative humidity (RH). Before the exposure experiments, BSA solutions (0.6 ml, 0.33 mg mL⁻¹) were loaded into the glass tube and dried by passing a nitrogen (N₂, 99.999%) flow at ~ 1 L min⁻¹ through a specific rotating device²⁷, which is essential to ensure the homogeneous coating and experiment reproducibility. The BSA-coated glass tube was then connected to the experimental setup. The experimental setup (Fig. S1, ESI) described previously,²⁰ was extended by incorporating an additional flow of NO₂ after the humidifier.

Briefly, ozone was produced from synthetic air passed through a UV lamp (L.O.T.-Oriol GmbH & Co.KG, Germany) at ~1.9 L min⁻¹. The gas flow was then split and one flow was passed through a Nafion

gas humidifier (MH-110-12F-4, PermaPure, USA) operated with autoclaved high purity water, while the other flow remained dry. RH could be varied in a wide range by adjusting the ratio between the dry and humidified air flow. During the experiments, the standard deviation from the set RH values was < 2% RH. The gas flow with a set O₃ concentration and RH was then mixed with a N₂ flow containing ~5 ppmV NO₂ (AIR LIQUIDE, Germany). The NO₂ concentrations were adjusted by varying the flow rate (20-80 mL min⁻¹) of the ~5 ppmV NO₂ flow. The combined gas flow was then directed through the BSA-coated glass tube. The concentrations of O₃ and NO₂ as well as RH were measured by commercial monitoring instruments (Ozone analyzer, 49i, Thermo Scientific, Germany; NO_x analyzer, 42i-TL, Thermo Scientific, Germany; RH sensor FHA 646-E1C with ALMEMO 2590-3 instrument, Ahlborn, Mess- und Regelungstechnik, Germany). After exposure, the proteins were extracted from the glass tube with 1.5 mL 1×Tris/Glycine/SDS buffer to avoid precipitation of protein oligomers in the extract solution.

For homogeneous bulk solution reactions, the O₃/NO₂ gas mixtures were directly bubbled through 1.5 mL of 0.13 mg mL⁻¹ BSA aqueous solutions (pH 7.0 ± 0.2; measured by a pH meter model WTW multi 350i; WTW, Germany) at a flow rate of 60 mL min⁻¹ using a Teflon tube (ID: 1.59 mm). All heterogeneous and homogeneous exposure experiments were performed in duplicate.

2.3. SEC-HPLC-DAD analysis

Product analysis was performed using high-performance liquid chromatography coupled to diode array detection (HPLC-DAD, Agilent Technologies 1200 series). The HPLC-DAD system consisted of a binary pump (G1379B), an autosampler with thermostat (G1330B), a column thermostat (G1316B), and a photodiode array detector (DAD, G1315C). ChemStation software (Rev. B.03.01, Agilent) was used for system control and data analysis. Molecular weight (MW) separation by size exclusion chromatography (SEC) was carried out using an AdvanceBio SEC column (Agilent, 300 Å, 300 × 4.6 mm, 2.7 μm). Isocratic separation at a flow rate of 0.35 mL min⁻¹ was carried out using a mobile phase of 150 mM NaH₂PO₄ buffer (adjusted to pH 7 with 10 M NaOH (aq)) after injecting 40 μL of sample. The absorbance was monitored with the DAD at wavelengths of 220, 280 and 357 nm. Each chromatographic run was performed in duplicate.

A protein standard mix 15-600 kDa (69385, Sigma-Aldrich, Germany) containing bovine thyroglobulin (MW = 670 kDa), γ-globulin from bovine blood (MW = 150 kDa), chicken egg albumin, grade VI (MW = 44.3 kDa), and ribonuclease A (MW = 13.7 kDa) was used for the SEC column calibration (elution time vs log MW). Details can be found in Fig. S2 in the ESI. It should be noted that SEC separates molecules according to their hydrodynamic sizes, thus only approximate molecular masses can be obtained by this calibration method.

2.4. Determination of protein oligomer mass fractions and nitration degrees

A detailed description of the simultaneous determination of protein oligomer mass fractions and nitration degrees using the SEC-HPLC-DAD analysis described above can be found in Liu *et al.*²⁸ Briefly, we report the formation of BSA oligomers as the temporal evolution in

the ratios of the respective oligomers (dimer, trimer, and oligomers with $n \geq 4$) to the sum of monomer and all oligomer peak areas at the absorption wavelength of 220 nm. Assuming that the molar extinction coefficients of the individual protein oligomer fractions are multiples of the monomer extinction coefficient, the calculated oligomer ratios correspond to the mass fractions (ω) of the individual oligomers. Nitration degrees (NDs), defined as the concentration of nitrotyrosine (NTyr) divided by the sum of the concentrations of NTyr and Tyr, were obtained for BSA monomers and dimers, using the respective peak areas of the monomer and dimer signals at wavelengths of 280 nm and 357 nm. For the calculation of the total protein ND, the sum of the peak areas of all protein signals at wavelengths of 280 nm and 357 nm was used. Note that corresponding to the definition of the ND, the same number of nitrated Tyr residues in a BSA monomer and dimer will lead to a factor of 2 difference in the individual NDs, because a BSA dimer contains twice the number of Tyr residues compared to the monomer. Further information on the calculation of NDs can be found in Liu *et al.*²⁸ The values and errors of the calculated NDs and oligomer mass fractions represent arithmetic mean values and standard deviations of duplicate experiments.²⁹ The commercially available BSA also contained dimers and trimers of the protein as well as pre-nitrated monomers and dimers (\sim NDs 0.9%). Therefore, the reported values of oligomer mass fractions and NDs were corrected for these background signals.

3. Results and discussion

3.1. Protein oligomerization

Figures 1 and 2 show the effects of varying NO_2 and O_3 concentrations on protein oligomerization for homogeneous bulk solution and coated-wall flow-tube experiments, respectively. Exposures were carried out at fixed NO_2 concentrations with varying O_3 concentrations and vice versa. The exposure time was varied from 0.5 up to 12 h. While in bulk solution experiments dimers were generally observed as the major reaction products of BSA with O_3 and NO_2 , trimers or higher oligomers can be dominant products in the coated-wall flow-tube experiments at longer exposure times, depending on the experimental conditions.

The results of the bulk solution experiments on protein oligomerization are illustrated in Fig. 1. Generally, the mass fractions of dimers, trimers, and higher oligomers increase with increasing reaction times, reaching up to $21 \pm 1\%$ for dimers, $9 \pm 1\%$ for trimers, and $4 \pm 1\%$ for oligomers with $n \geq 4$ after 12 h of exposure. The minimum mass fraction of monomers correspondingly was found to be 66%. While varying the O_3 concentrations (Fig. 1a-d, fixed 50 ppb of NO_2) from 5 to 200 ppb significantly affected the temporal evolutions observed for the mass fractions of the different oligomers, changing the NO_2 concentration (Fig. 1e-h, fixed 50 ppb of O_3) in the same range did not result in significant changes in oligomer mass fractions. The solubility of O_3 and NO_2 in water is $\sim 10^{-5}$ mol mL⁻¹ (derived from their Henry's law constants: $K_{\text{sol, cc, O}_3} \approx K_{\text{sol, cc, NO}_2} \approx 10^{-2}$ M atm⁻¹)³⁰ under our experimental conditions. Increasing O_3 and NO_2 gas concentrations between 5 to 200 ppb should result in concentrations of O_3 and NO_2 between 7×10^{-11} to 3×10^{-9} M in the aqueous phase. Thus, the insignificant change of oligo-

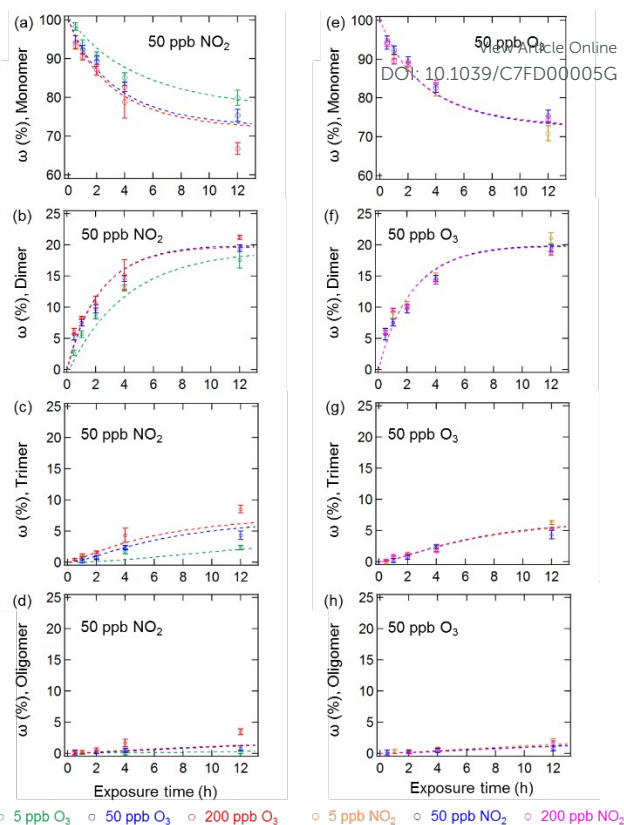


Fig. 1 Temporal evolution of protein oligomer mass fractions (ω (%), monomer, dimer, trimer and oligomer ($n \geq 4$)) in the aqueous phase reaction of BSA with O_3/NO_2 : ((a)-(d)) at a fixed NO_2 concentration of 50 ppb with varied O_3 concentrations; ((e)-(h)) at a fixed O_3 concentration of 50 ppb with varied NO_2 concentrations. The data points and error bars represent the arithmetic mean values and standard deviations of duplicate experiments. The dashed lines are the results of the kinetic model.

mer mass fractions with varied NO_2 concentration should not be caused by a saturation of dissolved NO_2 in the investigated concentration range (5 to 200 ppb).

Mechanistically, the reactions between O_3/NO_2 and protein Tyr residues involve the formation of ROIs (tyrosyl radicals) resulting from the reaction of Tyr with O_3 . These ROIs can then either react with NO_2 to form NTyr residues or cross-link due to intermolecular DTyr formation.^{6,20} Ozonolysis of Tyr may also result in other oxidized products such as 3,4-dihydroxyphenylalanine (DOPA).³¹ However, the reaction mechanism for the formation of these oxidized products is not the focus of this study and we only consider these modified Tyr derivatives in the proposed mechanism (Table S1) as a portion of the oxidized amino acid residues. Regardless, an inhibition of intermolecular DTyr cross-linking would be expected with increasing NO_2 concentrations. However, no such behavior was observed. Furthermore, similar protein oligomer mass fractions were observed previously in the absence of NO_2 for BSA exposed to O_3 in bulk solution experiments with comparable levels of O_3 (50 and 200 ppb).²⁰ This observation may be due to the high number of accessible Tyr residues on the dissolved BSA molecules in solution, because after 12 h of exposure still 66% of BSA (Fig. 1a) is present in monomeric form.

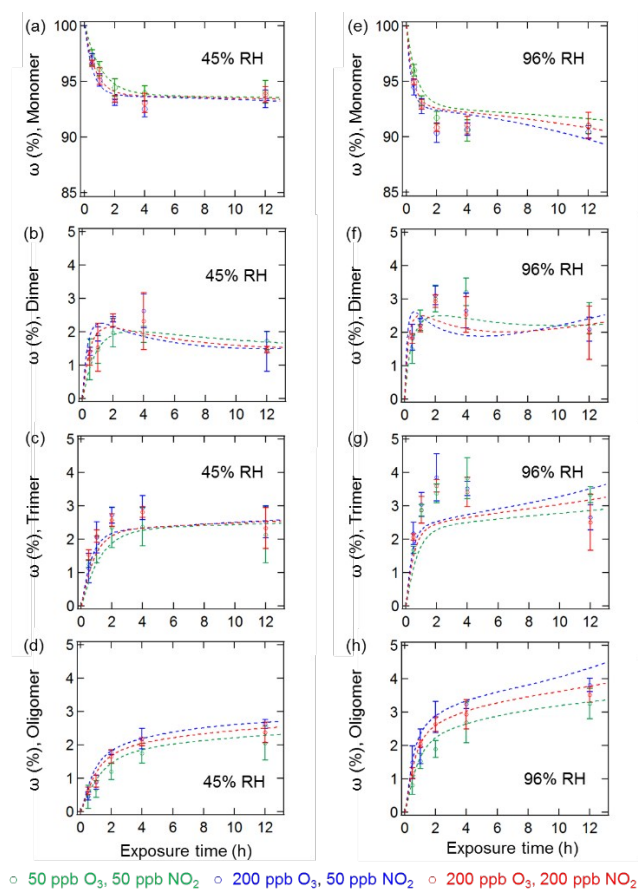


Fig. 2 Temporal evolution of protein oligomer mass fractions (ω (%), monomer, dimer, trimer and oligomer ($n \geq 4$)) upon exposure of BSA films (thickness 34 nm) to various O₃/NO₂ concentrations: ((a)-(d)) at 45% RH; ((e)-(h)) at 96% RH. The data points and error bars represent the arithmetic mean values and standard deviations of duplicate experiments. The dashed lines are the results of the kinetic model.

The results of the coated-wall flow-tube experiments on protein oligomerization are illustrated in Fig. 2. In these experiments, thin protein films were exposed to O₃/NO₂ mixtures. A film thickness of ~34 nm, or roughly five layers of BSA, can be calculated assuming an even distribution of the BSA molecules on the inner surface of the glass tube.²⁰ The experiments were performed at 45% and 96% RH with O₃/NO₂ concentrations of 50/50, 200/50, and 50/200 ppb, respectively. Generally, the reactive sites accessible for oligomerization reactions of the proteins are limited here compared to aqueous solutions, leading to smaller mass fractions of protein oligomers. Furthermore, we observed a 30-40% reduction of the overall oligomer mass fraction (dimer, trimer, and oligomer ≥ 4) compared to similar flow-tube experiments in the absence of NO₂ for comparable RH and O₃ concentrations.²⁰ Apparently, the lower diffusivity of the proteins in this solid (45% RH) or semi-solid (96% RH) state induces a competition between DTyr and NTyr formation, also indicated by the observation of slower reaction rates for oligomerization in the bulk of the thin protein film compared to its surface.^{20, 23}

In contrast to the bulk solution experiments, which showed a steady increase of the oligomer mass fractions with exposure time, dimer and trimer mass fractions in the flow tube experiments peaked

at exposure times of 2 – 4 h, depending on RH and trace gas concentrations, while only higher oligomers steadily increased over the course of the reaction time (see Fig. 2). This result indicates that as the exposure proceeds, the formation of dimers and trimers becomes slower than their consumption converting them into higher oligomers. The characteristic residence times (lifetimes) of biological particles in the atmosphere can range from hours to weeks, depending on their sizes, aerodynamic, and hygroscopic properties.³² Our observation indicates that initial exposure (< 2 – 4 h) of proteins to O₃ and NO₂ mainly leads to the formation of protein dimers and trimers, and as exposure proceeds, protein oligomers could be the dominant protein species, e.g., on the surface of bioaerosol particles.

3.2. Protein nitration

Figures 3 and 4 show the effects of varying NO₂ and O₃ concentrations on the nitration of protein monomers and dimers in homogeneous bulk solution and coated-wall flow-tube experiments, respectively. Exposures were carried out at fixed NO₂ concentrations with varying O₃ concentrations and vice versa. The exposure time was varied from 0.5 up to 12 h. While in previous studies total protein nitration degrees (NDs) were investigated upon exposure to O₃ and NO₂,^{12, 33} we explicitly explored and characterized the reaction kinetics of protein nitration, resolving the individual NDs of the protein monomer and its various oligomers over the course of reaction time.

The results of the bulk solution experiments on protein nitration are illustrated in Fig. 3. The maximum ND of protein monomers and dimers were found to be 7 % and 5 % after 12 h exposure to 200 ppb O₃ and 50 ppb NO₂, respectively. These results correspond to 1.4 NTyr residues per monomer molecule and 2 NTyr residues per dimer molecule (NTyr/Monomer and NTyr/Dimer are shown as secondary y-axis in Figs. 3 and 4). We found a positive relationship between the NDs and O₃ concentration (Fig. 3a and b), particularly the increase of

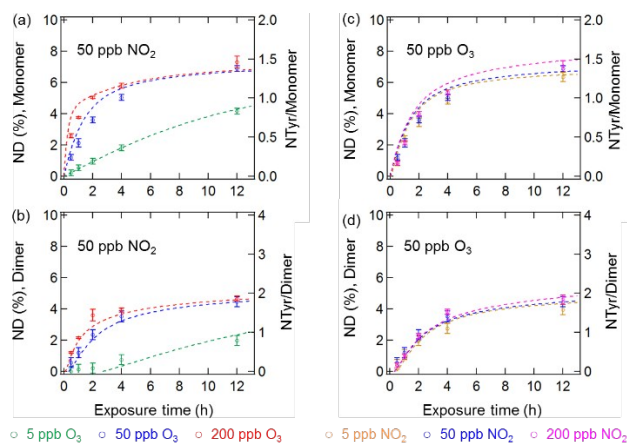


Fig. 3 NDs of protein monomer and dimer (primary y-axis), and NTyr number per monomer and dimer (secondary y-axis) plotted against reaction time in the aqueous phase reaction of BSA with O₃/NO₂: (a) and (b) at a fixed NO₂ concentration of 50 ppb with varied O₃ concentrations; (c) and (d) at a fixed O₃ concentration of 50 ppb with varied NO₂ concentrations. The data points and error bars represent the arithmetic mean values and standard deviations of duplicate experiments. The dashed lines are the results of the kinetic model.

O₃ concentration by one order of magnitude from 5 to 50 ppb resulted in an increase of NDs from $4.2 \pm 0.2\%$ to $6.9 \pm 0.2\%$, and $2.0 \pm 0.3\%$ to $4.5 \pm 0.3\%$ after 12 h exposure for the monomer and dimer, respectively. Also, for protein nitration, no significant difference was found when concentrations of NO₂ were varied from 5 to 200 ppb at a fixed O₃ concentration of 50 ppb, as shown in Fig. 3c and d. These results are in accordance with the observation by Shiraiwa *et al.*²³ on the study of the reactive uptake of NO₂ by aerosolized proteins. They found that the uptake coefficient of NO₂ (γ_{NO_2}) increased with increasing O₃ concentrations while γ_{NO_2} decreased gradually with increasing NO₂ concentration. Thus, our results confirmed that the protein reaction with O₃ and formation of ROI is the rate-limiting step for protein nitration.^{21,23} Shiraiwa *et al.*²³ have excluded NO₃ or N₂O₅ (formed through NO₂ oxidation by O₃) as major contributors for protein nitration. Ghiani *et al.*³⁴ reported that nitration of proteins can also occur by nitrate ions in bulk solutions without UV irradiation under acidic conditions (pH < 3 for BSA). The reaction of NO₂ with water can form nitric acid and thereby nitrate ions might appear in the BSA solution. However, we found that the pH of the BSA solutions stayed relatively constant (pH 6.6 ± 0.2 ; pH meter model WTW multi 350i) for a reaction time of 12 h at 200 ppb NO₂ and 50 ppb O₃, indicating that nitration induced by nitrate ions is likely a minor or negligible pathway in this study. This hypothesis is consistent with the results in Fig. 3c and d that show only a slight increase in ND (monomer, $6.3 \pm 0.3\%$ to $6.9 \pm 0.2\%$, and dimer, $4.0 \pm 0.3\%$ to $4.5 \pm 0.3\%$, for 12 h reaction) for a one order of magnitude increase in the NO₂ concentration from 5 to 50 ppb.

The results of the temporal increase of NDs of monomer and dimer for reactions of the thin protein films with O₃ and NO₂ concentrations of 50 and 200 ppb at 45% and 96% RH are illustrated in Fig. 4. Here, the NDs for monomer and dimer at 45% RH were found to be around 1% and 0.8% for 12 h exposure, corresponding to 0.2 NTyr/monomer molecule and 0.3 NTyr/dimer molecule. Note that the protein coating consisted of ~5 layers. Therefore, the results

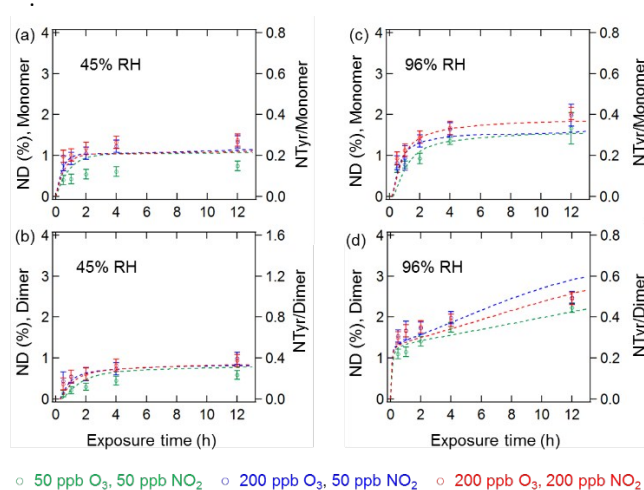


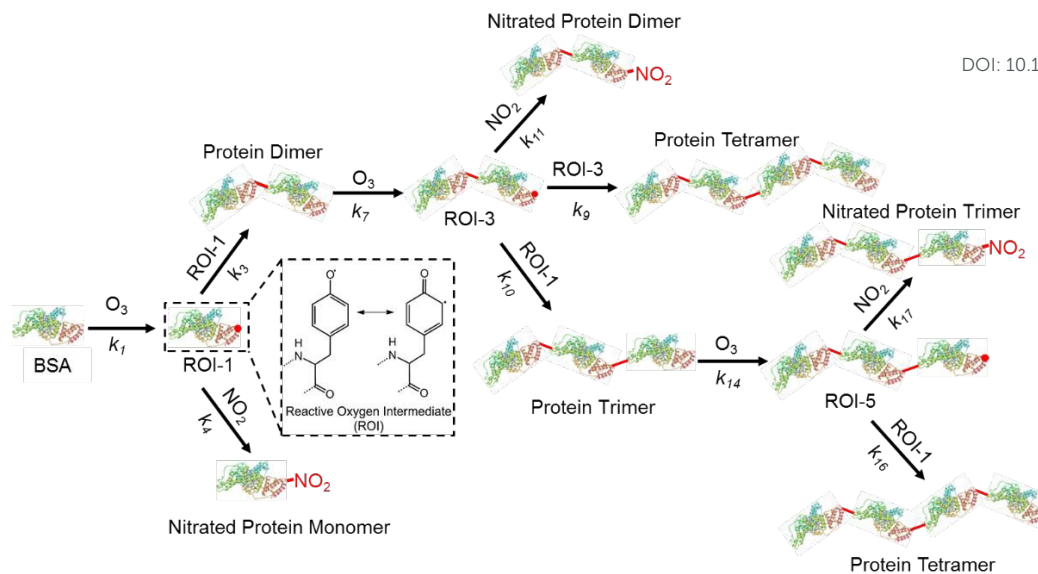
Fig. 4 NDs of protein monomer and dimer (primary y-axis), and NTyr number per monomer and dimer (secondary y-axis) plotted against exposure time upon exposure of BSA films (thickness 34 nm) to various O₃/NO₂ concentrations: (a) and (b) at 45% RH; (c) and (d) at 96% RH. The data points and error bars represent the arithmetic mean values and standard deviations of duplicate experiments. The dashed lines are the results of the kinetic model.

likely indicate that on average one Tyr per BSA monomer molecule located on the surface of the protein film were efficiently nitrated, while the bulk nitration occurred at much slower rates. This highly reactive site could be the Tyr residue at position 161 (Y161), as suggested by Zhang *et al.*³⁵ The maximum NDs for monomer and dimer reached up to $2.5 \pm 0.1\%$ and $2.0 \pm 0.1\%$ at 96% RH, respectively. However, both of the maximum NDs at 45% and 96% RH were much lower than those obtained for O₃/NO₂ exposure in aqueous solutions (200 ppb O₃ and 50 ppb NO₂). This discrepancy can be explained by a decrease in viscosity and an increase in diffusivity going from an amorphous solid (45% RH) or semisolid (96% RH) protein on a coated wall to an aqueous protein solution and was able to be reproduced using a model (see below).^{36,37} Furthermore, the NDs of BSA in this study are comparable to those found by Yang *et al.*³³ using the same protein, whereas the nitration efficiency of BSA in general is found to be much lower than the one observed for the major birch pollen allergen Bet v 1 in similar exposure experiments,¹² indicating a strong influence of molecular structure and potentially the amino acid sequence of the reacting protein. From previous mass spectrometric analysis of the site-selectivity of protein nitration by O₃/NO₂, it is known that only 3 out of 21 Tyr residues in BSA can be detected in nitrated form, while in Bet v 1, 4 out of 7 Tyr residues can be nitrated.^{12,35} Thus, besides the types of nitrating agents (e.g. ONOO⁻ or O₃/NO₂) and reaction conditions (in aqueous solution or heterogeneous exposure), the nitration efficiency also depends on the fraction of reactive Tyr residues in the investigated protein.

3.3. Kinetics and mechanism of protein nitration and oligomerization by O₃/NO₂

The model results for the reactions of proteins with O₃/NO₂ under the various exposure conditions are shown as the dashed lines in Figs. 1-4. A chemical mechanism involving 19 reactions (see Table S1 for details) was applied in two kinetic models, i.e., a box model for bulk solution experiments and the kinetic multilayer model for aerosol surface and bulk chemistry (KM-SUB)²⁶ for flow tube experiments to fit the experimental data. The most relevant reactions for this mechanism are illustrated in Fig. 5. The first step in the mechanism is the reaction of a Tyr residue with O₃ forming tyrosyl radicals as long-lived reactive oxygen intermediates (ROIs). In the second step of the process, the ROIs can react with each other to form dimers, or with NO₂ to form nitrated monomers. Note that for simplification, each molecule only contains one reactive tyrosine residue, while nitrated and oxidized monomers, dimers and trimers are unable to take part in further reactions in the kinetic model. A dimer can react further with O₃ to form a dimeric ROI, which may react with NO₂ to form a nitrated protein dimer, with monomeric ROI to form a protein trimer or with another dimeric ROI to form a protein tetramer.

The following assumptions were made to enable modelling the reaction system for bulk solution and coated-wall flow-tube experiments using the sets of physicochemical parameters shown in Table S1 (ESI): BSA molecules have reactive amino acid residues on their surface (AA1) and in their bulk (AA2), both of them reactive towards O₃. While ROIs formed in the protein bulk can only react with NO₂ to form NTyr, they are unable to form intermolecular DTyr due to steric hindrance.³⁸ These assumptions were also applied to di-



View Article Online
DOI: 10.1039/C7FD00005G

Fig. 5 Schematic overview of the most relevant reactions for protein nitration and oligomerization upon exposure to ozone and nitrogen dioxide. The reactions are corresponding to protein surface Tyr nitration and oligomerization in the mechanism presented in Table S1. The molecular structure of the protein (BSA, PDB accession number 3V03) was created using the RCSB PDB protein workshop (4.2.0) software.

mers and trimers. Besides Tyr, O_3 can also oxidize other amino acid residues, i.e., cysteine (Cys), tryptophan (Trp), methionine (Met) and histidine (His).³¹ Among them, only Cys is able to cross-link proteins directly upon O_3 exposure, yielding intermolecular disulfide bridges, as one free Cys is available in BSA.³⁹ This reversible cross-linking mechanism has been shown to be only a minor contributor to protein oligomerization upon O_3/NO_2 exposure previously.²⁰ The kinetic parameters were obtained using a global optimization method combining a uniformly-sampled Monte-Carlo search with a genetic algorithm (MCGA method).^{40, 41} The genetic algorithm was terminated when the correlation between experimental data and model output reached an optimum. Concentrations of O_3 and NO_2 in the aqueous phase can be estimated using the published Henry's law constant of $K_{sol, cc, O_3} \approx K_{sol, cc, NO_2} \approx 10^{-2} \text{ M atm}^{-1}$, which were used as fixed values in the model.³⁰

The temporal evolution of NDs and oligomer mass fractions in aqueous solution is well-reproduced by the model (Figs. 1 and 3). For the heterogeneous reactions studied in the coated-wall flow-tube experiments at 45% RH and 96% RH, some substantial deviations between modelled and measured data can be observed, and the coefficient of determination (R^2 value) is approximately a factor of two lower than for the aqueous data. For example, the oligomer mass fractions ω at 45% RH in Fig. 2 a-d are qualitatively captured fairly well, while the model fails to reproduce their evolution at higher RH, especially for the dimer and trimer (Fig. 2 f and g). The observed reduction of dimers in flow tube experiments could be reproduced by the model including the reactions on the surface, where the rates are four orders of magnitude higher than that of bulk reactions. Despite simple model assumptions when describing the complex reaction system that was studied, the model reproduces the experimental data reasonably well with an overall R^2 value of 0.88 for Figures 1-4. Most of the optimized parameters obtained for the flow tube experiments were close to or the same as those for

aqueous solutions (for details see Table S1, ESI). However, note that some of the rate coefficients would be expected to change as the liquid water content and viscosity varies. Water could actively take part in some of the reactions and its presence at different concentrations could lead to changes in experimental conditions, such as pH, which would influence the rate of the reactions. As the viscosity increases it is also expected that some rate coefficients would decrease as they become diffusion-limited as per the Smoluchowski diffusion equation.^{42, 43}

The second-order rate coefficients obtained as model outputs and shown in Table S1 are mostly consistent with previous studies.^{20, 23} However, as the complex reaction mixture has been reflected in only 19 chemical reactions, the absolute numbers of the rate coefficients obtained for the individual reactions likely do not reflect reality, because further secondary chemistry of various kinds is not included explicitly. It should also be noted that different types of tyrosine residues have not been explicitly included within the model, although these can nitrate at different rates and have different surface accessibilities.^{35, 44} Nevertheless, qualitatively, the model results suggest that protein nitration occurs at faster rates than protein oligomerization. The observed and modelled preference of nitration over oligomerization can be rationalized by comparing the mass fraction of nitrated monomer (calculated by multiplying the mass fraction of monomer with NTyr/monomer) with the total oligomer mass fraction. Nitrated monomers were observed to have two times or higher mass fractions compared to all other oligomer mass fractions combined under all experimental conditions. This result indicates the Tyr nitration outcompetes the dimerization/oligomerization process.^{22, 45}

4. Implications and conclusions

In this study we investigated the kinetics and mechanism of nitration and oligomerization of proteins induced by O_3 and NO_2 under different atmospherically-relevant conditions. We showed the concentration and time dependence of the formation of dimers, trimers and higher protein oligomers as well as their individual nitration degrees. The temporal evolution of the concentrations of these multiple reaction products were well reproduced by a kinetic model with 19 chemical reactions. Protein nitration was found to be kinetically favored over protein oligomerization under the experimental conditions studied in this work. On the basis of the observation of nitrated oligomers formed upon exposure to O_3/NO_2 , we suggest further investigation on allergenic and immunogenic effects by nitrated protein oligomers. The nitrated oligomers were also found in the physiologically-relevant peroxyxynitrite-induced protein nitration and oligomerization,⁴⁶ in which the mechanism is similar to the one we reported here.^{25, 47}

The implications of protein chemistry with O_3 and NO_2 under atmospherically relevant conditions are illustrated in Fig. 6. The overall nitration and oligomerization rates were both almost one order of magnitude higher in aqueous phase than for 45% RH, indicating an increased relevance of the processes under cloud-processing conditions. Also, the yields of protein nitration and oligomerization can be strongly influenced by changes in relative humidity leading to changes of phase states. The protein dimers can yield up to 20% (by mass) for 12h exposure in the liquid phase and the NDs of monomers and dimers can be up to 7% and 5%, respectively. This result indicates that on average, 1.4 Tyr residues in each monomeric protein molecule and 2 Tyr residues in each dimeric molecule are present in their nitrated forms. For proteins in solid or semi-solid phase states, our measurement and model results suggest that higher protein oligomers are likely to be found at lower RH, e.g., on the surface of bioaerosols, whereas the NDs of monomers and dimers remain at ~1-2%. Using ab initio calculations, Sandiya *et al.*²²

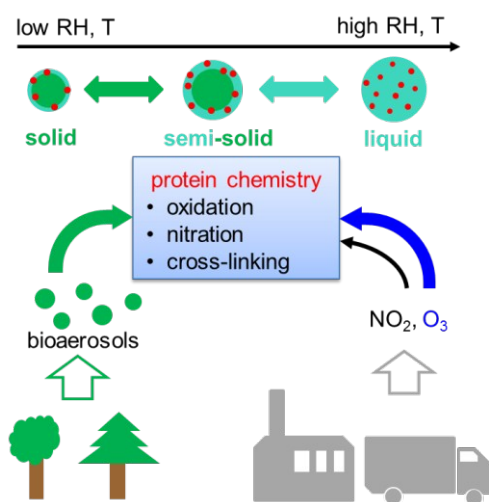


Fig. 6 Atmospheric protein chemistry by ozone (O_3) and nitrogen dioxide (NO_2). Reaction rates are limited by the phase state of proteins and hence the diffusivity of oxidants and protein molecules, which changes with relative humidity (RH) and temperature (T). Air pollutants such as NO_2 and O_3 can enhance the allergen release from bioaerosols (e.g., pollen), with O_3 being more important in triggering the nitration, cross-linking and oxidation of allergenic proteins in bioaerosols and other protein-containing particles (e.g., Bet v 1 on urban road dust¹⁵).

also showed that increased temperature can speed up the formation of tyrosyl radicals by ozonolysis. Thus, it is expected that nitrated and dimeric protein species could be important products of exposure to O_3 and NO_2 under tropical or summer smog conditions. These differences in reaction kinetics should be taken into account in studies on the physiological effects of proteins exposed to anthropogenic air pollutants, as the allergenic proteins in various oligomerization and nitration states might have a different immunogenic potential.

Both increasing levels of O_3 and NO_2 are able to damage pollen grains and facilitate the release of allergen in polluted environments.^{3, 8, 9} However, our results showed that the tyrosine nitration and cross-linking of proteins are sensitive towards the increase of O_3 concentration and rather insensitive towards change in ambient NO_2 concentrations. Therefore, an effective control of the enhanced allergenicity induced by air pollutants-modified aeroallergens should point towards the decrease of ambient ozone concentrations.

Acknowledgements

F.L. and S.L. acknowledge financial support from China Scholarship council (CSC). C.J.K. and T.B. acknowledge support by the Max Planck Graduate Center with the Johannes Gutenberg University Mainz (MPGC). C.J.K. acknowledges financial support by the German Research Foundation (DFG; grant no. KA 4008/1-2).

Notes and references

- M. I. Asher, S. Montefort, B. Björkstén, C. K. Lai, D. P. Strachan, S. K. Weiland, H. Williams and I. P. T. S. Group, *Lancet*, 2006, 368, 733-743.
- R. Pawankar, C. E. Baena-Cagnani, J. Bousquet, G. W. Canonica, A. A. Cruz, M. A. Kaliner and B. Q. Lanier, *World Allergy Organ. J.*, 2008, 1, S4-S17.
- U. Frank and D. Ernst, *Front. Plant. Sci.*, 2016, 7.
- K.-H. Kim, S. A. Jahan and E. Kabir, *Environ. Int.*, 2013, 59, 41-52.
- U. Pöschl and M. Shiraiwa, *Chem. Rev.*, 2015, 115, 4440-4475.
- K. Reinmuth-Selzle, C. J. Kampf, K. Lucas, N. Lang-Yona, J. Fröhlich-Nowoisky, M. Shiraiwa, S. Lai, F. Liu, F. Shen, R. Sgarbanti, B. Weber, M. G. Weller, I. Bellinghausen, J. Saloga, A. Duschl, D. Schuppan and U. Pöschl, *Environ. Sci. Technol.*, 2017, Submitted.
- D. Diaz-Sanchez, M. P. Garcia, M. Wang, M. Jyrala and A. Saxon, *J. Allergy. Clin. Immun.*, 1999, 104, 1183-1188.
- I. Beck, S. Jochner, S. Gilles, M. McIntyre, J. T. Buters, C. Schmidt-Weber, H. Behrendt, J. Ring, A. Menzel and C. Traidl-Hoffmann, *PLoS One*, 2013, 8, e80147.
- Y. Ouyang, Z. Xu, E. Fan, Y. Li and L. Zhang, *Int. Forum. Allergy. Rhinol.*, 2016, 6, 95-100.
- C. Ackaert, S. Kofler, J. Horejs-Hoecck, N. Zulehner, C. Asam, S. von Grafenstein, J. E. Fuchs, P. Briza, K. R. Liedl and B. Bohle, *PLoS one*, 2014, 9, e104520.
- N. Lang-Yona, T. Shuster-Meiseles, Y. Mazar, O. Yarden and Y. Rudich, *Sci. Total Environ.*, 2016, 541, 365-371.
- K. Reinmuth-Selzle, C. Ackaert, C. J. Kampf, M. Samonig, M. Shiraiwa, S. Kofler, H. Yang, G. Gadermaier, H. Brandstetter and C. G. Huber, *J. Proteome Res.*, 2014, 13, 1570-1577.
- A. D. Estillore, J. V. Trueblood and V. H. Grassian, *Chem. Sci.*, 2016, 7, 6604-6616.

- 14 J. Fröhlich-Nowoisky, C. J. Kampf, B. Weber, J. A. Huffman, C. Pöhlker, M. O. Andreae, N. Lang-Yona, S. M. Burrows, S. S. Gunthe, W. Elbert, H. Su, P. Hoor, E. Thines, T. Hoffmann, V. R. Després and U. Pöschl, *Atmos. Res.*, 2016, 182, 346-376.
- 15 T. Franze, M. G. Weller, R. Niessner and U. Pöschl, *Environ. Sci. Technol.*, 2005, 39, 1673-1678.
- 16 J. T. Buters, A. Kasche, I. Weichenmeier, W. Schober, S. Klaus, C. Traidl-Hoffmann, A. Menzel, J. Huss-Marp, U. Krämer and H. Behrendt, *Int. Arch. Allergy Immunol.*, 2007, 145, 122-130.
- 17 F. Liu, S. Lai, K. Reinmuth-Selzle, J. F. Scheel, J. Fröhlich-Nowoisky, V. R. Després, T. Hoffmann, U. Pöschl and C. J. Kampf, *Anal. Bioanal. Chem.*, 2016, 408, 6337-6348.
- 18 P. Taylor, R. Flagan, A. Miguel, R. Valenta and M. Glovsky, *Clin. Exp. Allergy.*, 2004, 34, 1591-1596.
- 19 G. F. Schäppi, P. E. Taylor, I. A. Staff, C. Suphioglu and R. B. Knox, *Sex. Plant. Reprod.*, 1997, 10, 315-323.
- 20 C. J. Kampf, F. Liu, K. Reinmuth-Selzle, T. Berkemeier, H. Meusel, M. Shiraiwa and U. Pöschl, *Environ. Sci. Technol.*, 2015, 49, 10859-10866.
- 21 M. Shiraiwa, Y. Sosedova, A. Rouvière, H. Yang, Y. Zhang, J. P. Abbatt, M. Ammann and U. Pöschl, *Nat. Chem.*, 2011, 3, 291-295.
- 22 L. Sandhiya, P. Kolandaivel and K. Senthilkumar, *J. Phys. Chem. B*, 2014, 118, 3479-3490.
- 23 M. Shiraiwa, K. Selzle, H. Yang, Y. Sosedova, M. Ammann and U. Pöschl, *Environ. Sci. Technol.*, 2012, 46, 6672-6680.
- 24 M. Shiraiwa, K. Selzle and U. Pöschl, *Free. Radic. Res.*, 2012, 46, 927-939.
- 25 S. Pfeiffer, K. Schmidt and B. Mayer, *J. Biol. Chem.*, 2000, 275, 6346-6352.
- 26 M. Shiraiwa, C. Pfrang and U. Pöschl, *Atmos. Chem. Phys.*, 2010, 10, 3673-3691.
- 27 G. Li, H. Su, X. Li, U. Kuhn, H. Meusel, T. Hoffmann, M. Ammann, U. Pöschl, M. Shao and Y. Cheng, *Atmos. Chem. Phys.*, 2016, 16, 10299-10311.
- 28 F. Liu, K. Reinmuth-Selzle, S. Lai, M. G. Weller, U. Pöschl and C. J. Kampf, *J. Chromatogr. A*, 2017, Submitted.
- 29 S. L. Ellison, M. Rosslein and A. Williams, in *Quantifying uncertainty in analytical measurement*, Eurachem, 2000.
- 30 R. Sander, *Atmos. Chem. Phys.*, 2015, 15.
- 31 V. K. Sharma and N. J. Graham, *Ozone Sci. Eng.*, 2010, 32, 81-90.
- 32 V. R. Després, J. A. Huffman, S. M. Burrows, C. Hoose, A.S. Safatov, G. Buryak, J. Fröhlich-Nowoisky, W. Elbert, M. O. Andreae, U. Pöschl, R. Jaenicke, *Tellus B*, 2012, 64, 1-58.
- 33 H. Yang, Y. Zhang and U. Pöschl, *Anal. Bioanal. Chem.*, 2010, 397, 879-886.
- 34 A. Ghiani, M. Bruschi, S. Citterio, E. Bolzacchini, L. Ferrero, G. Sangiorgi, R. Asero and M. G. Perrone, *Sci. Total Environ.*, 2016.
- 35 Y. Zhang, H. Yang and U. Pöschl, *Anal. Bioanal. Chem.*, 2011, 399, 459-471.
- 36 M. Shiraiwa, M. Ammann, T. Koop and U. Pöschl, *Proc. Natl. Acad. Sci. U. S. A.*, 2011, 108, 11003-11008.
- 37 E. Mikhailov, S. Vlasenko, S. Martin, T. Koop and U. Pöschl, *Atmos. Chem. Phys.*, 2009, 9, 9491-9522.
- 38 W. H. Heijnis, H. L. Dekker, L. J. de Koning, P. A. Wierenga, A. H. Westphal, C. G. de Koster, H. Gruppen and W. J. van Berkel, *J. Agric. Food Chem.*, 2010, 59, 444-449.
- 39 T. Ueki, Y. Hiragi, M. Kataoka, Y. Inoko, Y. Amemiya, Y. Izumi, H. Tagawa and Y. Muroga, *Biophys. Chem.*, 1985, 23, 115-124.
- 40 T. Berkemeier, S. S. Steimer, U. K. Krieger, T. Peter, U. Pöschl, M. Ammann and M. Shiraiwa, *Phys. Chem. Chem. Phys.*, 2016, 18, 12662-12674.
- 41 A. M. Arangio, J. H. Slade, T. Berkemeier, U. Pöschl, D. A. Knopf and M. Shiraiwa, *J. Phys. Chem. A*, 2015, 119, 4533-4544.
- 42 W. Scheider, *J. Phys. Chem.*, 1972, 76, 349-361.
- 43 L. J. Lapidus, W. A. Eaton and J. Hofrichter, *Proc. Natl. Acad. Sci. U. S. A.*, 2000, 97, 7220-7225.
- 44 B. Petersen, T. N. Petersen, P. Andersen, M. Nielsen and C. Lundegaard, *BMC. Struct. Biol.*, 2009, 9, 10.1039/C7FD00005G
- 45 J. M. Souza, G. Peluffo and R. Radi, *Free. Radic. Biol. Med.*, 2008, 45, 357-366.
- 46 Y. J. Zhang, Y. F. Xu, X. Q. Chen, X. C. Wang and J.-Z. Wang, *FEBS Lett.*, 2005, 579, 2421-2427.
- 47 R. Radi, *Proc. Natl. Acad. Sci. U. S. A.*, 2004, 101, 4003-4008.

Supporting Information for “Atmospheric protein chemistry influenced by anthropogenic air pollutants: nitration and oligomerization upon exposure to ozone and nitrogen dioxide”

Faraday Discussions

Fobang Liu,^a Pascale S. J. Lakey,^a Thomas Berkemeier,^{a,b} Haijie Tong,^a Anna Theresa Kunert,^a Hannah Meusel,^a Yafang Cheng,^a Hang Su,^a Janine Fröhlich-Nowoisky,^a Senchao Lai,^c Michael G. Weller,^d Manabu Shiraiwa,^e Ulrich Pöschl,^a and Christopher J. Kampf^{*,f,a}

^aMultiphase Chemistry Department, Max Planck Institute for Chemistry, Hahn-Meitner-Weg 1, 55128 Mainz, Germany

^bSchool of Chemical & Biomolecular Engineering, Georgia Tech, Atlanta, GA, USA

^cSchool of Environment and Energy, South China University of Technology, Higher Education Mega Center, Guangzhou 510006, P.R. China

^dDivision 1.5 Protein Analysis, Federal Institute for Materials Research and Testing (BAM), Richard-Willstätter-Str. 11, 12489 Berlin, Germany

^eDepartment of Chemistry, University of California, Irvine, CA, USA

^fInstitute for Organic Chemistry, Johannes Gutenberg University Mainz, Duesbergweg 10-14, 55128 Mainz, Germany

*Correspondence to Christopher J. Kampf, email: kampf@uni-mainz.de, phone: +49 6131 39 22417

Table S1 The chemical mechanism with 19 equations and the corresponding parameters used in the kinetic model for the reactions of proteins with O₃ and NO₂ at 45% RH, 96% RH and aqueous solutions. The bulk diffusion coefficients of O₃ and NO₂ were estimated to be $1.9 \times 10^{-10} \text{ cm}^2 \text{ s}^{-1}$ at 45% RH and $1.0 \times 10^{-9} \text{ cm}^2 \text{ s}^{-1}$ at 96% RH; self-diffusion coefficients of protein were estimated to be $9.0 \times 10^{-21} \text{ cm}^2 \text{ s}^{-1}$ at 45% RH and $1.0 \times 10^{-18} \text{ cm}^2 \text{ s}^{-1}$ at 96% RH. Note that reactions on the surface were also included for the flow tube experiments with rate constants determined using the following equation: $k_{\text{surface}} (\text{cm}^2 \text{ s}^{-1}) = 1 \times 10^4 \times k_{\text{bulk}} (\text{cm}^3 \text{ s}^{-1})$.

No.	Equation	Parameters		
		45% RH	96% RH	Aqueous
	Total BSA = x_I AA ₁ + (1- x_I) AA ₂	$x_I = 0.56$	$x_I = 0.65$	$x_I = 0.69$
R1	O ₃ + AA ₁ → c_I ROI-1 + (1- c_I) oxidized monomer	$k_I = 3.41 \times 10^{-15} \text{ cm}^3 \text{ s}^{-1}$ $c_I = 0.97$	$k_I = 5.99 \times 10^{-15} \text{ cm}^3 \text{ s}^{-1}$ $c_I = 0.99$	$k_I = 5.00 \times 10^{-14} \text{ cm}^3 \text{ s}^{-1}$ $c_I = 0.97$
R2	O ₃ + AA ₂ → c_2 ROI-2 + (1- c_2) oxidized monomer	$k_2 = 4.55 \times 10^{-15} \text{ cm}^3 \text{ s}^{-1}$ $c_2 = 0.15$	$k_2 = 3.83 \times 10^{-14} \text{ cm}^3 \text{ s}^{-1}$ $c_2 = 0.25$	$k_2 = 8.32 \times 10^{-16} \text{ cm}^3 \text{ s}^{-1}$ $c_2 = 0.13$
R3	ROI-1 + ROI-1 → x_2 dimer ₁ + (1- x_2) dimer ₂	$k_3 = 4.26 \times 10^{-19} \text{ cm}^3 \text{ s}^{-1}$ $x_2 = 0.85$	$k_3 = 6.11 \times 10^{-19} \text{ cm}^3 \text{ s}^{-1}$ $x_2 = 0.84$	$k_3 = 3.45 \times 10^{-20} \text{ cm}^3 \text{ s}^{-1}$ $x_2 = 0.54$
R4	ROI-1 + NO ₂ → nitrated monomer	$k_4 = 5.00 \times 10^{-19} \text{ cm}^3 \text{ s}^{-1}$	$k_4 = 5.00 \times 10^{-19} \text{ cm}^3 \text{ s}^{-1}$	$k_4 = 5.00 \times 10^{-19} \text{ cm}^3 \text{ s}^{-1}$
R5	ROI-1 → AA ₁	$k_5 = 1.98 \times 10^{-8} \text{ s}^{-1}$	$k_5 = 9.38 \times 10^{-8} \text{ s}^{-1}$	$k_5 = 6.95 \times 10^{-4} \text{ s}^{-1}$
R6	ROI-2 + NO ₂ → nitrated monomer	$k_6 = 1.00 \times 10^{-13} \text{ cm}^3 \text{ s}^{-1}$	$k_6 = 1.00 \times 10^{-13} \text{ cm}^3 \text{ s}^{-1}$	$k_6 = 1.00 \times 10^{-13} \text{ cm}^3 \text{ s}^{-1}$
R7	dimer ₁ + O ₃ → c_3 ROI-3 + (1- c_3) oxidized dimer	$k_7 = 1.64 \times 10^{-13} \text{ cm}^3 \text{ s}^{-1}$ $c_3 = 0.57$	$k_7 = 1.81 \times 10^{-13} \text{ cm}^3 \text{ s}^{-1}$ $c_3 = 0.78$	$k_7 = 1.01 \times 10^{-15} \text{ cm}^3 \text{ s}^{-1}$ $c_3 = 0.67$
R8	dimer ₂ + O ₃ → c_4 ROI-4 + (1- c_4) oxidized dimer	$k_8 = 9.94 \times 10^{-15} \text{ cm}^3 \text{ s}^{-1}$ $c_4 = 0.13$	$k_8 = 9.94 \times 10^{-15} \text{ cm}^3 \text{ s}^{-1}$ $c_4 = 0.14$	$k_8 = 1.41 \times 10^{-15} \text{ cm}^3 \text{ s}^{-1}$ $c_4 = 0.14$
R9	ROI-3 + ROI-3 → tetramer	$k_9 = 9.76 \times 10^{-21} \text{ cm}^3 \text{ s}^{-1}$	$k_9 = 8.88 \times 10^{-21} \text{ cm}^3 \text{ s}^{-1}$	$k_9 = 2.29 \times 10^{-20} \text{ cm}^3 \text{ s}^{-1}$
R10	ROI-1 + ROI-3 → x_3 trimer ₁ + (1- x_3) trimer ₂	$k_{10} = 4.80 \times 10^{-20} \text{ cm}^3 \text{ s}^{-1}$ $x_3 = 0.80$	$k_{10} = 4.77 \times 10^{-20} \text{ cm}^3 \text{ s}^{-1}$ $x_3 = 0.80$	$k_{10} = 3.75 \times 10^{-20} \text{ cm}^3 \text{ s}^{-1}$ $x_3 = 0.80$

R11	ROI-3 + NO ₂ → nitrated dimer	$k_{11} = 5.32 \times 10^{-18} \text{ cm}^3 \text{ s}^{-1}$	$k_{11} = 6.18 \times 10^{-17} \text{ cm}^3 \text{ s}^{-1}$	$k_{11} = 2.77 \times 10^{-19} \text{ cm}^3 \text{ s}^{-1}$
R12	ROI-3 → dimer ₁	$k_{12} = 7.63 \times 10^{-9} \text{ s}^{-1}$	$k_{12} = 9.58 \times 10^{-8} \text{ s}^{-1}$	$k_{12} = 1.06 \times 10^{-5} \text{ s}^{-1}$
R13	ROI-4 + NO ₂ → nitrated dimer	$k_{13} = 1.00 \times 10^{-13} \text{ cm}^3 \text{ s}^{-1}$	$k_{13} = 1.00 \times 10^{-13} \text{ cm}^3 \text{ s}^{-1}$	$k_{13} = 1.00 \times 10^{-13} \text{ cm}^3 \text{ s}^{-1}$
R14	trimer ₁ + O ₃ → c ₅ ROI-5 + (1-c ₅) oxidized trimer	$k_{14} = 1.00 \times 10^{-12} \text{ cm}^3 \text{ s}^{-1}$ c ₅ = 0.15	$k_{14} = 1.00 \times 10^{-12} \text{ cm}^3 \text{ s}^{-1}$ c ₅ = 0.15	$k_{14} = 1.00 \times 10^{-12} \text{ cm}^3 \text{ s}^{-1}$ c ₅ = 0.15
R15	trimer ₂ + O ₃ → c ₆ ROI-6 + (1-c ₆) oxidized trimer	$k_{15} = 1.00 \times 10^{-15} \text{ cm}^3 \text{ s}^{-1}$ c ₆ = 0.15	$k_{15} = 1.00 \times 10^{-15} \text{ cm}^3 \text{ s}^{-1}$ c ₆ = 0.15	$k_{15} = 1.00 \times 10^{-15} \text{ cm}^3 \text{ s}^{-1}$ c ₆ = 0.15
R16	ROI-1 + ROI-5 → tetramer	$k_{16} = 5.00 \times 10^{-20} \text{ cm}^3 \text{ s}^{-1}$	$k_{16} = 5.00 \times 10^{-20} \text{ cm}^3 \text{ s}^{-1}$	$k_{16} = 5.00 \times 10^{-20} \text{ cm}^3 \text{ s}^{-1}$
R17	ROI-5 + NO ₂ → nitrated trimer	$k_{17} = 5.00 \times 10^{-16} \text{ cm}^3 \text{ s}^{-1}$	$k_{17} = 5.00 \times 10^{-16} \text{ cm}^3 \text{ s}^{-1}$	$k_{17} = 5.00 \times 10^{-16} \text{ cm}^3 \text{ s}^{-1}$
R18	ROI-5 → trimer ₁	$k_{18} = 1.00 \times 10^{-7} \text{ s}^{-1}$	$k_{18} = 1.00 \times 10^{-7} \text{ s}^{-1}$	$k_{18} = 1.00 \times 10^{-7} \text{ s}^{-1}$
R19	ROI-6 + NO ₂ → nitrated trimer	$k_{19} = 1.00 \times 10^{-13} \text{ cm}^3 \text{ s}^{-1}$	$k_{19} = 1.00 \times 10^{-13} \text{ cm}^3 \text{ s}^{-1}$	$k_{19} = 1.00 \times 10^{-13} \text{ cm}^3 \text{ s}^{-1}$

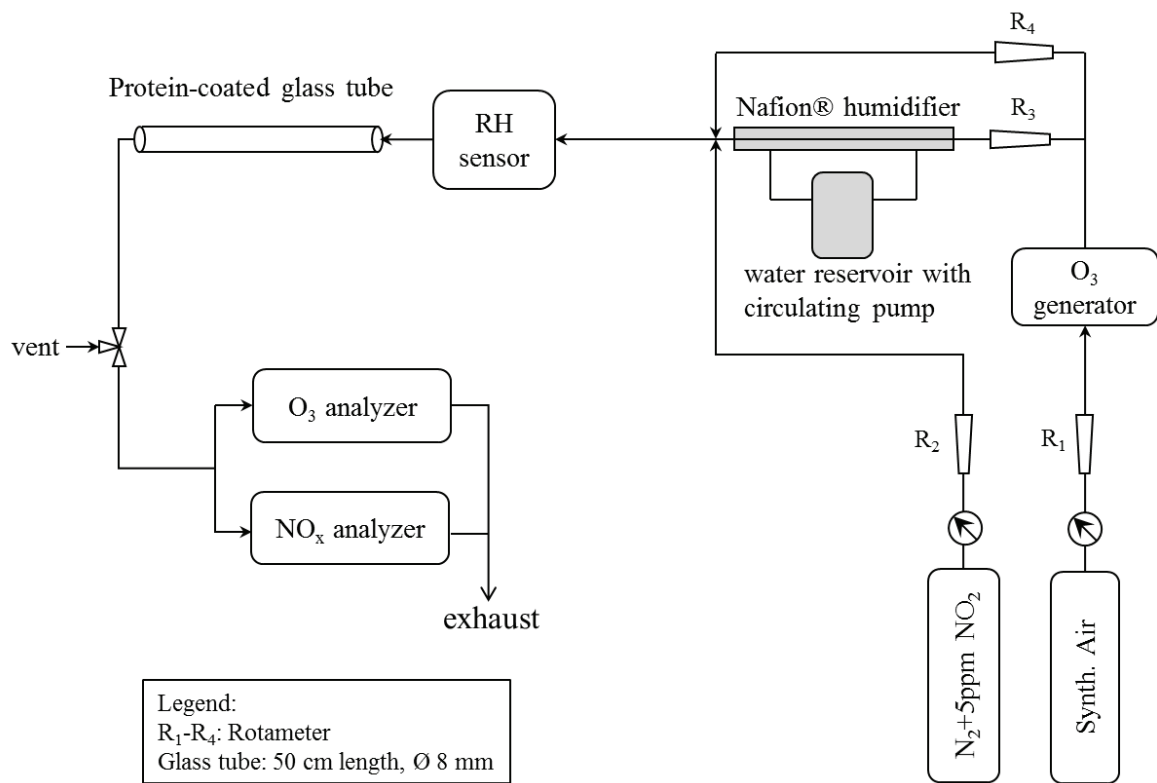


Fig. S1 Experimental setup for protein exposure to O₃/NO₂.

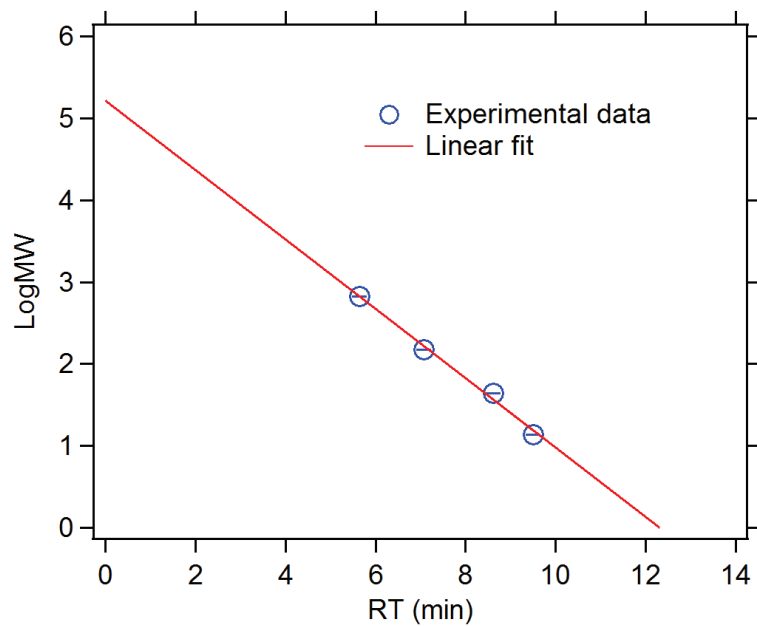


Fig. S2 Calibration curve plotting the logarithm of molecular weight (Log MW) against retention time (RT) of the protein standard mix. The fitting equation was $y = -0.42x + 5.21$, $R^2 = 0.99$.

B.5. Liu et al., Anal. Bioanal. Chem., 2017

Release of free amino acids upon oxidation of peptides and proteins by hydroxyl radicals

Fobang Liu¹, Senchao Lai², Haijie Tong¹, Pascale S. J. Lakey¹, Manabu Shiraiwa^{3,1}, Michael G. Weller⁴, Ulrich Pöschl¹, and Christopher J. Kampf^{1,5,6,*}

¹Multiphase Chemistry Department, Max Planck Institute for Chemistry, Hahn-Meitner-Weg 1, 55128 Mainz, Germany

²School of Environment and Energy, South China University of Technology, Higher Education Mega Center, Guangzhou 510006, P.R. China

³Department of Chemistry, University of California, Irvine, 1102 Natural Sciences II, Irvine, CA 92697-2025

⁴Federal Institute for Materials Research and Testing (BAM), Division 1.5 Protein Analysis, Richard-Willstätter-Str. 11, 12489 Berlin, Germany

⁵Institute for Inorganic and Analytical Chemistry, Johannes Gutenberg University Mainz, Duesbergweg 10-14, 55128 Mainz, Germany

⁶Institute for Organic Chemistry, Johannes Gutenberg University Mainz, Duesbergweg 10-14, 55128 Mainz, Germany

*Correspondence to Christopher J. Kampf, email: c.kampf@mpic.de

Analytical and Bioanalytical Chemistry, 2017; 1-10.

Release of free amino acids upon oxidation of peptides and proteins by hydroxyl radicals

Fobang Liu¹ · Senchao Lai² · Haijie Tong¹ · Pascale S. J. Lakey¹ · Manabu Shiraiwa^{1,3} · Michael G. Weller⁴ · Ulrich Pöschl¹ · Christopher J. Kampf^{1,5,6}

Received: 28 October 2016 / Revised: 20 December 2016 / Accepted: 3 January 2017
© The Author(s) 2017. This article is published with open access at Springerlink.com

Abstract Hydroxyl radical-induced oxidation of proteins and peptides can lead to the cleavage of the peptide, leading to a release of fragments. Here, we used high-performance liquid chromatography tandem mass spectrometry (HPLC-MS/MS) and pre-column online *ortho*-phthalaldehyde (OPA) derivatization-based amino acid analysis by HPLC with diode array detection and fluorescence detection to identify and quantify free amino acids released upon oxidation of proteins and peptides by hydroxyl radicals. Bovine serum albumin (BSA), ovalbumin (OVA) as model proteins, and synthetic tripeptides (comprised of varying compositions of the amino acids Gly, Ala, Ser, and Met) were used for reactions with hydroxyl radicals, which were generated by the Fenton

reaction of iron ions and hydrogen peroxide. The molar yields of free glycine, aspartic acid, asparagine, and alanine per peptide or protein varied between 4 and 55%. For protein oxidation reactions, the molar yields of Gly (~32–55% for BSA, ~10–21% for OVA) were substantially higher than those for the other identified amino acids (~5–12% for BSA, ~4–6% for OVA). Upon oxidation of tripeptides with Gly in C-terminal, mid-chain, or N-terminal positions, Gly was preferentially released when it was located at the C-terminal site. Overall, we observe evidence for a site-selective formation of free amino acids in the OH radical-induced oxidation of peptides and proteins, which may be due to a reaction pathway involving nitrogen-centered radicals.

Electronic supplementary material The online version of this article (doi:10.1007/s00216-017-0188-y) contains supplementary material, which is available to authorized users.

✉ Christopher J. Kampf
c.kampf@mpic.de

- ¹ Multiphase Chemistry Department, Max Planck Institute for Chemistry, Hahn-Meitner-Weg 1, 55128 Mainz, Germany
- ² School of Environment and Energy, South China University of Technology, Higher Education Mega Center, Guangzhou 510006, China
- ³ Department of Chemistry, University of California, Irvine, 1102 Natural Sciences II, Irvine, CA 92697-2025, USA
- ⁴ Division 1.5 Protein Analysis, Federal Institute for Materials Research and Testing (BAM), Richard-Willstätter-Str. 11, 12489 Berlin, Germany
- ⁵ Institute for Inorganic and Analytical Chemistry, Johannes Gutenberg University Mainz, Duesbergweg 10-14, 55128 Mainz, Germany
- ⁶ Institute for Organic Chemistry, Johannes Gutenberg University Mainz, Duesbergweg 10-14, 55128 Mainz, Germany

Keywords Peptides · Proteins · Oxidation · Hydroxyl radicals · HPLC-MS · Amino acid analysis

Introduction

Reactive oxygen species (ROS) have been associated with various diseases (e.g., diabetes and cancer), as they can cause oxidative stress, biological aging, and cell death [1–7]. The hydroxyl radical (OH), the most reactive form of ROS, can oxidize most organic compounds such as proteins and DNA [8]. Hydroxyl radicals can be generated in biological systems endogenously and exogenously [9], and the sources include a variety of different processes such as cellular metabolic processes, radiolysis, photolysis, and Fenton chemistry [10–12]. Elucidation of the OH-induced oxidation mechanism of amino acids, peptides, and proteins is of exceptional importance for physiological chemistry (e.g., for understanding the relationship between protein oxidation and aging) [13–16] and also of considerable interest for the Earth's atmosphere [17, 18].

Hydroxyl radicals undergo several types of reactions with amino acids, peptides, and proteins. Typical reactions include addition, electron transfer, and hydrogen abstraction [14, 15]. The OH radicals can attack both amino acid side chains and the peptide backbone, generating a large number of different radical derivatives of proteins [19, 20]. With respect to the peptide backbone cleavage, the main reaction pathway is initiated by an H abstraction at the α -carbon position. This is followed by a reaction with O₂ to give a peroxy radical, which ultimately results in fragmentation and cleavage of the backbone of the protein, thereby mainly forming amide and carbonyl fragments [11, 21]. Several studies have demonstrated that the H abstraction from the α -carbon position is the dominant pathway for the OH-mediated fragmentation of proteins and occurs at specific sites or amino acid residues as shown by computational and experimental investigations [9, 22, 23]. Also, the metal-catalyzed oxidation (MCO) of proteins was found to be an important pathway for protein degradation, as metal ions preferentially bind particular sites of proteins, resulting in selective damage [14, 24–26]. Among the multiple oxidation products, carbonyl compounds, peptide-bound hydroperoxides, and larger protein fragments were predominantly identified [27–30]. For example, Morgan et al. [28] investigated the site selectivity of peptide-bound hydroperoxide and alcohol group formation, as well as fragment species formed through protein oxidation by OH/O₂ using a mass spectrometry (MS) approach.

The high reactivity of proteins with OH radicals, however, may result in various products due to different reaction mechanisms [31, 32]. In this study, we focus on the identification and quantification of amino acids as oxidation products of proteins and peptides generated by hydroxyl radicals from the Fenton reaction. For this purpose, we introduced two robust analytical methods based on mass spectrometry and liquid chromatography, which have been widely used for the determination of amino acids in various environments (e.g., plasma and plant extracts) [33, 34]. These methods provide analytical evidence for the release of amino acids due to the OH-mediated oxidation of peptides and enable their yields to be quantified.

Bovine serum albumin (BSA) and ovalbumin (OVA) were used as model proteins, and tripeptides with varying amino acid sequences were used to study yields and site selectivity for reactions with OH radicals. The amino acids consisted of the tripeptides (glycine (Gly), alanine (Ala), serine (Ser), and methionine (Met)) were chosen due to their reactivity towards OH radicals; i.e., Gly, Ala, and Ser show a low reactivity towards OH, while the rate constant of Met with OH is about 2 orders of magnitude higher [19]. Oxidation products were analyzed by high-performance liquid chromatography tandem mass spectrometry (HPLC-MS/MS) using a Q-ToF mass spectrometer and pre-column online *ortho*-phthalaldehyde (OPA) derivatization-based amino acid analysis by HPLC

with diode array detection and fluorescence detection to identify and quantify free amino acids. We report the release of free amino acids in the OH radical-induced oxidation of peptides and proteins. Furthermore, effects of amino acid side chains on the release are discussed with regard to product identification and site selectivity.

Experimental

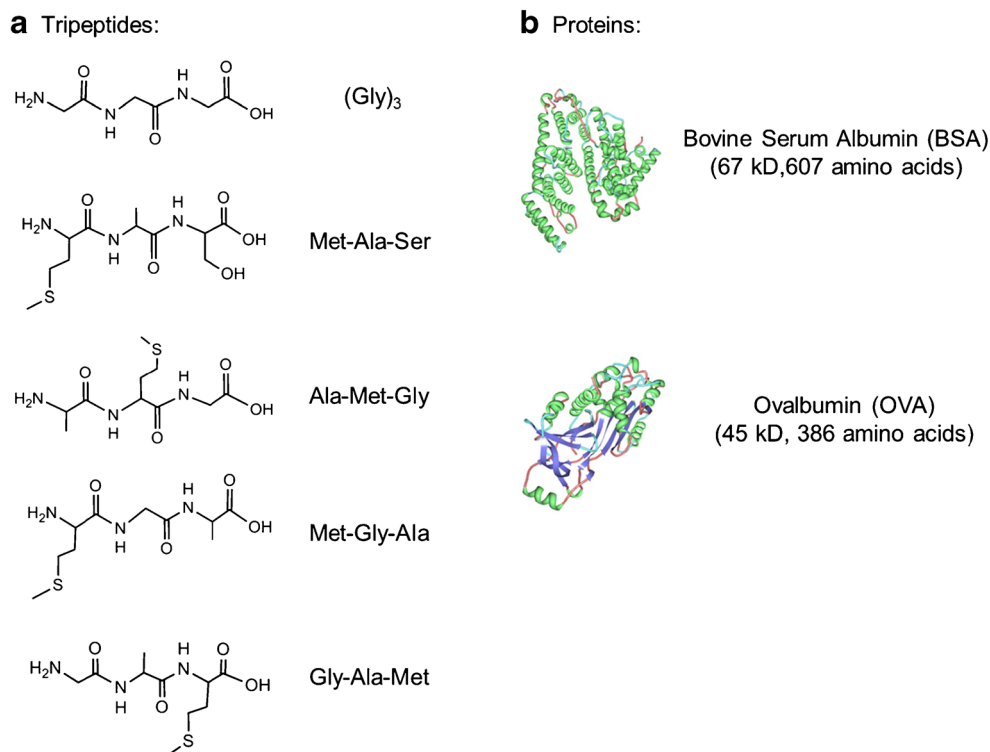
Reagents

BSA (A5611), OVA (grade V, A5503), Gly-Gly-Gly ((Gly)₃, G1377), Met-Ala-Ser (M1004), NaH₂PO₄·H₂O (71504), OPA (P0657), 9-fluorenylmethoxycarbonyl chloride (Fmoc-Cl, 23186), 3-mercaptopropionic acid (63768), acetonitrile (ACN, 34998), methanol (MeOH, 494291), amino acid standards (AAS18), asparagine (A0884), glutamine (49419), tryptophan (93659), sodium tetraborate decahydrate (Na₂B₄O₇·10H₂O, S9640), FeSO₄·7H₂O (F7002), H₂O₂ solution (30%, w/v, 16911), and HCl solution (0.1 M, 318965) were purchased from Sigma-Aldrich (Germany). Sodium hydroxide (NaOH, 0583) was from VWR (Germany). Met-Gly-Ala, Gly-Ala-Met, and Ala-Met-Gly were obtained from GeneCust (Luxembourg) and were delivered in the desalted form with a purity >95%. High purity water (18.2 M Ω cm) was taken from an ELGA LabWater system (PURELAB Ultra, ELGA, UK) and autoclaved before use if not specified otherwise.

Protein/peptide oxidation reactions

Reaction mixtures of proteins/peptides (structures shown in Fig. 1) with Fenton oxidants (FeSO₄-H₂O₂) were stirred (Multistirrer 15, Fischer Scientific, Germany) in closed screw-cap vials at room temperature. Hydroxyl radicals were generated under two oxidation conditions, and the estimated effective OH concentrations are listed in Table 1. The pH of the reaction solutions was adjusted to 3 by adding 1 M NaOH and measured by a pH meter (Multi 350i; WTW, Weilheim, Germany). Although ethylenediaminetetraacetic acid (EDTA) is a common chelator to stimulate the generation of radicals under physiological pH conditions (pH 6–8) [35], no EDTA was added in this study as glycine was found to be one of the degradation products of EDTA in the presence of OH [36]. For protein oxidation reactions, the proteins BSA and OVA were pretreated with a size-exclusion column (PD-10, GE Healthcare, Germany) using ultrapure H₂O to remove low molecular components (<5 kDa). From the purified 25 mg mL⁻¹ protein solutions, 100- μ L aliquots were added to the Fenton oxidant solutions to a final volume of 2.5 mL. After the respective reaction times, the oxidized samples were immediately eluted on a PD-10 column pre-equilibrated with ultrapure H₂O to separate the protein and the low molecular

Fig. 1 Structures of the investigated peptides (a) and proteins (b) in this study. The molecular structures of proteins (BSA, PDB accession number 3V03; OVA, PDB accession number 1OVA) were created using the RCSB PDB protein workshop (4.2.0) software



weight fraction (<5 kDa). For peptide oxidation reactions, 100 μL of 100 mM solutions of the investigated peptides were added as described before. Control reactions were performed using either H_2O_2 or FeSO_4 alone at the same concentrations and pH conditions, adjusted by 0.1 M HCl and 1 M NaOH, respectively.

In addition, oxidation experiments were performed for peptides with UV-induced OH generation via the homolysis of H_2O_2 in aqueous solution. Briefly, 4 mM (Gly)₃ were mixed with 50 mM H_2O_2 or 200 mM H_2O_2 in a $10 \times 10 \times 40$ mm UV quartz cuvette (Hellma Analytics, Müllheim, Germany) and subsequently irradiated by four UV lamps (wavelength of 254 nm, LightTech, Hungary) for 1 h. The pH of these samples was also adjusted to 3 by adding 0.1 M HCl. Control samples were either treated the same way as described above, but without UV irradiation, or prepared without H_2O_2 and irradiated for 1 h.

All experiments described above were performed in duplicate, and the samples were lyophilized (-40 $^\circ\text{C}$, ~ 12 h) immediately after reaction to stop the reaction by removing the hydrogen peroxide. The dry residues were stored at -20 $^\circ\text{C}$ and redissolved in 100 μL H_2O for analysis.

Amino acid analysis

The oxidized peptides and low molecular weight fraction of proteins were analyzed with the HPLC-DAD-FLD system (Agilent Technologies 1200 Series) consisting of a binary pump (G1312B), a four-channel microvacuum degasser (G1379B), a column thermostat (G1316B), an autosampler with a thermostat (G1330B), a photo-diode array detector (DAD, G1315C), and a fluorescence detector (FLD, G1321A). ChemStation software (version B.03.01, Agilent) was used to control the system and for the data analysis.

Table 1 Oxidation conditions for the generation of OH radical in aqueous solutions

Condition	Compositions		pH (adjusted by 1 M NaOH)	[OH] (molecule cm^{-3}) ^a
	FeSO_4 (mM)	H_2O_2 (mM)		
Ox1	5	50	3	1.5×10^8
Ox2	5	150	3	2.1×10^8

^a The decay of (Gly)₃ was monitored and allowed for an estimation of the effective OH concentration based on a pseudo-first-order kinetic rate function: $[(\text{Gly})_3] = [(\text{Gly})_3]_0 e^{-k([\text{OH}]t)}$, where $[(\text{Gly})_3]$ is the recovery of (Gly)₃, $[(\text{Gly})_3]_0$ is the initial recovery (i.e., 100%), k (1.2×10^{-12} $\text{cm}^3 \text{s}^{-1}$) is the second-order rate constant for the reaction of OH with (Gly)₃ [16], [OH] is the effective concentration of hydroxyl radical (assuming it remains constant during the reaction), and t is the reaction time. The fitting curves are shown in Fig. S6 in ESM

Chromatographic conditions were in accordance with the instructions by Agilent Technologies [37]. Briefly, automatic pre-column derivatization with OPA and FMOC was performed at room temperature, according to the injector programs (for details, see Table S1 in Electronic Supplemental Material (ESM)) listed in Henderson et al. [37]. After derivatization, an amount equivalent to 0.5 μL of each sample was injected on a Zorbax Eclipse amino acid analysis (AAA) column (150 mm \times 4.6 mm i.d., 3.5 μm , Agilent) at a temperature of 40 $^{\circ}\text{C}$. Mobile phase A was 40 mM NaH_2PO_4 (aq), adjusted to pH 7.8 with 10 N NaOH (aq), while mobile phase B was acetonitrile/methanol/water (45:45:10, v/v/v). The flow rate was 2 mL min^{-1} with a gradient program that started with 0% B for 1.9 min followed by a 16.2-min step that raised eluent B to 57%. Then, eluent B was increased to 100% within 0.5 min and kept for another 3.7 min. The mobile phase composition was reset to initial conditions within 0.9 min, and the column was equilibrated for 2.8 min before the next run. Primary amino acids were detected by monitoring the UV absorbance at 338 nm, with a reference at $\lambda = 390$ nm, bandwidth = 10 nm, slit of 4 nm, and peak width of >0.1 min, simultaneously detected by FLD with excitation 340 nm, emission 450 nm, and photomultiplier tube (PMT) gain of 10. Secondary amino acids were detected by FLD with excitation 266 nm, emission 305 nm, and PMT gain of 9. A mixture of 20-amino acid standards (see ESM Table S2) was used to obtain calibration curves for quantification as illustrated in Fig. S1 in ESM. The limits of detection (LODs, defined as a signal-to-noise ratio of 3) for 20 individual amino acids are in the range of 0.1 to 5 pmol. Linearity is demonstrated for the concentration range of 20 to 500 μM for all amino acids by detection using a DAD or FLD.

LC-Q-TOF-MS

Identification of OH-mediated reaction products of peptides and the low molecular weight fraction of proteins was also carried out using an HPLC-MS/MS system (Agilent). The LC-MS/MS system consists of a quaternary pump (G5611A), an autosampler (G5667A) with a thermostat (G1330B), a column thermostat (G1316C), and an electrospray ionization (ESI) source interfaced to a Q-ToF mass spectrometer (6540 UHD Accurate-Mass Q-ToF, Agilent Technologies). All modules were controlled by MassHunter software (Rev. B. 06.01, Agilent). The LC column was a Zorbax Extend-C18 Rapid Resolution HT (2.1 \times 50 mm, 1.8 μm) and was operated at a temperature of 30 $^{\circ}\text{C}$. Eluents used were 3% (v/v) acetonitrile (Chromasolv, Sigma, Seelze, Germany) in water/formic acid (0.1% v/v, Chromasolv, Sigma, Seelze, Germany) (eluent A) and 3% water in acetonitrile (eluent B). The flow rate was 0.2 mL min^{-1} with a gradient program starting with 3% B for 1.5 min followed by an 18-min step that raised eluent B

to 60%. Further, eluent B was increased to 80% at 20 min and returned to initial conditions within 0.1 min, followed by column re-equilibration for 9.9 min before the next run. The sample injection volume was 1–5 μL .

The ESI-Q-TOF instrument was operated in the positive ionization mode (ESI+) with a drying gas temperature of 325 $^{\circ}\text{C}$, 20 psig nebulizer pressure, 4000 V capillary voltage, and 75 V fragmentor voltage. Fragmentation of protonated ions was conducted using the targeted MS/MS mode with a collision energy of 10 V (16 V for m/z 76). Spectra were recorded over the mass range of m/z 50–1000 for MS mode and m/z 20–1000 for MS/MS mode. Data analysis was performed using the qualitative data analysis software (Rev. B. 06.00, Agilent).

Results and discussion

Identification of amino acid products in the hydroxyl radical-induced oxidation of peptides and proteins

Figure 1 shows the tripeptides and proteins investigated in this study. The oxidation products generated by OH radicals from the Fenton reaction were analyzed by AAA and LC-MS/MS in order to identify and quantify amino compounds and, in particular, amino acid products.

Figure 2 shows the exemplary AAA chromatograms of an amino acid standard, as well as protein and peptide samples oxidized by OH radicals. The signal corresponding to glycine-OPA derivative at a retention time (RT) of 7.8 min was detected in all oxidized samples of glycine-containing peptides and proteins. Moreover, the peak was absent when the oxidized peptide did not contain glycine (i.e., Met-Ala-Ser). LC-MS/MS analysis of underivatized samples further confirmed the free amino acid glycine to be an oxidation product of proteins and peptides reacting with hydroxyl radicals. Figure 3 shows the MS/MS spectra of a glycine standard (m/z 76) and those of precursor ions with m/z 76 found in oxidized BSA, (Gly)₃, and Ala-Met-Gly samples. In all cases, identical fragmentation patterns were observed and the loss of 16 Da from the precursor ions corresponds to the loss of NH_2 [34]. In addition, the signal intensity of extracted ion chromatograms (EICs) for m/z 76 in the oxidized samples increased significantly compared to the control samples (see ESM Fig. S2), indicating the formation of an OH-mediated reaction product with m/z 76 in these samples. Thus, glycine, which does not contain an oxidation sensitive side chain, could be identified as a product of all studied reaction systems of peptides and proteins comprising glycine in their amino acid sequences.

In addition to glycine, three other peaks exhibiting the RT of OPA derivatives of aspartic acid (Asp), asparagine (Asn), and Ala were detected in the AAA of oxidized protein (BSA and OVA) samples, i.e., at 2.1 min for Asp, 6.4 min for Asn,

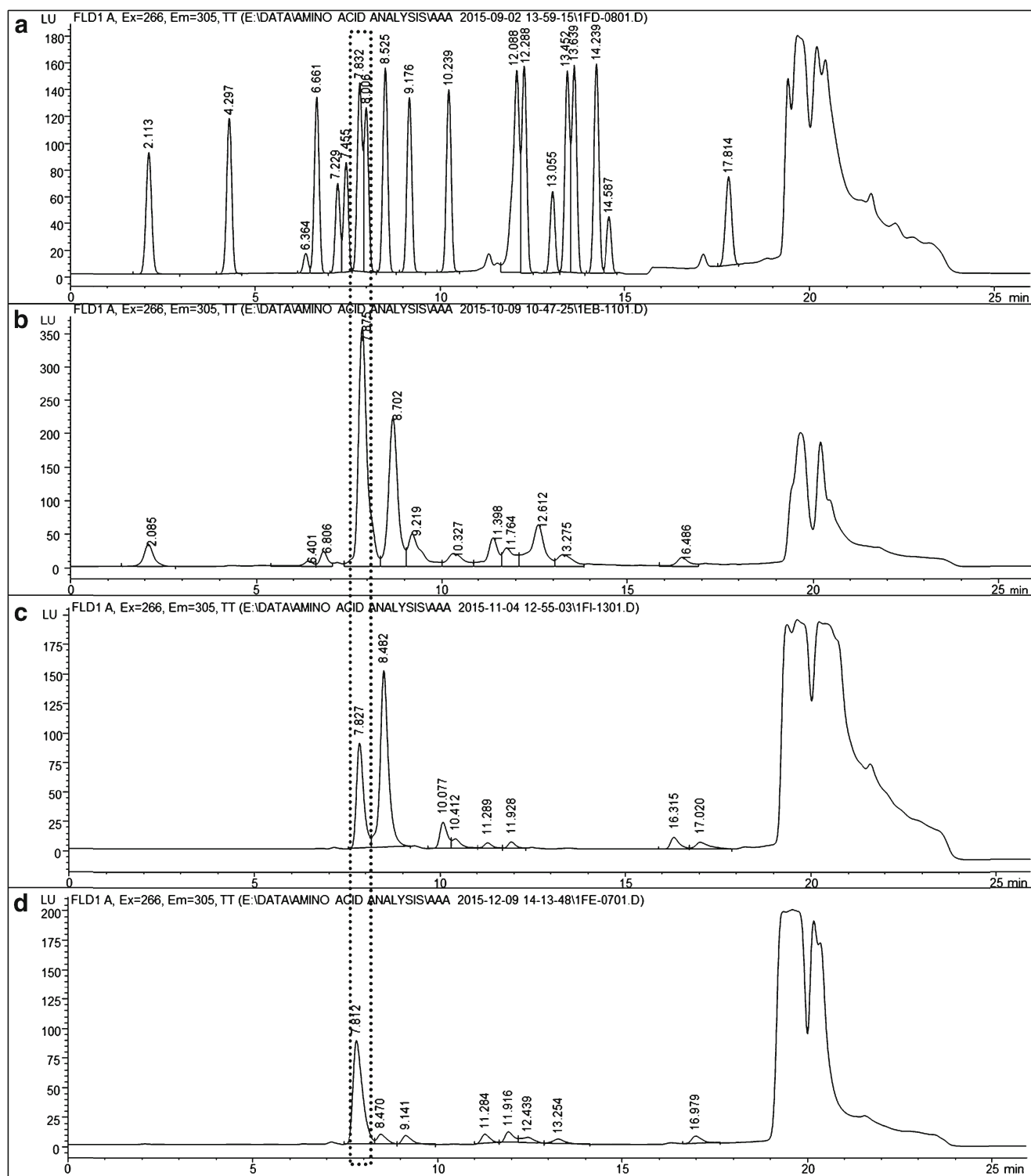
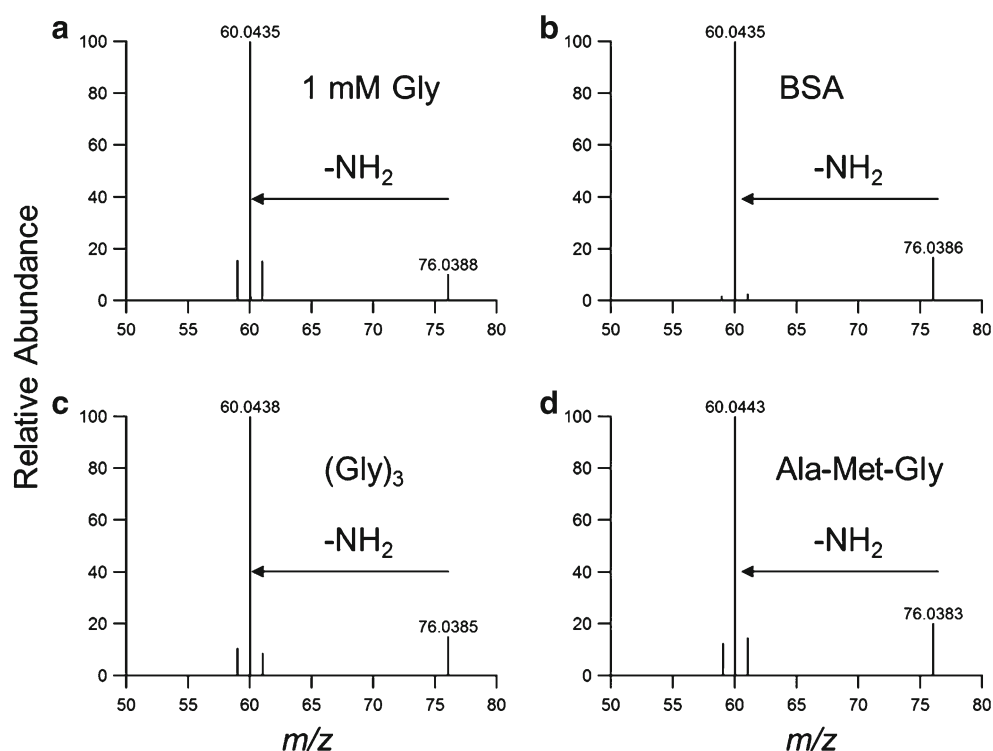


Fig. 2 Amino acid analysis (AAA) with fluorescence detection of OPA-derivatized amino acids: **(A)** 200 μ M of a 20-amino acid standard; **(B)** 15 μ M BSA, Ox2, 24 h; **(C)** 4 mM tri-Gly, Ox1, 0.25 h; and **(D)** 4 mM Ala-Met-Gly, Ox1, 19 h. The dotted box indicates the signal of glycine in all samples

and 9.2 min for Ala, as illustrated in Fig. 2B. The LC-MS/MS analysis of reference compounds and samples confirmed the identity of the amino acids as shown in Fig. S3 in ESM [34, 38]. It should be noted that the four free amino acids (Asp,

Asn, Gly, and Ala) identified in oxidized protein samples, all exhibit a low rate constant for reactions with OH [19, 39], resulting in a higher stability towards further reactions with OH radicals and enabling their identification in the analysis.

Fig. 3 The MS² spectra of *m/z* 76 in (A) 1 mM Gly, (B) oxidized BSA sample in Ox2 condition, (C) (Gly)₃ in Ox1 condition, and (D) Ala-Met-Gly in Ox1 condition (Ox1, 5 mM FeSO₄–50 mM H₂O₂; Ox2, 5 mM FeSO₄–150 mM H₂O₂). The oxidized samples show an accurate mass of precursor ion *m/z* 76 with the glycine standard, and they exhibit the same fragments of *m/z* 60. The extracted ion chromatograms (EICs) of *m/z* 76 for the above samples are shown in Fig. S2 in ESM



Furthermore, Ala and Asp were unambiguously identified by LC-MS/MS in the oxidized Met-Gly-Ala and Gly-Ala-Met samples. Exemplary MS² spectra of reference standards and samples are shown in Fig. S4 in ESM. The presence of Asp in the tripeptide samples can be explained by the OH-induced oxidative modification of methionine (Met), as suggested by Xu and Chance [11] and illustrated in Fig. S5 in ESM. Note that Asp was not identified in the oxidized Ala-Met-Gly sample. This discrepancy may be explained by the formation of other oxidation products of Met, which can be formed when Met is located in the middle of the peptide, as Met is highly reactive towards OH and the reaction could result in different oxidized species [11]. In the oxidized Met-Ala-Ser sample, the amino acids Asp, Ala, and Ser were identified. Here, Ser could be released directly from the C-terminal position or it could be formed by the oxidation of the methyl side chain of Ala released from the peptide [40]. Therefore, from the combined AAA and LC-MS/MS results, we can confirm that free amino acids are products in the OH-induced oxidation of proteins and peptides.

Quantification and site selectivity of amino acid formation

Figure 4 shows the molar yields of free amino acids for the OH oxidation of two model proteins (BSA and OVA) quantified by AAA, whereby yields increased with increasing oxidant concentrations. The yields of Gly were found to be the highest among the quantified amino acids and ranged from ~32 to 55% for BSA and from ~10 to 21% for OVA.

Notably, the Gly yield of BSA was approximately two to three times higher than that of OVA under the same conditions, despite the higher number of Gly residues in OVA (19) compared to BSA (17). The factors influencing the yields of individual free amino acids in the studied reactions might be multiple, including different tertiary and primary structures and thus different numbers of accessible sites available for the OH attack, as well as differences in adjacent amino acids in BSA and OVA, influencing OH site selectivity [19].

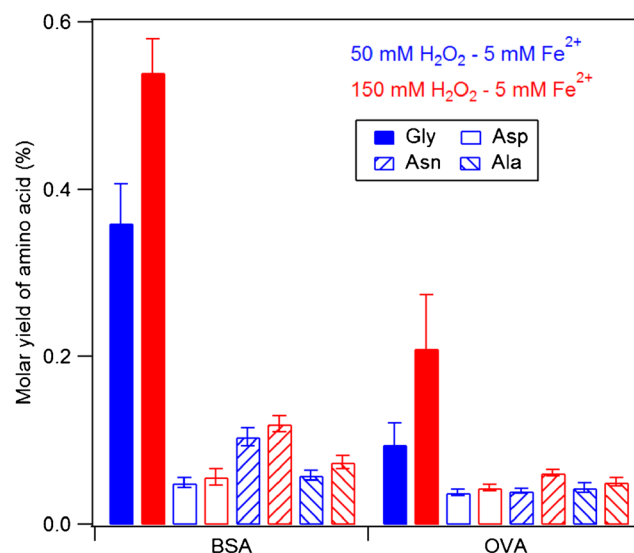


Fig. 4 Molar yields of amino acids obtained in the oxidation of BSA and OVA samples with different concentrations of oxidants (50 and 150 mM H₂O₂ with 5 mM FeSO₄, respectively)

Figure 5 shows the temporal evolution of the Gly yield during the oxidation of (Gly)₃ by OH radicals. The corresponding recovery of (Gly)₃ (see ESM Fig. S6) was obtained through AAA analysis using a calibration curve made by a set of (Gly)₃ solutions (see ESM Fig. S7). We found that the recovery of (Gly)₃ has declined to 50% after 1 h of reaction (see ESM Fig. S6), while the molar yield of glycine only reached 6% of (Gly)₃. Additionally, the molar ratio of free Gly to reacted (Gly)₃ ($\Delta(\text{Gly})_3 = (\text{Gly})_3, t=0 - (\text{Gly})_3, t=x$) was relatively stable over the reaction time with a value of $\sim 12\%$. These results indicate that other reaction products than Gly are accounting for $\sim 88\%$ of the reacted peptide. These products may include, e.g., carbonyl species known to be products of the α -carbon H abstraction pathway [28]. To exclude an influence of acidic or basic hydrolysis on the observed formation of glycine [41], control experiments were conducted, in which (Gly)₃ was incubated under acidic (pH 2) and basic (pH 12) conditions for 24 h, respectively. No glycine formation was observed in these experiments. Furthermore, we found that amino acids were also released in the absence of iron ions. This was confirmed through control experiment, in which OH radicals were generated by the photolysis of H₂O₂, and a positive relationship between glycine yield and H₂O₂ concentrations was observed (see ESM Fig. S8).

Furthermore, we found the amino acid yields of three small peptides (Ala-Met-Gly, Met-Gly-Ala, and Gly-Ala-Met) are dependent on the sequence of Gly, Ala, and Met, as shown in Fig. 6. The highest yields of Gly and Ala were obtained when they were located at the C-terminus, followed by the mid-chain position and the N-terminal site. While the Gly concentration was increasing with reaction time, the Ala concentration already showed a reduction after 2 h of reaction time when located at the C-terminal site (Met-Gly-Ala), which may be due to further oxidation of free Ala by OH radicals. Besides, comparing the results in the case of Gly and Ala both located in the same position of the respective tripeptide, the yield of Gly was about 50% higher than that of Ala when they are located C-terminally. For mid-chain and N-terminal sites, their yields were more comparable. These results suggest that the OH attack for the release of free amino acids preferably occurs at Gly, particularly for Gly located at the C-terminal site and, to a less extent, at Ala. Previous studies have suggested that OH-mediated fragmentation of proteins likely occur at specific sites rather than giving rise to random fragments [23, 28, 42]. Glycine residues could be favorable sites for OH attacking the polypeptide backbone due to its low steric hindrance [11]. It should be noted that the highest molar yield of Gly was found to be $\sim 2\%$ of the corresponding tripeptide (Ala-Met-Gly), confirming free amino acids to

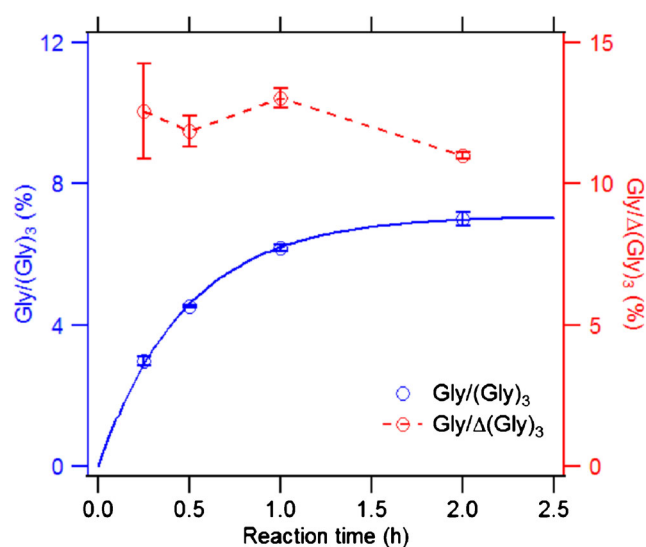
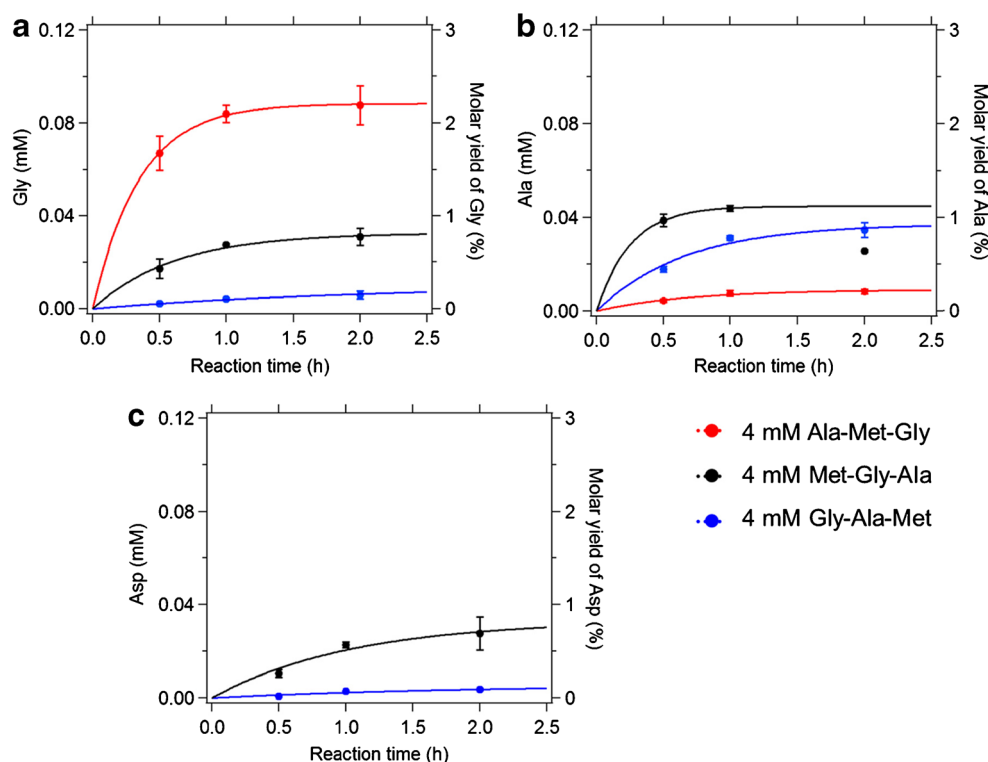


Fig. 5 The temporal evolution of molar yield Gly/(Gly)₃ (blue dots) and the product ratio of Gly to $\Delta(\text{Gly})_3$ (red dots) in the oxidation of 4 mM (Gly)₃ with 5 mM FeSO₄–50 mM H₂O₂ condition (Ox1). $\Delta(\text{Gly})_3$ was quantified by a calibration curve made by a set of (Gly)₃ solutions (see ESM Fig. S7) monitored at a UV absorbance of 338 nm. The solid line (blue) is fitted with a pseudo-first-order kinetic rate function: $[\text{AA}] = a[\text{TriPep}]_0(1 - e^{-k[\text{OH}]t})$, as discussed in the “Quantification and site selectivity of amino acid formation” section

be low yield products and explaining the lack of reports in the literature.

Aspartic acid, the OH oxidation product of Met, was found in Met-Gly-Ala and Gly-Ala-Met. In contrast to the observed increasing yield of Gly and Ala for the C-terminal site, the Asp yields were found to be higher for the N-terminal site than for the C-terminal site, i.e., 0.7% in Met-Gly-Ala and only 0.1% in Gly-Ala-Met. The site selectivity for the OH attack at Gly may also explain why the yield of Asp was higher for Met at the N-terminal site than at the C-terminal site, since in Met-Gly-Ala, the attack on Gly may lead to the formation of Met or its oxidized product as a “byproduct”. Additionally, the temporal evolution of release for amino acids in Figs. 5 and 6 can be fitted with a pseudo-first-order rate function: $[\text{AA}] = a[\text{TriPep}]_0(1 - e^{-k[\text{OH}]t})$, where the coefficient a stands for the maximum molar yield for the release of the specific amino acid, k is the second-order rate coefficient, t is the reaction time, and $[\text{AA}]$, $[\text{TriPep}]_0$, and $[\text{OH}]$ are the concentrations of amino acids, tripeptide (4 mM), and OH ($1.5 \times 10^8 \text{ mol cm}^{-3}$, assuming $[\text{OH}]$ is constant), respectively. The second-order rate coefficient for the release of amino acids from the four investigated tripeptides is in the order of magnitude of $10^{-12} \text{ cm}^3 \text{ s}^{-1}$. The maximum molar yield for all the amino acids was from 0.0014 ± 0.0018 to 0.0709 ± 0.0011 , with the highest found for Gly in (Gly)₃ (0.0709 ± 0.0011); the detailed coefficients from fittings can be found in Table S3 in ESM. The kinetics and mechanism will be further investigated in follow-up studies.

Fig. 6 Temporal evolution of the concentration (*left axis*) and molar yield (*right axis*) of glycine (A), alanine (B), and aspartic acid (C) from Gly-Ala-Met, Met-Gly-Ala, and Ala-Met-Gly subjected to the oxidation with 5 mM FeSO₄–50 mM H₂O₂ (Ox1). The *solid lines* are fitted with a pseudo-first-order kinetic rate function: $[AA] = a[\text{TriPep}]_0[1 - e^{-k[\text{OH}]t}]$, as discussed in the “Quantification and site selectivity of amino acid formation” section. For the fitting for Ala in Ala-Met-Gly, it is only fitted for the first two data points



Conclusions

Free amino acids were identified as products in the OH-induced oxidation of proteins and peptides by LC-MS/MS analysis. In addition, the molar yields of the formation of amino acids were quantified by AAA analysis. Glycine was released at higher yields than the other identified amino acids, which is likely to be due to the absence of a side chain resulting in low rate constants for further reactions with OH and low steric hindrance of the initial radical generation on the peptide backbone, especially when Gly was in the C-terminal position. Note that the molar yields and production rates of amino acids for different peptides and proteins cannot be interchangeably used, as release of amino acids is not equal to their presence in the solution due to possible side chain oxidations of amino acids.

The formation of free amino acids, however, has not been reported for the main backbone cleavage process through α -carbon H abstraction, which results in the formation of amide and carbonyl products, as outlined in the “Introduction” section. Thus, another reaction pathway may be responsible for the formation of free amino acids. The peptide which was only composed of glycine ((Gly)₃) appears to be a good candidate for the investigation of such pathways, because H abstraction by OH radicals can only occur at the α -carbon and the amide nitrogen. For other amino acids, however, hydroxyl radicals can attack at the side chain and polypeptide backbone sites, complicating investigations of the reaction mechanism. In

previous studies, Štefanić et al. [43] determined that the amide nitrogen is the preferred site for OH attack through pulse radiolysis on free glycine and a glycine anion, whereas Doan et al. [9] concluded that H abstraction from the peptide nitrogen atom is the least preferred site for OH attack at the peptide backbone by ab initio calculations. The key difference for the contradiction in the above two studies is that the former investigated isolated amino acids while the latter used peptide systems for their calculation methods. Also, the electron transfer between sites resulting in secondary fragmentation or rearrangement [14, 44], should be considered for the formation of nitrogen-centered radicals. Further verification of the generation of nitrogen-centered radicals and the investigation of their role for the release of amino acids via protein/peptide oxidation by hydroxyl radicals could be obtained by techniques such as electron paramagnetic resonance (EPR) spectroscopy in follow-up studies [45, 46].

Acknowledgements Open access funding provided by Max Planck Society. F.L. and S.L. acknowledge the financial support from the China Scholarship Council (CSC), and C.J.K. acknowledges the support by the Max Planck Graduate Center (MPGC) with the Johannes Gutenberg University Mainz and the financial support by the German Research Foundation (DFG, grant no. KA4008/1-2).

Compliance with ethical standards

Conflict of interest The authors declare that they have no competing interests.

Ethical approval This article does not contain any research with human participants or animals.

All authors of this manuscript were informed and agreed for submission.

Open Access This article is distributed under the terms of the Creative Commons Attribution 4.0 International License (<http://creativecommons.org/licenses/by/4.0/>), which permits unrestricted use, distribution, and reproduction in any medium, provided you give appropriate credit to the original author(s) and the source, provide a link to the Creative Commons license, and indicate if changes were made.

References

- Waris G, Ahsan H. Reactive oxygen species: role in the development of cancer and various chronic conditions. *J Carcinog*. 2006;5:14.
- Valko M, Jomova K, Rhodes CJ, Kuča K, Musílek K. Redox- and non-redox-metal-induced formation of free radicals and their role in human disease. *Arch Toxicol*. 2016;90:1–37.
- Oyinloye BE, Adenowo AF, Kappo AP. Reactive oxygen species, apoptosis, antimicrobial peptides and human inflammatory diseases. *Pharmaceuticals*. 2015;8:151–75.
- Pöschl U, Shiraiwa M. Multiphase chemistry at the atmosphere–biosphere interface influencing climate and public health in the anthropocene. *Chem Rev*. 2015;115:4440–75.
- Wang Y, Chen J, Ling M, López JA, Chung DW, Fu X. Hypochlorous acid generated by neutrophils inactivates ADAMTS13 an oxidative mechanism for regulating ADAMTS13 proteolytic activity during inflammation. *J Biol Chem*. 2015;290:1422–31.
- Chen X, Mou Y, Ling J, Wang N, Wang X, Hu J. Cyclic dipeptides produced by fungus *Eupenicillium brefeldianum* HMP-F96 induced extracellular alkalization and H₂O₂ production in tobacco cell suspensions. *World J Microbiol Biotechnol*. 2015;31:247–53.
- Abu-Soud HM, Maitra D, Shaieb F, Khan SN, Byun J, Abdulhamid I, et al. Disruption of heme-peptide covalent cross-linking in mammalian peroxidases by hypochlorous acid. *J Inorg Biochem*. 2014;140:245–54.
- Kocha T, Yamaguchi M, Ohtaki H, Fukuda T, Aoyagi T. Hydrogen peroxide-mediated degradation of protein: different oxidation modes of copper- and iron-dependent hydroxyl radicals on the degradation of albumin. *BBA-Protein Struct M*. 1997;1337:319–26.
- Doan HQ, Davis AC, Francisco JS. Primary steps in the reaction of OH radicals with peptide systems: perspective from a study of model amides. *J Phys Chem A*. 2010;114:5342–57.
- Apel K, Hirt H. Reactive oxygen species: metabolism, oxidative stress, and signal transduction. *Annu Rev Plant Biol*. 2004;55:373–99.
- Xu G, Chance MR. Hydroxyl radical-mediated modification of proteins as probes for structural proteomics. *Chem Rev*. 2007;107:3514–43.
- Watson C, Janik I, Zhuang T, Charvátová O, Woods RJ, Sharp JS. Pulsed electron beam water radiolysis for submicrosecond hydroxyl radical protein footprinting. *Anal Chem*. 2009;81:2496–505.
- Stadtman E, Levine R. Free radical-mediated oxidation of free amino acids and amino acid residues in proteins. *Amino Acids*. 2003;25:207–18.
- Davies MJ. Protein oxidation and peroxidation. *Biochem J*. 2016;473:805–25.
- Štefanić I, Ljubić I, Bonifačić M, Sabljčić A, Asmus K-D, Armstrong DA. A surprisingly complex aqueous chemistry of the simplest amino acid. A pulse radiolysis and theoretical study on H/D kinetic isotope effects in the reaction of glycine anions with hydroxyl radicals. *Phys Chem Chem Phys*. 2009;11:2256–67.
- Stadtman ER. Protein oxidation and aging. *Science*. 1992;257:1220–4.
- Cape J, Cornell S, Jickells T, Nemitz E. Organic nitrogen in the atmosphere—where does it come from? A review of sources and methods. *Atmos Res*. 2011;102:30–48.
- McGregor KG, Anastasio C. Chemistry of fog waters in California's Central Valley: 2. Photochemical transformations of amino acids and alkyl amines. *Atmos Environ*. 2001;35:1091–104.
- Sharma VK, Rokita SE. Oxidation of amino acids, peptides, and proteins: kinetics and mechanism. John Wiley & Sons; 2012.
- Stadtman ER. Protein oxidation and aging. *Free Radic Res*. 2006;40:1250–8.
- Davies MJ. The oxidative environment and protein damage. *BBA-Proteins Proteom*. 1703;2005:93–109.
- Rauk A, Armstrong DA. Influence of β -sheet structure on the susceptibility of proteins to backbone oxidative damage: preference for α -centered radical formation at glycine residues of antiparallel β -sheets. *J Am Chem Soc*. 2000;122:4185–92.
- Hawkins C, Davies M. EPR studies on the selectivity of hydroxyl radical attack on amino acids and peptides. *J Chem Soc Perk Trans*. 1998;2:2617–22.
- Dufield DR, Wilson GS, Glass RS, Schöneich C. Selective site-specific Fenton oxidation of methionine in model peptides: evidence for a metal-bound oxidant. *J Pharm Sci*. 2004;93:1122–30.
- Uehara H, Luo S, Aryal B, Levine RL, Rao VA. Distinct oxidative cleavage and modification of bovine [Cu–Zn]-SOD by an ascorbic acid/Cu (II) system: identification of novel copper binding site on SOD molecule. *Free Radic Bio Med*. 2016;94:161–73.
- Zhou X, Mester C, Stemmer PM, Reid GE. Oxidation-induced conformational changes in calcineurin determined by covalent labeling and tandem mass spectrometry. *Biochemistry-US*. 2014;53(43):6754–65.
- Morgan PE, Pattison DI, Hawkins CL, Davies MJ. Separation, detection, and quantification of hydroperoxides formed at side-chain and backbone sites on amino acids, peptides, and proteins. *Free Radic Biol Med*. 2008;45:1279–89.
- Morgan PE, Pattison DI, Davies MJ. Quantification of hydroxyl radical-derived oxidation products in peptides containing glycine, alanine, valine, and proline. *Free Radic Biol Med*. 2012;52:328–39.
- Guedes S, Vitorino R, Domingues R, Amado F, Domingues P. Oxidation of bovine serum albumin: identification of oxidation products and structural modifications. *Rapid Commun Mass Spectrom*. 2009;23:2307–15.
- Marx G, Chevion M. Site-specific modification of albumin by free radicals. Reaction with copper(II) and ascorbate. *Biochem J*. 1986;236:397–400.
- Catalano CE, Choe YS, de Montellano PO. Reactions of the protein radical in peroxide-treated myoglobin. Formation of a heme-protein cross-link. *J Biol Chem*. 1989;264:10534–41.
- Lee SH, Kyung H, Yokota R, Goto T, Oe T. Hydroxyl radical-mediated novel modification of peptides: N-terminal cyclization through the formation of α -ketoamide. *Chem Res Toxicol*. 2014;28:59–70.
- Schwarz EL, Roberts WL, Pasquali M. Analysis of plasma amino acids by HPLC with photodiode array and fluorescence detection. *Clin Chim Acta*. 2005;354:83–90.
- Thiele B, Füllner K, Stein N, Oldiges M, Kuhn AJ, Hofmann D. Analysis of amino acids without derivatization in barley extracts by LC-MS-MS. *Anal Bioanal Chem*. 2008;391:2663–72.
- Baron CP, Refsgaard HH, Skibsted LH, Andersen ML. Oxidation of bovine serum albumin initiated by the Fenton reaction—effect of EDTA, tert-butylhydroperoxide and tetrahydrofuran. *Free Radic Res*. 2006;40:409–17.

36. Oviedo C, Contreras D, Freer J, Rodriguez J. Fe(III)-EDTA complex abatement using a catechol driven Fenton reaction combined with a biological treatment. *Environ Technol.* 2004;25:801–7.
37. Henderson J, Ricker R, Bidlingmeyer B, Woodward C. Rapid, accurate, sensitive, and reproducible HPLC analysis of amino acids. Agilent Technologies. Technical Note 5980-1193E, J. R. Soc. Interface 9. 2000.
38. Gómez-Ariza J, Villegas-Portero M, Bernal-Daza V. Characterization and analysis of amino acids in orange juice by HPLC–MS/MS for authenticity assessment. *Anal Chim Acta.* 2005;540:221–30.
39. Buxton GV, Greenstock CL, Helman WP, Ross AB. Critical review of rate constants for reactions of hydrated electrons, hydrogen atoms and hydroxyl radicals ($\cdot\text{OH}/\cdot\text{O}^-$ in aqueous solution). *J Phys Chem Ref Data.* 1988;17:513–886.
40. Bachi A, Dalle-Donne I, Scaloni A. Redox proteomics: chemical principles, methodological approaches and biological/biomedical promises. *Chem Rev.* 2012;113:596–698.
41. Le Maux S, Nongonierma AB, Barre C, FitzGerald RJ. Enzymatic generation of whey protein hydrolysates under pH-controlled and non pH-controlled conditions: impact on physicochemical and bioactive properties. *Food Chem.* 2016;199:246–51.
42. Uchida K, Kato Y, Kawakishi S. A novel mechanism for oxidative cleavage of prolyl peptides induced by the hydroxyl radical. *Biochem Biophys Res Commun.* 1990;169:265–71.
43. Štefanić I, Bonifačić M, Asmus K-D, Armstrong DA. Absolute rate constants and yields of transients from hydroxyl radical and H atom attack on glycine and methyl-substituted glycine anions. *J Phys Chem A.* 2001;105:8681–90.
44. Hawkins CL, Davies MJ. Generation and propagation of radical reactions on proteins. *BBA-Bioenergetics.* 2001;1504:196–219.
45. Tong H, Arangio AM, Lakey PS, Berkemeier T, Liu F, Kampf CJ, et al. Hydroxyl radicals from secondary organic aerosol decomposition in water. *Atmos Chem Phys.* 2016;16:1761–71.
46. Arangio AM, Tong H, Socorro J, Pöschl U, Shiraiwa M. Quantification of environmentally persistent free radicals and reactive oxygen species in atmospheric aerosol particles. *Atmos Chem Phys.* 2016;16:13105–19.

Analytical and Bioanalytical Chemistry

Electronic Supplementary Material

Release of free amino acids upon oxidation of peptides and proteins by hydroxyl radicals

Fobang Liu, Senchao Lai, Haijie Tong, Pascale S. J. Lakey, Manabu Shiraiwa,
Michael G. Weller, Ulrich Pöschl, Christopher J. Kampf

Table S1 Injector program for the automatic pre-column derivatization for amino acid analysis

Step	Function	Reagent	Amount
1	draw	borate buffer	2.5 μL
2	draw	sample	0.5 μL
3	mix		3.0 μL
4	wait		0.5 min
5	draw	water (needle wash)	0 μL
6	draw	OPA-3MPA	0.5 μL
7	mix		3.5 μL
8	draw	water (needle wash)	0 μL
9	draw	FMOC	0.5 μL
10	mix		4 μL
11	draw	water	32 μL
12	mix		18 μL
13	Inject		(0.5 μL)

Table S2 A list of 20 amino acid standards used for making a calibration curve for amino acid analysis. “Peak No.” is the amino acid elution order using Eclipse-AAA column

Peak No.	Amino acid (Abbreviation)	Molecular weight (g mol ⁻¹)	Retention Time (min)
1	Aspartic acid (Asp)	133.04	2.1
2	Glutamic acid (Glu)	147.05	4.3
3	Asparagine (Asn)	132.05	6.4
4	Serine (Ser)	105.04	6.7
5	Glutamine (Gln)	146.07	7.2
6	Histidine (His)	155.07	7.5
7	Glycine (Gly)	75.03	7.8
8	Threonine (Thr)	119.06	8.0
9	Arginine (Arg)	174.11	8.5
10	Alanine (Ala)	89.05	9.2
11	Tyrosine (Tyr)	181.07	10.2
12	Cystine (Cy2)	240.02	11.5*
13	Valine (Val)	117.08	12.1
14	Methionine (Met)	149.05	12.3
15	Tryptophan (Trp)	204.09	13.1
16	Phenylalanine (Phe)	165.08	13.5
17	Isoleucine (Ile)	131.09	13.6
18	Leucine (Leu)	131.09	14.2
19	Lysine (Lys)	146.10	14.6
20	Proline (Pro)	115.06	17.8

* Cy2 does not fluoresce under these derivatization conditions and thereby the retention time is monitored in DAD signal (338 nm).

Table S3 The fitting coefficients with a pseudo-first order rate equation: $[AA] = a[TriPep]_0(1 - e^{-k[OH]t})$, for the temporal evolution of release of amino acids in the four investigated tripeptides

Tripeptide	a			k (cm ³ s ⁻¹)			Chisquare		
	Gly	Ala	Asp	Gly	Ala	Asp	Gly	Ala	Asp
(Gly) ₃	0.0709 ± 0.0011			(3.87 ± 0.28) × 10 ⁻¹²			2.05× 10 ⁻⁶		
Ala-Met-Gly	0.0221 ± 0.0001	0.0023 ± 0.0002		(5.32 ± 0.21) × 10 ⁻¹²	(2.69 ± 1.06) × 10 ⁻¹²		4.13× 10 ⁻⁷	4.06× 10 ⁻⁷	
Met-Gly-Ala	0.0082 ± 0.0006	0.0112	0.0083 ± 0.0022	(3.02 ± 0.88) × 10 ⁻¹²	7.36 × 10 ⁻¹²	(1.77 ± 1.33) × 10 ⁻¹²	2.77× 10 ⁻⁶	*	1.05 × 10 ⁻⁵
Gly-Ala-Met	0.0019 ± 0.0002	0.0093 ± 0.0011	0.0014 ± 0.0018	(1.47 ± 0.40) × 10 ⁻¹²	(2.78 ± 1.26) × 10 ⁻¹²	(0.99 ± 2.65) × 10 ⁻¹²	4.82× 10 ⁻⁸	9.41× 10 ⁻⁶	9.32 × 10 ⁻⁷

*: Chisquare cannot be achieved due to only two datapoints were used for the fitting.

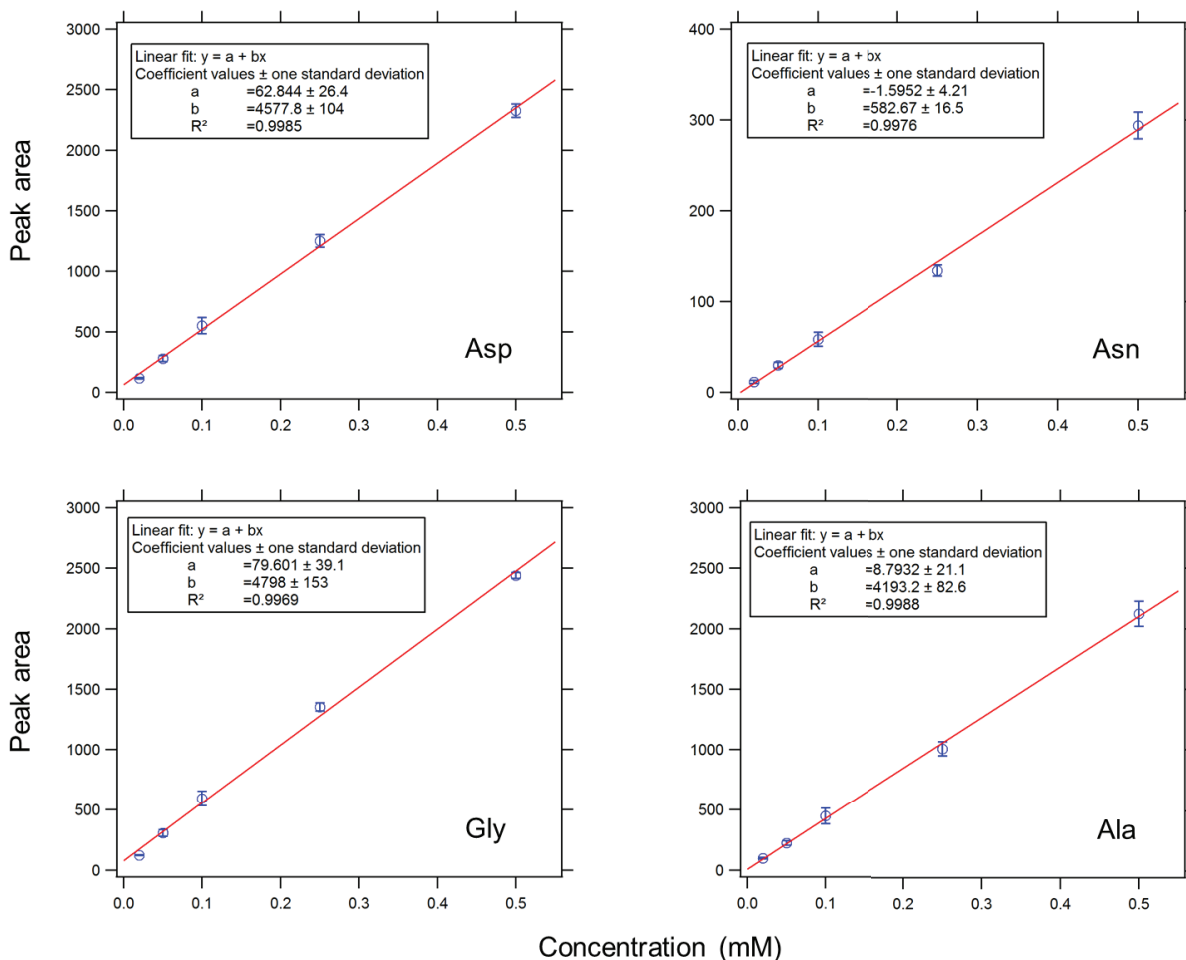


Fig. S1 Calibration curves plotting the peak area detected by FLD detection against the concentration of amino acids. (A) Aspartic acid, the fitting equation was: $y = 4577.8x + 62.84$, $R^2 = 0.999$, (B) Asparagine, the fitting equation was: $y = 582.67x - 1.60$, $R^2 = 0.998$, (C) Glycine, the fitting equation was: $y = 4798x + 79.60$, $R^2 = 0.999$, (D) Alanine, the fitting equation was: $y = 4193.2x + 8.79$, $R^2 = 0.999$

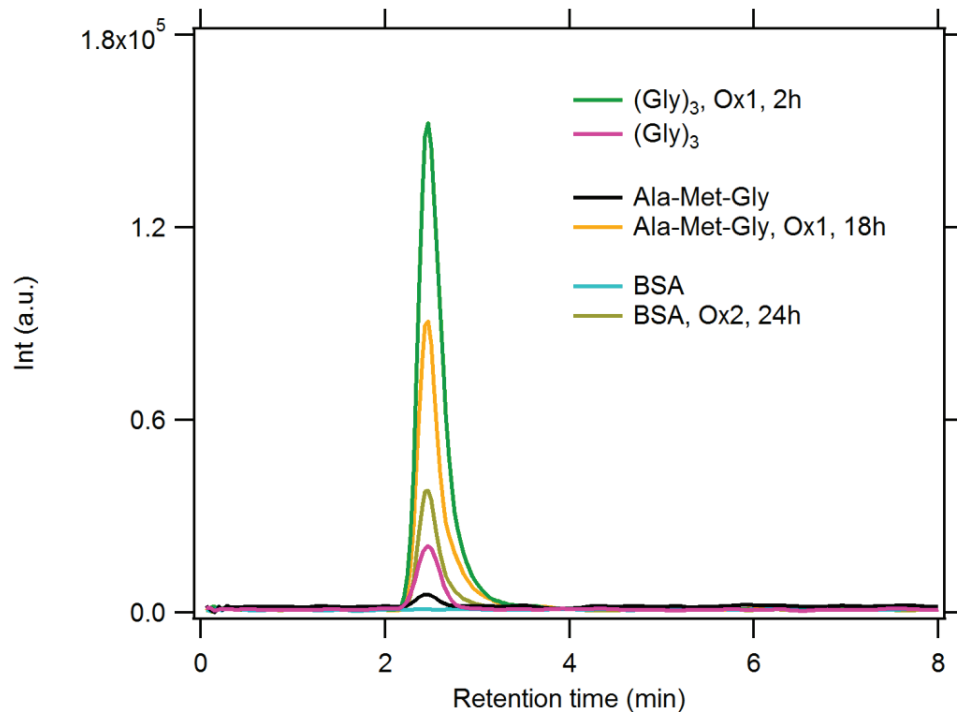


Fig. S2 The extracted ion chromatograms (EIC) of m/z 76 in oxidized proteins/peptides samples and respective control samples

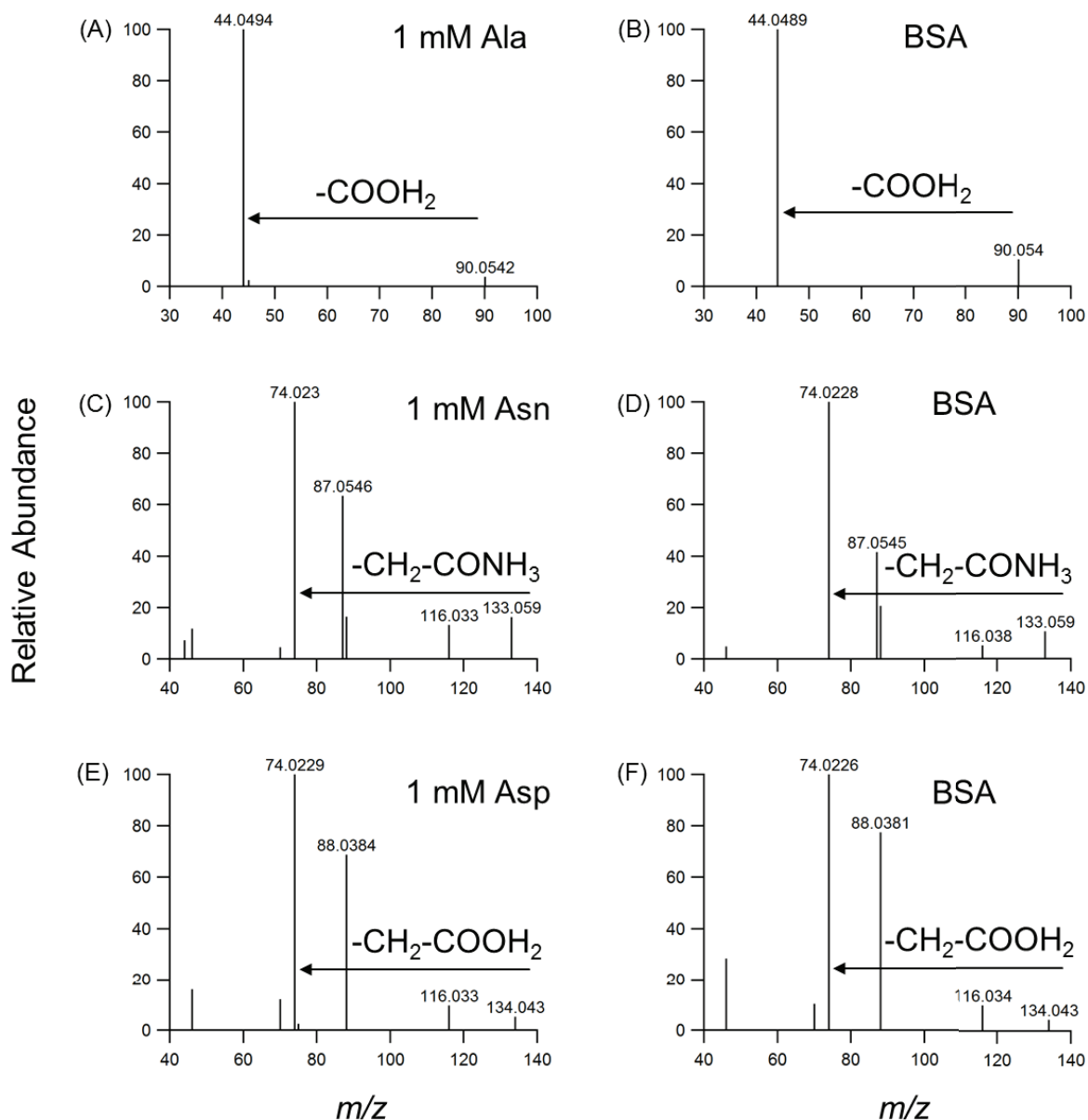


Fig. S3 The MS² spectra of *m/z* 90 (B), *m/z* 133 (D) and *m/z* 134 (F) in the oxidized BSA sample, in Ox2 condition (5 mM FeSO₄-150 mM H₂O₂). The precursor ion *m/z* 90, *m/z* 133 and *m/z* 134 was identified as alanine, asparagine and aspartic acid as they exhibited the same fragmentation patterns with *m/z* 90 in 1 mM Ala (A), *m/z* 133 in 1 mM Asn (C) and *m/z* 134 in 1 mM Asp (E), respectively

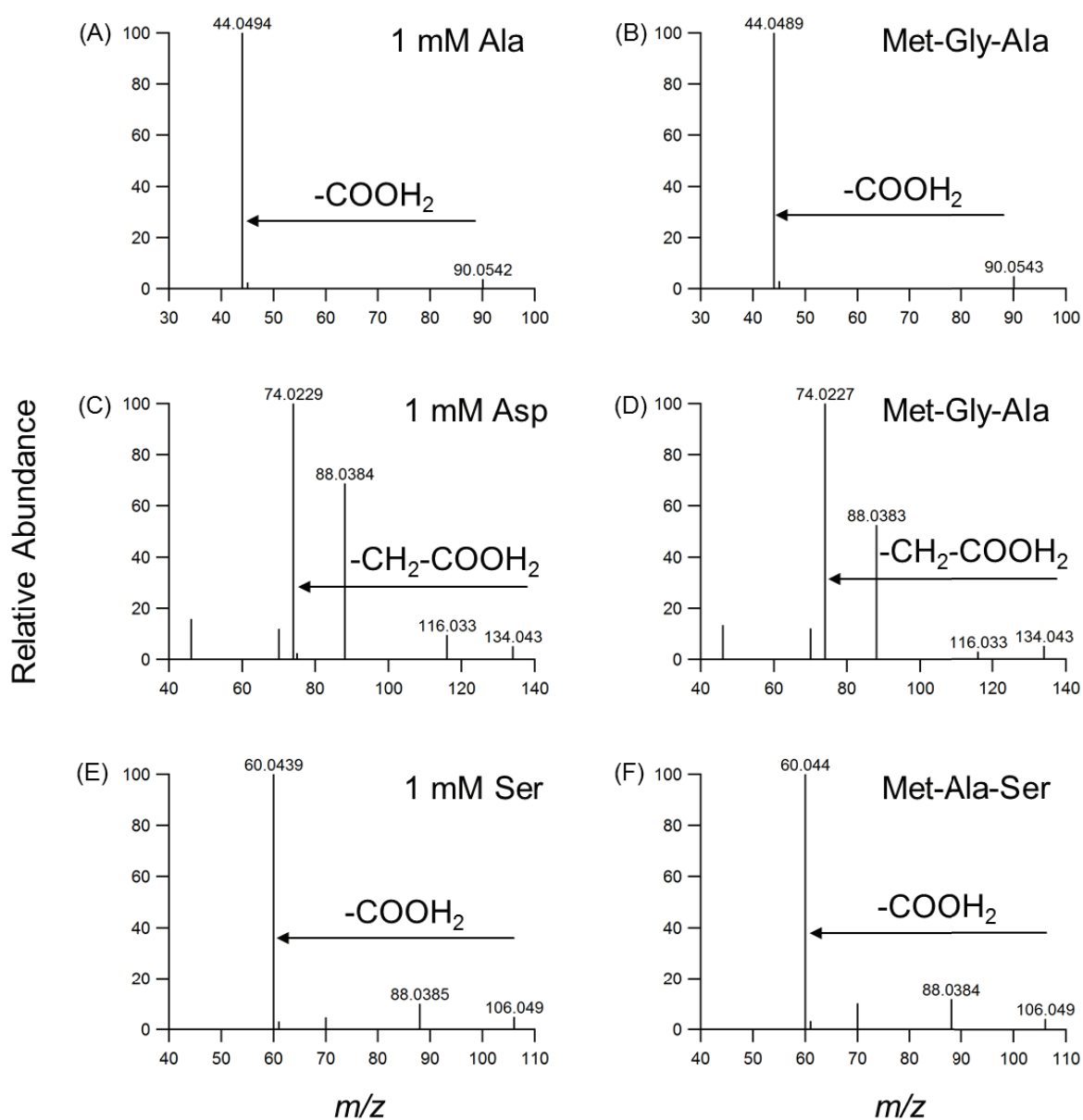


Fig. S4 The representative MS² spectra of *m/z* 90 (B) and *m/z* 134 (D) in the oxidized Met-Gly-Ala sample, and *m/z* 134 (F) in the oxidized Met-Ala-Ser sample in Ox1 condition (5 mM FeSO₄-50 mM H₂O₂). The precursor ion *m/z* 90, *m/z* 134 and *m/z* 106 was identified as alanine, aspartic acid and serine by comparison with the fragments of *m/z* 90 in 1 mM Ala (A), *m/z* 134 in 1 mM Asp (C) and *m/z* 106 in 1 mM Ser (E), respectively

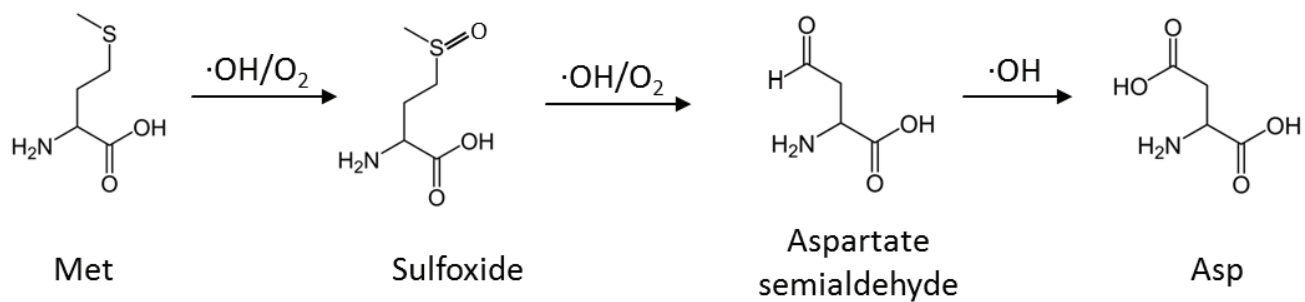


Fig. S5 Oxidation of methionine (Met) by OH radical for Met to aspartic acid (Asp) conversion. The major steps involve a first step of the oxidation of methionine to sulfoxide, followed by the formation of aldehyde at γ - carbon, which is further oxidized to yield Asp

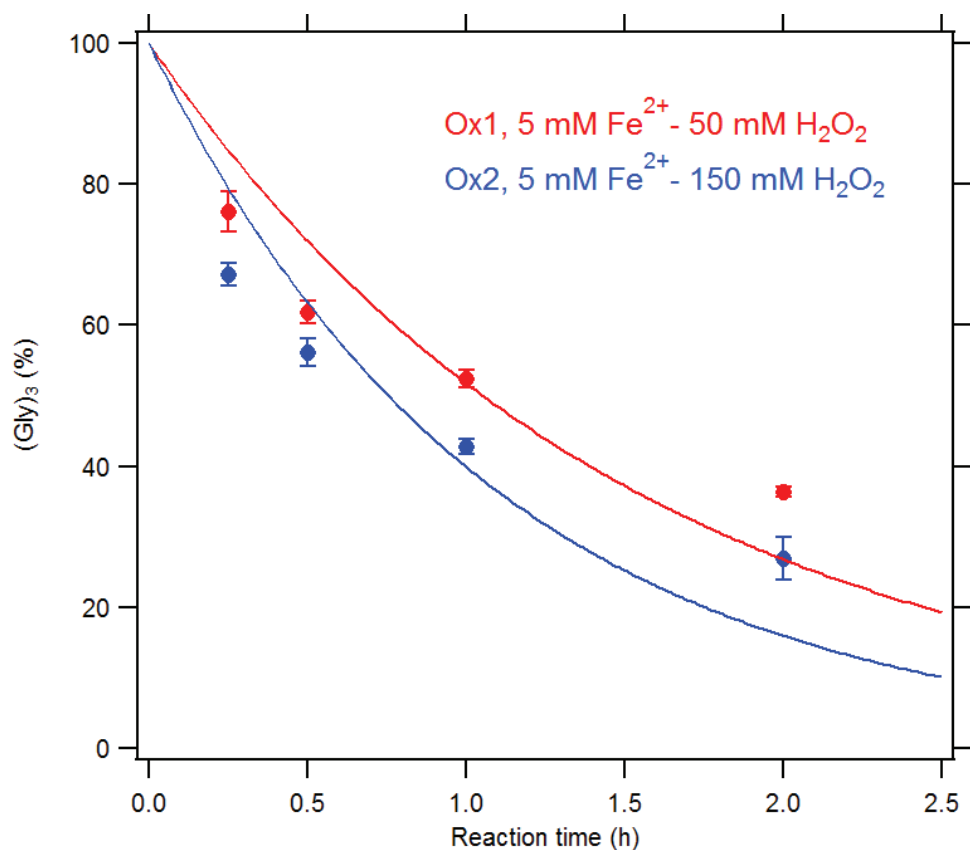


Fig.S6 The decay of (Gly)₃ under two different oxidation conditions. Both curves were fitted with a pseudo-first order kinetic rate function: $[(Gly)_3] = [(Gly)_3]_0 e^{(-k[OH]t)}$, where $[(Gly)_3]$ is the recovery of (Gly)₃, $[(Gly)_3]_0$ is the initial recovery (i.e., 100%), k ($1.2 \times 10^{-12} \text{ cm}^3 \text{ s}^{-1}$) is the second order rate constant for the reaction of OH with (Gly)₃, $[OH]$ is the concentration of hydroxyl radical, t is the reaction time. For simplification, we assumed that $[OH]$ remained constant during the reaction in order to obtain a rough $[OH]$ from the fitting function

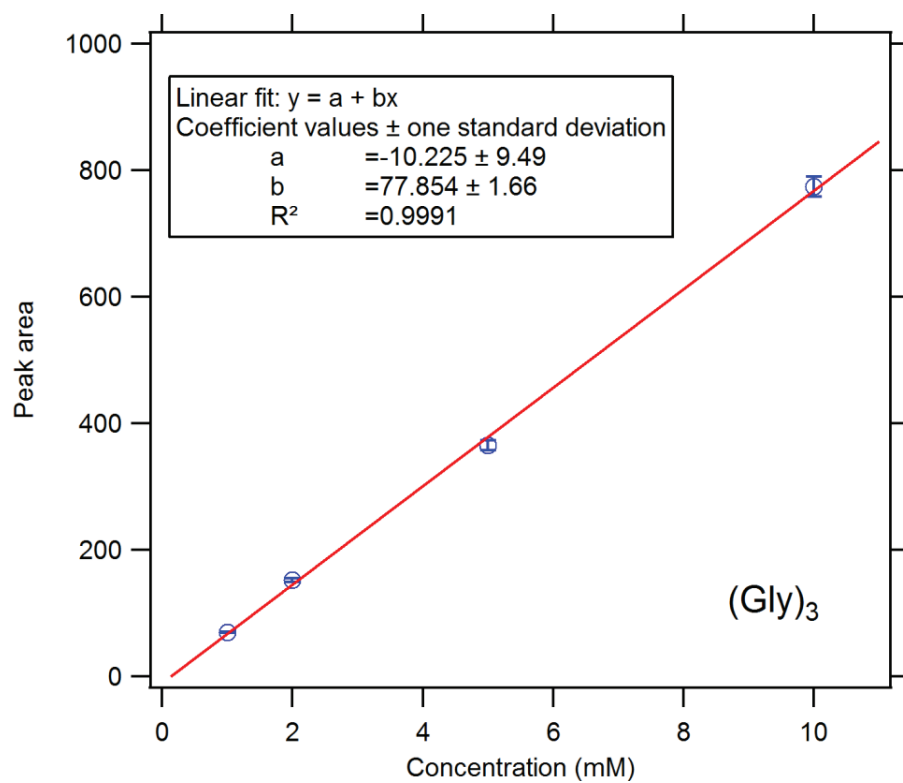


Fig. S7 Calibration curve plotting the peak area detected by DAD detection against concentration of (Gly)₃. The fitting equation was $y = 77.85x - 10.23$, $R^2 = 0.999$

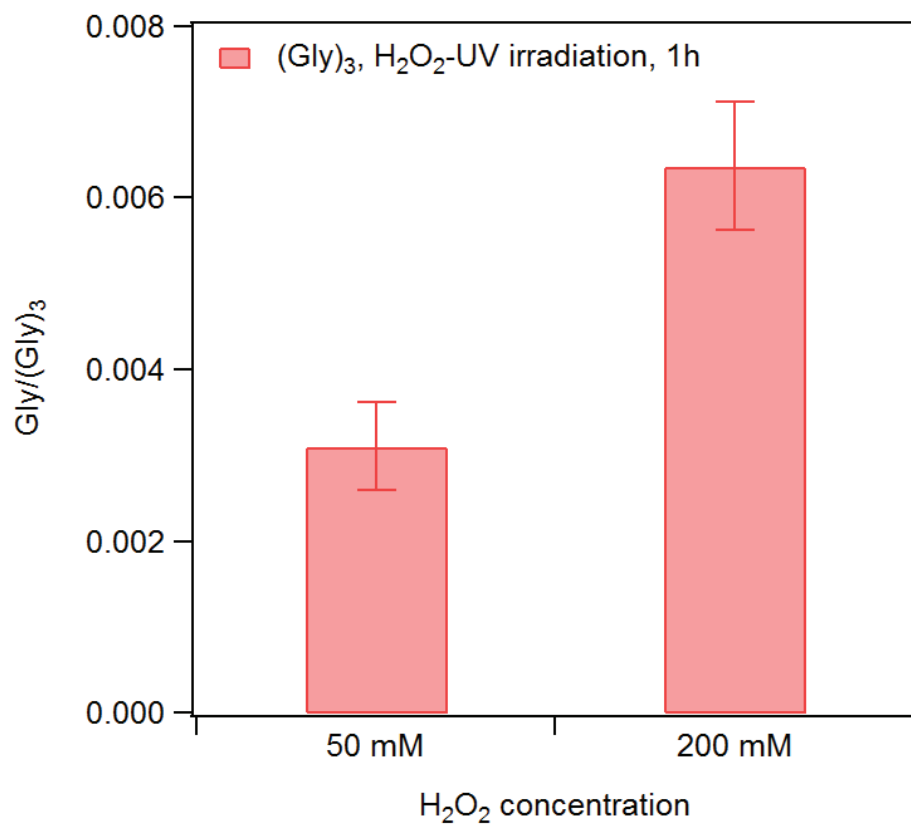


Fig. S8 Molar yield of glycine obtained in the oxidation of 4 mM (Gly)₃ with UV photolysis of 50 and 200 mM H₂O₂ solutions

Curriculum Vitae

Name Fobang Liu
Date of birth 20 July 1987
Place of birth Guangzhou, China

Education

11/2013-06/2017 PhD study, Max Planck Institute for Chemistry, Department of Multiphase Chemistry, Mainz, Germany
Supervisor: Prof. Dr. Ulrich Pöschl
Dissertation: “Chemical modification of proteins by air pollutants and metaproteomic analysis of atmospheric aerosol samples”

09/2010-06/2013 Master study, Sun Yat-sen University, School of Marine Science, Guangzhou, China
Supervisor: Prof. Dr. Shichun Zou
Thesis: “Characteristics, source apportionment of Polycyclic Aromatic Hydrocarbons (PAHs) and water soluble ions in marine aerosols”

09/2006-06/2010 Bachelor study, Sun Yat-sen University, School of Chemistry, Guangzhou, China
Supervisor: Prof. Dr. Shichun Zou
Thesis: “Characterization of bioaerosols in the atmosphere of livestock farm in Zhuhai, China”